Thaisa Baccarin

DESENVOLVIMENTO DE NANOEMULSÕES CONTENDO CONSTITUINTES DE *Punica granatum* PARA APLICAÇÃO CUTÂNEA VISANDO SUA UTILIZAÇÃO NA FOTOPROTEÇÃO

Tese submetida ao Programa de Pós-Graduação em Farmácia da Universidade Federal de Santa Catarina para obtenção do Grau de Doutora em Farmácia.
Orientadora: Profª. Drª. Elenara Lemos Senna

Florianópolis

2015

Ficha de identificação da obra elaborada pelo autor,
através do Programa de Geração Automática da Biblioteca Universitária da UFSC.

Baccarin, Thaisa
Desenvolvimento de nanoemulsões contendo constituintes de Punica granatum para aplicação cutânea visando sua utilização na fotoproteção / Thaisa Baccarin ; orientadora, Elenara Lemos Senna - Florianópolis, SC, 2015.
296 p.

Tese (doutorado) - Universidade Federal de Santa Catarina, Centro de Ciências da Saúde. Programa de Pós Graduação em Farmácia.

Inclui referências

1. Farmácia. 2. Nanoemulsão. 3. Punica granatum. 4. Fotoproteção. 5. Liberação tópica. I. Lemos Senna, Elenara. II. Universidade Federal de Santa Catarina. Programa de Pós Graduação em Farmácia. III. Título.

"DESENVOLVIMENTO DE NANOEMULSÕES CONTENDO CONSTITUINTES DE Punica granatum PARA APLICAÇÃO CUTÂNEA VISANDO SUA UTILIZAÇÃO NA FOTOPROTEÇÃO"

POR

Thaisa Baccarin

Tese julgada e aprovada em sua forma final pelo(a) Orientador(a) e membros da Banca Examinadora, composta pelos Professores Doutores:

Banca Examinadora:

Prof(a). Dr(a). Simone Gonçalves Cardoso (UFSC – Membro Titular)

Prof(a). Dr(a). Danilo Wilhelm Filho (UFSC – Membro Titular)

Prof(a). Dr(a). Simone Quintana de Oliveira (UFSC – Membro Titular)

Prof(a). Dr(a). Helder Ferreira Teixeira (UFRGS – Membro Titular)

Prof(a). Dr(a). Lucas Antônio Miranda Ferreira (UFMG – Membro Titular)

Prof(a). Dr(a). Elenara Lemos Senna (UFSC – Orientadora)

Profa. Dra. Tânia Beatriz Creczynski Pasa
Coordenadora do Programa de Pós-Graduação em Farmácia da UFSC

Florianópolis, **29 de outubro de 2015**.

Aos meus maiores exemplos de vida, meus pais Antônio e Lenir, por todo apoio, compreensão, amor, carinho e dedicação que destinaram a mim durante toda minha vida.

AGRADECIMENTOS

À Deus, por sempre iluminar meu caminho.

Aos meus pais Antônio e Lenir, por estarem sempre presentes na minha vida, pelo incentivo, apoio, compreensão e amor incondicional.

Ao meu irmão Marcelo e a todos meus familiares, pelo apoio e incentivo.

À Profª. Drª. Elenara Lemos Senna, pela oportunidade e orientação, pela liberdade em conduzir esta tese, e pela confiança em meu trabalho.

À Profª. Drª. Maria Pilar Vinardell, por ter me recebido tão bem na Universitat de Barcelona durante meu doutorado sanduíche. Obrigada por todos os ensinamentos e atenção, e principalmente por confiar em meu trabalho e contribuir não apenas com meu crescimento profissional, mas também pessoal.

À Profª. Drª. Montserrat Mitjans, pelos ensinamentos e risadas compartilhadas.

Aos demais funcionários, pesquisadores e professores do Departamento de Fisiologia da Falcultat de Farmàcia da Universitat de Barcelona por terem me acolhido.

Aos colegas de Barcelona, Ledy, Andrèu, Roberta, Jordi, Marinela, Marta, Teresa, Carol, Gema e Itsazo, pelas risadas, conversas e aprendizado.

À minha família espanhola, Paquita, Juan, Oscar e Andréia pela recepção calorosa, e por tornar minha estadia em Barcelona tão agradável e inesquecível.

À Profª. Drª. Ruth Meri Lucinda Silva, do Laboratório de Tecnologia Farmacêutica da Universidade do Vale do Itajaí pela amizade, apoio e incentivo.

À amiga Alexandra, pelo apoio e pelas conversas divertidas.

À Elis, pela compreensão, apoio e assistência na utilização do UFLC.

Aos colegas e amigos do Laboratório de Farmacotécnica da Universidade Federal de Santa Catarina, por estarem sempre presentes nos momentos de alegria e de dificuldades durante a realização deste

trabalho. Em especial, à amiga Letícia, pelos conhecimentos compartilhados, pelo incentivo, compreensão e companheirismo durante os todos esses anos de doutorado, e à amiga Janaína, por toda ajuda, coleguismo, incentivo, pelas eternas divagações sobre as dificuldades de trabalhar com plantas e principalmente, por nossas risadas nada discretas compartilhadas.

Aos demais colegas e professores da Pós-Graduação em Farmácia.

À CAPES, pela concessão de bolsas e apoio financeiro.

RESUMO

O presente trabalho descreve o desenvolvimento de nanoemulsões do tipo óleo em água contendo constituintes de *Punica granatum* (romã) e hidrogéis termosensíveis incluindo nanoemulsões para aplicação cutânea visando sua utilização na fotoproteção. A fração acetato de etila foi obtida por partição líquido-líquido, a partir do extrato seco das cascas de *P. granatum*, e caracterizada pela quantificação de polifenóis totais, ácido gálico, ácido elágico e punicalagina - 638,1 mg/g, 238,6 mg/g, 84,7 mg/g e 296,7 mg/g - respectivamente. As nanoemulsões contendo óleo de semente de romã (EAF-PSO-NE) ou triglicerídeo de cadeia média (EAF-MCT-NE) como fase oleosa, encapsulando a fração acetato de etila, foram obtidas através de dois métodos: emulsificação-evaporação do solvente e emulsificação espontânea, respectivamente. As nanoemulsões apresentaram forma esférica e distribuição monodispersa das gotículas. O tamanho médio das gotículas obtido pela técnica de espalhamento de luz dinâmico (DLS) foi de aproximadamente 180 nm e 220 nm, para EAF-PSO-NE e EAF-MCT-NE, respectivamente. Estes dados foram confirmados por microscopia eletrônica de transmissão (MET). O teor médio de fenóis totais, ácido elágico, ácido gálico e punicalagina para EAF-PSO-NE foi de 2,3 mg/mL, 35,1 µg/mL, 1248,9 µg/mL, 425,6 µg/mL, respectivamente; para EAF-MCT-NE foi de 2,3 mg/mL, 89,9 µg/mL, 1320,7 µg/mL, 383,6 µg/mL, respectivamente. As nanoemulsões apresentaram valores de eficiência de encapsulação de acordo com a lipofilicidade de cada composto polifenólico e considerável ação antioxidade frente aos ensaios de DPPH e FRAP. As nanoemulsões foram caracterizadas como não irritantes/fotoirritantes em ensaio preliminar utilizando eritrócitos humanos. Ainda empregando eritrócitos humanos como modelo de biomembrana, verificou-se que as nanoemulsões foram capazes de interagir com a bicamada lipídica e proteger a mesma de danos oxidativos induzidos pelo iniciador de radical livre AAPH. O efeito fotoprotetor das nanoemulsões contra radiação UVB foi evidenciado pela proteção a danos no DNA celular. O fator de proteção solar (FPS) determinado *in vitro* foi de até 25 para EAF-PSO-NE. Estudos *in vitro* demonstraram que nas concentrações testadas as nanoemulsões e fração livre não foram citotóxicas ou fototóxicas. O comportamento das nanoemulsões na presença do meio de cultura foi verificado pela técnica de DLS e crio-microscopia eletrônica de transmissão (Crio-MET). Nos estudos de internalização celular as nanoemulsões demonstraram

habilidade de se acumularem ao redor da célula e também internalizar. A estabilidade físico-química (exceto teor de punicalagina) das nanoemulsões foi evidenciada por 60 dias. A fotoestabilidade das formulações foi verificada pela exposição a doses mínimas preconizadas de radiação UVA e UV-visível; as nanoemulsões foram consideradas fotoestáveis. A baixa viscosidade das nanoemulsões inviabiliza sua aplicação na pele, deste modo um copolímero termosensível foi incorporado nas mesmas. A presença das nanoemulsões nos hidrogéis foi confirmada pela técnica de DLS e por microscopia eletrônica de varredura de alta resolução (SEM-FEG). Os hidrogéis foram caracterizados físicamente e quimicamente e foi verificado que na concentração mais baixa de copolímero um hidrogel de textura agradável e de fácil aplicação em spray foi obtido. Estudos de permeação e retenção dos compostos fenólicos através de pele de orelha suína também foram conduzidos. A fração nanoemulsionada aumentou substancialmente a liberação tópica dos compostos polifenólicos quando comparada com a fração livre. A permeação e retenção dos compostos polifenólicos dependeram de suas características físico-químicas, do veículo e de possíveis interações com a pele. As concentrações dos compostos polifenólicos retidos no *stratum corneum*, e permeados até a epiderme viável e derme evidenciaram a possibilidade de aplicação das formulações como fotoprotetor atuando na absorção de fótons e complementando a ação antioxidante na pele. Com o intuito de visualizar a permeação e retenção a partir da aplicação tópica de nanoemulsões ou de hidrogéis contendo as nanoemulsões, um agente fluoróforo (vermelho de nilo) foi juntamente nanoemulsionado com a fração acetato de etila. As imagens obtidas por microscopia confocal de varredura laser (MCVL) corroboraram os resultados obtidos nos estudos de permeação e retenção cutânea. Assim, os resultados obtidos indicam que as nanoemulsões e hidrogéis contendo constituintes de *P. granatum* (óleo da semente e fração), oferecem uma estratégia promissora para liberação tópica de compostos polifenólicos (ácido gálico, ácido elágico e punicalagina) com potencial aplicação na fotoproteção.

Palavras-chave: *Punica granatum*; Romã; Nanoemulsão; Óleo de semente de romã; Fração acetato de etila; Ácido gálico; Ácido elágico; Punicalagina; Polifenóis; Aplicação tópica; Validação analítica; Atividade antioxidante; Potencial irritante e fotoirritante; Fotoproteção; Radiação UVB; Citotoxicidade *in vitro*; Dano ao DNA; Internalização celular; Fototoxicidade; Hidrogel termosensível; Liberação tópica.

ABSTRACT

This work describes the development of oil in water nanoemulsions containing *Punica granatum* (pomegranate) constituents and thermosensitive hydrogels thickened nanoemulsions for topical application aiming its use in photoprotection. The polyphenol-rich ethyl acetate fraction (EAF) was obtained by liquid-liquid partition from the dry peel extract of *P. granatum* and characterized by quantification of total polyphenols, gallic acid, ellagic acid, and punicalagin - 638.1 mg/g, 238.6 mg/g, 84.7 mg/g and 296.7 mg/g - respectively. The nanoemulsions containing pomegranate seed oil (EAF-PSO-NE), or medium chain triglyceride (EAF-MCT-NE) as oil phase entrapping the EAF was obtained by two methods: emulsification-evaporation of the solvent and spontaneous emulsification, respectively. Nanoemulsions presented spherical shape and monodisperse distribution of droplets. The average droplet size obtained through dynamic light scattering (DLS) was around 180 nm and 220 nm for EAF-PSO-NE and EAF-MCT-NE, respectively. These data were confirmed by transmission electron microscopy (TEM). The average of total phenolic content, ellagic acid, gallic acid and punicalagin for EAF-PSO-NE were 2.3 mg/mL, 35.1 µg/mL, 1248.9 µg/mL and 425.6 µg/mL, respectively; for EAF-MCT-NE were 2.3 mg/mL, 89.9 µg/mL, 1320.7 µg/mL and 383.6 µg/mL, respectively. The encapsulation efficiency values were according to the lipophilicity of each polyphenol compound and considerable antioxidant activity was observed for nanoemulsions through DPPH and FRAP assays. In preliminary testing using human erythrocytes the nanoemulsions were characterized as non-irritant/photoirritant. Also employing human erythrocytes as a biomembrane model, it was found that the nanoemulsions were able to interact with the lipid bilayer and protect against oxidative damage induced by the free-radical initiator AAPH. The photoprotective effect of nanoemulsions was demonstrated by cellular protection against UVB radiation induced DNA damage. The *in vitro* sun protection factor (SPF) was up to 25 for EAF-PSO-NE. *In vitro* studies showed that the concentrations tested for free EAF and nanoemulsions were not cytotoxic or phototoxic. The droplet size and zeta potential of the nanoemulsions in contact with culture medium were verified by DLS technique and cryo-transmission electron microscopy (Cryo-TEM). In the cellular internalization studies nanoemulsions demonstrated an ability to accumulate around the cell and also to internalize. The

nanoemulsions were physically and chemically stable for 60 days (except for punicalagin content). The photostability of the formulations was verified by UVA and UV-visible exposure at recommended minimum doses; nanoemulsions were considered photostable. Since the nanoemulsions exhibit low viscosities, which restrain their application to the skin surface, a thermoreversible copolymer was incorporated into the formulations. The presence of nanoemulsions in the hydrogels was confirmed by DLS technique and by high resolution scanning electron microscopy (FEG-SEM). The hydrogels were physically and chemically characterized. It was noticed that when the lowest concentration of the copolymer was employed, a hydrogel easy to spray and with pleasant texture was obtained. Permeation and retention studies of phenolic compounds across the porcine ear skin were also conducted. The nanoemulsified EAF increased substantially the topical delivery of polyphenolic compounds compared with the free EAF. The skin permeation and retention of polyphenolic compounds depended on its physico-chemical characteristics, the vehicle and possible interactions with the skin. The amounts of polyphenolic compounds retained in the *stratum corneum* and that permeated into the viable epidermis and dermis, highlight the possible application of the formulations as photoprotectors acting in the absorption of photons and complementing the antioxidant protection in the skin. In order to visualize the permeation and retention after topical application of nanoemulsions or hydrogels containing nanoemulsions, a fluorophore agent (nile red) was nanoemulsified together with the ethyl acetate fraction. The images obtained by confocal laser scanning microscopy (CLSM) corroborated the results obtained in the skin permeation and retention studies. Thus, the results indicated that nanoemulsions and hydrogels containing constituents of *P. granatum* (seed oil and EAF), offer a promising strategy for topical delivery of polyphenolic compounds (gallic acid, ellagic acid, and punicalagin) with potential application in photoprotection.

Keywords: *Punica granatum*; pomegranate; Nanoemulsion; Pomegranate seed oil; Polyphenol-rich ethyl acetate fraction (EAF); Gallic acid; Ellagic acid; Punicalagin; Polyphenols; Topical application; Analytical validation; Antioxidant activity; Irritant and photoirritant potential; Photoprotection; UVB Radiation; DNA damage; *In vitro* cytotoxicity; Cellular internalization; Phototoxicity; Thermosensitive hydrogel; Topical delivery.

LISTA DE FIGURAS

Publicação: "*Pomegranate seed oil nanoemulsions encapsulating pomegranate peel polyphenol-rich ethyl acetate fraction: Development and antioxidant assessment*"

Publicação: *"Protection against oxidative damage in human erythrocytes and preliminary photosafety assessment of Punica granatum seed oil nanoemulsions entrapping polyphenol-rich ethyl acetate fraction"*

Publicação: "*Nanoemulsion drug delivery systems for potential application in skin delivery of polyphenol constituents from pomegranate*"

LISTA DE TABELAS

Publicação: *"Pomegranate seed oil nanoemulsions entrapping pomegranate peel polyphenol-rich extract fraction: Development and antioxidant evaluation"*

Publicação: *"Protection against oxidative damage in human erythrocytes and preliminary photosafety assessment of Punica granatum seed oil nanoemulsions entrapping polyphenol-rich ethyl acetate fraction"*

Publicação: ***"Photoprotection by Punica granatum seed oil nanoemulsion entrapping polyphenol-rich ethyl acetate fraction against UVB-induced DNA damage in human keratinocytes (HaCaT) cell line"***

Publicação: ***"Nanoemulsion drug delivery systems for potential application in skin delivery of polyphenol constituents from pomegranate"***

LISTA DE ABREVIATURAS E SIGLAS

AAPH – 2,2'-azobis (2-amidinopropane) dihydrochloride; 2,2'-azobis (2-aminopropano) dicloridrato.
ANOVA – Analysis of Varience; Análise de Variância.
BSA – Bovine Serum Albumin; Albumina Sérrica Bovina.
CAT – Catalase; Catalase.
CLSM – Confocal laser scanning microscopy; Microscopia confocal de varredura laser.
CPD – Cyclobutane-Pyrimidine Dimers; Dímeros de Pirimidina Ciclobutano.
DAD – Diode Array Detector ; Detector de Diodos.
DAPI – 4',6-diamidino-2-phenylindole; 4',6-diamidino-2-fenilindol.
DE – Dermis ; Derme.
DEM – Minimal Erythema Dose ; Dose Eritematosa Mínima.
DLS – Dynamic Light Scattering ; Espalhamento de Luz Dinâmico.
DMEM – Dulbecco's Modified Eagle's Medium; Meio Eagle Modificado por Dulbecco.
DMSO – Dimethyl Sulfoxide; Dimetilsulfóxido.
DNA – Deoxyribonucleic Acid; Ácido Desoxirribonucleico.
DPH – 1,6-diphenyl-1,3,5-hexatriene; 1,6-difenil-1,3,5-hexatrieno.
EA – Ellagic Acid; Ácido Elágico.
EAF – Ethyl Acetate Fraction from pomegranate peel extract ; Fração Acetato de Etila do extrato das cascas da romã.
EAF-PSO-NE – Pomegranate seed oil nanoemulsion encapsulating the ethyl acetate fraction from pomegranate peel extract ; Nanoemulsão contendo o óleo de semente de romã encapsulando a fração acetato de etila do extrato das cascas da romã.
EAF-MCT-NE –Medium chain trigliceryde nanoemulsion encapsulating the ethyl acetate fraction from pomegranate peel extract ; Nanoemulsão contendo triglicerídeo de cadeia média encapsulando a fração acetato de etila do extrato das cascas da romã.
EAF-PSO-NE gel_{18} – Poloxamer 18% hydrogel thikened pomegranate seed oil nanoemulsion encapsulating the ethyl acetate fraction from pomegranate peel extract ; Hidrogel de poloxamer 18% contendo nanoemulsão com óleo de semente de romã encapsulando a fração acetato de etila do extrato das cascas da romã.
EAF-PSO-NE gel_{28} – Poloxamer 28% hydrogel thikened pomegranate seed oil nanoemulsion encapsulating the ethyl acetate fraction from pomegranate peel extract ; Hidrogel de poloxamer 28% contendo

nanoemulsão com óleo de semente de romã encapsulando a fração acetato de etila do extrato das cascas da romã.
EAF-MCT-NE gel_{18} – Poloxamer 18% hydrogel thikened medium chain trigliceryde nanoemulsion encapsulating the ethyl acetate fraction from pomegranate peel extract ; Hidrogel de poloxamer 18% contendo nanoemulsão com triglicerídeo de cadeia média encapsulando a fração acetato de etila do extrato das cascas da romã.
EAF-MCT-NE gel_{28} – Poloxamer 28% hydrogel thikened medium chain trigliceryde nanoemulsion encapsulating the ethyl acetate fraction from pomegranate peel extract ; Hidrogel de poloxamer 28% contendo nanoemulsão com triglicerídeo de cadeia média encapsulando a fração acetato de etila do extrato das cascas da romã.
EAF_{NR}-PSO-NE – Pomegranate seed oil nanoemulsion encapsulating the ethyl acetate fraction from pomegranate peel extract and nile red ; Nanoemulsão contendo o óleo de semente de romã encapsulando a fração acetato de etila do extrato das cascas da romã e o vermelho de nilo.
EAF_{NR}-MCT-NE – Medium chain trigliceryde nanoemulsion encapsulating the ethyl acetate fraction from pomegranate peel extract ; Nanoemulsão contendo triglicerídeo de cadeia média encapsulando a fração acetato de etila do extrato das cascas da romã e vermelho de nilo.
EDTA – Ethylenediamine tetraacetic acid; Ácido etilenodiamino tetra-acético.
EE – Entrapment Efficiency ; Eficiência de Encapsulação.
EP – Viable epidermis ; Epiderme viável.
ERN – Reactive Nitrogen Species ; Espécies Reativas de Nitrogênio.
FBS – Fetal Bovine Serum; Soro fetal bovino.
FEG-SEM – Field Emission Gun Scanning Electron Microscopy; Microscopia Eletrônica de Varredura por Emissão de Campo.
FPS – Fator de Proteção Solar.
GA – Gallic Acid ; Ácido Gálico.
GAE – Gallic Acid Equivalent ; Equivalentes em Ácido Gálico.
GPx – Glutathione Peroxidase ; Glutationa Peroxidase.
HC_{50} – 50% Hemolitic Concentration ; Concentração Hemolítica 50%.
HMW – High Molecular Weight Proteins ; Proteínas de Alto Peso Molecular.
HPLC – High Performance Liquid Chromatography; Cromatografia Líquida de Alta Eficiência
IC_{50} – 50% Inhibitory Concentration; Concentração Inibitória 50%.

ICH – International Conference Harmonization.
IL-8 – Interleukin 8 ; Interleucina 8.
LOD – Limit of Detection ; Limite de Detecção.
LOQ – Limit of Quantification ; Limite de Quantificação.
MCT – Medium Chain Trigliceryde; Triglicerídeo de Cadeia Média.
MCT-NE – Medium chain trigliceryde nanoemulsion ; Nanoemulsão contendo o triglicerídeo de cadeia média como fase interna.
MTT – 3-(4,5-Dimethiazol-Zyl)-2-5-Diphenyltetrazolium Bromide; Brometo de 3-(4,5-Dimetiltiazol-2-il)-2,5-Difeniltetrazólio.
MW – Molecular Weight ; Peso Molecular.
NE – Nanoemulsion ; Nanoemulsão.
NER – Nucleotide Excision Repair ; Reparo por Excisão de Nucleotídeos.
NRU – Neutral Red Uptake ; Captura do Vermelho Neutro.
NR – Nile red ; Vermelho de nilo.
OECD – Organization for Economic Co-operation and Development.
PC – Punicalagin ; Punicalagina.
PBS – Phosphate Buffered Saline ; Tampão Fosfato Salino.
PI – Polidispersity Index; Índice de Polidispersão.
PSO – Pomegranate seed oil; Óleo de Semente de Romã.
PSO-NE – Pomegranate seed oil nanoemulsion ; Nanoemulsão contendo o óleo da semente de romã como fase interna.
PTFE – Polytetrafluorethylene ; Politetrafluoretileno.
RE – Refrigerator ; Refrigerador ;
RBCs – Human Red Blood Cells ; Eritrócitos Humanos.
ROS – Reactive Oxygen Species ; Espécies Reativas de Oxigênio
RSD – Relative Standard Deviation ; Desvio Padrão Relativo.
RT – Room Temperature ; Temperatura Ambiente.
SC – *Stratum corneum* ; Estrato córneo.
SC_{50} – 50% Scavenging Concentration ; Concentração para reduzir 50% do radical.
SD – Standard Deviation ; Desvio Padrão.
SE – Standard Error ; Erro Padrão.
SEM – Scanning Electron Microscopy; Microscopia Eletrônica de Varredura.
SEM – Standard Error of the Mean; Desvio Padrão da Média.
SOD – Superoxide Dismutase ; Superóxido Dismutase.
TEM – Transmission Electron Microscopy; Microscopia Eletrônica de Transmissão.

TMA-DPH – 1-(4-trimethylammoniumphenyl)-6-phenyl-1,3,4-hexatriene p-toluenesulfonate;
TPC – Total Phenolic Content; Concentração de Fenóis Totais.
TPTZ – 2,4,6-tris(2-pyridyl)-S-triazine; 2,4,6-tris(2-piridil)-S-triazina.
UFLC – Ultra fast liquid chromatography ; Cromatografia Líquida Ultra Rápida.
UV/VIS – Ultraviolet-Visible Spectrophotometry ; Espectrofotometria no Ultravioleta-Visível.

LISTA DE SÍMBOLOS

λ – Light wavelenght; Comprimento de onda.
μ – Micro; Micro.
D – Drug difussion coefficient; Coeficiente de difusão do fármaco.
J – Flux; Fluxo.
m – Mass; Massa.
t – Time; Tempo.
ΔC – Drug concentration gradiente. Gradiente de concentração do fármaco.
K_p – Permeability coefficient; Coeficiente de permeabilidade.
K_{oct} – Octanol-water partition coefficient; Coeficiente de partição octanol-água.
C_0 – Initial concentration; Concentração inicial.

SUMÁRIO

INTRODUÇÃO

A pele é o órgão que reveste o corpo humano limitando o seu contato com o meio externo. Ela desempenha funções como a regulação da temperatura corporal, da perda de água e a proteção frente a agressões químicas, físicas e microbiológicas do meio externo. Caracteriza-se como uma membrana heterogênea, sendo o estrato córneo a principal camada que promove a proteção e controla a absorção de fármacos. Ele é composto por um feixe de queratina insolúvel cercado por células estabilizadas por proteínas interligadas e limitado por lipídeos, como colesterol e ácidos graxos (HADGRAFT, 2001).

Os efeitos da radiação ultravioleta sobre a pele têm sido amplamente estudados. A exposição crônica à radiação solar tem sido considerada como sendo a maior causa de câncer de pele e fotoenvelhecimento. O espectro da luz ultravioleta consiste das radiações UVA (320-400nm), UVB (280-320nm) e UVC (200-280nm). As radiações UVA e UVB são responsáveis pela diminuição de sistemas antioxidantes cutâneos, bem como pelo aumento de sistemas oxidantes, por diversos mecanismos, alterando assim o balanço redox celular e, conseqüentemente, a homeostasia cutânea (GARATINI et al., 2007).

A aplicação tópica de antioxidantes representa uma estratégia interessante de proteção cutânea contra a radiação ultravioleta e malefícios ocasionados por ela, como o aumento do estresse oxidativo, danos ao DNA, entre outros.

A *Punica granatum* (L.), conhecida popularmente como pomegranate ou romã pertence à família Punicaceae, é uma planta nativa da área do Irã ao Himalaia no norte da Índia, e tem sido cultivada e naturalizada na região Mediterrânea, como também nas áreas mais secas dos Estados Unidos, China, Japão e Rússia (MEERTS et al., 2009). Os frutos são consumidos frescos ou utilizados na preparação de suco, geléia, pasta e também como flavorizante (FADAVI et al., 2005; MOUSAVINEJAD et al., 2009).

No Brasil, o plantio da romãzeira vem sendo avaliado desde 2010 e algumas variedades de romã estão sendo cultivadas nos estados de São Paulo, Bahia e Pernambuco. Pesquisas realizadas pela Empresa Brasileira de Pesquisa Agropecuária (EMBRAPA) têm demonstrado que existe a possibilidade de cultivo de espécies de climas tropical úmido, subtropical e temperada, com potencial econômico para as áreas irrigadas do semiárido brasileiro (OLIVEIRA et al., 2012).

A composição química dos frutos difere dependendo do cultivo, região, clima, maturidade da planta e condição de armazenamento (BARZEGAR et al., 2004). Cerca de 30-50% do peso total do fruto

corresponde à casca, e é fonte de compostos bioativos como polifenóis, flavonóides, elagitaninos, compostos proantocianidina (LI et al., 2006), minerais, especialmente potássio, cálcio, fósforo, magnésio e sódio (MIRDEHGHAN e RAHEMI, 2007), e polissacarídeos complexos (JAHFAR et al., 2003). Além dos elagitaninos, a casca contém ácidos hidroxibenzóicos como o ácido gálico e ácido elágico; antocianidinas e flavonóides como o campferol, luteolina, e quercetina (VIUDA-MARTOS et al., 2010). As sementes são ricas em lipídeos; o óleo da semente é caracterizado pela alta concentração de ácidos graxos poli-insaturados como o ácido punícico, linolênico, linoléico, e outros lipídeos como ácido oléico, esteárico e palmítico. As sementes ainda contem proteína, fibras, vitaminas e minerais, pectina, polifenóis, isoflavonas (genisteína), o fitoestrógeno coumestrol, e o esteróide estrona (EL-NEMR et al., 2006; FADAVI et al., 2006).

Várias atividades biológicas têm sido relatadas para os compostos presentes na casca da *P. granatum*, incluindo as atividades antioxidante (ÇAM et al., 2009), antitumoral (HAMAD e AL-MOMENE, 2009), hepatoprotetora (CELIK et al., 2009), além de melhorar a condição cardiovascular (DAVIDSON et al., 2009). Possui também atividades antimicrobiana (DUMAN et al, 2009), anti-inflamatória (LEE et al., 2010), antiviral (HAIDARI et al., 2009), e antidiabética (XU et al., 2009). Em particular, estudos têm mostrado a capacidade dos extratos da casca da romã em inibir a geração de radicais livres em modelos *in vivo* frente à radiação UVA e UVB, protegendo contra o eritema, espessamento da epiderme e fragmentação do DNA (KASAI et al., 2006; PACHECO-PALENCIA et al., 2008; MANASATHIEN et al., 2011).

A utilização do óleo da semente de *P. granatum* também é promissora. A aplicação tópica do óleo da semente de *P. granatum* reduziu significativamente a incidência e crescimento do tumor de pele em camundongos (HORA et al., 2003), como também regenerou a epiderme pela estimulação da proliferação dos queratinócitos (ASLAM et al., 2006).

Apesar dos efeitos benéficos dos antioxidantes na pele, a administração tópica cutânea ainda é um desafio, devido à eficiente função barreira exercida pelo estrato córneo que impede a absorção da maioria dos fármacos. Diversas estratégias têm sido empregadas para contornar as limitações impostas pela baixa absorção percutânea de fármacos. Os promotores de absorção, como por exemplo, etanol, polisorbato 80, taurocolato de sódio, demonstraram ser efetivos em

atingir este objetivo. Todavia, muitos deles são potentes irritantes, induzindo ao aparecimento de dermatite irritativa, a qual está de fato associada ao aumento de até 80 vezes na penetração cutânea de substâncias ativas (SCHÄFER-KORTING et al., 2007).

A incorporação de fármacos em sistemas carreadores coloidais tem mostrado ser uma estratégia promissora para o aumento da retenção e permeação cutânea, além de permitir o direcionamento dos mesmos nas subestruturas da pele. Eles diferem entre si em função da sua composição, capacidade de incorporar fármacos e aplicabilidade, mas a característica comum é o tamanho de partícula nanométrico. Entre os carreadores coloidais com potencial aplicação tópica destacam-se as nanoemulsões. Estes sistemas nanoestruturados são constituídos por lipídios purificados e misturas complexas de glicerídeos, apresentando tamanho de partícula variável. Suas principais características incluem excelente estabilidade física, capacidade de proteção de fármacos instáveis frente à degradação, capacidade de controle da liberação, possibilidade de vetorização e aprimoramento da biodisponibilidade de fármacos (MEHNERT e MADER, 2001; NEMEN e LEMOS-SENNA, 2011; ZHAI e ZHAI, 2014).

As nanoemulsões geralmente são compostas por um núcleo oleoso disperso em um meio aquoso (óleo em água-O/A) ou por um núcleo aquoso disperso em um meio oleoso (água em óleo-A/O). Óleos de origem vegetal ou semisintética, constituídos principalmente de triglicerídeos de cadeia média (TCM) e longa (TCL) são frequentemente empregados. No preparo das nanoemulsões também são empregados tensoativos de caráter lipofílico e hidrofílico, que podem ser incorporados isoladamente ou associados (FRONZA et al., 2004).

Algumas hipóteses têm sido propostas para explicar as propriedades de promoção da permeação cutânea de fármacos quando associados a sistemas nanoemulsionados. O fármaco é apresentado em uma forma finamente dispersa que assegura o contato íntimo com o estrato córneo, facilitando o seu transporte através da pele. As partículas de tamanho nanométrico podem se acumular nos folículos pilosos ou nos espaços entre os corneócitos, onde podem se desintegrar ou fundir junto aos lipídios da pele, afetando positivamente a permeação. Os lipídios podem ainda formar um filme na superfície da pele, aumentando a permeação cutânea por um efeito de oclusão. Finalmente, alguns componentes da formulação, como os surfactantes, podem agir como promotores de absorção, reduzindo a função barreira da pele

(SCHÄFER-KORTING et al., 2007; CEVC e VIERL, 2010; ZHAI e ZHAI, 2014).

Nos últimos anos, considerável atenção tem sido dada ao desenvolvimento de novos sistemas de liberação para fármacos de origem vegetal. Na pesquisa de fito-formulações, o desenvolvimento de formas nanométricas (nanopartículas, lipossomas, nanoemulsão etc.) contendo derivados vegetais, proporciona infinitas vantagens como aumento da solubilidade e biodisponibilidade, redução da toxicidade, melhora da estabilidade e proteção contra degradação química, quando comparado com os derivados vegetais em preparações convencionais (SARAF, 2010).

Levando em consideração os aspectos mencionados, a proposta deste trabalho consiste em desenvolver nanoemulsões contendo a fração acetato de etila do extrato da casca da romã, rica em compostos polifenólicos, usando o óleo da semente de romã como fase oleosa, com vistas à aplicação tópica cutânea. A utilização de ambos polifenóis e óleo da romã permitiria combinar em uma única formulação os efeitos benéficos destes compostos na fotoproteção, além de permitir o aumento da permeação cutânea e a melhoria da atividade antioxidante na pele.

Este trabalho é apresentado em quatro capítulos, sendo três deles na forma de publicações. O primeiro refere-se a uma breve revisão da literatura sobre o assunto. O segundo versa sobre o desenvolvimento das nanoemulsões, incluindo a preparação e caracterização da fração acetato de etila rica em polifenóis, a preparação e caracterização fisicoquimica das nanoemulsões, o desenvolvimento de uma metodologia analítica por cromatografia líquida de alta eficiência (CLAE) para determinação dos compostos polifenólicos majoritários, e a avaliação da atividade antioxidante *in vitro*. Ainda neste capítulo, o efeito protetor contra dano oxidativo em modelos *in vitro* usando eritrócitos humanos e a fotosegurança preliminar da fração acetato de etila e das nanoemulsões são determinados. O terceiro capítulo descreve um estudo sobre a caracterização das nanoemulsões em meio de cultura, a internalização celular das nanoemulsões, citotoxicidade, fototoxicidade e fotoproteção *in vitro* da fração acetato de etila e nanoemulsões em cultura monocamada de queratinócitos humanos (HaCaT) e fibroblasto murino (3T3). Finalmente, o quarto capítulo refere-se à incorporação das nanoemulsões em um hidrogel e avaliação da permeação e retenção cutânea destas formulações. Os estudos de estabilidade e fotoestabilidade das nanoemulsões são descritos no Apêndice A desta tese.

OBJETIVOS

Objetivo Geral

Desenvolver nanoemulsões contendo constituintes de *Punica granatum* para aplicação cutânea visando sua utilização na fotoproteção.

Objetivos Específicos

- Obter a fração acetato de etila a partir do extrato seco das cascas de *Punica granatum* pelo método de partição líquido-líquido;
- Desenvolver e validar metodologia analítica por cromatografia líquida de alta eficiência para a determinação dos principais compostos fenólicos, ácido elágico, ácido gálico e punicalaginas na fração acetato de etila e nanoemulsões;
- Caracterizar a fração acetato de etila quanto ao teor de fenólicos totais e concentração dos principais compostos fenólicos, ácido elágico, ácido gálico e punicalaginas.
- Preparar nanoemulsões a partir do óleo da semente da romã e fração acetato de etila rica em polifenóis da casca da romã pela técnica de emulsificação/evaporação do solvente;
- Preparar nanoemulsões a partir de triglicerideos de cadeia média e fração acetato de etila rica em polifenóis da casca da romã pela técnica de emulsificação espontânea;
- Caracterizar as nanoemulsões quanto ao tamanho de gota, morfologia e potencial zeta;
- Determinar o teor e a eficiência de encapsulação dos principais compostos fenólicos, ácido elágico, ácido gálico e punicalaginas nas nanoemulsões;
- Determinar a estabilidade e fotoestabilidade das nanoemulsões;
- Determinar a atividade antioxidante das nanoemulsões através de ensaios *in vitro*.
- Determinar o potencial irritante e fotoirritante das nanoemulsões em modelo de eritrócito humano;
- Avaliar e comparar a citotoxicidade e fototoxicidade das nanoemulsões contendo constituintes de *P. granatum* em cultura de fibroblastos murino 3T3 e queratinócitos humanos HaCaT *in vitro*;

- Avaliar a fotoproteção contra radiação UVB das nanoemulsões contendo constituintes de *P. granatum* em cultura de queratinócitos HaCaT *in vitro*;
- Preparar hidrogéis a partir das nanoemulsões contendo constituintes de *P. granatum*;
- Caracterizar os hidrogéis contendo nanoemulsão quanto ao tamanho de partícula, potencial zeta, viscosidade, análise de textura e morfologia;
- Desenvolver e validar metodologia analítica por cromatografia líquida ultra rápida para a determinação dos principais compostos fenólicos, ácido elágico, ácido gálico e punicalaginas nos estudos de permeação e retenção cutânea;
- Avaliar e comparar a permeação e retenção dos principais compostos fenólicos em modelo bicompartimental de célula de difusão tipo Franz, usando pele de orelha suína como membrana.

CAPÍTULO 1: REVISÃO DE LITERATURA

1 ADMINISTRAÇÃO TÓPICA CUTÂNEA

1.1 A pele

A pele não apenas é o maior órgão do corpo humano, mas também uma excelente barreira biológica. Apesar de possuir menos que 2 mm de espessura, a pele corresponde a aproximadamente 4% do peso corporal total (AULTON, 2005) e desempenha várias e complexas funções como, o controle da perda de água através da pele, da perda de eletrólitos, regulação da temperatura corporal, atua como órgão sensorial (tato, percepção de dor) e executa funções do sistema endócrino (síntese de vitamina D). Entretanto, sua função primordial é a de barreira protetora contra agentes químicos, mecânicos, microbiológicos, radiação solar (MENON, 2002; AULTON, 2005; PROW et al., 2011). O pH da pele pode variar entre 4 e 6,5, dependendo da região do corpo e da condição em que se encontra a mesma (saudável e íntegra ou ferida e/ou em dado estado patológico) (LAMBERS et al., 2006).

A pele humana compõe-se de três camadas de tecidos: a epiderme, a derme e a hipoderme (Figura 1).

Figura 1. Representação esquemática da estrutura da pele.

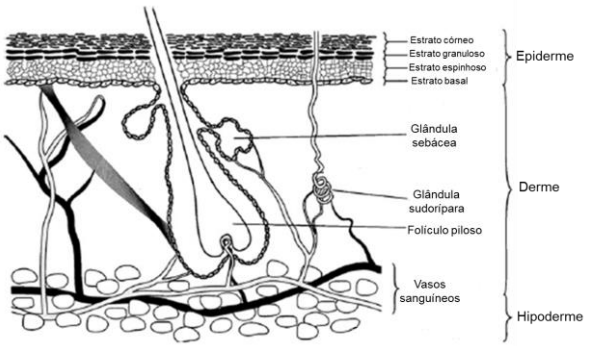

Fonte: adaptado de Maghraby; Barry; Williams (2008) e Barry (2001).

1.1.1 Epiderme

A epiderme é a camada mais externa da pele que primeiramente entra em contanto com produtos cosméticos, farmacêuticos, tecidos, agentes externos. Sua espessura é variável, oscilando desde 0,8 mm até 0,006 mm dependendo da região do corpo. A epiderme encontra-se em constante autorrenovação, este processo é dinâmico e definido pela perda das células da superfície do estrato córneo (descamação) e crescimento das células da epiderme inferior (MENON, 2002). Possui quatro camadas de células distintas: camada basal, espinhosa, granulosa e córnea.

- *Camada basal*: Composta por células colunares contendo organelas e filamentos de queratina aderidas à membrana via hemidesmossomos (MENON, 2002). As células presentes da camada basal dividem-se, diferenciam-se por meio de um processo de queratinização e migram ascendentemente para formarem o estrato córneo ou a camada córnea (AULTON, 2005; TANG e BHUSHAN, 2010).

-*Camada espinhosa*: Devido à abundância de desmossomos presentes nesta camada, as células apresentam morfologia espinhosa. Além das típicas organelas e filamentos de queratina, as células desta camada possuem corpos lamelares - discos lipídicos compostos por fosfolipídios, colesterol e glicosilceramidas empacotados (MENON, 2002).

-*Camada granulosa*: Os grânulos de queratohialina caracterizam histologicamente esta camada. As células apresentam-se mais alongadas e achatadas. Há um aumento nos filamentos de queratina, na síntese de proteínas e na lipogênese; os corpos lamelares são secretados para o meio extracelular nesta etapa final de diferenciação destas células em corneócitos (MENON, 2002).

-*Camada córnea ou estrato córneo*: Consiste de corneócitos anucleares ricos em queratina. Esses corneócitos ficam dispostos em regiões lamelares lipídicas de forma a aparentar uma organização do tipo “tijolo e argamassa” (Figura 2). As regiões lipídicas são formadas por bicamadas lipídicas (ceramidas, colesterol e ácidos graxos livres) e água dando origem a uma estrutura intercelular multilamelar e altamente lipofílica. Devido a estas regiões de caráter hidrofílico e lipofílico, o que possibilita meios de difusão de naturezas opostas, o estrato córneo é considerado como principal obstáculo à administração tópica de medicamentos. Assim, a camada córnea tem como função promover a hidratação cutânea e proteger o organismo contra agentes externos

(WERTZ, 1996; FOLDVARI, 2000; MENON, 2002; BOUWSTRA et al., 2003; TANG e BHUSHAN, 2010; GEUSENS et al., 2011).

Outras células encontram-se na epiderme viável juntamente com os queratinócitos, e incluem os melanócitos, que produzem melanina; as células de Langerhans, que exercem função imunológica; e as células de Merkel, que atuam na percepção sensorial (FOLDVARI, 2000; PROW et al., 2011).

1.1.2 Derme

A derme consiste em uma matriz de tecido conectivo, entremeada de proteínas fibrosas (colágeno tipo I e III, elastina e reticulina) que se encontram rodeadas por uma substância de fundo amorfa composta por mucopolissacarídeos (FOLDVARI, 2000). Ela também apresenta fibroblastos, macrófagos e leucócitos (CEVC e VIERL, 2010). Através dela atravessam nervos, vasos sanguíneos e linfáticos, e os apêndices da pele (glândulas sudoríparas, glândulas sebáceas e folículos pilosos). O suprimento sanguíneo deve ser eficiente para remover produtos de degradação, regular a temperatura, mobilizar células de defesa e transportar nutrientes não apenas nesta camada, mas também para epiderme, já que esta última não é vascularizada (MENON, 2002; AULTON, 2005; CEVC e VIERL, 2010; PROW et al., 2011).

1.1.3 Hipoderme

A hipoderme ou tecido subcutâneo é composto basicamente de células que armazenam gordura (adipócitos). Essa gordura subcutânea funciona como fonte de energia, amortecedor mecânico e barreira térmica (AULTON, 2005).

1.2 Liberação de fármacos na pele

A principal vantagem da administração tópica cutânea reside no fato que esta via contorna o meio hostil do estômago e o metabolismo pré-sistêmico intestinal e hepático, acarretando em uma maior aderência ao tratamento pelo paciente. Como desvantagem, a administração via tópica pode levar à ocorrência de irritação, dermatite de contato ou reação alérgica causada pelo fármaco e/ou veículo, além da dificuldade de fármacos em permear a camada córnea devido a sua complexa estrutura e a alta lipofilicidade (ASHARA et al., 2014; LIU et al., 2014).

A permeação de um fármaco pela pele ocorre predominantemente por difusão passiva através de três vias: a via transepidermal, a qual é subdividida entre as microvias intercelular (por entre as células, passando pelos lipídeos intercelulares) e transcelular (passando através das células e dos lipídeos intercelulares) (Figura 2), e a via transpedicular (através de folículos pilosos, glândulas sebáceas e sudoríparas) (BARRY, 2001; MAGHRABY et al., 2008). Visto que os apêndices da pele constituem apenas 0,1% da área superficial, estima-se que a principal via de permeação de fármacos é a via transepidermal (AULTON, 2005).

Figura 2. Representação da estrutura do estrato córneo (modelo "tijolo e argamassa"), e organização lamelar dos espaços intercelulares. As flechas indicam as vias transepidermais de penetração de fármacos através da pele: via intercelular e via transcelular.

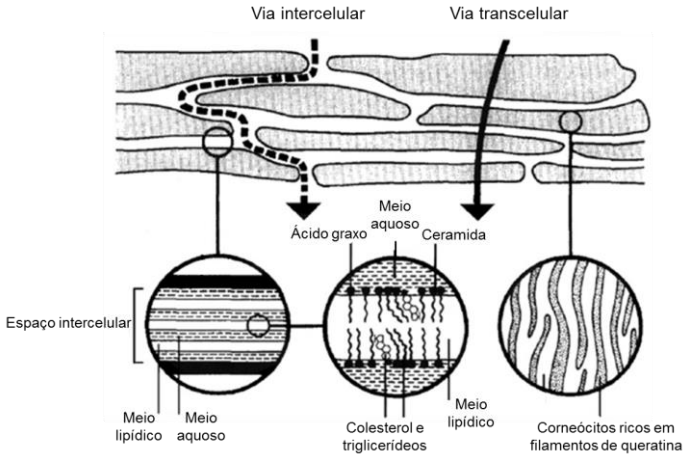

Fonte: adaptado de Maghraby; Barry; Williams (2008) e Barry (2001).

A absorção percutânea de fármacos através das diferentes camadas da pele pode ser descrita pela primeira lei de difusão de Fick.

$$J = \frac{dm}{dt} = \frac{D \times \Delta C \times k}{h} \qquad \text{Equação 1}$$

onde J é o fluxo por unidade de área no estado estacionário, m é a massa, t é o tempo, D é o coeficiente de difusão através da pele, ΔC é o

gradiente de concentração do fármaco entre o veículo e a pele, *k* é o coeficiente de partição e *h* é o comprimento da rota difusional do fármaco através da pele.

Segundo Hadgraft and Pugh (1998) em circunstâncias normais a concentração de fármaco aplicada na superfície da pele é muito maior que a permeada, assim a equação anterior pode ser simplificada para a seguinte equação:

$$J = K_p \times C_0 \qquad \text{Equação 2}$$

onde K_p é o coeficiente de permeabilidade (=kD/h) (cm.h^{-1}) e C_0 é a concentração de fármaco aplicada na pele. O coeficiente de permeabilidade pode ainda ser estimado pela equação empírica descrita por Potts e Guy (1992):

$$Log\ k_p\ (cm.h^{-1}) = -2{,}7 + 0{,}71 \log K_{oct} - 0{,}006\ \text{PM} \qquad \text{Equação 3}$$

onde K_{oct} é o coeficiente de partição octanol-água e *PM* é o peso molecular. Moléculas grandes tendem a se difundir lentamente pela pele, por isso o PM na equação.

O valor de fluxo pode ser obtido por meio da construção de um gráfico de massa difusante acumulada, *m*, que passa por unidade de área através da pele, em função do tempo (Figura 3). Nos tempos maiores, o gráfico aproxima-se de uma linha reta, correspondente ao estado estacionário. A inclinação da reta fornece o valor de fluxo (*J*) e a extrapolação da mesma até o eixo das abcissas fornece o tempo de latência (L, *m*=0) (MOSER et al., 2001; AULTON, 2005).

Figura 3. Gráfico representativo da quantidade cumulativa de difusante atravessando uma unidade de área de membrana em função do tempo.

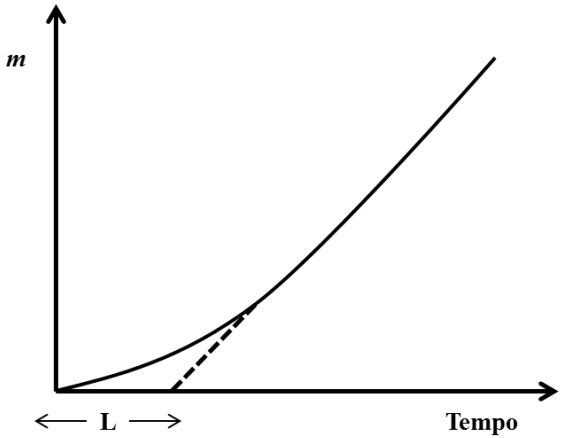

Fonte: adaptado de Aulton (2005).

Vários fatores influenciam o transporte de susbstâncias através da pele, incluindo fatores fisiológicos como a espessura da pele, a produção sebácea e o grau de hidratação. A hidratação do estrato córneo é um dos fatores mais importantes para aumentar a velocidade de penetração de fármacos, pois a água intumesce o tecido descompactando a camada córnea (AULTON, 2005). Esses fatores também podem estar relacionados a propriedades inerentes do fámaco como coeficiente de partição, coeficiente de difusão, solubilidade, peso molecular e grau de ionização (ASHARA et al., 2014; LIU et al., 2014). Fármacos que apresentem boa solubilidade tanto em óleo como na água tendem a permear melhor através da pele. Moléculas não ionizadas atravessam prontamente as membranas lipídicas, já as moléculas ionizadas penetram no estrato córneo até determinado nível. Entretanto, uma vez que apresentam solubilidade aquosa superior às espécies neutras, as moléculas ionizadas podem exercer uma contribuição significativa para o fluxo total quando presentes em solução saturada ou próxima da saturação, sendo que o fluxo máximo é obtido quando a concentração de fármaco aplicado na pele é igual à solubilidade (HADGRAFT, 2004; AULTON, 2005; BAROLI, 2010).

A liberação de fármacos na pele pode ocorrer em duas regiões diferentes e pode ser distinguida em liberação tópica e transdérmica.

Na liberação tópica, o fármaco é geralmente incorporado em uma forma farmacêutica semissólida e aplicado diretamente na pele para exercer sua função no tratamento de doenças dermatológicas. A ação é local, ocorrendo principalmente na epiderme.

Quando o fármaco é veiculado a uma forma farmacêutica e aplicado na pele, ele entra em contato com a principal barreira à permeação, o estrato córneo, juntamente com resíduos celulares, suor, sebo e microorganismos. O seu transporte através da pele ocorre normalmente por um processo de difusão passiva pelas vias transcelular, intercelular, folículo piloso, glândula sebácea e sudorípara (PROW et al., 2011; ASHARA et al., 2014).

A liberação transdérmica tem como alvo o alcance do fármaco na derme e passagem para a circulação sanguínea para obtenção de um efeito sistêmico. Tratam-se de formas farmacêuticas de liberação prolongada que reduzem o número de doses administradas e as flutuações da concentração plasmática, minimizando os efeitos indesejados do fármaco, além de ser de fácil acesso para os pacientes e indolor. Assim como na liberação tópica, o maior desafio é permear o estrato córneo e normalmente o transporte do fármaco ocorre por difusão passiva. Alguns tratamentos para dor crônica, reposição ou contracepção hormonal e doenças cardiovasculares são disponibilizados em formas farmacêuticas de liberação transdérmica (ex. adesivos, géis) (LIU et al., 2014).

1.3 Estudos de permeação cutânea

A verificação da permeação cutânea é uma das principais etapas no delineamento de novas formas farmacêuticas de liberação tópica ou transdérmica, pois permitem compreender os fatores que determinam o bom desempenho *in vivo*. Indubitavelmente, os dados mais confiáveis de absorção através da pele são obtidos de estudos em humanos, no entanto, esses estudos geralmente não são possíveis durante a fase inicial de desenvolvimento de um novo medicamento ou de novos candidatos a fármacos. Visto que é praticamente impossível realizar estudos de permeação cutânea somente em modelos *in vivo*, modelos *ex vivo* e *in vitro* têm sido freqüentemente empregados para avaliar os parâmetros cinéticos da permeação de fármacos através da pele (GODIN e TOUITOU, 2007). Os estudos de permeação cutânea proporcionam informações relevantes para avaliar o comportamento de sistemas de liberação de fármacos quanto ao aumento do perfil de penetração do

fármaco, rota de permeação, mecanismo de ação do sistema carreador e quantificação do fármaco nas camadas da pele (DEPIERI et al., 2015).

O modelo de células de difusão de Franz, conhecido também como modelo estático, representa uma opção de ampla aplicabilidade para estudos de permeação cutânea (FRANZ, 1975). As células de difusão são fabricadas em vidro e divididas em dois compartimentos, o doador e o receptor (Figura 4). Entre os dois compartimentos é colocada a pele com o estrato córneo voltado para o compartimento doador, enquanto que o tecido conectivo da derme para o receptor. Comumente utiliza-se a pele de orelha suína para realizar este estudo visto que se assemelha à pele humana quanto à composição lipídica e permeabilidade, todavia são empregadas também pele de rato e pele humana (SARTORELLI et al., 2000). No ensaio, a formulação é aplicada no compartimento doador e permanece diretamente em contato com o estrato córneo. No compartimento receptor é colocado um fluido receptor, o qual é mantido sob agitação constante e em aquecimento. Trata-se normalmente de uma solução na qual a substância teste é solúvel a fim de garantir a condição *sink*. As coletas do meio receptor são realizadas em tempos pré-determinados para quantificação da substância teste, sendo que posterior a cada coleta o fluido receptor é sempre reposto (DEPIERI et al., 2015).

Figura 4. Representação esquemática da célula de difusão de Franz.

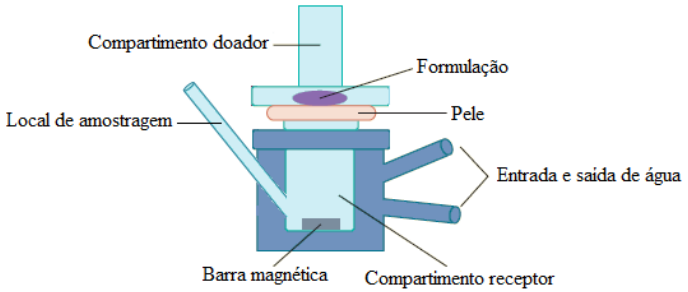

Fonte: adaptado de Depieri et al (2015).

Uma técnica complementar para a quantificação de substâncias na pele empregada de forma isolada ou posterior ao ensaio de permeação cutânea é o *tape stripping*. A técnica do *tape stripping* consiste basicamente da retirada do estrato córneo (corneócitos) por

meio de fitas adesivas aplicadas na pele (Figura 5). É uma técnica simples, de fácil execução e minimamente invasiva que possibilita determinar a localização e a distribuição de substâncias no estrato córneo como também quantificá-las através de técnicas de doseamento (ESCOBAR-CHÁVEZ et al., 2008). O *tape stripping* também é empregado em estudos de biodisponibilidade tópica e de bioequivalência, os fármacos de uso tópico se distribuem inicialmente pelo estrato córneo e a partir dele, atingem a epiderme viável e a derme. Geralmente, a concentração do fármaco presente no estrato córneo está diretamente relacionada com a concentração que se difunde para as demais camadas (SHAH et al., 1998; ESCOBAR-CHÁVEZ et al., 2008).

Figura 5. Representação esquemática da separação do estrato córneo pela técnica do *tape stripping*.

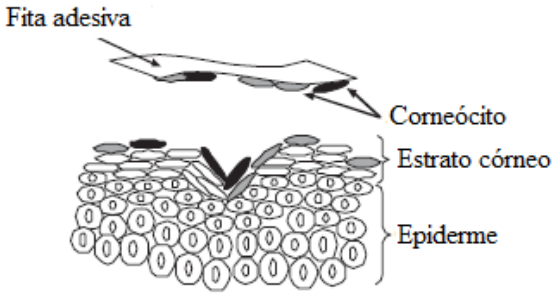

Fonte: adaptado de Pailler-Mattei et al (2011).

Apesar de amplamente utilizada, certos parâmetros são limitantes na retirada do estrato córneo como a variabilidade individual, a localização anatômica da pele, a hidratação da pele, a presença de sulcos na pele, o tipo de fita adesiva, a pressão exercida sobre a fita na pele, a duração desta pressão e o processo de remoção da fita (BASHIR et al., 2001; LADEMANN et al., 2009). O número de fitas adesivas aplicadas na pele pode variar de 10 a 15 fitas e sabe-se que este número não é proporcional à espessura do estrato córneo, porém assume-se que é suficiente para a remoção total do mesmo (DEPIERI et al., 2015).

Para a quantificação de fármacos na epiderme e derme, técnicas de separação destas camadas são amplamente descritas, como a raspagem mecânica com auxílio de bisturi, o aquecimento e a digestão enzimática. A homogeneização do tecido total (epiderme+derme) em

solvente apropriado também é outra técnica utilizada (BADEN e GIFFORD, 1970; FORT e MITRA, 1994; MAHARLOOEI et al., 2011; DEPIERI et al., 2015).

1.4 Estratégias para melhorar a permeação de fármacos na pele

Embora o tratamento tópico apresente vantagens irrefutáveis, a adequada permeação cutânea de compostos ativos para produzir uma resposta terapêutica ainda é um grande desafio no desenvolvimento de novos medicamentos e cosméticos. O estrato córneo, constituído por uma estrutura lipídica altamente ordenada, age como principal barreira protetora, tanto para evitar a perda excessiva de água quanto para proteger contra agentes externos danosos. Neste sentido, inúmeras substâncias ativas quando veiculadas em formas farmacêuticas convencionais apresentam grande dificuldade de permear até camadas mais profundas da pele, e quando permeiam somente quantidades subterapêuticas são detectadas, fazendo-se necessário o emprego de estratégias que aumentem a permeação cutânea das mesmas (SCHÄFER-KORTING et al., 2007).

Diferentes estratégias para contornar as limitações impostas pela baixa permeação de fármacos são relatadas na literatura. Promotores de absorção são compostos conhecidos por desordenar ou modificar a fluidez da estrutura lipídica do estrato córneo, afetar os desmossomos, que mantêm a coesão entre os corneócitos, ou ainda por interagir com a queratina (VAN HAL et al., 1996; WILLIAMS e BARRY, 2012). Idealmente, os promotores de permeação devem ser farmacologicamente inertes, atóxicos, não irritantes, não alérgicos, de ação imediata e reversível e ser compatível com os demais componentes do sistema (LANE, 2013).

Em condições oclusivas, a água age como um promotor primário, especialmente tratando-se de fármacos hidrofílicos, devido à hidratação das regiões polares das bicamadas lipídicas e consequente desestruturação lipídica (VAN HAL et al., 1996; BOLZINGER et al., 2012; WILLIAMS e BARRY, 2012). Outros exemplos de promotores de absorção são os ésteres, álcoois, sulfóxidos, pirrolidonas, ácidos graxos, surfactantes (catiônico, aniônico e não iônico), terpenos, amidas (uréia), azona, glicóis entre outros (BARRY, 2001; BENSON, 2005; WILLIAMS e BARRY, 2012; LANE, 2013). Muitos desses promotores provocam irritações na pele causadas pela solubilização dos lipídeos do estrato córneo em micelas. Este evento leva a perda da propriedade de

barreira do estrato córneo afetando o transporte de substâncias hidrofílicas e levando ao ressecamento da pele (BOLZINGER et al., 2012).

Além dos promotores químicos citados anteriormente, há também métodos físicos para promover a permeação, dentre os quais destacam-se: (*i*) a iontoforese, uma técnica não invasiva baseada na aplicação de uma corrente elétrica de baixa intensidade para facilitar a permeação de fármacos carregados; (*ii*) a eletroporação, que envolve a criação de poros aquosos na bicamada lipídica por meio da aplicação de pulsos elétricos curtos; (*iii*) a fonoforese, que consiste na utilização do ultrassom de alta frequência que provoca uma perturbação do empacotemento lipídico nos espaços intercelulares do estrato córneo por meio de efeitos de cavitação e aquecimento; (*iv*) a microdermoabrasão, que promove a permeação por remover o estrato córneo através do jateamento de micropartículas abrasivas, quimicamente inertes, sobre a superfície cutânea durante a aplicação tópica; (*v*) e o arranjo de microagulhas, que consiste em um dispositivo com centenas de microagulhas revestidas ou preenchidas com o fármaco que, quando aplicadas sobre a pele, penetram no estrato córneo sem rompê-lo e sem estimular a enervação nas camadas mais profundas (HENRY et al., 1998; BARRY, 2001; AULTON, 2005; SARAF et al., 2011; ALEXANDER et al., 2012).

A administração cutânea de pró-fármacos e a formação de pares iônicos são outras estratégias descritas na literatura com o intuito de melhorar a permeação cutânea de fármacos (BENSON, 2005). Na primeira, faz-se uso de um pró-fármaco de coeficiente de partição maior, que ao atingir a epiderme viável, é hidrolisado pelas esterases, liberando o fármaco na forma ativa (SLOAN e WASDO, 2003). Na segunda, devido ao fato de moléculas carregadas não permearem prontamente através da pele, a formação de um par iônico, por meio da adição de um contra íon, neutraliza a carga e facilita a passagem do complexo formado através do estrato córneo. Ao atingir a epiderme viável, que é mais hidrofílica, o par iônico se dissocia liberando o fármaco carregado (MEGWA et al., 2000; VALENTA et al., 2000).

A aplicação de sistemas nanoestruturados em produtos farmacêuticos e cosméticos tem sido extensivamente pesquisada. Trata-se de sistemas caracterizados por apresentar tamanho dentro da escala nanométrica e possuir uma grande área superficial, o que confere certas vantagens para a aplicação tópica como a melhora na permeação cutânea de fármacos, a vetorização dos mesmos nas diversas camadas da pele, a

incorporação de concentrações maiores de fármacos nas formas farmacêuticas com provável aumento da liberação nos tecidos, e a possibilidade de obtenção de perfis de liberação sustentados (SCHÄFER-KORTING et al., 2007; GOLUBOVIC-LIAKOPOULOS et al., 2011).

2 ESTRESSE OXIDATIVO E FOTOPROTEÇÃO

A radiação solar é essencial para a vida na Terra e seus efeitos sobre o corpo humano dependem das características individuais da pele exposta, intensidade, frequência e tempo de exposição. A radiação solar ultravioleta (UV) pode ser dividida em três faixas, considerando sua propagação: UVC (100-290 nm) que normalmente não chega à superfície da Terra por ser filtrada pela camada de ozônio; UVB (290-320 nm) que atua principalmente na epiderme basal e é responsável pelos danos imediatos da radiação solar (eritema, edema, queimadura), e danos ao ácido desoxirribonucleico (DNA), levando ao estresse oxidativo e ao envelhecimento precoce; e UVA (320-400 nm) que atua na epiderme e derme, agindo como agente mutagênico e carcinogênico, estando também relacionada com o fotoenvelhecimento (RÜNGER, 1999; DE GRUIJL, 2000; NICHOLS e KATIYAR, 2010).

2.1 Estresse oxidativo

Mais que qualquer outro tecido, a pele é exposta a inúmeros agentes químicos, físicos e microbiológicos, muitos dos quais induzem à formação de radicais livres, os quais são átomos apresentando um ou mais elétrons desemparelhados. Esses radicais livres podem ser espécies reativas de oxigênio (EROS) ou de nitrogênio (ERN) (ex. óxido nítrico). Dentre as EROS formadas na pele, destacam-se os radicais hidroxila ($HO^{\bullet}$) e superóxido ($O_2^{\bullet -}$), peroxila e alcoxila ($RO_2^{\bullet}$ e $RO^{\bullet}$) e peróxido de hidrogênio (H_2O_2). Estas espécies são fundamentais em diversos processos fisiológicos e bioquímicos, mantendo a homeostase celular, sendo que há um equilíbrio refinado entre sua formação e remoção. Quando ocorrem alterações neste equilíbrio, um estado pró-oxidante é gerado, levando assim ao chamado estresse oxidativo (ARUOMA, 1998; GUARATINI et al., 2007).

O sistema antioxidante cutâneo é formado por substâncias enzimáticas e não-enzimáticas. Dentre as substâncias enzimáticas tem-se a glutationa peroxidase (GPx), a catalase (CAT) e a superóxido

dismutase (SOD). A SOD converte $O_2^{\bullet -}$ em H_2O_2, podendo estar presente no citosol, em organelas celulares específicas ou extracelularmente. Já a CAT e GPx são as principais responsáveis pela remoção imediata do H_2O_2. A CAT, encontrada principalmente nos peroxissomos, catalisa especificamente a decomposição do H_2O_2, gerando moléculas de água e oxigênio. A GPx catalisa reações de doação de elétrons, no qual utiliza da glutationa reduzida (GSH) como agente redutor, formando a glutationa oxidada (FRIDOVICH, 1998; ROVER JÚNIOR et al., 2001). Entre os antioxidantes não-enzimáticos ou de baixo peso molecular, destacam-se a GSH, vitamina E (α-tocoferol), o estradiol, a melatonina, ácido lipóico e a melanina (KAY et al., 1986; REITER e MAESTRONI, 1999; SERGEEV et al., 1999).

As radiações UVA e UVB são responsáveis pela redução de sistemas antioxidantes cutâneos e aumento dos sistemas oxidantes, alterando assim a homeostasia cutânea. A primeira resposta observada após a exposição ao sol é a inflamação, caracterizada por eritema, edema e calor, seguido do recrutamento e estimulação de células de defesa que geram uma série de espécies reativas (JURKIEWICZ e BUETTNERF, 1996; THIELE et al., 1998; GUARATINI et al., 2007). Dentre os principais alvos das espécies reativas geradas estão os lipídeos, proteínas e DNA.

Nos lipídeos, as EROS causam a peroxidação lipídica pela retirada de um átomo de hidrogênio de um ácido graxo insaturado pelo radical $HO^{\bullet}$. Após isto, há a formação de radicais $RO_2^{\bullet}$ na presença de oxigênio molecular e se não forem contidos, esses eventos podem originar uma reação em cadeia resultando na desintegração da membrana celular lipídica. Nas proteínas, os aminoácidos aromáticos, como o triptofano, tirosina e fenilalanina, por apresentarem grupamentos cromóforos, possuem a capacidade de absorver a radiação UV. Esses aminoácidos, também presentes na queratina da camada córnea da pele, absorvem uma parte da radiação UV, antes desta atingir as células viáveis. Entretanto ao atingirem, a oxidação das proteínas acarreta em uma modificação da cadeia polipeptídica formando derivados carbonilados (GUTTERIDGE, 1995; SANDER et al., 2002; PATTISON e DAVIES, 2006).

Os danos genéticos provocados pela radiação UV envolvem não somente a absorção de energia direta pelo DNA, como também a formação de radical hidroxila, que reage com esta biomolécula, podendo acarretar mutações (PELLE et al., 2003; GUARATINI et al., 2007). As bases do DNA são capazes de absorver diretamente os fótons

provenientes da radiação UVC e UVB, e quando este evento ocorre, pirimidinas adjacentes podem se ligar covalentemente gerando, principalmente, dímeros de pirimidina ciclobutano (CPDs) e fotoprodutos pirimidina (6-4) pirimidona, modificações estas capazes de causar uma distorção na dupla hélice do DNA. Estas modificações também são consideradas como o "gatilho" molecular responsável pela indução da imunossupressão e iniciação da fotocarcinogênese. A absorção de fótons no comprimento de onda da radiação UVA é muito baixa, mas alterações no DNA podem ser causadas de forma indireta via geração de EROS (RAVANAT et al., 2001; YOU et al., 2001).

Os danos causados no DNA, se não reparados, podem levar a sérias consequências celulares. O reparo por excisão de nucleotídeos (NER) é um dos mais importantes mecanismos de reparo de danos ao DNA causados por agentes externos, como a radiação solar. O processo do NER envolve cinco passos sucessivos: *i*) reconhecimento do dano; *ii*) abertura da dupla hélice do DNA onde está localizado o dano; *iii*) dupla incisão nas extremidades deste dano; *iv*) síntese do novo DNA utilizando como molde a fita não danificada; *v*) ligação da porção nova da fita sintetizada à sequencia original (DE BOER e HOEIJMAKERS, 2000).

2.2 Fotoproteção

A fotoproteção refere-se às medidas preventivas contra os danos causados pela exposição ao sol como é o caso de melanomas, carcinomas e fotoenvelhecimento. A utilização de fotoprotetores de uso tópico é a principal abordagem cosmética contra os efeitos nocivos causados pela radiação UV. Os fotoprotetores almejados devem proteger a pele contra as radiações UVB e UVA, atuar sobre os radicais livres, prevenir e/ou estimular a reparação do DNA. Além disso, devem ser estáveis e seguros para o uso humano. Os protetores solares contem filtros que são moléculas ou complexos moleculares que podem absorver, refletir ou dispersar a radiação UV. Existem duas classes de filtros solares: os inorgânicos e os orgânicos, conhecidos também como filtros físicos e químicos, respectivamente (FLOR et al., 2007; GONZÁLEZ et al., 2008).

Os filtros inorgânicos, também conhecidos como bloqueadores, são partículas derivadas de metais, ou óxidos metálicos, que atuam através de mecanismos ópticos, refletindo ou dispersando os raios solares por meio de uma barreira opaca formada pelo filme de partículas

sobre a pele. Os principais filtros físicos empregados são o óxido de zinco e dióxido de titânio, e quando incorporados às formulações ficam suspensos no veículo (GILABERTE e GONZÁLEZ, 2010).

Os filtros orgânicos ou químicos são moléculas que absorvem a radiação ultravioleta (cromóforo exógeno), impedindo que ela danifique as células da pele. São moléculas compostas por anéis aromáticos com grupamentos carboxílicos e grupamentos doadores de elétrons, como a amina ou um grupo metoxila, na posição orto ou para. Ao absorver a radiação UV, os elétrons situados no orbital π HOMO (orbital molecular preenchido de mais alta energia) são excitados para orbital π^* LUMO (orbital molecular vazio de baixa energia), ao retornarem para o estado inicial, liberam energia na forma de calor. Quanto menor a diferença de energia entre os orbitais, maior será o comprimento de onda de absorção (FLOR et al., 2007). Dependendo da faixa de absorção que cada molécula atue, ela será considerada um filtro solar de amplo espectro (atua em ambos os tipos de radiações UVA e UVB) ou exclusivamente UVA ou UVB.

Em relação aos filtros inorgânicos, os filtros orgânicos possuem uma menor estabilidade fotoquímica, podem ser fotoirritantes e promover reações alérgicas (GILABERTE e GONZÁLEZ, 2010). Alguns exemplos de filtros orgânicos utilizados em protetores solares são as benzofenonas, os cinamatos, o butil-metoxi-dibenzoil-metano e o ácido p-aminobenzóico (PABA).

O fator de proteção solar pode ser determinado por meio de ensaios *in vivo*, calculando-se a razão numérica entre a Dose Eritematosa Mínima (DEM) da pele protegida pelo fotoprotetor, aplicado na quantidade de 2 mg/cm^2, e a DEM da pele não protegida (MANSUR et al., 1986). Entretanto, métodos espectrofotométricos podem auxiliar na determinação do FPS. Os resultados *in vivo* e *in vitro* apresentam boa correlação para os protetores com filtros orgânicos (SAYRE et al., 1979; MANSUR et al., 1986), além de ser desejável uma previsão do FPS antes da condução dos testes em humanos, reduzindo assim os riscos de queimadura nos voluntários submetidos aos ensaios *in vivo*.

Métodos *in vitro* empregando linhagens celulares como queratinócitos e fibroblastos, na avaliação do potencial fotoprotetor de substâncias e/ou produtos, são descritos na literatura. A implementação e validação destes métodos *in vitro* vem sendo de grande importância principalmente após a proibição da comercialização de produtos cosméticos (ex. fotoprotetores) cuja formulação tenha sido objeto de

ensaios em animais (UE nº1223, 2009). No Brasil, conforme a normativa nº 17 de 2014 publicada pelo Conselho Nacional de Controle de Experimentação Animal (CONCEA), após a validação do método alternativo pelo CONCEA, as empresas devem substituir o método original *in vivo* pelo método alternativo *in vitro* dentro de um prazo de 5 anos (CONCEA, 2014).

2.3 Antioxidantes

A aplicação tópica de antioxidantes representa uma estratégia interessante na proteção cutânea contra o estresse oxidativo ocasionado por diferentes agentes (GUARATINI et al., 2007). Substâncias antioxidantes como o ácido ascórbico (vitamina C) e a vitamina E são frequentemente encontrados em formulações fotoprotetoras de uso tópico e muitas vezes associados entre si. A vitamina E, além de estabilizar as bicamadas lipídicas no estrato córneo, é um dos mais importantes inibidores da peroxidação lipídica (KAGAN et al., 1990). Há também os carotenoides, como o betacaroteno e retinol (vitamina A), que são compostos lipofílicos encontrados no tecido adiposo, lipoproteínas e membranas celulares. São isoprenóides geralmente constituídos por oito unidades de isopreno, formando uma longa cadeia poliênica contendo de 2 a 15 duplas ligações conjugadas na molécula, as quais estão relacionadas à eficácia da ação antioxidante pelo livre deslocamento de elétrons (FRASER e BRAMLEY, 2004; CERQUEIRA et al., 2007).

Devido à alta ação antioxidante, outra classe química de compostos que têm ganhado cada vez mais atenção da indústria farmacêutica e cosmética, são os compostos polifenólicos. O uso destes compostos na proteção solar será relatado a seguir.

2.3.1 Polifenóis

Os polifenóis são metabólitos secundários de plantas caracterizados quimicamente por apresentarem um anel aromático contendo ao menos um grupamento hidroxila. Os grupamentos hidroxilas também podem estar metilados, sulfonados e glicosilados por açúcares. Os polifenóis glicolisados apresentam melhor solubilidade aquosa que a forma aglicona, porém devido ao alto peso molecular e baixa lipofilicidade, exibem baixa a biodisponibilidade e permeabilidade cutânea (GROOT e RAUEN, 1998; FANG et al., 2006; RATZ-ŁYKO et

al., 2015). Nessa classe de compostos químicos encontram-se os ácidos fenólicos, flavonoides, quinonas, cumarinas, lignanas, estilbenos e taninos (HARBORNE, 1989; BRAVO, 1998). Algumas estruturas químicas dos compostos polifenólicos são apresentadas na figura 6.

Figura 6. Estruturas químicas básicas dos principais polifenóis encontrados nas plantas (a) flavonoides, (b) ácidos fenólicos, (c) cumarinas, (d) lignanas e (e) estilbenos.

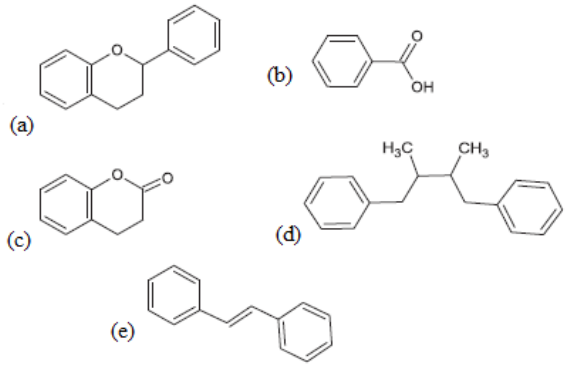

Fonte: adaptado de Razt-Lyko et al (2015).

A capacidade antioxidante dos polifenóis é atribuída principalmente ao poder redutor do grupo hidroxila aromático, que reduz os radicais livres reativos compensando o desemparelhamento de elétrons, e gerando o radical correspondente estabilizado por ressonância. Essa capacidade é influenciada pelo número e posição das hidroxilas, assim como pelas posições da glicosilação. Ao contrário das vitaminas C e E, que agem em meio aquoso e na membrana fosfolipídica, respectivamente, os polifenóis podem se localizar nos dois sítios (CERQUEIRA et al., 2007; RATZ-ŁYKO et al., 2015). Outra característica dos polifenóis é a habilidade em complexar íons metálicos como ferro, cobre, zinco e manganês. Essa habilidade é benéfica no sentido de limitar a atividade de enzimas envolvidas na remodelagem do tecido conectivo e inibir o processo inflamatório (AN et al., 2005; ARCT e PYTKOWSKA, 2008; THRING et al., 2009).

Polifenóis isolados ou presentes em extratos vegetais são candidatos promissores para minimizar os efeitos da radiação ultravioleta na pele. Os mecanismos pelos quais estes compostos reduzem os efeitos deletérios da radiação solar incluem: *i*) absorção

direta da radiação ultravioleta (agentes cromóforos); *ii*) inibição da inflamação pela inibição de enzimas e citocinas pró-inflamatórias; *iii*) modulação da imunosupressão; *iv*) indução de apoptose; *v*) ação antioxidante direta, por meio do sequestro de EROS e ERN e indireta por meio da indução de respostas citoprotetoras intrínsecas; *vi*) reparação do DNA (ALMEIDA et al., 2008; DINKOVA-KOSTOVA, 2008; NICHOLS e KATIYAR, 2010; AFAQ, 2011; AFAQ e KATIYAR, 2011; PASTORE et al., 2012; ALMEIDA et al., 2015; RATZ-ŁYKO et al., 2015).

3 ROMÃ

A *Punica granatum L* (Punicaceae) (Figura 7), é uma planta nativa do Himalaia, Afeganistão, Irã, Índia, China e a partir do oeste do Irã seu cultivo se expandiu pelo Mediterrâneo (MORTON, 1987). O seu plantio também é realizado em outros países, como Estados Unidos, Argentina, Austrália, Chile e Brasil, em regiões subtropicais, tropicais, em condições climáticas variáveis, evidenciando flexibilidade e adaptabilidade do plantio (TEIXEIRA DA SILVA et al., 2013). A romã, seu fruto, é consumida mundialmente, sendo considerada por religiosos um fruto sagrado, um símbolo da prosperidade e ambição.

No Brasil, algumas variedades de romã estão sendo cultivadas nos estados de São Paulo, Bahia e Pernambuco, sendo os principais fornecedores do fruto para diferentes regiões do país. Pesquisas realizadas têm demonstrado que existe a possibilidade de cultivo de espécies de climas tropical úmido, subtropical e temperada, com potencial econômico para as áreas irrigadas do semiárido brasileiro. Assim, o plantio da romãzeira está sendo avaliada, desde 2010, com o objetivo de encontrar uma nova opção de cultivo para os produtores da região. Estão em avaliação as cultivares "Wonderful" e "Bagawa", importadas dos Estados Unidos e de Israel, no campo experimental da Embrapa Semiárido em Petrolina – Pernambuco (OLIVEIRA et al., 2012).

A romãzeira pode chegar a 3-5 metros de altura. Suas folhas são brilhantes e apresentam forma de lança. Conforme a árvore cresce e atinge idade adulta, os galhos apresentam coloração cinza; as flores são grandes e apresentam coloração vermelha, branca ou uma mescla de ambas, e possuem um cálice tubular que eventualmente gera o fruto. A romã possui sementes que se encontram separadas por um pericarpo branco membranoso e cada uma delas é envolvida pela polpa vermelha

que origina o suco do fruto (LAWRENCE, 1951; DAHLGREN e THORNE, 1984). Variações na coloração e tamanho do fruto, porte da árvore e ciclo de poda podem ser afetados por mutações e agroecossistemas (SARKHOSH et al., 2006; BEDAF et al., 2011).

Figura 7. *Punica granatum* Linn. I- Galhos com flores; II- Cálice tubular; III- Fruto seccionado ao meio; IV- Semente envolvida pela polpa; V-Fruto inteiro.

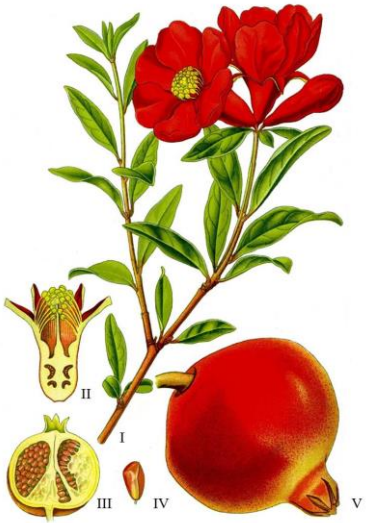

3.1 Composição química

As cascas correspondem até 50% do peso do fruto e são caracterizadas por uma rede de membranas internas. Elas são ricas em compostos polifenólicos, incluindo flavonoides (antocianinas, catequinas), mas predominantemente os ácidos hidroxibenzóicos gálico e elágico, e elagitaninos como a punicalina, punicalagina e peduncalagina (Figura 8) (BEN NASR et al., 1996; FISCHER et al., 2011). As punicalaginas são encontradas na forma dos isômeros anoméricos, alfa e beta (LU et al., 2008). Esses compostos são taninos hidrolizáveis e complexos, de alto peso molecular (>1000 g/mol), derivados do ácido elágico, e geralmente são compostos lábeis quando em solução ou expostos ao meio externo (CLIFFORD e SCALBERT, 2000). Na hidrólise ácida ou básica dos elagitaninos, as ligações ésteres

são hidrolisadas e o ácido hexahidroxidifênico liberado sofre espontânea lactonização rendendo ácido elágico (QUIDEAU e FELDMAN, 1996). O ácido elágico e o ácido gálico são compostos polifenólicos de baixo peso molecular, 302,20 g/mol e 170,12 g/mol, respectivamente, sendo que o ácido gálico é hidrossolúvel e o ácido elágico apresenta baixa solubilidade aquosa e em vários solventes orgânicos (BALA, BHARDWAJ, HARIHARAN e RAVI KUMAR, 2006).

Alguns dos compostos citados anteriormente podem também ser encontrados no suco e em outras partes da romãzeira (LANSKY e NEWMAN, 2007), como nas folhas (ERCISLI et al., 2007; LAN et al., 2009), nas flores (AVIRAM et al., 2008) e caule (NEUHOFER et al., 1993). Contudo, eles se encontram muito mais concentrados nas cascas e são responsáveis por 90% da atividade antioxidante atribuída a planta (AFAQ et al., 2005a; VIUDA-MARTOS et al., 2010; ISMAIL et al., 2012; TEIXEIRA DA SILVA et al., 2013). Já as sementes são ricas em óleo, o qual é constituído de uma mistura de ácidos graxos como o ácido oleico, esteárico, linoleico e o componente majoritário (65-80%), ácido punícico (9-trans,11-cis,13-trans, ácido octadecatrienóico) (Figura 8) (SCHUBERT et al., 1999; GOULA e ADAMOPOULOS, 2012). Evidentemente, tanto a composição química de cada parte do fruto quanto a concentração de cada composto difere conforme a região do plantio, clima, maturidade, manejo do plantio, condições de estocagem entre outros (VIUDA-MARTOS et al., 2010).

Figura 8. Estruturas dos principais compostos polifenólicos presentes nas cascas de *P. granatum* – (1) Ácido Gálico; (2) Ácido Elágico; (3) Punicalagina. (4) Principal composto encontrado no óleo da semente de *P. granatum*: Ácido punícico.

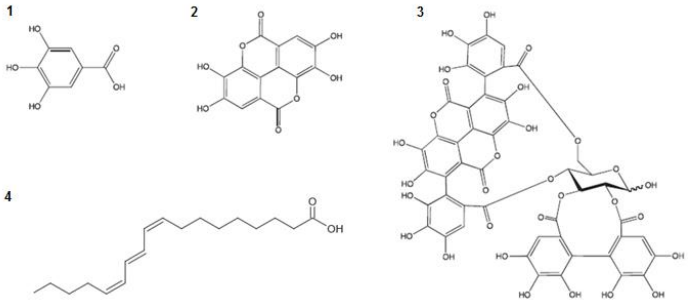

Fonte: adaptado de Qu et al. (2012) e Melo; Carvalho; Mancini-Filho (2014).

3.2 Propriedades biológicas

Na medicina popular as cascas são normalmente utilizadas no tratamento da inflamação, diarreia, úlcera (LANSKY et al., 2000) e como antiparasitário (NAQVI et al., 1991). Estudos científicos apontam várias aplicações e atividades biológicas relacionadas à romã que geralmente são atribuídas à presença de punicalaginas, ao ácido elágico e ácido gálico. Algumas das atividades relatadas incluem: melhoria da atividade cardiovascular e do perfil lipidêmico (AVIRAM et al., 2000; ESMAILLZADEH et al., 2006; LARROSA et al., 2010); anti-inflamatória (LEE et al., 2010; NEYRINCK et al., 2013), antitumoral (AFAQ et al., 2005a; MALIK et al., 2005; SEERAM et al., 2005; SYED et al., 2007; FJAERAA e NÅNBERG, 2009; GEORGE et al., 2011), hipoglicemiante (KATZ et al., 2007; BANIHANI et al., 2013); cicatrizante (CHIDAMBARA MURTHY et al., 2004; HAYOUNI et al., 2011); antimicrobiana (BRAGA et al., 2005; NAZ et al., 2007) e antioxidante (GIL et al., 2000; SINGH et al., 2002; NEGI e JAYAPRAKASHA, 2003; NEGI et al., 2003; LI et al., 2006; ÇAM et al., 2009; MANASATHIEN et al., 2012). A capacidade antioxidante dos compostos presentes no suco e extratos da romã está diretamente correlacionada com o grau de hidroxilação que os mesmos apresentam (GIL et al., 2000; LANDETE, 2011).

Além das propriedades biológicas citadas anteriormente, vários trabalhos científicos relatam a potencial ação fotoprotetora dos extratos da romã. Zaid e colaboradores (2007) observaram que o pré-tratamento de queratinócitos humanos com o extrato da romã reduziu os efeitos do estresse oxidativo provocados pela radiação UVB e também inibiu o aumento os marcadores de fotoenvelhecimento, como as metaloproteinases de matriz envolvidas na degradação de tecido cutâneo conectivo e colágeno (ASLAM et al., 2006). Manasathien e colaboradores (2011) relataram que o pré-tratamento tópico do dorso de ratas com o extrato etanólico das cascas da romã reduziu o eritema, o espessamento epidérmico e a fragmentação do DNA causados pela radiação UVB. Similarmente, outros autores demonstraram que o pré-tratamento de queratinócitos, fibroblastos e pele humana reconstituída com extrato da romã preveniu contra danos celulares provocados pela radiação UVA e UVB (SYED et al., 2006; PACHECO-PALENCIA et al., 2008; AFAQ et al., 2009).

Atividades biológicas também foram atribuídas ao óleo da semente de romã, como agente promotor de regeneração da epiderme

(ASLAM et al., 2006), quimiopreventivo (HORA et al., 2003), neuroprotetora (MIZRAHI et al., 2014) e antioxidante (SCHUBERT et al., 1999).

Apesar da potencial utilização de extratos da romã, principalmente das cascas, em produtos cosméticos e farmacêuticos, sua aplicação é limitada devido às propriedades biofarmacêuticas desfavoráveis de alguns compostos químicos presentes nos mesmos, como baixa solubilidade aquosa, baixa permeabilidade e instabilidade. Com o intuito de contornar essas limitações, a encapsulação destes compostos tem sido proposta. A Tabela 1 resume alguns dos benefícios relatados na encapsulação dos constituintes ativos presentes na romã.

Tabela 1. Resumo dos efeitos benéficos alcançados pela aplicação de sistemas nanoestruturados contendo compostos presentes na romã.

Sistema nanoestruturado	Composto	Via de administração pretendida	Benefícios relatados	Referências
Nanopartículas poliméricas	Ácido elágico	Oral	Melhora da permeabilidade intestinal quando comparado ao composto livre em solução.	(BALA, BHARDWAJ, HARIHARAN, KHARADE, et al., 2006).
Nanopartículas poliméricas	Ácido elágico	Oral	Maior inibição do crescimento celular de linhagem celulares humana de carcinoma oral (KB).	(ARULMOZHI et al., 2013).
Nanopartículas poliméricas	Ácido elágico, punicalagina ou extrato da romã	Oral	Maior inibição do crescimento celular de células tumorais humanas de adenocarcinoma mamário (MCF-7 e Hs578T) quando comparado aos	(SHIRODE et al., 2015).

			compostos livres em solução.	
Sistema auto-nanoemulsionante	Ácido elágico	Oral	Melhora da biodisponibilidade oral e permeabilidade quando comparado ao composto em suspensão.	(AVACHAT e PATEL, 2015).
Niossomas	Ácido elágico	Tópica	Niossomas contendo o ácido elágico liberaram o composto na epiderme e derme, já o composto livre em solução, ficou retido na camada mais externa da pele.	(JUNYAPRASERT et al., 2013).
Niossomas	Ácido gálico	Tópica	Melhora da permeação do composto presente na fração semipurificada de	(MANOSROI et al., 2011).

Niossomas	Ácido gálico	Tópica	*Terminalia chebula*. Melhora da liberação transdérmica do ácido gálico a partir dos niossomas quando comparado ao composto livre ou ao creme contendo extrato de chá preto.	(YEH et al., 2013).

4 NANOEMULSÕES

Nanoemulsões são sistemas heterogêneos, cineticamente estáveis, constituídas de uma dispersão uniforme de gotículas de um líquido em outro na qual ele é imiscível e, estabilizadas por um ou mais surfactantes. O tamanho da gotícula normalmente varia de 100 a 500 nm e o sistema pode ser classificado como óleo em água (O/A) ou água em óleo (A/O), dependendo da natureza das fases interna e externa (Figura 9) (TADROS et al., 2004; USÓN et al., 2004).

Figura 9: Estrutura das nanoemulsões do tipo A/O e O/A.

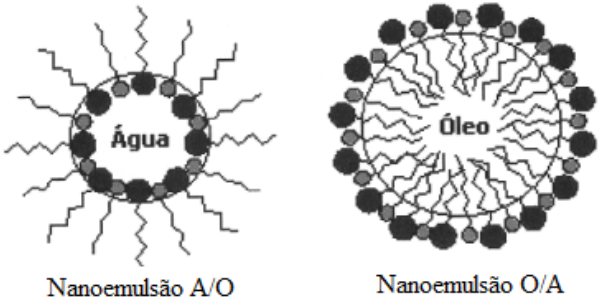

Fonte: adaptado de Schulman; McRoberts (1946).

4.1 Preparação e caracterização

As nanoemulsões apresentam-se como preparações de baixa viscosidade e comportamento Newtoniano, onde substâncias ativas de reduzida solubilidade aquosa podem ser incorporadas, sendo encontradas preferencialmente solubilizadas na fase oleosa e/ou adsorvidas na interface da gota (SONNEVILLE-AUBRUN et al., 2004). Na fase oleosa são geralmente utilizados óleos que apresentam ácidos graxos saturados, insaturados e ésteres de ácidos graxos em sua composição. Os surfactantes apresentam como função reduzir a tensão superficial entre água e óleo, e neste caso, o tipo e a concentração do surfactante utilizado devem ser cuidadosamente selecionados já que os mesmos estão relacionados com a estabilidade e toxicidade da nanoemulsão. Tensoativos não iônicos ou anfotéricos, ou ainda suas combinações são empregados com frequência para controlar o tamanho da gota e melhorar a estabilidade do sistema (CHEN et al., 2011). Os

tensoativos não iônicos também são mais seguros quando comparados com os tensoativos iônicos (CHIME et al., 2014).

As lecitinas são misturas complexas de fosfolipídeos extraídos da gema de ovo ou da soja, cujo componente majoritário é a fosfatidilcolina. São moléculas anfifílicas que adsorvem em interfaces óleo/água com a porção apolar direcionada para a fase oleosa e a porção polar para a fase aquosa, resultando em uma diminuição da tensão superficial de sistemas nanoemulsionados (XU et al., 2011). Lecitinas são amplamente utilizadas na área farmacêutica e cosmética por serem atóxicas e biocompatíveis. Geralmente conferem um alto valor de potencial zeta negativo, capazes de prevenir a coalescência das gotículas, sendo consideradas assim agentes estabilizadores (SCHMID e KORTING, 1993). Zhou e colaboradores (2010) relataram que nanoemulsões contendo lecitina melhoraram a permeação cutânea de uma substância lipofílica, o vermelho de nilo, quando comparadas com uma macroemulsão por reduzir o efeito barreira do estrato córneo através de mudanças na conformação dos lipídeos intercelulares, além da melhora na hidratação cutânea.

As nanoemulsões podem ser obtidas usando métodos de emulsificação de baixa e alta energia. Dentre os métodos de emulsificação de alta energia, os mais citados na literatura são a homogeneização ultrasônica, a homogeneização por alta pressão e a microfluidização. A emulsificação pela homogeneização ultrasônica ocorre por dois mecanismos. Primeiro, o uso de um campo acústico produz ondas interfaciais instáveis, que eventualmente resultam na formação de gotículas. Segundo, a aplicação de ultrassom de baixa frequência causa a cavitação; a formação e subsequente ruptura de microbolhas pela variação de pressão causa uma turbulência extremamente alta, que por sua vez é capaz de romper as gotas de óleo dispersas no meio em gotículas de tamanho nanométrico (MAA e HSU, 1999; KENTISH et al., 2008; SUTRADHAR KUMAR e AMIN MD, 2013). A intensidade do ultrassom e o efeito térmico são parâmetros que influenciam no processo. Com o aumento da intensidade de sonicação o tamanho de gota diminui, porém essa diminuição é limitada por um platô, onde o tamanho destas gotículas permanece constante. Durante o processo há um aumento da temperatura da dispersão a ser nanoemulsionada, resultante da energia dissipada na forma de calor, o que pode ser um fator limitante nos casos de materiais termolábeis (MAA e HSU, 1999; ALMEIDA et al., 2008). Este método tem sido muito empregado em escala laboratorial, entretanto, pode também ser

empregado em grande escala desde que a emulsão não seja muito viscosa para não comprometer a homogeneidade do sistema (MAA e HSU, 1999; BEHREND e SCHUBERT, 2001; ALMEIDA et al., 2008).

Outro método de alta energia é a utilização de homogeneizadores de alta pressão ou microfluidizadores. Estes equipamentos são projetados para que uma emulsão macroscópica seja forçada a passar por espaços extremamente estreitos, lacuna homogeneizadora ou microcanais, pela imposição de uma alta pressão. Como resultado, forças de cisalhamento, impacto e cavitação são aplicadas em um volume pequeno da dispersão líquida gerando gotículas de tamanho nanométrico. Geralmente, o diâmetro das gotículas obtidas por estes métodos pode ser afetado pela pressão imposta, temperatura e pelo tempo de processamento (número de ciclos de passagem) (FLOURY, BELLETTRE, et al., 2004; FLOURY, LEGRAND, et al., 2004; ALMEIDA et al., 2008; ANTON et al., 2008).

Os métodos de emulsificação de baixa energia fazem uso de propriedades físico-químicas do sistema e utilizam a alteração espontânea na curvatura do surfactante para a obtenção de gotículas. Pertencente a esta classe está o método de emulsificação espontânea.

A emulsificação espontânea baseia-se na adição de uma solução do óleo em um solvente orgânico miscível em água, a uma fase aquosa contendo um surfactante. A rápida difusão do solvente orgânico na fase aquosa gera uma turbulência interfacial, chamada de efeito Maragoni, que leva à redução da tensão interfacial e formação de nanogotículas da fase oleosa (VITALE e KATZ, 2003; BOUCHEMAL et al., 2004; XU e LUO, 2007; ANTON et al., 2008). Alguns fatores que afetam as características da nanoemulsão resultante incluem a viscosidade do óleo, o equilíbrio lipófilo-hidrófilo do tensoativo e a miscibilidade do solvente orgânico na água. Além disso, o gradiente de concentração entre a fase aquosa e oleosa afeta a velocidade de difusão do solvente e, consequentemente, o tamanho das gotículas (BOUCHEMAL et al., 2004).

A emulsificação espontânea é uma excelente alternativa para o preparo de nanoemulsões devido à simplicidade do método, pela possibilidade de preparação de pequenos volumes da formulação, além de não necessitar do aquecimento das fases oleosa e aquosa, o que a torna interessante na incorporação de fármacos termolábeis, e de dispensar o emprego de equipamentos sofisticados (BOUCHEMAL et al., 2004).

A caracterização dos sistemas nanoemulsionados incluem a determinação de propriedades físico-químicas como tamanho médio e distribuição de tamanho das gotículas, potencial zeta, pH e viscosidade. Fatores como componentes da formulação, técnica de preparo e incorporação de fármacos influenciam estas propriedades. Técnicas de microscopia eletrônica também são empregadas para avaliar a morfologia destes sistemas nanoestruturados e corroborar com a caracterização (ROLAND et al., 2003).

O tamanho e distribuição do tamanho, e do potencial zeta das gotículas são geralmente determinados por espectroscopia de correlação fotônica e da mobilidade eletroforética, respectivamente. O potencial zeta é definido como a diferença de potencial entre o meio de dispersão e a camada estacionária ligada à partícula dispersa, e indica o grau de repulsão entre as partículas de sistemas coloidais em uma dispersão. Seu valor reflete a composição da interface do sistema, em relação aos tensoativos formadores do filme interfacial ou em relação à presença de moléculas com carga, localizadas na interface. Um potencial zeta relativamente elevado em módulo conferirá estabilidade física ao sistema, uma vez que as forças repulsivas entre as gotículas superam as forças de atração (LIEBERMAN et al., 1989; ROLAND et al., 2003). O pH final dos sistemas nanoemulsionados deve levar em consideração aspectos como a solubilidade e estabilidade do fármaco no veículo, a estabilidade da forma farmacêutica e a via de administração. Para a aplicação cutânea, é indicado que as formulações apresentem um pH neutro a levemente ácido (ALVES et al., 2007; ARORA et al., 2014).

Em relação à estabilidade das nanoemulsões, o tamanho nanométrico confere estabilidade contra a sedimentação ou cremação devido ao movimento Browniano das partículas, onde a taxa de difusão é maior que a taxa de sedimentação induzida pela gravidade (TAYLOR, 1998; 2003; TADROS et al., 2004; SOLANS et al., 2005).

4.2 Aplicação tópica cutânea das nanoemulsões

As nanoemulsões têm sido estudadas para aplicação em produtos farmacêuticos e cosméticos como potenciais veículos para liberação e melhoria do perfil de distribuição dos compostos ativos nas diferentes camadas da pele (GUGLIELMINI, 2008). Neste aspecto, as nanoemulsões apresentam propriedades e vantagens peculiares. Tais sistemas permitem a solubilização de compostos lipifílicos e hidrofílicos (KOGAN e GARTI, 2006) e, devido ao tamanho nanométrico e elevada

área superficial das gotículas, elas promovem uma aplicação mais uniforme e prolongam o tempo de permanência do fármaco na pele (NGUYEN et al., 2013; FERREIRA et al., 2015). São cineticamente estáveis (dificilmente floculam, coalescem ou sedimentam), e melhoram a estabilidade química de compostos instáveis por proteger frente à oxidação (KOGAN e GARTI, 2006). As nanoemulsões também conduzem ao aumento da hidratação da pele e da permeação cutânea de compostos ativos, resultando na melhoria da biodisponibilidade de fármacos aplicados topicamente (SONNEVILLE-AUBRUN et al., 2004; TADROS et al., 2004; SOLANS et al., 2005; GUGLIELMINI, 2008; DEVARAJAN e RAVICHANDRAN, 2011; SHAH et al., 2012; SUTRADHAR KUMAR e AMIN MD, 2013; CHIME et al., 2014). Adicionalmente, tais sistemas podem restringir os efeitos desejados em tecidos específicos e também representar uma estratégia para a redução da toxicidade sistêmica (PRETE et al., 2006; GAOE et al., 2012; PUGLIA et al., 2014; YU et al., 2014).

Vários estudos têm evidenciado o aumento da permeação cutânea de fármacos hidrofílicos e lipofílicos incorporados às nanoemulsões, quando comparados às emulsões convencionais (FRIEDMAN et al., 1995; FERNANDEZ et al., 2000; WU et al., 2001; SHAKEEL et al., 2007; SHAKEEL et al., 2008). Basicamente, este aumento se deve a dois mecanismos distintos: aos altos gradientes de concentração de fármaco promovidos pela habilidade do sistema em dissolver consideráveis quantidades de ambos compostos lipofílicos e hidrofílicos sem aumentar, no entanto, a afinidade dos mesmos pelo veículo; e ao potencial promotor de permeação cutânea dos constituintes individuais do sistema nanoemulsionado (KREILGAARD, 2002). As nanoemulsões podem interagir com o estrato córneo desestruturando a bicamada lipídica do mesmo. Dessa forma, os lipídeos passam de uma forma ordenada para uma forma lipídica desordenada, aumentando a permeabilidade cutânea e a penetração de substâncias que normalmente não passariam através desta barreira. O tamanho reduzido das partículas permite o estreito contato com as junções superficiais dos corneócitos, favorecendo o acúmulo das partículas e sustentação da liberação do agente ativo (CEVC, 2004). Além disso, o efeito oclusivo proporcionado pelo filme lipídico hidrata a camada córnea e favorece a absorção (PARDEIKE et al., 2009).

Uma variedade de produtos cosméticos e farmacêuticos como loções, géis, sérum, podem ser obtidos a partir de sistemas nanoemulsionados, com diferencial no aspecto visual e sensorial

(SONNEVILLE-AUBRUN et al., 2004). Considerável atenção tem sido dada para o desenvolvimento de novos sistemas nanoemulsionados para a liberação de compostos naturais presentes em extratos ou frações de extratos vegetais (SARAF, 2010; CHIME et al., 2014).

Buranajaree e colaboradores (2011) avaliaram a ação despigmentante de nanoemulsões contendo 0,02% (p/p) de extrato de cerne de *Artocarpus incisus* em modelo *in vivo*. O dorso dos animais foi irradiado com luz UVB com o intuito de causar hiperpigmentação (melasma) cutânea; após seis semanas de tratamento tópico com o extrato nanoemulsionado ou com a solução aquosa de extrato livre, os autores observaram uma ação despigmentante melhor no tratamento com o extrato nanoemulsionado.

Mahdi e colaboradores (2011), obtiveram nanoemulsões contendo 0,05% (p/p) de extrato seco de *Phyllanthus urinaria* pelo método de emulsificação espontânea para futura aplicação como antioxidante e antienvelhecimento cutâneo. Chaiittianan e Sripanidkulchai (2014) desenvolveram nanoemulsões por homogeneização de alta pressão contendo 0,15% (p/p) de extrato hidroalcoólico da casca de *Phyllanthus emblica* apresentando vários compostos fenólicos incluindo o ácido gálico, ácido vanílico, epicatequinas entre outros.

Leelapornpisid e colaboradores (2014) desenvolveram nanoemulsões contendo o extrato da flor de *Tagetes erecta* pelo método de inversão de fases, e posteriormente incorporaram as mesmas em um gel para aplicação tópica cutânea visando a ação antienvelhecimento. Comparando o gel contendo o extrato nanoemulsionado com o gel contendo o extrato livre, os autores relataram uma maior atividade antioxidante *in vitro* e melhor retenção cutânea do composto majoritário, quercetagetina, nas diferentes camadas da pele para o gel contendo as nanoemulsões. Além disso, estudos em voluntários evidenciaram uma melhora na hidratação cutânea e diminuição de rugas após oito semanas de tratamento com o gel contendo o extrato de *T. erecta* nanoemulsionado.

Bidone e colaboradores (2014) desenvolveram nanoemulsões por emulsificação espontânea contendo extrato de *Achyrocline satureioides* para liberação cutânea de flavonoides, visando a obtenção de uma atividade anti-herpética (vírus de herpes simples). Estudos de permeação dos principais flavonoides em modelo *in vitro* empregando mucosa esofágica e orelha suína, foram realizados e os autores relataram a detecção de todos os flavonoides de interesse na superfície da mucosa e

na epiderme até oito horas após a aplicação tópica (BIDONE et al., 2015).

CAPÍTULO 2: DESENVOLVIMENTO E CARACTERIZAÇÃO DE NANOEMULSÕES CONTENDO CONSTITUINTES DE *Punica granatum* E AVALIAÇÃO DA ATIVIDADE ANTIOXIDANTE *IN VITRO*

A aplicação tópica de derivados vegetais (ex. extratos, frações extrativas) contendo compostos polifenólicos com o propósito de reduzir os efeitos nocivos causados pela radiação solar tem sido considerada. Entretanto, muitas vezes estes compostos apresentam baixa solubilidade e permeabilidade dificultando sua liberação e distribuição no tecido. O uso de sistemas nanoestruturados como as nanoemulsões constitui uma estratégia promissora para melhorar estas propriedades e possibilitar a liberação cutânea destes compostos.

Neste contexto, o desenvolvimento de nanoemulsões contendo o óleo da semente de romã como fase oleosa encapsulando a fração acetato de etila rica em compostos polifenólicos para aplicação tópica visando à fotoproteção é relatada neste trabalho. Com o intuito de comparar e verificar possível ação sinérgica entre o óleo da semente de romã e a fração acetato de etila, nanoemulsões contendo triglicerídeo de cadeia média (componente inerte) como fase oleosa encapsulando a fração acetato de etila rica em compostos polifenólicos também foram desenvolvidos.

Este capítulo encontra-se dividido em duas partes. A primeira parte descreve os resultados publicados no *Journal of Nanopharmaceutics and Drug Delivery, v. 2, p. 333-343, 2014* , que estão relacionados à obtenção por partição líquido-líquido e caracterização da fração acetato de etila rica em compostos polifenólicos a partir do extrato seco das cascas da romã bem como o desenvolvimento e caraterização das nanoemulsões contendo o óleo da semente de romã ou triglicerídeo de cadeia média encapsulando a fração acetato de etila rica em compostos polifenólicos através de dois métodos de preparo, emulsificação-evaporação do solvente e emulsificação espontânea, respectivamente. Os resultados referentes à validação de um método analítico por HPLC-DAD para a quantificação dos compostos polifenólicos na fração acetato de etila e nas nanoemulsões também são descritos. Ainda, a ação antioxidante da fração livre e nanoemulsionada foi determinada pelos métodos de DPPH e FRAP.

O método do DPPH (2,2-difenil-1-picril-hidrazil) consiste na descoloração de uma solução composta por radicais estáveis DPPH de cor violeta para uma solução amarela quando da adição de substâncias que podem doar um átomo de hidrogênio (antioxidantes) e reduzir o radical. Já o método de redução do ferro (FRAP) basea-se no potencial redutor férrico de compostos antioxidantes em reduzir o Fe^{3+} em Fe^{2+}. Diversos trabalhos científicos relatam o emprego destas metodologias para avaliar o potencial antioxidante de derivados de plantas e

nanoemulsões (ELFALLEH et al., 2011; MAHDI et al., 2011; MANASATHIEN et al., 2011; SESSA et al., 2013; ABLA e BANGA, 2014; RUDRA et al., 2014; HA et al., 2015).

Os estudos de estabilidade e fotoestabilidade das nanoemulsões contendo a fração acetato de etila do extrato das cascas da romã encontram-se descritas no Apêndice A.

A segunda parte do capítulo aborda os resultados publicados na revista *Toxicology in vitro*, artigo *in press* (2015), e são referentes aos estudos empregando eritrócitos humanos como modelo de biomembrana para avaliar a interação das nanoemulsões com a bicamada lipídica e o efeito protetor que as nanoemulsões conferem à biomembrana frente a um agente causador de dano oxidativo. Esse modelo também foi utilizado na avaliação preliminar do potencial irritante e fotoirritante das nanoemulsões.

Publicação: "Pomegranate seed oil nanoemulsions encapsulating pomegranate peel polyphenol-rich ethyl acetate fraction: Development and antioxidant assessment"

Journal of Nanopharmaceutics and Drug Delivery 2 (2014) 333-343

Pomegranate seed oil nanoemulsions encapsulating pomegranate peel polyphenol-rich ethyl acetate fraction: Development and antioxidant assessment

Thaisa Baccarin, Elenara Lemos-Senna*

Programa de Pós-Graduação em Farmácia, Centro de Ciências da Saúde, Universidade Federal de Santa Catarina, Campus Universitário Trindade, 88040-900 Florianópolis, SC, Brazil.

*Corresponding author: Elenara Lemos Senna. Programa de Pós-Graduação em Farmácia, Universidade Federal de Santa Catarina, 88040-970, Florianópolis, SC, Brazil. E-mail address: lemos.senna@ufsc.br - Telephone: (+55) 48 37325067

ABSTRACT

Nanoemulsions encapsulating a pomegranate peel polyphenol-rich ethyl acetate fraction (EAF) were developed and assessed regarding its antioxidant properties in order to obtain a new dosage form to protect the skin against UV radiation. Pomegranate seed oil (PSO) and medium chain triglyceride (MCT) nanoemulsions were prepared through ultrasonic emulsification/solvent evaporation and spontaneous emulsification methods, respectively. Both the unloaded and the EAF-loaded nanoemulsions were characterized according to their mean size and size distribution, zeta potential, and morphology. The Folin-Ciocalteu spectrophotometric method was used to determine total phenolic compounds, and a HPLC-DAD method was developed and validated to quantify the major polyphenol gallic acid, ellagic acid and punicalagin in both the EAF and the nanoemulsions. Antioxidant activity of free EAF and nanoemulsions was investigated by using FRAP and DPPH methods. All nanoemulsion formulations exhibited spherical-shaped droplets with mean size of about 200 nm and monodisperse size distribution. The droplets displayed negative surface charge as indicated by zeta potential measurements. Both the EAF and the nanoemulsions exhibited exceptionally high concentrations of pomegranate polyphenols, whose major compounds were gallic acic, ellagic acid, and punicalagin. However, entrapment efficiency varied

according to the partition coefficient of each polyphenol, with the most hydrophilic gallic acid exhibiting the lower entrapment efficient values. The nanoemulsions were stable at 4 ºC during 60 days storage. The EAF and EAF loaded-nanoemulsions displayed radical DPPH-scavenging activity similar to the ascorbic acid; no differences were found between nanoemulsions prepared with PSO and those prepared with MCT. Concerning the FRAP assay, the Trolox equivalent values were similar for EAF and EAF-loaded nanoemulsions prepared using MCT. However, lower Trolox equivalent values were found when PSO was employed, probably due to a limitation provided by the low solubility of PSO in the reaction medium. The results suggest that EAF-loaded nanoemulsion constitute a promising drug delivery system with antioxidant properties for topical administration on the skin.

Keywords: *Punica granatum*; pomegranate peel polyphenol-rich ethyl acetate fraction; pomegranate seed oil; nanoemulsions; antioxidant activity.

1. INTRODUCTION

Pomegranate (*Punica granatum* L., Punicaceae), a seeded or granular apple, is a delicious fruit consumed worldwide (CELIK et al., 2009; ISMAIL et al., 2012). It is widely cultivated throughout Iran, India, Mediterranean countries, China, Japan, drier parts of the United States and Mexico (FADAVI et al., 2006). The seeds are a rich source of lipids; pomegranate seed oil comprises 12% to 20% of total seed weight and consists of 65-80% conjugated fatty acids, whose main constituent is the 9-trans,11-cis,13-trans, octadecatrienoic acid, known as punicic acid, an omega-5 long-chain polyunsaturated fatty acid, and a positional, geometric isomer of α-linolenic acid (FADAVI et al., 2006; MELO et al., 2014). Therefore, pomegranate seed oil demonstrate potential health benefits related to the presence of conjugated fatty acids, including antioxidant (QU et al., 2010), anti-inflammatory (MELO et al., 2014), antitumor (MELO et al., 2014), immunomodulatory (MELO et al., 2014), anti-atherosclerotic (FADAVI et al., 2006) and anti-aging activities (RAHIMI et al., 2012).

Pomegranate peels, in turn, are rich in polyphenols compounds, including anthocyanins (delphinidin, cyanidin, and perlagonidin) and hydrolysable tannins (punicalin, pedunculagin, punicalagin, gallagic,

and ellagic esters of glucose), which account for 92% of the antioxidant activity associated with the fruit (AFAQ et al., 2005a; VIUDA-MARTOS et al., 2010; ISMAIL et al., 2012). Punicalagins are the major ellagitannins in the whole fruit and can be hydrolyzed to ellagic acid (EA) and other smaller polyphenols *in vivo* (BASU e PENUGONDA, 2009). Several *in vitro* and *in vivo* studies have demonstrated the antioxidant, anti-inflammatory, anticancer, and anti-angiogenesis activities of pure punicalagin, total pomegranate tannin extract, or pomegranate juice (RAHIMI et al., 2012; NEYRINCK et al., 2013). In particular, studies have demonstrated the ability of pomegranate peel extracts to inhibit free radical generation in UVA and UVB-irradiated hairless rat and human skin, protecting it against UV-induced erythema, epidermal thickness, skin burns, DNA fragmentation, and depigmentation (KASAI et al., 2006; PACHECO-PALENCIA et al., 2008; MANASATHIEN et al., 2011).

Taking into account the above-mentioned properties of pomegranate, the development of topical dosage form to deliver antioxidant compounds from pomegranate fruit directly into the skin seems to be valuable to protect the skin against oxidative stress caused by UV radiation. In this sense, nanoemulsion formulations would allow the association of both polyphenol and lipid compounds from pomegranate in a single dosage form. Nanoemulsions are kinetically stabilized dispersions consisted of nanometric-sized oil droplets finely dispersed in an aqueous phase, with the aid of a suitable surfactant system (SCHRAMM, 2005; MASON et al., 2006). Due to the large surface area and low surface tension of the oil droplets, nanoemulsions would exhibit the additional advantage to increase the permeation of incorporated polyphenol compounds through the skin, enhancing the topical effect (SCHRAMM, 2005; MASON et al., 2006; SILVA et al., 2009).

Considering our previous discussion, the objective of this study was to develop pomegranate seed oil nanoemulsions encapsulating a pomegranate polyphenol-rich extract fraction for topical administration. The polyphenol-rich extract fraction consisted of the ethyl acetate fraction obtained from commercial pomegranate peel spray-dried powder, considering the description that such fractioned extract has the highest polyphenol content and antioxidant properties (LUO et al., 2002; GANESAN et al., 2008; PANICHAYUPAKARANANT et al., 2010). In order to characterize and quantify the major phenolic compounds in both the extract fraction and the nanoemulsions, we developed and

validated a novel high-performance liquid chromatography-diode array detector (HPLC-DAD) method. Still, we investigated the antioxidant activity of the nanoemulsions, as well as the possible antioxidant synergic effect, provided by the association of polyphenols and polyunsaturated fatty acid in the same formulation. Although several studies have related the development of drug delivery systems containing pomegranate chemical constituents (HAYOUNI et al., 2011; LI e GU, 2011; MOHAGHEGHI et al., 2011; GOULA e ADAMOPOULOS, 2012; GUPTA et al., 2012; KAUR, CHANCHAL DEEP e SARAF, SWARNLATA . 2012; KAUR, CHANCHAL DEEP e SARAF, SWARNLATA, 2012a; b), the literature presents no reports on the approach of encapsulating an ethyl acetate fraction rich in polyphenols from pomegranate peel into nanoemulsions composed of pomegranate seed oil.

2. MATERIALS AND METHODS

2.1 Materials

Pomegranate seed oil and pomegranate peel dried extract were purchased from Via Farma (Sao Paulo, Brazil); according to the manufacturer, pomegranate seed oil contains 65% to 85% of punicic acid, and minor amounts of others polyunsaturated fatty acids, including linoleic acid, and α- and γ-linolenic acids. Pomegranate peel dried extract is a spray-dried powder standardized to contain at least 40% of ellagic acid. Soy lecithin (Lipoid® S100) and polysorbate 80 (Tween 80®) were purchased from PharmaNostra (Rio de Janeiro, Brazil) and Sigma-Aldrich (St. Louis, MO, USA), respectively. Medium chain triglyceride (Rittamolient®) was purchased from Brasquim (Porto Alegre, Brazil). Ellagic acid, gallic acid and punicalagin standards, Folin-Ciocalteu's reagent, Trolox (6-hydroxy-2,5,7,8-tetramethylchromane-2-carboxylic acid), 2,4,6-tris(2-pyridyl)-S-triazine (TPTZ), triethanolamine, ascorbic acid, and α-α-diphenyl-β-picrylhydrazyl (DPPH) were purchased from Sigma-Aldrich (St. Louis, MO, USA). Ferric chloride was purchased from Labsynth® (Sao Paulo, Brazil). Except for the methanol (Vetec®), acetonitrile (Panreac®) and acetic acid (Vetec®) (Sao Paulo, Brazil) of HPLC grade used in the analysis, all of the remaining used solvents and reagents were analytical grade.

2.2.1 Preparation of pomegranate polyphenol-rich extract fraction

Polyphenol-rich extract fraction from pomegranate fruit peel consisted of the ethyl acetate fraction obtained from a commercial pomegranate peel spray-dried extract powder. Briefly, 60 g of the spray-dried extract powder was extracted four times through dynamic maceration with 1000 mL of 90:10 (v/v) methanol:water mixture during 24 hours. The extractive solution was submitted to evaporation under reduced pressure to eliminate the solvent; subsequently, the precipitated was suspended with 500 mL of a 2% (v/v) aqueous acetic acid solution. The resulting mixture was partitioned with dichloromethane and ethyl acetate. Afterward, the pooled ethyl acetate fraction (EAF) was evaporated to dryness under reduced pressure. The colour of the obtained EAF was brown-green with a sticky and semisolid consistency.

2.2.2 Preparation of nanoemulsions

EAF-loaded pomegrante seed oil nanoemulsions (EAF-PSO-NE) were prepared using an ultrasonic emulsification method followed by solvent evaporation (ABISMAIL et al., 1999). Briefly, the ethyl acetate fraction (EAF) at different concentrations (0.1%, 0.3%, 0.4% or 0.5%; w/v), soy lecithin (0.4%; w/v), and PSO (2%; w/v) were dissolved in 10 mL of ethyl acetate. This ethyl acetate solution was subsequently poured slowly into 40 mL of a polysorbate 80 (2.1%; w/v) aqueous solution, and then adjusted to pH 5.0-6.5 with triethanolamine. The oil in water dispersion was sonicated for 1, 3 or 5 minutes using an Ultrasonic Processor UP200S (Hielscher, Germany), and it was subsequently maintained under magnetic stirring for 24 hours. The resulting nanoemulsion was evaporated under reduced pressure up to the volume of 15 mL.

EAF-loaded medium chain trygliceride nanoemulsions (EAF-MCT-NE) were prepared through the spontaneous emulsification method (BOUCHEMAL et al., 2004). Briefly, 10 mL of an ethanolic solution containing EAF at different concentrations (0.1%, 0.3%, 0.4% or 0.5%; w/v), soy lecithin (0.4%; w/V), and MCT (1.8%, w/v) was poured into a 2.1% (w/v) polysorbate 80 aqueous solution and adjusted to pH 5.0-6.5 with triethanolamine, under magnetic stirring. The

nanoemulsion was evaporated under reduce pressure to eliminate the organic solvent and concentration up to volume of 15 mL. All formulations were filtered through 8 µm quantitative filter paper. Unloaded PSO-NE and MCT-NE followed equal preparation. All formulations were prepared in triplicate.

2.4. Physicochemical and morphological characterization of the nanoemulsions

The mean droplet size and zeta potential were determined through dynamic light scattering (DLS) and laser-Doppler anemometry, respectively, using a Zetasizer Nano Series (Malvern Instruments, Worcestershire, UK). The analyses of size were performed at a scattering angle of 173°, after appropriated dilution of the samples in ultrapure water (Milli-Q®, Millipore, USA). For zeta potential analysis, the samples were diluted in Milli-Q® water and placed in electrophoretic cells where a potential of ±150 mV was applied. The zeta potential values were calculated as mean electrophoretic mobility values using Smoluchowski's equation. The pH of nanoemulsions was determined at 25 °C using a pH meter (Acorn® Series pH 5 meter Oakton) calibrated with pH 4.0 and 7.0 buffer solutions. All measurements were performed at 25 °C.

A short term physical stability of the nanoemulsions was carried out after storing the formulations at 4 ºC for 60 days. Mean particle size and size distribution, zeta potential and pH of the samples were determined on days 1, 7, 15, 30, and 60, as above mentioned.

The morphology of the nanoemulsions was examined using a Jeol-1011-100 kV transmission electron microscope (Jeol, Tokyo, Japan). The nanoemulsion was diluted in ultrapure water; subsequently, a drop of the samples was deposited on carbon-coated copper grids and negatively stained with 1% (w/v) fosfotungistic acid solution.

2.5. Determination of total phenolic content

The total phenolic content (TPC) in the EAF and EAF-loaded nanoemulsions (EAF-PSO-NE and EAF-MCT-NE) was determined according to the Folin-Ciocalteu procedure reported by Sousa et al (2007) with modifications. Briefly, 40 mg of EAF was accurately weighted, transferred to a 100 mL volumetric flask, dissolved in methanol, and completed to volume with the same solvent to obtain a

0.4 mg mL^{-1} solution. An aliquot of 250 µL of this solution was transferred to a 25 mL volumetric flask and, then, 500 µL of Folin-Ciocalteu's reagent and 10 mL of distilled water were added, and the mixture was shaken for 1 minute. Afterward, 2 mL of $NaCO_3$ (15% w/v) was added, the solution was stirred for 30 seconds, and the volume was adjusted to 25 mL with distilled water. The samples were incubated for 2 hours protected from light; subsequently, the absorbance of the samples was measured at 750 nm through a spectrophotometer Shimadzu® UV-1800, Software UV Probe 2.33.

To determine the TPC in the nanoemulsions, 1.0 mL of each formulation was transferred to a 10 mL volumetric flask. Next, the samples were dissolved with 1 mL of acetonitrile alone (EAF-MCT-NE) or ethyl acetate (EAF-PSO-NE), the mixtures were shaken vigorously in a vortex for 2 min, and acetonitrile was added to complete the volume. Afterward, 2 mL of this solution was transferred to a 25 mL volumetric flask, and the samples received the same treatment of EAF. Total phenolic content was determined from a linear equation of a gallic acid standard curve constructed in concentrations ranging from 2 to 8 µg mL^{-1}. The results were expressed as gallic acid equivalents (GAE) in milligrams per grams of ethyl acetate fraction or milligrams per milliliter of nanoemulsion. All samples were analysed in triplicate.

2.6. HPLC analysis of polyphenol compounds

2.6.1. Instrumentation and chromatographic conditions

The experiments were conducted using a Shimadzu-HPLC system equipped with a LC-20AT binary pump, CTO-20A oven, SPD-M20A photo diode array detector, and software LC Solution 1.2 (Shimadzu, Tokyo, Japan). The analyses were carried out with a Luna C18 5 µm Fusion RP 100 Å column (250 mm x 4.6 mm) (Phenomenex®, USA), coupled with a C18 guard column (Phenomenex®, USA), equilibrated at 30º C. Mobile phase consisted of acetonitrile (A) and 1% (v/v) acetic acid aqueous solution (B), filtered prior to use through 0.45 µm regenerated cellulose membrane filter. The mobile phase was eluted at flow rate of 1 mL min^{-1} using the following linear gradient program: 97% B at 0.01-3 min, 97%-94% B at 3-5 min; 94%- 90% B at 5-8 min; 90%-87% B at 8-12 min; 87%-84% B at 12-15 min, 84%-80% B at 15-18 min; 80%-77% B at 18-21 min; 77%-74% B at 21-24 min, 74%-97% B at 24-28 min; 97% B at 28-30 min. The

injection volume of the samples was 20 µL and the detection was achieved at wavelengths of 270 nm, 367 nm, and 378 nm for gallic acid, ellagic acid, and punicalagin, respectively.

2.6.2 Sample preparation

To determine ellagic acid, gallic acid, and punicalagin in EAF, 40 mg of the extract was accurately weighed, transferred to a 50 mL volumetric flask, dissolved with methanol using sonication during 5 minutes, and the volume was adjusted with the same solvent to obtain an EAF methanolic solution. The solution was then filtered through a 0.2 *µm* PTFE syringe filter and an aliquot of 400 µL was transferred to a vial followed by the addition of 600 µL of methanol. The sample was prepared in triplicate and injected three times in the chromatograph.

To determine the polyphenol compounds in the EAF-loaded nanoemulsions, 1 mL of each formulation was transferred to a 10 mL volumetric flask. Following, the samples were dissolved with 1 mL of acetonitrile alone (EAF-MCT-NE) or ethyl acetate (EAF-PSO-NE), the mixtures were shaken vigorously in a vortex for 2 min with subsequent addition of acetonitrile to complete the volume. The resulting solutions were filtered through a 0.2 µm PTFE syringe filter and injected in the chromatograph. All samples were analyzed in triplicate.

2.6.3 Validation of the HPLC-DAD method

To quantify the compounds ellagic acid, gallic acid and punicalagin in EAF and EAF-loaded nanoemulsions, a HPLC-DAD method was developed and validated according to the ICH and ANVISA guidelines (BRASIL, 2003; ICH, 2005). Methanolic stock solutions of gallic acid (510 µg mL^{-1}), ellagic acid (100 µg mL^{-1}), and punicalagin (100 µg mL^{-1}) were prepared and appropriately diluted with the same solvent to construct the calibration curves. Seven concentrations of each compound were injected in triplicate in the chromatograph at concentrations ranging from 3 to 30 µg mL^{-1} for gallic acid and ellagic acid, and from 15 to 100 µg mL^{-1} for punicalagin. The linearity of the method was verified through the calculation of the coefficient of regression of the calibration curves using the least squares method. The limit of detection (LOD) and limit of quantitation (LOQ) were determined at signal-to-noise ratios (S/N) of 3 and 10, respectively, based on the standard deviation of the y-intercepts of

regression curves (BRASIL, 2003). *A* recovery test was used to assess the accuracy of the method; accurate amounts of gallic acid (5, 15 and 25 µg mL^{-1}), ellagic acid (5, 15 and 25 µg mL^{-1}) and punicalagin (15, 25 and 75 µg mL^{-1}) standard solutions were added to diluted samples of EAF. Selectivity/specificity was determined by comparing of unloaded and EAF-loaded chromatographic profiles to verify whether any formulation compound interferes in the HPLC-DAD analysis. For repeatability (intra-day precision) determination, analyses of EAF were performed in sextuplicate for each compound at one level concentration three times in a single day. The intermediate precision (inter-day precision) was determined through a single analysis of the sample (EAF) in sextuplicate for another two consecutive days; relative standard deviation (%RSD) was determined. Robustness was assessed through the analysis of gallic acid, ellagic acid, and punicalagin standard solutions and EAF under different experimental conditions, making small changes in the oven temperature (29 ºC, 30 ºC and 31 ºC) and mobile phase flow rate (0.9, 1.0 and 1.1 mL min^{-1}). Data were analyzed through ANOVA ($p<0.05$).

2.7. Entrapment efficiency

Ellagic acid, gallic acid, and punicalagin were determined by HPLC and TPC was determined spectrophotometrically in the whole EAF-loaded nanoemulsions and in the supernatants obtained through the ultrafiltration/centrifugation of colloidal dispersions, using Amicon Centrifugal Filter Devices with Ultracel-100 membrane (100 kDa, Millipore Corp., USA). The entrapment efficiency (%) was estimated as the difference between the total concentration of each polyphenol or TPC found in the nanoemulsions and the concentrations found in the supernatants.

2.8. Antioxidant activity evaluation

2.8.1. DPPH radical-scavenging activity

The α,α-diphenyl-β-picrylhydrazyl (DPPH) radical scavenging activity was assessed as described by Choi et al, with some modifications (CHOI et al., 2002). EAF and ascorbic acid (positive control) were dissolved in ethanol to obtain the final concentration of 1.0 g mL^{-1}. EAF-MCT-NE and EAF-PSO-NE were dissolved in

acetonitrile and acetonitrile:ethyl acetate (3:1, v/v), respectively, to obtain solutions containing the theoretical concentration of EAF of 1.0 mg mL^{-1}. Each sample was transferred to glass tube and appropriately diluted to obtain concentrations ranging from 0.5 to 10 µg mL^{-1}. Afterward, 2 mL of a 0.3 mM DPPH ethanol solution was added into each glass tube and allowed to react at room temperature. After 30 min, the absorbance values were measured at 517 nm using an ethanolic EAF solution and DPPH solution as blank and negative control, respectively. The percentages of scavenging capacity (%) were calculated using equation $100-[((Abs_s-Abs_b)/Abs_c) \times 100]$, where Abs_s, Abs_b, and Abs_c were the absorbances of the sample, blank and control, respectively. The SC_{50} values were obtained through linear regression analysis of the EAF concentration *versus* percent inhibition curves obtained from triplicates. Statistical analyses were performed employing ANOVA ($p<0.05$).

2.8.2 Ferric reducing antioxidant power assay (FRAP)

The antioxidant capacity of EAF and EAF-loaded nanoemulsions was determined using the FRAP assay as described by Benzie and Strain (1996). The samples were diluted in water up to concentration of 50 µg mL with 10 µL subsequently transferred to a glass tube and mixed with 1 mL of working FRAP reagent ($FeCl_3$ 1.7 mM in sodium acetate 300 mM pH 3.6 and 2,4,6-tris(2-pyridyl)-s-triazine 0.83 mM in HCl 40 mM). The mixture was incubated for 15 min at 37 ºC followed by the measurement of absorbance using a spectrophotometer (Hitachi, U-1800, Tokio, Japan) at 593 nm. The antioxidants present in the EAF or EAF-loaded nanoemulsions were assessed as reducers of Fe^{3+} to Fe^{2+}, which is chelated by 2,4,6-tris(2-pyridyl)-S-triazine (TPTZ) to form a complex (Fe^{2+}-TPTZ). A standard curve of Trolox (water soluble vitamin E analogue) was prepared at a concentration ranging between 50 and 1000 µM and the results expressed as Trolox equivalents (mM). The assay was carried out in triplicate. Statistical analyses were performed employing ANOVA ($p<0.05$).

3. RESULTS AND DISCUSSION

3.1. Development of nanoemulsions

In this study, we aimed to develop pomegranate seed oil nanoemulsions encapsulating the polyphenol compounds present in the pomegranate peel as a novel topical dosage form that might be useful for skin protection against UV-radiation. Nanoemulsions were prepared using different concentrations of an ethyl acetate fraction rich in pomegranate polyphenols obtained from a pomegranate dried extract. Both polyunsaturated fatty acids and polyphenols of pomegranate are recognized for their antioxidant properties; however, we are interested in investigating a possible synergic antioxidant effect provided by their association in a single formulation. Therefore, medium chain triglyceride nanoemulsions containing pomegranate polyphenols were also prepared and characterized to be compared with the PSO-NE regarding physicochemical properties and antioxidant capacity.

Nanoemulsions may be prepared by using high- and low-energy methods. High-energy methods enclose the application of a mechanical energy during the emulsification step, generally by using high shear stirring, high-pressure homogenizers and/or ultrasound generators, while lower energy methods are based on the phase transitions taking place during the emulsification (CHIME et al., 2014; KOMAIKO e MCCLEMENTS, 2015). In this study, MCT-NE were prepared using the spontaneous emulsification method, consisting of a low energy emulsification process, where nanodroplets of the oil phase are formed due to an interfacial instability originated from the fast diffusion of a miscible organic phase into a aqueous phase, the so-called Maragoni effect (BOUCHEMAL et al., 2004; KOMAIKO and MCCLEMENTS, 2015). However, when PSO was employed as oil phase, the spontaneous emulsification method did not provide a monodisperse distribution of the droplets (data not shown), probably due to the high viscosity of PSO oil that prevented the formation of small droplets and a stable colloidal dispersion. Therefore, PSO nanoemulsions had to be prepared through an emulsification/solvent evaporation method, using the ultrasound energy to obtain the nanodispersions. The generation of nanodroplets by sonifiers is generally attributed to a mechanism of cavitation. The application of ultrasound waves in a coarse emulsion leads to a sequence of mechanical depressions and compressions, generating cavitation bubbles, which tend to implode, causing extreme levels of highly

localized turbulance. This turbulance provides sufficient energy to break up the primary droplets of dispersed oil into nanometric-scaled droplets, increasing the surface area (ABISMAïL et al., 1999; KENTISH et al., 2008). Evidently, the physicochemical properties of the resulting nanoemulsions are strongly dependent on the preparation method as well as the formulation composition (DIVSALAR et al., 2012). Table 1 describes the mean diameter and polydispersion index as well as zeta potential and pH values obtained for unloaded and EAF-loaded nanoemulsions prepared using PSO and MCT as oil.

Table 1. Physicochemical characteristics of unloaded and EAF-loaded nanoemulsions.

Sample	EAF[a] (%,w/v)	Size (nm ± SD)	Polydispersity Index	Zeta Potential (mV± SD)	pH
EAF-MCT-NE					
	0.1	206.2 ± 8.7	0.152	-23.1 ± 5.7	5.32
	0.3	217.2 ± 6.1	0.158	-26.2 ± 5.3	5.31
	0.4	220.3 ± 16.2	0.177	-28.7 ± 6.2	5.33
	0.5	215.6 ± 1.8	0.144	-30.6 ± 5.3	5.35
Unloaded MCT-NE	0.0	200.8 ± 8.2	0.159	-13.8 ± 4.9	5.94
EAF-PSO-NE					
	0.1	127.5 ± 7.7	0.143	-26.1 ± 5.6	5.65
	0.3	149.5 ± 1.4	0.127	-29.3 ± 6.4	5.43
	0.4	178.4 ± 5.9	0.105	-28.4 ± 6.0	5.72
	0.5	183.5 ± 14.8	0.122	-31.4 ± 5.9	5.57
Unloaded PSO-NE	0.0	141.2 ± 13.3	0.143	-20.4 ± 6.3	5.91

[a]Initial concentration of EAF in the formulations. Values are expressed as mean ± SD (n=3).

As observed on Table 1, the droplet size of nanoemulsions varied from 200.8 to 220.3 nm, and from 127.5 to 183.5 nm, for formulations prepared with MCT and PSO, respectively. Both the unloaded and the EAF-loaded nanoemulsions exhibited values of polydispersity index less than 0.2, indicating that monodisperse colloidal dispersions were obtained. In addition, it can be observed the tendency of droplet size to increase with the increase of EAF concentration in the formulations, especially when the emulsion/evaporation method was employed. These results may be associated with the semisolid characteristic of EAF, which probably increases the viscosity of the oil phase, increasing the ratio of dispersed to continuous phase viscosities, hampering the oil phase disruption by the ultrasonic homogenizer (TRONCOSO et al., 2011). The fact that this effect was not very evident when the spontaneous emulsification was employed to prepare MCT-NE, was consistent with results found by other authors who stated the inexistence of a correlation between bulk physicochemical properties of the oil and the final nanoemulsion droplet size (KOMAIKO and MCCLEMENTS, 2015).

The particle charge is one of the factors that may determine the physical stability of colloidal dispersions. In general, the higher the electrostatic repulsion between the particles the higher the physical stability (HEURTAULT et al., 2003). However, nonionic surfactants such as polysorbate 80 may stabilize colloidal dispersions through the steric effect produced by the location of polyethylene glycol chains of the hydrophilic moiety of the molecule at the droplet surface (HOELLER et al., 2009). In this study, zeta potential of nanoemulsions varied from -13.9 to -30.6 mV, and from -20.5 to -31.4 mV, for formulations prepared using MCT and PSO, respectively. It is worth to mention that unloaded PSO-NE exhibited a higher zeta potential than unloaded MCT-NE, probably due to the high content of punicic acid of pomegranate oil. Also, the zeta potential increased (in module) with the increase of the initial EAF concentration in the formulations, which may be related to the high concentration of carboxylated and hydroxylated compounds in this fraction. The pH of unloaded and EAF-loaded nanoemulsions varied from 5.0 to 6.0, which is compatible with that of the skin (LAMBERS et al., 2006). The incorporation of EAF caused the reduction of the pH values of the colloidal dispersions, which may also be related to the increase in acidic compounds in the formulations.

To assess the short time stability of the formulations, the nanoemulsions were visually inspected for eventual creaming,

coalescence, phase separation, and/or precipitation. In addition, droplet size and zeta potential were assessed over the 60 days of the study. Nanoemulsions maintained at 4 ºC were remarkably stable and no changes in the droplet size and zeta potential were observed (Fig.1). Moreover, no visual changes in the macroscopic characteristics and/or presence of any sign of phase separation were verified during the assay, evidencing that nanoemulsions were stable under the tested conditions.

Figure 1. Variation of droplet size (solid line and closed symbols) and zeta potential (dashed line and open symbols) during 60 days of stability study at 4 ºC. (circle) unloaded PSO-NE; (square) unloaded MCT-NE.

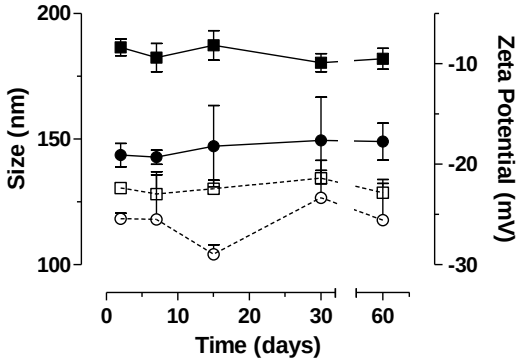

TEM images representing EAF-loaded nanoemulsions negatively stained showed spherical-shape particles with diameters of about 100-200 nm, which was in accordance with the dynamic light scattering analysis (Fig. 2). A dark outline can be seen on the droplets, which has been related to the fact that the film of dry phosphotungistic acid is rather thick and only the top part of the spherical particle protrudes out of the stain (DORA et al., 2012).

Figure 2. TEM micrographs of a representative EAF-loaded nanoemulsion (EAF-PSO-NE).

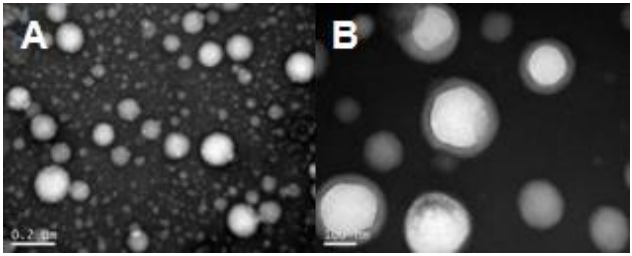

3.2. Validation of the HPLC-DAD method

Polyphenols represent the predominant class of phytochemicals of pomegranate fruits mainly consisting of hydrolysable tannins (FISCHER et al., 2011). The tannin fraction consists of gallic acid and ellagic acid and the combinations of monomers gives rise to structures that are subdivided into gallotannins and ellagitannins, including the most specific gallagylesters, such as the predominant hydrolysable tannin of pomegranates, known as punicalagin (HASLAM, 2007). Many methods for the determination of polyphenolic compounds in pomegranates and derived products have been reported (PANICHAYUPAKARANANT et al., 2010; QU et al., 2010; FISCHER et al., 2011). However, no reports were found concerning a HPLC-DAD method for the quantification of major phenolic compounds on the pomegranate polyphenol-rich EAF that can also be applied to quantify these compounds in EAF-loaded nanoemulsions.

Figure 3A illustrates a representative chromatogram profile of the three major identified phenolic compounds obtained for free EAF and EAF-loaded nanoemulsions. This chromatogram enabled the identification of the gallic acid (1) and ellagic acid (4) at retention times of 6.5 and 25.5 minutes, respectively. Punicalagin is found naturally as two reversible a- and b-anomers and detected at retention times of 14.5 and 16.5 minutes. For further analysis, total punicalagin was determined as the sum of the area peaks obtained for each anomer. The HPLC method was able to provide a satisfactory separation of the chemical markers in a short period of time, considering the matrix complexity. To determine the method specificity, unloaded nanoemulsions were also analyzed using the same conditions. All other components of the

nanoemulsions proved not to interfere in the peaks corresponding to the polyphenol compounds, evidencing the specificity of the method (Fig. 3B).

Figure 3. Phenolic compounds identified and quantified in pomegranate peel EAF: gallic acid (GA), punicalagin (PC) and ellagic acid (EA)**.** Representative chromatographic profiles obtained for (B) EAF-loaded nanoemulsions and (C) Unloaded nanoemulsions. In B: gallic acid (1), punicalagin anomers (2, 3) and ellagic acid (4).

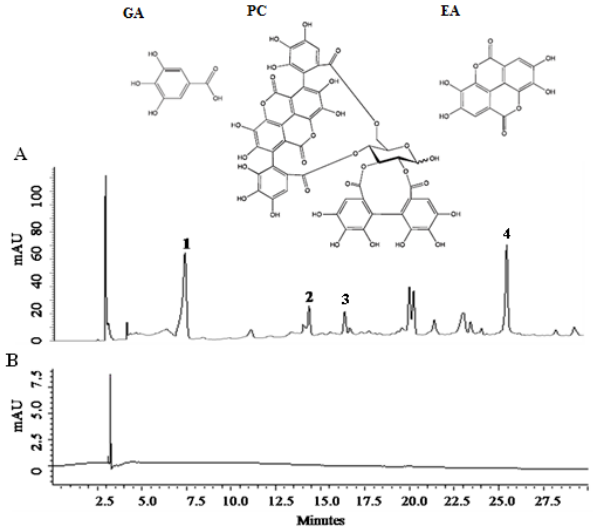

Calibration curve was found to be linear (r^2 >0.99) over the concentration range of 3-30 µg mL^{-1} for ellagic and gallic acid, and 15-100 µg mL^{-1} for punicalagin. The average recovery was near 100% for all compounds. The LOD values of gallic acid, total punicalagin, and ellagic acid were 0.21, 3.75, and 0.51 µg mL^{-1}, while their LOQ values were found to be 0.7, 1.71 and 12.5 µg mL^{-1}, respectively. The intra and inter-day precision analyses indicated %RSD of 1.56-3.31 and 4.36-5.19, respectively. The accuracy of the HPLC method was demonstrated by the recovery data revealing that the mean recovery values of different concentrations of gallic acid, total punicalagin, and ellagic acid were 99.98, 99.92 and 99.5%, respectively (Table 2).

Table 2. Results of the regression analysis, and determination of intra-day and inter-day precision of the HPLC method (n=6).

Compounds	λ (nm)	r^2	Regression line	LOD (μg mL^{-1})	LOQ (μg mL^{-1})	Precision (%RSD)		Recovery (% ± RSD)
						Intra-day	Inter-day	
Gallic acid	270	0.997	y = 34689x+5641	0.21	0.70	1.56	4.36	99.98 ± 1.57
Punicalagin	378	0.998	y = 2331x-9617	3.75	12.50	3.31	5.19	99.92 ± 1.64
Ellagic acid	367	0.996	y = 31664x-2685	0.51	1.71	2.19	5.11	99.45 ± 1.93

The robustness of the proposed method was determined through the analyses of the polyphenols under small changes in the oven temperature (29, 30 and 31ºC) and mobile phase flow rate (0.9, 1.0 and 1.1 mL min^{-1}), as presented on Table 3. The robustness was estimated using the overall mean and standard deviation for each variable on the concentration of ellagic acid, gallic acid and punicalagin. Standard deviation (SD) was less than 2% for all parameters and compounds. The developed method proved robust in terms of quantification of ellagic acid, gallic acid, and punicalagin in the ethyl acetate fraction from peel extract of *P. granatum*.

Table 3. Results obtained in the robustness determination of the HPLC method (n=3).

Parameters	**Concentration (μg mL^{-1} ± SD)**		
	Gallic acid	**Punicalagin**	**Ellagic acid**
Oven temperature			
29ºC	14.04 ± 0.31	22.30 ± 2.90	15.24 ± 0.05
30ºC	14.64 ± 0.11	22.49 ± 0.36	14.63 ± 0.26
31ºC	14.31 ± 1.72	22.58 ± 0.62	15.63 ± 0.31
Flow rate			
0.9 mL min^{-1}	14.25 ± 1.40	21.52 ± 0.94	14.62 ± 0.61
1.0 mL min^{-1}	12.64 ± 0.11	19.49 ± 0.36	14.63 ± 0.26
1.1 mL min^{-1}	13.43 ± 0.15	21.10 ± 0.99	14.21 ± 0.22

SD: Standard Deviation.

3.3. Determination of phenolic compounds in the EAF

Table 4 presents the results obtained after the spectrophotometric determination of total phenolic content, and HPLC analyses of the major polyphenols ellagic acid, gallic acid, and punicalagin through HPLC in the pomegranate polyphenol-rich EAF.

Table 4. Total phenolic content (TPC) and ellagic acid, gallic acid, and punicalagin content of pomegranate polyphenol rich ethyl acetate fraction.

	[a]TPC	[b]Ellagic acid	[b]Gallic acid	[b]Punicalagin
EAF	638.13 ± 13.24	84.7 ± 0.83	238.6 ± 1.28	296.7 ± 2.55

[a]Result expressed in mg g^{-1} ± SD of GAE.
[b]Results expressed in mg g^{-1} ± SD.
TPC = Total phenolic content.
GAE = Gallic acid equivalent.

The EAF obtained from *P. granatum* peel extract displayed an exceptionally high total phenolic content (638.13 mg g^{-1} GAE), as well as considerable concentrations of ellagic acid, gallic acid, and punicalagin, proving the efficiency of the proposed extraction method. The concentration of ellagic acid found in the EAF is in agreement with those concentrations reported by others authors (PANICHAYUPAKARANANT et al., 2010). Punicalagin proved to be the major polyphenol in the EAF, as expected, since pomegranate peel has been related to possess the highest concentration of punicalagin among the most commonly consumed fruits (ISMAIL et al., 2012). Elango et al. (2011) have reported that the gallic acid was the major compound isolated from pomegranate peel extract. Bekir et al. (2013) found that ethyl acetate fraction obtained from pomegranate leaves had a value of total phenolics of 127.3 mg g^{-1} GAE. Another study carried out by Oliveira et al. (2013) demonstrated a similar concentration of total phenolic (608.50 mg g^{-1} GAE) in the ethyl acetate fraction obtained from *Neoglaziovia variegate* leaves dried extracts. Indeed, the concentration of phenolic compounds may vary from plant to plant, the part of the plant used, seasonal changes, environment conditions, harvest period; but overall, considering the liquid-liquid partition process, these secondary metabolites have been predominantly found in the ethyl acetate fraction (CECHINEL FILHO and YUNES, 1998; LUO et al., 2002).

3.4. Determination of polyphenol content and entrapment efficiency in the nanoemulsions

Table 5 summarized the results of polyphenol content and entrapment efficiency obtained after the determination of total phenolic compounds (TPC) and the major polyphenols ellagic acid, gallic acid, and punicalagin in the nanoemulsions. The TPC concentration found in the formulations varied from 0.8 to 2.3 mg mL^{-1} GAE, and the entrapment efficiency – representing the amount of drug associated with the droplets – varied from 34.5 to 44.8%. In addition, the total polyphenol content increased with the increase in the initial amount of EAF added to the formulations; similar values were found for EAF-MCT-NE and EAF-PSO-NE. The increase of the concentration of major polyphenol compounds with the increasing of EAF added to the formulation was also observed after analyzes of these compounds by HPLC. These values varied from 17.4 to 89.9 µg mL^{-1}, 286.7 to 1320.7 µg mL^{-1}, and 33.7 to 425.6 µg mL^{-1} for ellagic acid, gallic acid and punicalagin, respectively. However, different values of entrapment efficiency were obtained for these tree compounds, with gallic acid displaying the lowest values. These results may be related to the lipophilicity of these compounds, expressed by their respective octanol/water partition coefficients. While ellagic acid and punicalagin displayed log P values of 2.44 and 2.36, respectively, gallic acid displays a log P of -0.53, which is particular to a more hydrophilic compound. Therefore, gallic acid was more partitioned towards the aqueous phase during the emulsification process, resulting in lower entrapment efficient values.

Table 5. Values of phenolic compounds content and entrapment efficiency found in the MCT and PSO nanoemulsions (n=3).

EAF	TPC		Ellagic acid		Gallic acid		Punicalagin	
(%, w/V)	Content ($mg\ mL^{-1}$)	EE (% ± SD)	Content ($\mu g\ mL^{-1}$)	EE (% ± SD)	Content ($\mu g\ mL^{-1}$)	EE (% ± SD)	Content ($\mu g\ mL^{-1}$)	EE (% ± SD)
MCT-NE								
0.1	0.8 ± 0.03	34.5 ± 7.87	23.6 ± 0.93	72.2 ± 5.87	350.2 ± 13.53	53.8 ± 1.14	62.1 ± 9.63	76.9 ± 3.54
0.3	1.4 ± 0.13	40.6 ± 7.97	41.7 ± 7.15	80.7 ± 4.83	824.0 ± 28.30	44.2 ± 1.71	123.0 ± 4.70	76.4 ± 4.39
0.4	1.9 ± 0.18	39.6 ± 4.77	66.9 ± 9.64	83.9 ± 1.44	1045.8 ± 47.07	50.2 ± 0.30	296.7 ± 33.47	86.7 ± 0.12
0.5	2.3 ± 0.14	39.7 ± 3.90	89.9 ± 3.59	85.7 ± 5.58	1320.7 ± 4.19	48.0 ± 1.77	383.6 ± 2.94	82.7 ± 5.53
PSO-NE								
0.1	0.9 ± 0.06	46.4 ± 1.64	17.4 ± 0.36	64.9 ± 3.37	286.7 ± 15.04	46.3 ± 2.42	33.7 ± 1.34	50.4 ± 3.65
0.3	1.5 ± 0.08	44.9 ± 2.41	27.0 ± 1.49	62.7 ± 3.88	638.5 ± 27.12	48.9 ± 3.67	142.0 ± 27.56	76.0 ± 4.30
0.4	1.9 ± 0.16	44.4 ± 3.37	30.3 ± 3.22	66.5 ± 8.89	827.3 ± 2.72	48.1 ± 4.16	249.5 ± 16.06	80.3 ± 3.19
0.5	2.3 ± 0.14	42.1 ± 4.79	35.1 ± 1.06	48.3 ± 8.11	1248.9 ± 20.11	48.4 ± 3.01	425.6 ± 16.42	83.4 ± 2.54

EE = Entrapment Efficiency; *TPC* = Total Phenolic Content

3.5 Assessment of antioxidant activity

Antioxidants have attracted considerable attention regarding radicals and oxidative stress since they are involved in the defense mechanism against the pathologies associated with the attack of free radicals. Besides, the interest in using these compounds to prevent the presumed deleterious effects of free radicals in the human body has been increasing. Numerous exogenous antioxidants are derived from natural sources, mainly plants, such as flavonoids and anthocyanines, which are the target analytes in many cases (SESSA et al., 2013). They have been considered promising compounds to be exploited as chemopreventive agents for a variety of skin disorders, in particular for skin cancer (HORA et al., 2003; AFAQ et al., 2005b; SYED et al., 2006; ISMAIL et al., 2012; RAHIMI et al., 2012).

The antioxidant properties of compounds found in the seed oil and peels of pomegranate fruits have been extensively demonstrated (SYED et al., 2006; LANDETE, 2011; MANASATHIEN et al., 2011; RAHIMI et al., 2012; MELO et al., 2014). In this study, our interest was to assess the antioxidant properties of a new nanoemulsion formulation containing high concentrations of polyphenols of pomegranate using PSO as the oil phase. DPPH and FRAP are two colorimetric methods available for the assessment of the antioxidant properties of plant extracts. DPPH is a stable free radical, due its delocalization of the spare electron on the whole molecule; the delocalization on the DPPH molecule determines the occurrence of a purple colour. When it reacts with a hydrogen donor, the reduced form is generated, accompanied by the disappearance of the violet colour. In this case, the decrease in absorbance depends linearly on the concentration of antioxidant compounds. In contrast, the FRAP method relies on the reduction of the complex ferric ion-TPTZ by the antioxidants. The binding of Fe^{2+} to the ligand creates a very intense navy blue color. The absorbance can be measured to test the amount of iron reduced and can be correlated to the amount of antioxidants in the sample. Trolox or ascorbic acid is usually used as reference (GÜLÇIN, 2006; SESSA et al., 2013).

The results obtained in the assessment of the antioxidant activity of free EAF as well as EAF-loaded nanoemulsions prepared using MCT and PSO are demonstrated in Table 6. With the application of the FRAP method, both the EAF and the EAF-loaded MCT-NE indicated similar antioxidant activity (54.98 and 54.56 mM of Trolox equivalent, respectively). Contrary to what expected, a lower value of trolox

equivalent antioxidant capacity was verified for EAF-loaded PSO-NE. The PSO is denser than MCT; therefore, it is more likely that the antioxidant compounds present in EAF are embedded by the PSO, hampering their solubilization in the reaction medium, and avoiding an optimal contact with the assay reagent. Similar results were obtained by Sessa et al. (2013), who evidenced the lower antioxidant capacity of grape marc extract loaded into lipid-based nanocarriers, when the antioxidant activity of encapsulated compounds was assessed using the FRAP method.

Table 6. Antioxidant activity of free EAF and EAF-loaded nanoemulsions assessed by FRAP and DPPH methods.

Samples	*FRAP* (*Trolox mM ± SD*)	*DPPH* *SC_{50} (*μg mL^{-1}* ± SD)*
EAF	54.98 ± 7.45[a]	3.10 ± 0.09
EAF-MCT-NE	54.56 ± 6.02[a]	3.58 ± 0.18[b]
EAF-PSO-NE	37.81 ± 6.45	3.95 ± 0.04[b]
Ascorbic Acid	-	3.46 ± 0.03[b]

For each assay, equal letters indicate no significant difference between the samples (F_{cal}/F_{crit} < 1.0). *SC_{50}: Radical-scavenging activity (concentration in μg mL^{-1} required for 50% reduction of DPPH radical). Values are expressed as mean ± SD (n=3).

In contrast, the SC_{50} for DPPH radical-scavenging activity was 3.10, 3.58 and 3.95 μg mL^{-1} for free EAF, EAF-MCT-NE, and EAF-PSO-NE, respectively. Among all the samples, free EAF displayed a slightly higher antioxidant activity than nanoemulsions. These SC_{50} values were considerably lower than those found by Manasathien et al. (2011) when testing the antioxidant activity of pomegranate peel ethanolic extract (SC_{50} of 51.51 μg mL^{-1}), and it may be related to the higher content of phenolic compounds in the EAF obtained from pomegranate peel dried extract. In addition, this study does not corroborate the hypothesis that the association of the polyunsaturated fatty acid of PSO and polyphenols from pomegranate peel fruits could produce a synergic effect, increasing antioxidant activity. However, studies on antioxidant activity should not be based on a single antioxidant test since there are differences between then in many aspects. Therefore, further studies concerning the antioxidant activity of free EAF and EAF-loaded nanoemulsions are still required.

4. CONCLUSIONS

In this study, we have successfully developed nanoemulsions encapsulating high concentrations of polyphenols from *P. granatum* peel fruit into PSO or MCT droplets, using emulsification/solvent evaporation and spontaneous emulsification techniques, respectively. The EAF obtained through liquid-liquid partition exhibited a great amount of phenolic compounds, which were the main compounds responsible for the antioxidant activity in both the EAF and the EAF-loaded nanoemulsions, as verified through the DPPH and FRAP assays. These compounds were quantified on the free EAF and EAF-loaded nanoemulsions using a validated HPLC-DAD method. EAF-loaded nanoemulsions developed in this study can be considered promising drug delivery systems to improve skin absorption and antioxidant effect of pomegranate polyphenols to protect skin against UV-radiation.

Conflict of interest

The authors declare the absence of conflict of interest.

Acknowledgments

The authors would like to thank the Coordination for the Improvement of Higher Education Personnel (CAPES-DS) for the financial support.

References

ABISMAIL, B.; CANSELIER, J. P.; WILHELM, A. M.; DELMAS, H.; GOURDON, C. Emulsification by ultrasound: drop size distribution and stability. **Ultrason Sonochem,** v. 6, n. 1–2, p. 75-83, 1999.

ABISMAïL, B.; CANSELIER, J. P.; WILHELM, A. M.; DELMAS, H.; GOURDON, C. Emulsification by ultrasound: drop size distribution and stability. **Ultrason Sonochem,** v. 6, n. 1–2, p. 75-83, 1999.

AFAQ, F.; SALEEM, M.; KRUEGER, C. G.; REED, J. D.; MUKHTAR, H. Anthocyanin- and hydrolyzable tannin-rich pomegranate fruit extract modulates MAPK and NF-κB pathways and

inhibits skin tumorigenesis in CD-1 mice. **Int J Cancer,** v. 113, n. 3, p. 423-433, 2005.

BASU, A.; PENUGONDA, K. Pomegranate juice: a heart-healthy fruit juice. **Nutr Rev,** v. 67, p. 49-56, 2009.

BEKIR, J.; MARS, M.; SOUCHARD, J. P.; BOUAJILA, J. Assessment of antioxidant, anti-inflammatory, anti-cholinesterase and cytotoxic activities of pomegranate (Punica granatum) leaves. **Food Chem Toxicol,** v. 55, n. 0, p. 470-475, 2013.

BENZIE, I. F. F.; STRAIN, J. J. The ferric reducing ability of plasma (FRAP) as a measure of "Antioxidant Power": The FRAP assay. **Anal Biochem,** v. 239, n. 1, p. 70-76, 1996.

BOUCHEMAL, K.; BRIANÇON, S.; PERRIER, E.; FESSI, H. Nano-emulsion formulation using spontaneous emulsification:solvent, oil and surfactant optimisation. **Int J Pharm,** v. 280, p. 241-251, 2004.

BRASIL. **Resolução RE 899 determina a publicação do "Guia para validação de métodos analíticos e bioanalíticos"**. Agência Nacional de Vigilância Sanitária 2003.

CECHINEL FILHO, V.; YUNES, R. A. Estrategies for obtaining pharmacologically active compounds from medicinal plants: concepts about structural modification for improve the activity. **Quim Nova,** v. 21, n. 1, p. 99-105, 1998.

CELIK, I.; TEMUR, A.; ISIK, I. Hepatoprotective role and antioxidant capacity of pomegranate (Punica granatum) flowers infusion against trichloroacetic acid-exposed rats. **Food Chem Toxicol,** v. 47, p. 145-149, 2009.

CHIME, S. A.; KENECHUKWU, F. C.; ATTAMA, A. A. **Nanoemulsions — Advances in formulation, characterization and applications in drug delivery**. Croatia: Intech Books, 2014.

CHOI, C. W.; KIM, S. C.; HWANG, S. S.; CHOI, B. K.; AHN, H. J.; LEE, M. Y.; PARK, S. H.; KIM, S. K. Antioxidant activity and free radical scavenging capacity between Korean medicinal plants and

flavonoids by assay-guided comparison. **Plant Sci,** v. 163, n. 6, p. 1161-1168, 2002.

DE OLIVEIRA JUNIOR, R. G.; DE SOUZA ARAÚJO, C.; SOUZA, G. R.; GUIMARÃES, A. L.; DE OLIVEIRA, A. P.; DE LIMA-SARAIVA, S. R. G.; MORAIS, A. C. S.; RIBEIRO, J. S. In vitro antioxidant and photoprotective activities of dried extracts from Neoglaziovia variegata (Bromeliaceae). **J Appl Pharm Sci,** v. 3, n. 01, p. 122-127, 2013.

DIVSALAR, A.; SABOURY, A. A.; NABIUNI, M.; ZARE, Z.; KEFAYATI, M. E.; SEYEDARABI, A. Characterization and side effect analysis of a newly designed nanoemulsion targeting human serum albumin for drug delivery. **Colloids Surf B,** v. 98, n. 0, p. 80-84, 2012.

DORA, C. L.; SILVA, L. F. C.; PUTAUX, J. L.; NISHIYANNA, Y.; PIGNOT-PAINTRAND, I.; BORSALI, R.; LEMOS-SENNA, E. Poly(ethylene glycol) hydroxystearate-based nanosized emulsions: effect of surfactant concentration on their formation and ability to solubilize quercetin. **J Biomed Nanotechnol,** v. 8, p. 1-9, 2012.

ELANGO, S.; BALWAS, R.; PADMA, V. V. Gallic acid isolated from pomegranate peel extract induces reactive oxygen species mediated apoptosis in A549 cell line. **J Cancer Ther,** v. 2, p. 638-645, 2011.

FADAVI, A.; BARZEGAR, M.; AZIZI, H. M. Determination of fatty acids and total lipid content in oilseed of 25 pomegranates varieties grown in Iran. **J Food Compost Anal,** v. 19, p. 676-680, 2006.

FISCHER, U. A.; CARLE, R.; KAMMERER, D. R. Identification and quantification of phenolic compounds from pomegranate (Punica granatum L.) peel, mesocarp, aril and differently produced juices by HPLC-DAD–ESI/MSn. **Food Chem,** v. 127, n. 2, p. 807-821, 2011.

GANESAN, P.; KUMAR, C. S.; BHASKAR, N. Antioxidant properties of methanol extract and its solvent fractions obtained from selected Indian red seaweeds. **Bioresour Technol,** v. 99, n. 8, p. 2717-2723, 2008.

GOULA, A. M.; ADAMOPOULOS, K. G. A method for pomegranate seed application in food industries: Seed oil encapsulation. **Food Bioprod Process,** v. 90, n. 4, p. 639-652, 2012.

GÜLÇIN, İ. Antioxidant activity of caffeic acid (3,4-dihydroxycinnamic acid). **Toxicol,** v. 217, n. 2–3, p. 213-220, 2006.

GUPTA, S. S.; GHOSH, S.; MAITI, P.; GHOSH, M. Microencapsulation of conjugated linolenic acid–rich pomegranate seed oil by an emulsion method. **Food Sci Technol Int,** v. 18, n. 6, p. 549-558, December 1, 2012 2012.

HASLAM, E. Vegetable tannins – Lessons of a phytochemical lifetime. **Phytochemistry,** v. 68, n. 22–24, p. 2713-2721, 2007.

HAYOUNI, E. A.; MILED, K.; BOUBAKER, S.; BELLASFAR, Z.; ABEDRABBA, M.; IWASKI, H.; OKU, H.; MATSUI, T.; LIMAM, F.; HAMDI, M. Hydroalcoholic extract based-ointment from Punica granatum L. peels with enhanced in vivo healing potential on dermal wounds. **Phytomedicine,** v. 18, n. 11, p. 976-984, 2011.

HEURTAULT, B.; SAULNIER, P.; PECH, B.; PROUST, J.-E.; BENOIT, J.-P. Physico-chemical stability of colloidal lipid particles. **Biomaterials,** v. 24, n. 23, p. 4283-4300, 2003.

HOELLER, S.; SPERGER, A.; VALENTA, C. Lecithin based nanoemulsions: A comparative study of the influence of non-ionic surfactants and the cationic phytosphingosine on physicochemical behaviour and skin permeation. **Int J Pharm,** v. 370, n. 1–2, p. 181-186, 2009.

HORA, J. J.; MAYDEW, E. R.; LANSKY, E. P.; DWIVEDI, C. Chemopreventive effects of pomegranate seed oil on skin tumor development in CD1 mice. **J Med Food,** v. 6, n. 3, p. 157-161, 2003.

ICH STEERING COMMITTEE. International Conference on Harmonization of Technical Requeriments for Registration of Pharmaceuticals for Human Use, Validation of analytical procedures: Text and methodology. Geneva, Switzerland 2005.

ISMAIL, T.; SESTILI, P.; AKHTAR, S. Pomegranate peel and fruit extracts: A review of potential anti-inflammatory and anti-infective effects. **J Ethnopharmacol,** v. 143, n. 2, p. 397-405, 2012.

KASAI, K.; YOSHIMURA, M.; KOGA, T.; ARII, M.; KAWASAKI, S. Effects of Oral Administration of ellagic acid-rich pomegranate extract on ultraviolet-induced pigmentation in the human skin. **J Nutr Sci Vitaminol,** v. 52, n. 5, p. 383-388, 2006.

KAUR, C. D.; SARAF, S. Development of photoprotective creams with antioxidant polyphenolic herbal extracts. **Res J Med Plant,** v. 6, p. 83-91, 2012.

KAUR, C. D.; SARAF, S. Photoprotective herbal extract loaded nanovesicular creams inhibiting ultraviolet radiations induced photoaging. **Int J Drug Delivery**, v. 3, n. 4, p. 699-711, 2012.

KENTISH, S.; WOOSTER, T. J.; ASHOKKUMAR, M.; BALACHANDRAN, S.; MAWSON, R.; SIMONS, L. The use of ultrasonics for nanoemulsion preparation. **Innov Food Sci Emerg Technol,** v. 9, n. 2, p. 170-175, 2008.

KOMAIKO, J.; MCCLEMENTS, D. J. Low-energy formation of edible nanoemulsions by spontaneous emulsification: Factors influencing particle size. **J Food Eng,** v. 146, n. 0, p. 122-128, 2015.

LAMBERS, H.; PIESSENS, S.; BLOEM, A.; PRONK, H.; FINKEL, P. Natural skin surface pH is on average below 5, which is beneficial for its resident flora. **Int J Cosmet Sci,** v. 28, n. 5, p. 359-370, 2006.

LANDETE, J. M. Ellagitannins, ellagic acid and their derived metabolites: A review about source, metabolism, functions and health. **Food Res Int,** v. 44, n. 5, p. 1150-1160, 2011.

LI, Z.; GU, L. Effects of mass ratio, pH, temperature, and reaction time on fabrication of partially purified pomegranate ellagitannin−gelatin nanoparticles. **J Agric Food Chem,** v. 59, n. 8, p. 4225-4231, 2011/04/27 2011.

LUO, X. D.; BASILE, M. J.; KENNELLY, E. J. Polyphenolic antioxidants from the fruits of Chrysophyllum cainito L. (Star Apple). **J Agric Food Chem,** v. 50, n. 6, p. 1379-1382, 2002.

MANASATHIEN, J.; KUPITTAYANANT, S.; INDRAPICHATE, K. Protective efficacy of pomegranate (Punica granatum Linn., Punicaceae) peel ethanolic extracts on UVB-irradiated rat skin. **American-Eurasian Journal of Toxicology Sciences 3,** v. 4, p. 250-258, 2011.

MASON, T. G.; WILKING, J. N.; MELESON, K.; CHANG, C. B.; GRAVES, S. M. Nanoemulsions: formation, structure, and physical properties. **J Phys Condens Matter,** v. 18, n. 41, p. R635, 2006.

MELO, I. L. P.; CARVALHO, E. B. T.; MANCINI-FILHO, J. Pomegranate seed oil (Punica granatum L.): A source of punicic acid (conjugated alpha-linolenic-acid). **Plant Foods Hum Nutr,** v. 2, n. 1, p. 1024, 2014.

MOHAGHEGHI, M.; REZAEI, K.; LABBAFI, M.; EBRAHIMZADEH MOUSAVI, S. M. Pomegranate seed oil as a functional ingredient in beverages. **Eur J Lipid Sci Technol,** v. 113, n. 6, p. 730-736, 2011.

NEYRINCK, A. M.; VAN HÉE, V. F.; BINDELS, L. B.; DE BACKER, F.; CANI, P. D.; DELZENNE, N. M. Polyphenol-rich extract of pomegranate peel alleviates tissue inflammation and hypercholesterolaemia in high-fat diet-induced obese mice: potential implication of the gut microbiota. **Br J Nutr,** v. 109, n. 05, p. 802-809, 2013.

PACHECO-PALENCIA, L. A.; NORATTO, G.; HINGORANI, L.; TALCOTT, S. T.; MERTENS-TALCOTT, S. U. Protective effects of standardized pomegranate (Punica granatum L.) polyphenolic extract in ultraviolet-irradiated human skin fibroblasts. **J Agric Food Chem,** v. 56, n. 18, p. 8434-8441, 2008/09/24 2008.

PANICHAYUPAKARANANT, P.; ITSURIYA, A.; SIRIKATITHAM, A. Preparation method and stability of ellagic acid-rich pomegranate fruit peel extract. **Pharm Biol,** v. 48, n. 2, p. 201-205, 2010.

QU, W.; PAN, Z.; MA, H. Extraction modeling and activities of antioxidants from pomegranate marc. **J Food Eng,** v. 99, n. 1, p. 16-23, 2010.

RAHIMI, H. R.; ARASTOO, M.; OSTAD, S. N. A Comprehensive review of Punica granatum (pomegranate) properties in toxicological, pharmacological, cellular and molecular biology researches. **Iran J Pharm Res,** v. 11, n. 2, p. 385-400, Spring 2012.

SCHRAMM, L. L. In: (Ed.). **Emulsions, foams and suspensions: fundamentals and applications**. Germany: Wiley-VCH, 2005. p.4-5.

SESSA, M.; CASAZZA, A.; PEREGO, P.; TSAO, R.; FERRARI, G.; DONSÌ, F. Exploitation of polyphenolic extracts from grape marc as natural antioxidants by encapsulation in lipid-based nanodelivery systems. **Food Bioprocess Technol,** v. 6, n. 10, p. 2609-2620, 2013.

SILVA, A. P. C.; NUNES, B. R.; DE OLIVEIRA, M. C.; KOESTER, L. S.; MAYORGA, P.; BASSANI, V. L.; TEIXEIRA, H. F. Development of topical nanoemulsions containing the isoflavone genistein. **Pharmazie,** v. 64, n. 1, p. 32-35, 2009.

SOUSA, C. M. M.; ROCHA-SILVA, H.; VIEIRA-JR, G. M.; AYRES, M. C. C.; COSTA, C. L. S.; ARAÚJO, D. S.; CAVALCANTE, L. C. D.; BARROS, E. D. S.; ARAÚJO, P. B. M.; BRANDÃO, M. S.; CHAVES, M. H. Fenóis totais e atividade antioxidante de cinco plantas medicinais. **Quim Nova,** v. 30, n. 2, p. 351-355, 2007.

SYED, D. N.; MALIK, A.; HADI, N.; SARFARAZ, S.; AFAQ, F.; MUKHTAR, H. Photochemopreventive effect of pomegranate fruit extract on UVA-mediated activation of cellular pathways in normal human epidermal keratinocytes. **Photochem Photobiol,** v. 82, n. 2, p. 398-405, 2006.

TRONCOSO, E.; AGUILERA, J.; MCCLEMENTS, D. Development of nanoemulsions by an emulsification-evaporation technique. Food process engineering in a changing world. Proceedings of the 11th International Congress on Engineering and Food, 2011. p.929-930.

VIUDA-MARTOS, M.; FERNÁNDEZ-LÓPEZ, J.; PÉREZ-ÁLVAREZ, J. A. Pomegranate and its many functional components as related to human health: A review. **Compr Rev Food Sci Food Saf,** v. 9, n. 6, p. 635-654, 2010.

Publicação: "Protection against oxidative damage in human erythrocytes and preliminary photosafety assessment of *Punica granatum* seed oil nanoemulsions entrapping polyphenol-rich ethyl acetate fraction"

Artigo *in press* (2015) no periódico Toxicology *In Vitro*

Protection against Oxidative Damage in Human Erythrocytes and Preliminary Photosafety Assessment of *Punica granatum* Seed Oil Nanoemulsions Entrapping Polyphenol-rich Ethyl Acetate Fraction

Thaisa Baccarin [a,b], *Montserrat Mitjans* [a], *Elenara Lemos-Senna* [b], *Maria Pilar Vinardell* [a*]

[a] Departament de Fisiologia, Facultat de Farmàcia, Universitat de Barcelona, Av. Joan XXIII s/n, E-08028 Barcelona, Spain.

[b] Programa de Pós-Graduação em Farmácia, Centro de Ciências da Saúde, Universidade Federal de Santa Catarina, Campus Universitário Trindade, 88040-970 Florianópolis, SC, Brazil.

Corresponding author email: mpvinardellmh@ub.edu. Departament de Fisiologia, Facultat de Farmàcia, Universitat de Barcelona, Av. Joan XXIII s/n, E-08028 Barcelona, Spain. Phone number: +34 934 024505; Fax number: +34 934035901.

ABSTRACT

The main purpose of the present study is to evaluate the ability of nanoemulsion entrapping pomegranate peel polyphenol-rich ethyl acetate fraction (EAF) prepared from pomegranate seed oil and medium chain triglyceride to protect human erythrocyte membrane from oxidative damage and to assess preliminary *in vitro* photosafety. In order to evaluate the phototoxic effect of nanoemulsions, human red blood cells (RBCs) are used as a biological model and the rate of haemolysis and photohaemolysis (5 J cm^{-2} UVA) is assessed *in vitro*. The level of protection against oxidative damage caused by the peroxyl radical generator AAPH in human RBCs as well as its effects on bilayer membrane characteristics such as fluidity, protein profile and RBCs morphology are determined. EAF-loaded nanoemulsions do not promote haemolysis or photohaemolysis. Anisotropy measurements show that nanoemulsions significantly retrain the increase in membrane fluidity caused by AAPH. SDS-PAGE analysis reveal that AAPH induced degradation of membrane proteins, but that nanoemulsions reduce the extend of degradation. Scanning electron microscopy examinations

corroborate the interaction between AAPH, nanoemulsions and the RBCs membrane bilayer. Our work demonstrates that *P. granatum* nanoemulsions are photosafe and protect RBCs against oxidative damage and possible disturbance of the lipid bilayer of biomembranes. Moreover it suggests that these nanoemulsions could be promising new topical products to reduce the effects of sunlight on skin.

Keywords: *Punica granatum*, seed oil, polyphenol-rich ethyl acetate fraction, fluorescent probes, haemolysis, photohaemolysis.

1. INTRODUCTION

The peel extract of *Punica granatum*, popularly known as pomegranate, contains a large quantity of phenolic compounds such as ellagic acid, gallic acid, punicalagin, punicalin, luteolin and others (AMAKURA et al., 2000; VAN ELSWIJK et al., 2004; SEERAM et al., 2005). Pomegranate seed oil (PSO) contains conjugated fatty acids, in which the main constituent is punicic acid (EL-NEMR et al., 2006; FADAVI et al., 2006), that it has been reported to have antioxidant properties (QU et al., 2010). Phenolic compounds are natural antioxidants and are candidates for the ultraviolet photoprotection and prevention of ultraviolet radiation-induced oxidative stress and skin alteration, especially given their capacity to reduce the production of radicals, and their ability to stabilize reactions induced by oxygen and its radical species (GONZÁLEZ et al., 2013); promising applications of polyphenols exist in the cosmetic and pharmaceutical industries.

In a previous study, we developed PSO and medium chain triglyceride (MCT) nanoemulsion entrapping a pomegranate polyphenol-rich ethyl acetate fraction (EAF) for UV photoprotection application. Nanoemulsions (NEs) have attracted considerable attention for cosmetic and personal care as potential vehicles for releasing and improving the permeation of active compounds through the skin (GUGLIELMINI, 2008). The *in vitro* antioxidant activity of free EAF and NE loaded with EAF (EAF-PSO-NE and EAF-MCT-NE) was confirmed using the ferric reducing antioxidant power (FRAP) and 2,2-diphenyl-1-picrylhydrazyl (DPPH) methods (BACCARIN and LEMOS-SENNA, 2014).

The assessment of the toxicity potential of new molecules and formulations for human use is fundamental and it has become

imperative for the nonclinical toxicologist to establish new approaches for early screening of potential cosmetic and pharmaceutical products candidates (Ahuja and Sharma, 2014). In particular, phototoxicity is of increasing concern in dermatology because of the increased level of ultraviolet radiation reaching the earth from the sun (ONOUE et al., 2009). Phototoxicity can be caused by several classes of pharmaceuticals and cosmetics, which have the potential to provoke photoirritant, photoallergic and photogenotoxic events in light-exposed tissues through oxidation and chemical modification under exposure to sunlight (Stein et al., 2007; Elkeeb et al. 2012).

Although there is no single method that provides all the toxicity information required, and since different nanosized systems elicit different biological responses, during the process of determining and studying the toxicological behaviour of a sample a combination of assays is often required. *In vitro* haemolysis is one of these assays (DOKTOROVOVA et al., 2014) and evaluates the biocompatibility of nanodroplets and formulation components (*i.e.* surfactants, lipid) (SCHUBERT and MÜLLER-GOYMANN, 2005; SÖDERLIND and KARLSSON, 2006) via the impact of their physico-chemical characteristics on human red blood cells (RBCs), which is evaluated by quantifying the release of haemoglobin (ARORA et al., 2012).

Therefore, the aim of this work was to evaluate the potential protective effect of free EAF, unloaded and EAF-loaded NEs against oxidative damage caused by the peroxyl radical generator 2,2′-azobis (amidinopropane dihydrochloride) (AAPH) in human erythrocytes and also to identify any possible irritant reactions; the potential irritancy and photo irritancy were assessed by *in vitro* haemolysis and photohaemolysis, respectively. The erythrocyte was chosen as an *in vitro* model since its membrane is rich in polyunsaturated fatty acids, which are extremely susceptible to free radical-mediated peroxidation; besides, erythrocytes have no internal organelles and because they are the simplest cell model available, they are the most popular cell membrane system for verifying possible membrane interactions and are considered to be representative of the plasma membrane in general (SVETINA et al., 2004; MAGALHÃES et al., 2009). Oxidative damage of the erythrocyte membrane may cause its malfunctioning by altering its fluidity and protein profile, manifested by decreased reduction in cytoskeletal protein content (low-molecular-weight, LMW) and the production of high-molecular-weight (HMW) proteins (FLYNN et al., 1983; SNYDER et al., 1985) and abnormalities in erythrocyte shape

(YANG et al., 2006). Since these events have been proposed as a general mechanism leading to the haemolysis involved in cell injury and death (ALVAREZ-SUAREZ et al., 2012), we also evaluated them after RBCs were incubated with treatments.

To the best of our knowledge, this is the first time that the protective effect against oxidative damage in human erythrocytes of NE entrapping *P. granatum* peel polyphenol-rich EAF prepared using PSO or MCT as oil phases and their preliminary photosafety have been assessed using the above mentioned assays.

2. MATERIALS AND METHODS

2.1. Materials

Polysorbate 80 (Tween 80®), 2,2'-Azobis(2-methyl-propionamidine) dihydro-chloride (AAPH), triethanolamine, hydrogen peroxide 30% (w/w), sodium azide, sodium dodecyl sulfate (SDS), Triton X-100 and glycine were purchased from Sigma-Aldrich (St. Louis, MO, USA). NaCl, Na_2HPO_4 and KH_2PO_4 were purchased from Merck (Darmstadt, Germany). Ethyl acetate, dichloromethane, acetic acid and methanol were obtained from Vetec® (Rio de Janeiro, Brazil). Pomegranate seed oil and pomegranate fruit peel dry extract were purchased from Via Farma (Sao Paulo, Brazil). Soy lecithin (Lipoid® S100) was from Lipoid AG (Steinhausen, Switzerland). Medium chain triglyceride was from Brasquim (Porto Alegre, Brazil). Fluorescent probes DPH (1,6-diphenyl-1,3,5-hexatriene) and TMA-DPH (1-(4-trimethylammonium phenyl)-6-phenyl-1,3,4-hexatriene *p*-toluenesulfonate) were purchased from Molecular Probes (Eugene, OR). Acrylamide PAGE 40%, methylenebisacrylamide 2%, TEMED, mercaptoethanol, ammonium persulfate and bromophenol blue used for SDS-PAGE were obtained from GE Healthcare Amersham Biosciences (Uppsala, Sweden). Finally, water was purified in a Milli-Q system (Millipore, Bedford, MA).

2.2 Methods

2.2.1 Ethyl acetate fraction (EAF)

The pomegranate polyphenol-rich ethyl acetate fraction (EAF) was obtained from a commercial pomegranate peel dried extract and

characterized through a high performance liquid chromatography (HPLC) method and spectrophotometric method (Folin-Ciocalteu) as described in our previously work (BACCARIN and LEMOS-SENNA, 2014). Briefly, the dried powder was extracted by 24 hour dynamic maceration with a 90:10 (v/v) methanol:water mixture. The extractive solution was evaporated under reduced pressure for solvent removal, and the precipitate was suspended with a 2% aqueous acetic acid solution. The resulting mixture was then partitioned with dichloromethane and ethyl acetate. After that, the pooled ethyl acetate fraction was evaporated under reduced pressure to dryness.

2.2.2 Preparation of nanoemulsions

EAF-loaded pomegranate seed oil nanoemulsion (EAF-PSO-NE) or EAF-loaded medium chain triglyceride nanoemulsion (EAF-MCT-NE) were prepared using an ultrasonic emulsification method followed by solvent evaporation or spontaneous emulsification method, respectively (BACCARIN and LEMOS-SENNA, 2014). Briefly, for the EAF-PSO-NE, the ethyl acetate fraction (EAF) (0.5%; w/v), soy lecithin (0.4%; w/v) and PSO (2%; w/v) were dissolved in 10 mL of ethyl acetate. This ethyl acetate solution was slowly poured into 40 mL of a polysorbate 80 (2.1%; w/v) aqueous solution. The oil in water dispersion was sonicated for 3 minutes using an Ultrasonic Processor UP200S (Hielscher, Germany), adjusted to pH 5.0-6.5 with triethanolamine (2%; w/v) and then it was and kept under magnetic stirring for 24 hours. The resulting nanoemulsion was evaporated under reduced pressure up to volume of 15 mL.

For the EAF-MCT-NE, 10 mL of an ethanolic solution containing EAF (0.5%; w/v), soy lecithin (0.4%; w/v), and MCT (1.8%, w/v) was poured into a 2.1% (w/v) polysorbate 80 aqueous solution under magnetic stirring and adjusted to pH 5.0-6.5 with triethanolamine (2%; w/v). The nanoemulsion was then evaporated under reduce pressure to eliminate the organic solvent and concentrated up to volume of 15 mL. All formulations were filtered through 8 µm quantitative filter paper. Unloaded PSO-NE and MCT-NE were prepared in the same manner.

2.2.3 Physicochemical characterization of nanoemulsions

The mean droplet size and zeta potential were determined by dynamic light scattering (DLS) and laser-Doppler anemometry, respectively, using a Zetasizer Nano Series (Malvern Instruments, Worcestershire, UK). The size analyses were performed at a scattering angle of 173^{o}, after appropriated dilution of the samples in ultrapure water (Milli-Q®, Millipore, USA). For zeta potential analysis, the samples were diluted in Milli-Q® water and placed in electrophoretic cells where a potential of ±150 mV was applied. The zeta potential values were calculated as mean electrophoretic mobility values by using Smoluchowski's equation.

2.2.4 Preparation of red blood cell suspensions

Blood samples were obtained from anesthetized rats by cardiac puncture or from healthy volunteers from the Blood Bank of "Hospital Clinic" (Barcelona, Spain). All procedures followed the ethical guidelines of the University of Barcelona. Red blood cells (RBCs) were isolated by centrifugation at 3000 rpm at 4 ºC for 10 minutes, and washed three times in isotonic PBS containing 123.3 mM NaCl, 22.2 mM Na_2HPO_4 and 5.6 mM KH_2PO_4 in distilled water (pH 7.4).

2.2.5 Haemolysis assay

The membrane-lytic activity of EAF, NE and formulation components (polysorbate 80, lecithin, MCT and PSO) was determined through haemolysis assay. A 25 µL aliquot of rat or human erythrocyte suspension was exposed to each sample at various concentrations: EAF (10-1000 µg mL^{-1}), polysorbate 80 (0.5-80 mg mL^{-1}), lecithin (0.1-10 mg mL^{-1}), MCT (1-55 mg mL^{-1}), PSO (1-60 mg mL^{-1}), unloaded (MCT-NE and PSO-NE) and EAF-loaded nanoemulsions (EAF-MCT-NE and EAF-PSO-NE) (5-500 µg mL^{-1}) diluted in PBS solution in a total volume of 1 mL. Negative and positive controls were prepared by resuspending erythrocyte in buffer alone or distilled water, respectively. The samples were incubated at room temperature under constant shaking for 10 min, and then centrifuged at 10,000 rpm for 5 min. The absorbance of the haemoglobin released in the supernatant was measured at 540 nm using a Shimadzu UV-160A spectrophotometer (Shimadzu, Kyoto, Japan), and the percentages of haemolysis were

obtained by comparing the sample absorbance with the positive control (totally haemolysed). Dose-response curves were plotted from haemolysis results and the concentrations inducing 50% haemolysis (HC_{50}) were calculated .(NOGUEIRA, D. et al., 2012).

2.2.6 Haemolysis induced by H_2O_2

The haemolysis induced by H_2O_2 was measured as reported by Ugartondo and collaborators (UGARTONDO et al., 2009) with modifications. First, 250 µL of the human erythrocyte suspension, previously incubated with sodium azide (2 mM), was mixed with various concentrations of EAF (25-150 µg mL^{-1}), EAF-MCT-NE (25-100 µg mL^{-1}), EAF-PSO-NE (50-200 µg mL^{-1}). Then H_2O_2 was added and the mixture incubated for 90 min at 37 ºC under stirring. The volume of each sample was adjusted to 1 mL with PBS. After final incubation, the samples were centrifuged at 10,000 rpm for 5 min, the supernatant was diluted 1:10 in PBS and the absorbance of the haemoglobin released was measured at 540 nm using a Shimadzu UV-160A spectrophotometer (Shimadzu, Kyoto, Japan). The percentages of haemolysis were obtained by comparing the sample absorbance with the positive control (totally haemolysed). The concentration inhibiting 50% of the haemolysis caused by H_2O_2 (IC_{50}) was determined for each sample. The experiment was carried out three times using three replicate samples for each sample concentration tested.

2.2.7 Photohaemolysis assay

Twenty-five microliter of rat or human red blood cell suspension were added to a 24-well plate containing 500 µg mL^{-1} of EAF, EAF-MCT-NE, EAF-PSO-NE, MCT-NE or PSO-NE. Then, one plate was exposed to UVA (TL-D 15 W/10 UVA lamp, Royal Philips Eletronics-The Netherlands) and the other was kept in the dark. Irradiance was measured using a Delta OHM photoradiometer (HD2302-Italy) to determine the time of exposure, using the formula:

$$E\ (J/cm^2) = t(s) \times P(W/cm^2) \qquad \text{Eq. 1}$$

where E is UV dose, t is the time expressed in seconds and, finally, P is the lamp potency. Cells were irradiated with 1.6-2.1 mW/cm^2 to give a final exposure of 5 J cm^2.

After irradiation the contents of each well were transferred to a tube and centrifuged at 1000 rpm for 5 minutes. The absorbance of the supernatant was measured at 525 nm using a Shimadzu UV-160A spectrophotometer (Shimadzu, Kyoto, Japan). The HC_{50} was determined for plates exposed and non-exposed to the UVA irradiation. The photohaemolysis factor (PHF) was calculated by dividing the HC_{50} of the non-irradiated cells by the HC_{50} of the irradiated cells. The haemoglobin oxidation assay measured the formation of intracellular and extracellular methaemoglobin. The same assay conditions as those of the photohaemolysis assay were used, except that 100 µL of Triton X-100 1% (v/v) solution was added to each irradiated and non-irradiated well and the absorbance of methaemoglobin was measured at 630 nm. The amount of methaemoglobin in the sample was determined by the difference in optical density (ΔOD) between the irradiated and non-irradiated plate. A product is considered photoirritant if the PHF is ≥ 3.0 or if the ΔOD is ≥ 0.05 (PAPE et al., 2001).

2.2.8 Haemolysis mediated by AAPH

The haemolysis mediated by AAPH followed a method previously described in the literature, with some modifications (MIKI et al., 1987). The addition of AAPH (a peroxyl radical initiator) to the human erythrocyte suspension induces the oxidation of cell membrane lipids and proteins, resulting in haemolysis. Aliquots of 83 µL of the human erythrocyte suspension were incubated with AAPH at a final concentration of 50 mM for 2.5 h in a shaker at 37 ºC to achieve 100% haemolysis. The antihaemolytic activity of EAF (0.5-50 µg mL^{-1}), MCT-NE (5-100 µg mL^{-1}), EAF-MCT-NE (5-100 µg mL^{-1}), PSO-NE (5-100 µg mL^{-1}) and EAF-PSO-NE (5-100 µg mL^{-1}) was tested by adding several concentrations of each sample to the erythrocyte suspension in the presence of AAPH. A negative control (erythrocyte suspension with PBS alone) was included in all experiments to monitor spontaneous haemolysis. Samples plus erythrocyte suspension were also incubated without AAPH to determine whether the sample alone could cause haemolysis during 2.5 h of incubation. After incubation, the samples were centrifuged at 10,000 rpm for 5 min and the absorbance of

the supernatant was measured at 540 nm in a Shimadzu spectrophotometer. The concentration inhibiting 50% of the haemolysis (IC_{50}) was determined for each sample.

2.2.9 Scanning electron microscopy – SEM

After 2.5 h of incubation, unwashed samples were fixed by adding 1 mL of 5.0% glutaraldehyde in PBS solution and incubated at 4 ºC for 2 h. The samples were then centrifuged (1500 rpm for 10 min), the supernatant was discarded, and 1 mL of 2.5% glutaraldehyde in PBS was added. Fixed samples were washed with PBS solution, post-fixed with 1% osmium tetroxide, placed over a glass coverslip, dehydrated in an ascending series of ethyl alcohol (50–100%), air-dried using the critical point drying method in a CPD 7501 apparatus (Polaron, Watford, UK), and finally mounted on an aluminium stub and gold-coated in an SEM coating system SC 510 (Fisons Instruments, East Grinstead, UK). The resulting specimens were examined in a Zeiss DSM 940A scanning electron microscope (Carl Zeiss SMT AG, Jena, Germany).

2.2.10 Erythrocyte ghost preparation

After treatments and incubation for 2.5 hours, human erythrocyte ghost membranes were prepared following the procedure proposed by Fairbanks (FAIRBANKS et al., 1971). Samples were centrifuged and the erythrocyte pellet was resuspended and washed with buffer (Na_2HPO_4 5mM, pH 8.0) several times until white ghost membranes were obtained. The protein content of erythrocytes ghost cell membranes was measured using the Bio-Rad assay (Bio-Rad, Hercules, CA), which is based on the dye-binding procedure of Bradford (BRADFORD, 1976), using bovine serum albumin (BSA) as a protein standard.

2.2.11 SDS-PAGE

Sodium dodecyl sulfate-polyacrylamine gel electrophoresis of membrane proteins was performed according to Miki and collaborators (MIKI et al., 1987) using a Mini-PROTEAN Tetra Cell unit (Bio-Rad, Hercules, CA). Erythrocyte ghost membranes were mixed with SDS sample buffer, heated at 95 ºC for 5 min and then a total of 25 µg of

protein was electrophoresed in parallel into 12.5% SDS-polyacrylamide gel under reducing conditions (slab gel consisted of 7.5% polyacrylamide resolving gel and 5% polyacrilamide stacking gel). Electrophoresis was carried out at 60V for 10 min followed by 35 min at 200V. Protein bands were viewed by staining with Coomassie brilliant blue R-250 for 50 min under gentle shaking and destained with a mixture of 7.5% methanol and 10% acetic acid. The molecular weight of the membrane proteins was estimated from the molecular size marker (Bio-Rad Precision Plus Unstained Standard), ranging from 10 to 250 kDa. Electrophoresis gel was digitized on a computer through a video camera. Thereafter, ImageJ software was used to calculate the average pixel intensity of bands 1, 2, 3, 4.1, 4.2 and 5 within regions of interest (ROI) drawn on the collected gel images. Bands colour intensity was measured in triplicate for each treatment. The results were expressed as percentage of band colour intensity compared with control (100%) (NOGUEIRA, D. R. et al., 2012).

2.2.12 Cell membrane fluidity

To determine cell membrane fluidity, fluorescence anisotropy measurements were carried out using DPH and TMA-DPH fluorescent probes.(NOGUEIRA, D. R. et al., 2012) Treated and non-treated human red blood cells suspensions (haematocrit of 0.01%) in PBS were labelled with the fluorescent probes (final concentration in samples 10^{-6} M) at room temperature for 1 hour in dark conditions. Changes in membrane fluidity were also evaluated in samples incubated without AAPH to determine whether treatment alone can interfere in cell membrane fluidity. Steady-state anisotropy was measured using an SLM-Amino AB-2 spectrofluorometer, with polarizers in the L configuration in a quartz cuvette at room temperature. Samples were illuminated with linearly (vertically or horizontally) polarized monochromatic light (λ_{ex} = 365 nm), and the fluorescence intensities (λ_{em} = 425 nm), emitted parallel or perpendicular to the direction of the excitation beam (slit widths of 8 nm), were recorded. Fluorescence anisotropy (*r*) was calculated automatically by software provided with the instrument, according to the following equation:

$$r = \frac{(Ivv - Ivh \times G)}{(Ivv + 2Ivh \times G)} \qquad \text{Eq. 2}$$

where I_{vv} and I_{vh} represent the components of the light intensity emitted in parallel and perpendicular, respectively, to the direction of the vertically polarized excitation light. The factor $G = I_{hv}/I_{hh}$ was used to correct the inequality of the detection beam to horizontally and vertically polarized emission.

2.2.13 Statistical analysis

Each assay was carried out on three independent experiments using three replicate samples for each sample concentration tested. Statistical analyses were performed using one-way analysis of variance (ANOVA) followed by Dunnett's or Tukey's post-hoc test for multiple comparisons using GraphPad Prism 5.0 software. Differences were considered significant for $p < 0.05$ and $p < 0.001$.

3. RESULTS

3.1 Physicochemical characterization of the nanoemulsions

It is important to determine the physicochemical characteristics of NE since these characteristics may not only alter the biological but also the toxicological response (RIVERA GIL et al., 2010). Table 1 summarizes the physicochemical characteristics of unloaded and EAF-loaded NEs. The average size of all formulations, were about 200 nm, with the unloaded NE smaller than the loaded ones. The polydispersity indexes (PI) were < 0.2, indicating that monodisperse colloidal dispersions were obtained. Zeta potential, which describes the surface charge of the NE droplets, varied from -20.1 to -24.7 mV, giving an indication of the physical stability of the colloidal dispersions (MISHRA et al., 2009; MITRI et al., 2011).

Table 1. Physicochemical characterization of unloaded and EAF-loaded nanoemulsions.

Samples	Size (nm)	Zeta potential (mV)	Polydispersity Index
EAF-PSO-NE	201.2 ± 3.8	-21.9 ± 2.2	0.17 ± 0.02
PSO-NE	180.7 ± 4.0	-20.1 ± 1.8	0.17 ± 0.01
EAF-MCT-NE	202.5 ± 1.3	-25.7 ± 4.0	0.11 ± 0.03
MCT-NE	186.5 ± 3.3	-22.3 ± 0.3	0.18 ± 0.01

*Results are expressed as mean ± SD of at least 3 independent analyses.

3.2 Haemocompatibility and photohaemolysis studies

In the haemolysis assay the HC_{50} for the isolated formulations components was 7.25 ± 0.02 mg mL^{-1}, 1790 ± 1.83 mg mL^{-1}, 45.9 ± 0.07 mg mL^{-1}, 15.37 ± 0.54 mg mL^{-1} and > 1 mg mL^{-1}, for soy lecithin, polysorbate 80, PSO, MCT and free EAF, respectively; for EAF-loaded nanoemulsions (EAF-PSO-NE; EAF-MCT-NE) and unloaded nanoemulsions (PSO-NE; MCT-NE) was > 0.5 mg mL^{-1}. When the RBCs were irradiated, the EAF-loaded NEs (EAF-PSO-NE; EAF-MCT-NE) did not demonstrate a photohaemolitic behaviour.

3.3 Haemolysis mediated by H_2O_2 and AAPH

After verifying the haemolytic capacity of EAF and EAF-loaded NEs, their capacity to protect human RBCs against haemolysis induced by H_2O_2 and AAPH was evaluated (Figure. 1).

Figure 1. Protective effect of *P. granatum* EAF and EAF-loaded nanoemulsions against oxidative haemolysis induced by H_2O_2 and AAPH. Results are expressed as mean ± SEM of at least 3 independents assays. Statistical analyses were performed by ANOVA followed by Tukey's multiple comparison test (p<0.05). Same letters mean no statistical difference.

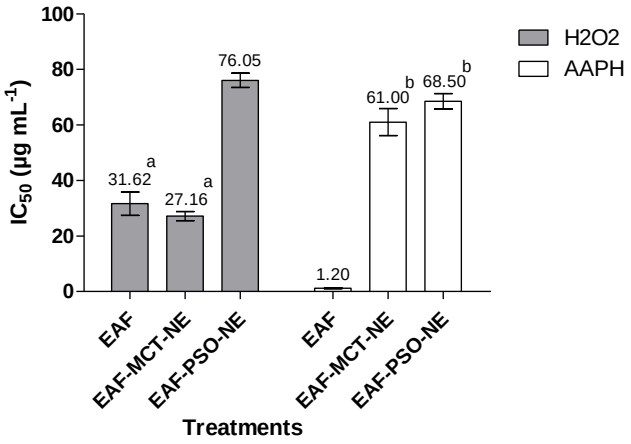

Oxygen free radicals are implicated in many biological processes and for the most part, the endogenous antioxidant system can manage their detoxification. However, certain external events can trigger the production of these damaging free radicals. Hydroxyl ($OH^{\bullet}$) and superoxide ($O_2^{\bullet-}$) free radical are two oxygen free radical species in biological systems. Normally, the enzymes catalase, superoxide dismutase, and glutathione peroxidase maintain these free radicals at low levels, but under certain circumstances, higher levels of these compounds may be available, thus leading to oxidative damage (FLOYD and LEWIS, 1983).

Hydrogen peroxide is generated by the dismutation of superoxide radical, catalysed by superoxide dismutase enzymes and directly produced by oxidase enzymes. It can lead the production of hydroxyl free radicals either by exposure to ultraviolet light or by interaction with transition metal ions, mostly iron (Fenton-type reaction) (HALLIWELL et al., 2000). Also, hydrogen peroxide may enter the human body through skin contact; it crosses the RBC lipid membrane and acts on the

intracellular moiety, forming hydroxyl radicals that can initiate lipid peroxidation and cause cell damage (BLASA et al., 2007; ALAM et al., 2013). In the case of haemolysis induced by H_2O_2 the IC_{50} of EAF and EAF-MCT-NE did not differ significantly, being 31.62 and 27.16 µg mL^{-1}, respectively; EAF-PSO-NE presented a slightly higher IC_{50}, at 76.05 µg mL^{-1}. During AAPH-induced haemolysis the EAF showed an IC_{50} of 1.20 µg mL^{-1} which places it at the same level of two well-known antioxidants, ascorbic acid IC_{50} 7.5 µg mL^{-1} (AMAN et al., 2013) and curcumin IC_{50} 2.94 µg mL^{-1} (BANERJEE et al., 2008). In the absence of AAPH, RBCs were stable and haemolysis was negligible (data not shown). The percentage of haemolysis in RBCs incubated only with EAF or EAF-loaded NEs was almost identical to that of the control sample (RBCs + PBS) indicating that EAF and EAF-loaded NEs themselves do not induce haemolysis.

3.4 Erythrocyte membrane fluidity

Table 2 shows the anisotropy values for both probes after AAPH assay. An increase in the *r* values (anisotropy measurement) of a probe is indicative of a decrease in the fluidity of the membrane. The baseline fluorescence for DPH and TMA-DPH was 0.2404 ± 0.0059 and 0.2456 ± 0.0065, respectively. Free EAF and EAF-loaded NEs containing PSO (EAF-PSO-NE) or MCT (EAF-MCT-NE) maintained the fluidity in the outer and inner parts of erythrocytes membranes at around baseline levels (control PBS). The presence of AAPH alone increased anisotropy values, indicating a decrease in membrane fluidity. In AAPH-induced peroxidation, free radicals are formed in the solution and attack the membranes from the external medium forming lipid hydroperoxides (ARORA et al., 2012). Co-incubated free EAF or EAF-loaded NEs managed to retrain the fluidity diminution caused by AAPH, suggesting that the polyphenols present in the EAF stop the free radicals attacking and accessing the bilayer.

Table 2. Steady-state Fluorescence Anisotropy of the probes DPH and TMA-DPH incorporated into erythrocyte membrane after AAPH assay.

Samples (μg mL^{-1})	**(r^a) DPH (mean ± SE)**	**(r^a) TMA-DPH (mean ± SE)**
Control	0.2404 ± 0.0059	0.2456 ± 0.0065
AAPH (50 mM)	0.3427 ± 0.0069^b	0.3315 ± 0.0053^b
EAF (1)	0.2488 ± 0.0060^c	0.2465 ± 0.0064^c
*EAF (1)	0.2351 ± 0.0073^c	0.2534 ± 0.0066^c
EAF-MCT-NE (50)	0.2498 ± 0.0060^c	0.2489 ± 0.0059^c
*EAF-MCT-NE (50)	0.2465 ± 0.0058^c	0.2443 ± 0.0060^c
EAF-PSO-NE (50)	0.2329 ± 0.0058^c	0.2382 ± 0.0052^c
*EAF-PSO-NE (50)	0.2449 ± 0.0079^c	0.2496 ± 0.0076^c

*Samples incubated without AAPH.
$^a r$ values = anisotropy measurements. $^b p < 0.01$ when compared to control PBS (Dunnett's post hoc test). $^c p < 0.01$ when compared to AAPH (Dunnett's post hoc test). Data represent the means of three independent experiments ± SE, each conducted in triplicate.

3.5 SDS-PAGE

Given the changes in membrane fluidity, the next step was to run an SDS-PAGE experiment to assess possible changes in membrane proteins in human erythrocytes. Oxidants basically alter the erythrocyte membrane by decreasing the LMW proteins and producing HMW proteins (FLYNN et al., 1983; SNYDER et al., 1985). Figure 2 shows the electrophoretic profile of the erythrocyte membrane proteins.

Figure 2. Protective effect of *P. granatum* EAF and EAF-loaded nanoemulsions for human erythrocyte membrane skeletal proteins after incubation with AAPH, determined by SDS-PAGE. Following preincubation of the erythrocytes for 2.5 hours in the absence or presence of AAPH and treatments, membranes were separated and washed as described in section 2.12. The major cytoskeletal protein bands are identified following the classification of Fairbanks *et al.* (FAIRBANKS et al., 1971) and are given on the right of the gel. Each lane corresponds to a different treatment: (1) protein standard; (2) control PBS (untreated membrane); (3) AAPH control; treatment with ethyl acetate fraction and nanoemulsions in the presence of AAPH (4) EAF (1 μg mL^{-1}), (5) EAF-PSO-NE (50 μg mL^{-1}), (6) EAF-MCT-NE (50 μg mL^{-1}).

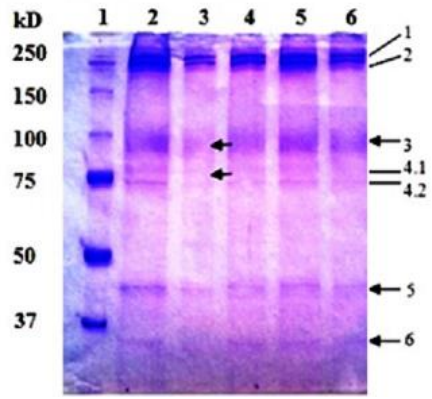

When RBCs were incubated with EAF or NE alone, the level of in erythrocyte-membrane proteins was maintained at a background level similar to that in the untreated samples (control) (data not shown). The well-established normal distribution of the major membrane cytoskeletal proteins is shown in lane 2, which contains untreated erythrocytes ghosts. AAPH treatment produced changes in the protein pattern, leading to a remarkable loss of spectrins (band 1 and 2), and band 3, 4.1, 4.2 and 5, as seen in lane 3, confirming previous results from other authors (HSEU et al., 2002; YANG et al., 2006; MARTÍNEZ et al., 2012). As shown in lanes 4, 5 and 6, the analysis of LMW proteins revealed that EAF and EAF-loaded NEs protected against AAPH-induced changes in the amount of erythrocytes membrane proteins. Table 3 shows the results expressed as the percentage of band colour intensity compared with the control (100%).

Table 3. Effect of AAPH and EAF and EAF-loaded nanoemulsions (EAF-PSO-NE and EAF-MCT-NE) on protein bands of human erythrocyte membrane.

Treatment	*Band 1 and 2*	*Band 3*	*Band 4.1 and 4.2*	*Band 5*
AAPH 50 Mm	37.42 ± 1.45*	39.65 ± 2.42*	4.96 ± 4.97*	22.94 ± 1.06*
AAPH + EAF 1 µg mL^{-1}	59.28 ± 2.05*#a	70.03 ± 4.32*#b	32.63 ± 3.49*#	50.43 ± 1.01*#
AAPH + EAF-PSO-NE 50 µg mL^{-1}	81.08 ± 1.24*#	88.02 ± 4.47*#c	61.10 ± 3.40*#d	69.08 ± 0.85*#e
AAPH + EAF-MCT-NE 50 µg mL^{-1}	60.35 ± 1.90*#a	75.29 ± 4.18*#b,c	59.49 ± 2.42*#d	65.80 ± 0.45*#e

The results are expressed as percentage of control taking control as 100%. Values are mean ± SEM of three experiments. See the Materials and Methods section for details of the analysis performed. Statistical analyses were performed by ANOVA followed by Tukey's multiple comparison tests (same letter means no statistical difference).

*Significant difference from control group ($p < 0.01$).

#Significant difference from AAPH group ($p < 0.01$).

After AAPH treatment, the amount of band 1, 2, 3, 4 and 5 proteins dropped to 37%, 40%, 5% and 23 %, respectively, in comparison with untreated erythrocytes. On the other hand, the co-treatment of erythrocytes with AAPH and EAF or EAF-loaded NEs containing PSO (EAF-PSO-NE) or MCT (EAF-MCT-NE) as the oil phase, reduced the effects of the oxidant agent on those proteins. This reduction was better and more evident when the EAF was nanoemulsified (EAF-PSO-NE or EAF-MCT-NE).

3.6 SEM analysis

The protein organization network found mainly in the inner membrane layer is responsible for the maintenance of shape and stability; once the protein network is compromised the shape of the erythrocyte may change (VITTORI et al., 2002). As mentioned previously, oxidative damage in cell membranes leads to changes in the protein profile. The effect of AAPH alone, EAF and EAF-loaded NEs co-incubated with AAPH on erythrocyte morphology was studied by SEM analysis (Figure. 3).

Figure 3. Scanning electron micrograph of normal human erythrocyte and protective effects of ethyl acetate fraction (EAF) and nanoemulsions of *P. granatum* peel extract against AAPH induced oxidative damage on RBC. A) AAPH at 50 mM; B-1) Control in PBS and B-2) Control in PBS after 2.5 h incubation; C) EAF (1.5 µg mL^{-1}) with AAPH at 50 mM; D) EAF-loaded NEs (50 µg mL^{-1}) with AAPH at 50 mM. Scale bars correspond to 10 µm.

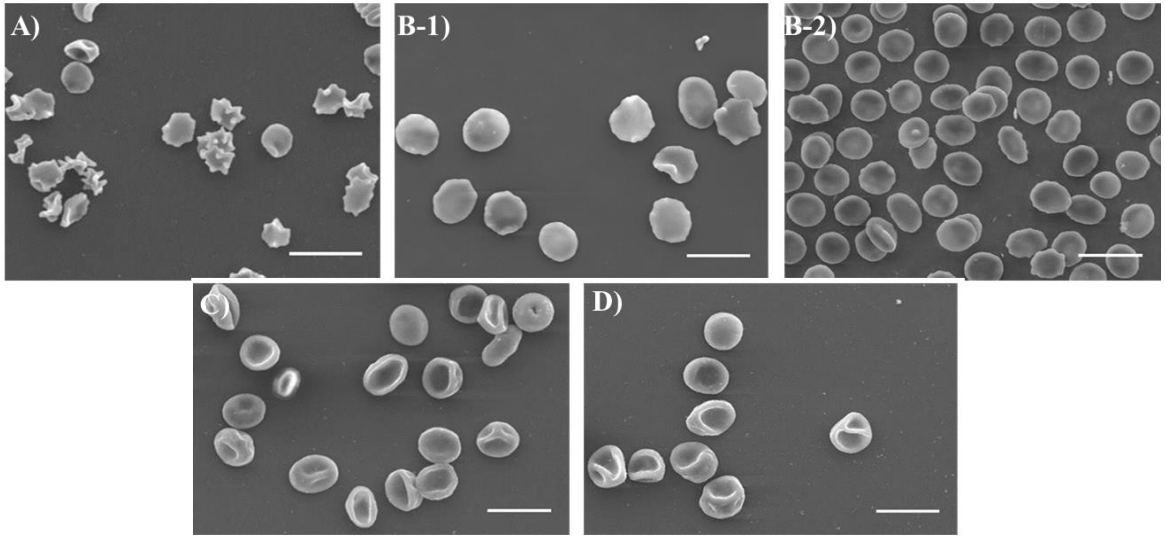

SEM examinations corroborated that AAPH, nanoemulsions and the EAF interacted with the lipid bilayer by altering the normal morphology of the RBCs. Treatment of erythrocytes with AAPH alone resulted in a significant change in shape to echinocytic or acanthocytic (Figure. 3A). In our study the control erythrocytes incubated with PBS solution for 2.5 hours presented a leptocyte-type shape (Fig. 4B-1), *i.e.* a flattened cell with reduced volume; assuming that the long incubation time was somehow deforming the RBCs, SEM preparation was then conducted immediately after adding RBCs to the PBS solution, but the findings were the same (Figure. 3B-2); it is thus likely that this was a blood sample characteristic. EAF (Figure. 3C) and EAF-loaded NEs (Figure. 3D) incubated with AAPH showed the knizocyte and stomatocyte-type deformation; knizocyte is a cell with two or three concavities while a stomatocyte is a cell with one concavity in the shape of a mouth. The EAF and EAF-loaded NEs incubated with RBCs alone did not alter the morphology of the erythrocytes that remained as the control ones (data not shown).

4. DICUSSION

Punica granatum is well known for its considerable polyphenolics content; they are bioactive secondary metabolites widely distributed in plants (HARBORNE, 1989) and contain one or more aromatic hydroxyl groups that actively scavenge free radicals and are responsible for antioxidant activity. It is essential to identify and quantify the polyphenolic compounds in both free EAF and EAF-loaded NEs, given that their capacity to protect erythrocytes against oxidation is largely related to the characteristics of these compounds. EAF contains at least 600 mg g^{-1} GAE (gallic acid equivalents) of total phenolic content, among which ellagic acid, gallic acid, and punicalagin are the major ones (8.47%, 23.86% and 29.67% w/w, respectively). The nanoemulsions presented entrapment efficiency near or above 50% depending on the chemical compound lipophilicity. Details of the polyphenol identification and quantification through HPLC method are described in a previous study (BACCARIN and LEMOS-SENNA, 2014).

Haemocompatibility testing, a major part of biocompatibility testing, comprises the evaluation of interactions of foreign material such as active compounds, excipients and/or formulations with human red blood cells and to explore possible damaging effects arising from these

combined exposure (SZEBENI, 2012). Haemolysis of human RBCs is a very good model not only for studying free radical induced oxidative damage to membranes and to evaluate the antioxidant activity of new compound or formulation, but also to determine the topical irritation and/or phototoxic potential (photohaemolysis) of these substances (PAPE et al., 1987; PAPE and HOPPE, 1991). With respect to the potential topical application of EAF-loaded NEs as a photoprotector and according to the Safety Evaluation Guide for Cosmetic Products (BRASIL, 2003a) it is extremely important to evaluate their potential topical irritation and photoirritation. Some studies have reported the photohaemolytic potential of hydroalcoholic extracts (MADARIAGA et al., 2010; TOLEDO et al., 2012). Nevertheless, there are few studies in the literature related to the effects of nanodispersions (*i.e.* nanoemulsion) and even fewer related to nanoemulsions loaded with plant extracts or extract fractions.

Several studies support the use of RBCs as a model of oxidative damage induced by AAPH (HSEU et al., 2002; YANG et al., 2006; BLASA et al., 2007; AJILA and PRASADA RAO, 2008; BANERJEE et al., 2008; CHIRINOS et al., 2008; MAGALHÃES et al., 2009; ALVAREZ-SUAREZ et al., 2012; MARTÍNEZ et al., 2012; BOTTA et al., 2014). When AAPH is added as a radical initiator, it decomposes at physiological temperature in aqueous solution to generate alkyl radicals, which in the presence of oxygen are converted to the corresponding peroxyl radicals; in turn, these peroxyl radicals induce oxidation of polyunsaturated lipids in the RBCs membrane, causing a chain reaction known as lipid peroxidation (BANERJEE et al., 2008).

Both EAF and EAF-loaded NEs demonstrated antioxidant properties against oxidative damage in the erythrocyte membrane induced by H_2O_2 or AAPH. The different IC_{50} values obtained for the H_2O_2 and AAPH assays only emphasizes the fact that conclusions about antioxidant activity should not be based on a single test model, because each assay represents a different type of oxidative damage and varies in different respects; therefore samples may also behave differently. With regard to AAPH assay, it was observed that the NE presented a higher IC_{50} than the free EAF, which can be explained by the fact that as the EAF is encapsulated it is not totally available in the assay medium in order to directly neutralize the peroxyl radicals generated from AAPH.

The incorporation of EAF and NE into RBCs could cause conformational alterations in membrane cytoskeletal proteins and changes in the internal viscosity of the cells. To determine whether free

EAF or EAF-loaded NEs disturb the phospholipid bilayer across its thickness, steady-state fluorescence anisotropy (*r*) was measured to test membrane fluidity, as this is a sensitive indicator for monitoring fluorophore binding to regions of biomembranes with constrained movement (HOU et al., 2011; NOGUEIRA, D. R. et al., 2012). This is an important parameter related to the structure and functional state of the cell membrane (MARCZAK, 2009).

The fluorescent probes, DPH and TMA-DPH, were incorporated into the human erythrocyte membranes to detect possible changes in membrane fluidity. DPH is incorporated within the hydrophobic region of the bilayer membrane, while TMA-DPH is incorporated near the surface of the cell membrane (MARCZAK, 2009). The fluorescence anisotropy values are inversely proportional to cell membrane fluidity. A high degree of fluorescence anisotropy, represents a high structural order and/or low cell membrane fluidity. Therefore, it is possible to assess the arrangement and mobility of membrane components in different regions of the bilayer (MARCZAK, 2009).

Our findings suggest that the possible localization of phenolic compounds of EAF-loaded NEs on the erythrocyte membrane is not restricted to one determined zone since EAF-loaded NEs when together with AAPH were able to elevate the fluidity of both the inner and outer layer, allowing better interaction between the antioxidant compounds and lipophilic radicals.

The degree of protection afforded by free EAF and EAF-loaded NEs against human erythrocyte oxidation might be attributed to different features. First, the partition coefficient or degree of lipophilicity of phenolic compounds determines their interaction with biomembranes and influences their antioxidant capacity and/or ability to interact with free radicals present in the aqueous medium of the oxidation system (LIAO and YIN, 2000). Second, the chemical structure of the phenolic compounds determines their ability to react with free radicals; for phenolic acids, the free radical-scavenging properties depend mainly on their number of hydroxyl groups that have the ability to donate hydrogen, thereby forming a stable end-product, which does not initiate or propagate further oxidation of the lipid (HSIEH et al., 2005). Third, in phenolic mixtures *i.e* extract and/or extract fraction, the presence of synergism may modify the characteristics of oxidation inhibition (CHIRINOS et al., 2008).

Regarding the membrane protein profile, when the RBCs were treated with the EAF-loaded NEs (EAF-PSO-NE or EAF-MCT-NE) a

more efficient protection against the oxidant agent on the membrane proteins was observed. This is probably due to the fact that one of the advantages of NE is that they better solubilize lipophilic compounds and enhance their transportation through lipid layers. In this way, it is not only the water-soluble radical scavengers present in the EAF that efficiently scavenge the peroxyl radicals in the medium before they attack the erythrocytes, but also the lipid-soluble ones which are located in lipophilic regions of the membrane (BLASA et al., 2007). Furthermore, EAF-PSO-NE appears to deliver an even better cell membrane protection, since PSO also presents antioxidants compounds that may act in a synergistic manner with EAF.

SEM studies corroborated the interaction of AAPH, EAF-PSO-NE and EAF-MCT-NE and free EAF with the lipid bilayer, as demonstrated by the changes in cell shape. According to the bilayer couple hypothesis, the shape changes induced in erythrocytes by foreign molecules are due to deferential expansion of the two monolayers of the RBCs membrane. Thus, stomatocytes are formed when the compound inserts into the inner monolayer, whereas speculated-shaped echinocytes are produced when it inserts into the outer moiety, causing surface expansion (SHEETZ and SINGER, 1974; LIM H. W. et al., 2002).

Finally, nanoemulsions entrapping pomegranate peel polyphenol-rich EAF have a great potential for cosmetic application as antioxidant and photoprotector. The present study indicates that EAF-PSO-NE and EAF-MCT-NE were photosafe in a preliminary *in vitro* test and protected the RBC membrane against oxidative damage.

Conflict of Interest

The authors declare no competing financial interest.

Acknowledgments

The authors acknowledge financial support from CAPES (CAPES/PDSE Project No. BEX 5613/13-2), the Ministerio de Economía y Competitividad - Spain (Project MAT2012-38047-C02-01) and European Union (FEDER). The authors would like to thank Professor Dr. Lourdes Pérez for Malvern Zetasizer Nano ZS use and Professor Dr. Maria Antonia Busquets for SLM-Amino AB-2 Spectrofluorometer use.

References

AJILA, C. M.; PRASADA RAO, U. J. S. Protection against hydrogen peroxide induced oxidative damage in rat erythrocytes by Mangifera indica L. peel extract. **Food Chem Toxicol,** v. 46, p. 303-309, 2008.

ALAM, M. N.; BRISTI, N. J.; RAFIQUZZAMAN, M. Review on in vivo and in vitro methods evaluation of antioxidant activity. **Saudi Pharm J,** v. 21, n. 2, p. 143-152, 2013.

ALVAREZ-SUAREZ, J. M.; GIAMPIERI, F.; GONZÁLEZ-PARAMÁS, A. M.; DAMIANI, E.; ASTOLFI, P.; MARTINEZ-SANCHEZ, G.; BOMPADRE, S.; QUILES, J. L.; SANTOS-BUELGA, C.; BATTINO, M. Phenolics from monofloral honeys protect human erythrocyte membranes against oxidative damage. **Food Chem Toxicol,** v. 50, n. 5, p. 1508-1516, 2012.

AMAKURA, Y.; OKADA, M.; TSUJI, S.; TONOGAI, Y. High-performance liquid chromatographic determination with photodiode array detection of ellagic acid in fresh and processed fruits. **J Chromatogr A,** v. 896, n. 1–2, p. 87-93, 2000.

AMAN, S.; MOIN, S.; OWAIS, M.; SIDDIQUI, M. U. Antioxidant activity of thymol: protective role in AAPH-induced hemolysis in diabetic erythrocytes. **Int J Pharm Sci Invent,** v. 2, n. 3, p. 55-60, 2013.

ARORA, S.; RAJWADE, J. M.; PAKNIKAR, K. M. Nanotoxicology and in vitro studies: The need of the hour. **Toxicol Appl Pharmacol,** v. 258, n. 2, p. 151-165, 2012.

BACCARIN, T.; LEMOS-SENNA, E. Pomegranate seed oil nanoemulsions encapsulating pomegranate peel polyphenol-rich ethyl acetate fraction: Development and antioxidant assessment. **J Nanopharmaceutics and Drug Delivery,** v. 2, n. 4, p. 333-343, 2014.

BANERJEE, A.; KUNWAR, A.; MISHRA, B.; PRIYADARSINI, K. I. Concentration dependent antioxidant/pro-oxidant activity of curcumin: Studies from AAPH induced hemolysis of RBCs. **Chem Biol Interact,** v. 174, n. 2, p. 134-139, 2008.

BLASA, M.; CANDIRACCI, M.; ACCORSI, A.; PIACENTINI, M. P.; PIATTI, E. Honey flavonoids as protection agents against oxidative damage to human red blood cells. **Food Chem,** v. 104, n. 4, p. 1635-1640, 2007.

BOTTA, A.; MARTÍNEZ, V.; MITJANS, M.; BALBOA, E.; CONDE, E.; VINARDELL, M. P. Erythrocytes and cell line-based assays to evaluate the cytoprotective activity of antioxidant components obtained from natural sources. **Toxicol In Vitro,** v. 28, n. 1, p. 120-124, 2014.

BRADFORD, M. M. A rapid and sensitive method for the quantitation of microgram quantities of protein utilizing the principle of protein-dye binding. **Anal Biochem,** v. 72, n. 1–2, p. 248-254, 1976.

BRASIL. Guia para avaliação de segurança de produtos cosméticos. **Agência Nacional de Vigilância Sanitária**, p. 1-47, 2003.

CHIRINOS, R.; CAMPOS, D.; WARNIER, M.; PEDRESCHI, R.; REES, J.-F.; LARONDELLE, Y. Antioxidant properties of mashua (Tropaeolum tuberosum) phenolic extracts against oxidative damage using biological in vitro assays. **Food Chem,** v. 111, n. 1, p. 98-105, 2008.

DOKTOROVOVA, S.; SOUTO, E. B.; SILVA, A. M. Nanotoxicology applied to solid lipid nanoparticles and nanostructured lipid carriers – A systematic review of in vitro data. **Eur J Pharm Biopharm,** v. 87, n. 1, p. 1-18, 2014.

EL-NEMR, S. E.; ISMAIL, I. A.; RAGAB, M. Chemical composition of juice and seeds of pomegranate fruit. **Die Nahrung,** v. 34, n. 7, p. 601-606, 2006.

FADAVI, A.; BARZEGAR, M.; AZIZI, H. M. Determination of fatty acids and total lipid content in oilseed of 25 pomegranates varieties grown in Iran. **J Food Compost Anal,** v. 19, p. 676-680, 2006.

FAIRBANKS, G.; STECK, T. L.; WALLACH, D. F. H. Electrophoretic analysis of the major polypeptides of the human erythrocyte membrane. **Biochemistry,** v. 10, n. 13, p. 2606-2617, 1971/06/01 1971.

FLOYD, R. A.; LEWIS, A. C. Hydroxyl Free Radical Formation from Hydrogen Peroxide by Ferrous Iron-Nucleotide Complexes. **Biochem,** v. 22, p. 2645-2649, 1983.

FLYNN, T. P.; ALLEN, D. W.; JOHNSON, G. J.; WHITE, J. G. Oxidant damage of the lipids and proteins of the erythrocyte membranes in unstable hemoglobin disease. Evidence for the role of lipid peroxidation. **J Clin Invest,** v. 71, p. 1215-1223, 1983.

GONZÁLEZ, N.; RIBEIRO, D.; FERNANDES, E.; NOGUEIRA, D. R.; CONDE, E.; MOURE, A.; VINARDELL, M. P.; MITJANS, M.; DOMÍNGUEZ, H. Potential use of Cytisus scoparius extracts in topical applications for skin protection against oxidative damage. **J Photochem Photobiol B,** v. 125, n. 0, p. 83-89, 2013.

GUGLIELMINI, G. Nanostructured novel carrier for topical application. **Clinics in Dermatology,** v. 26, n. 4, p. 341-346, 2008.

HALLIWELL, B.; CLEMENT, M. V.; LONG, L. H. Hydrogen peroxide in the human body. **FEBS Lett,** v. 486, p. 10-13, 2000.

HARBORNE, J. B. General procedures and measurements of total phenolics. In: HARBORNE, J. B. (Ed.). **Methods in plant biochemistry. Plant phenolics**. London: Academic Press, v.1, 1989.

HOU, S.-Z.; SU, Z.-R.; CHEN, S.-X.; YE, M.-R.; HUANG, S.; LIU, L.; ZHOU, H.; LAI, X.-P. Role of the interaction between puerarin and the erythrocyte membrane in puerarin-induced hemolysis. **Chem Biol Interact,** v. 192, n. 3, p. 184-192, 2011.

HSEU, Y.-C.; CHANG, W.-C.; HSEU, Y.-T.; LEE, C.-Y.; YECH, Y.-J.; CHEN, P.-C.; CHEN, J.-Y.; YANG, H.-L. Protection of oxidative damage by aqueous extract from Antrodia camphorata mycelia in normal human erythrocytes. **Life Sci,** v. 71, n. 4, p. 469-482, 2002.

HSIEH, C.-L.; YEN, G.-C.; CHEN, H.-Y. Antioxidant activities of phenolic acids on ultraviolet radiation-induced erythrocyte and low density lipoprotein oxidation. **J. Agric Food Chem,** v. 53, n. 15, p. 6151-6155, 2005.

LIAO, K.-L.; YIN, M.-C. Individual and combined antioxidant effects of seven phenolic agents in human erythrocyte membrane ghosts and phosphatidylcholine liposome systems: Importance of the partition coefficient. **J Agric Food Chem,** v. 48, n. 6, p. 2266-2270, 2000.

LIM H. W., G.; WORTIS, M.; MUKHOPADHYAY, R. Stomatocyte–discocyte–echinocyte sequence of the human red blood cell: Evidence for the bilayer– couple hypothesis from membrane mechanics. **Proc Natl Acad Sci U. S. A.,** v. 99, n. 26, p. 16766-16769, 2002.

MADARIAGA, Y. G.; CÁRDENAS, M. B.; TOLEDO, D. B.; ALFONSO, O. C.; MONTALBÁN, C. M. M.; BERNAL, Y. M. In vitro photohemolitic assessment of Cissus sicyoides L. and Achyranthes aspera. **Rev Cubana Plant Med,** v. 15, n. 3, p. 126-132, 2010.

MAGALHÃES, A. S.; SILVA, B. M.; PEREIRA, J. A.; ANDRADE, P. B.; VALENTÃO, P.; CARVALHO, M. Protective effect of quince (Cydonia oblonga Miller) fruit against oxidative hemolysis of human erythrocytes. **Food Chem Toxicol,** v. 47, n. 6, p. 1372-1377, 2009.

MARCZAK, A. Fluorescence anisotropy of membrane fluidity probes in human erythrocytes incubated with anthracyclines and glutaraldehyde. **Bioelectrochemistry,** v. 74, n. 2, p. 236-239, 2009.

MARTÍNEZ, V.; UGARTONDO, V.; VINARDELL, M. P.; TORRES, J. L.; MITJANS, M. Grape Epicatechin Conjugates Prevent Erythrocyte Membrane Protein Oxidation. **J Agric Food Chem,** v. 60, p. 4090-4095, 2012.

MIKI, M.; TAMAI, H.; MINO, M.; YAMAMOTO, Y.; NIKI, E. Free-radical chain oxidation of rat red blood cells by molecular oxygen and its inhibition by α-tocopherol. **Arch Biochem Biophys,** v. 258, n. 2, p. 373-380, 1987.

MISHRA, A.; RAM, S.; GHOSH, G. Dynamic light scattering and optical absorption in biological nanofluids of gold nanoparticles in poly(vinyl pyrrolidone) molecules. **J Phys Chem C,** v. 113, n. 17, p. 6976-6982, 2009.

MITRI, K.; SHEGOKAR, R.; GOHLA, S.; ANSELMI, C.; MÜLLER, R. H. Lipid nanocarriers for dermal delivery of lutein: preparation, characterization, stability and performance. **Int J Pharm,** v. 414, n. 1, p. 267-275, 2011.

NOGUEIRA, D.; MITJANS, M.; MORÁN, M. C.; PÉREZ, L.; VINARDELL, M. P. Membrane-destabilizing activity of pH-responsive cationic lysine-based surfactants: role of charge position and alkyl chain length. **Amino Acids,** v. 43, n. 3, p. 1203-1215, 2012.

NOGUEIRA, D. R.; MITJANS, M.; BUSQUETS, M. A.; PÉREZ, L.; VINARDELL, M. P. Phospholipid Bilayer-Perturbing Properties Underlying Lysis Induced by pH-Sensitive Cationic Lysine-Based Surfactants in Biomembranes. **Langmuir,** v. 28, n. 32, p. 11687-11698, 2012.

ONOUE, S.; SETO, Y.; GANDY, G.; YAMADA, S. Drug-induced phototoxicity; an early in vitro identification of phototoxic potential of new drug entities in drug discovery and development. **Curr Drug Saf,** v. 4, n. 2, p. 123-136, 2009.

PAPE, W. J. W.; HOPPE, U. In vitro methods for the assessment of primary local effects of topically applied preparations. **Skin Pharmacol,** v. 4, n. 3, p. 205-212, 1991.

PAPE, W. J. W.; MAURER, T.; PFANNENBECKER, U.; STEILING, W. The red blood cell phototoxicity test (photohaemolysis and haemoglobin oxidation): EU/COLIPA validation programme on phototoxicity (phase II). **ATLA, Altern Lab Anim,** v. 29, n. 2, p. 145-162, 2001.

PAPE, W. J. W.; PFANNENBECKER, U.; HOPPE, U. Validation of the red blood cell system as in vitro assay for rapid screening of irritation potential of surfactants. **Mol Toxicol,** v. 1, n. 4, p. 525-536, 1987.

QU, W.; PAN, Z.; MA, H. Extraction modeling and activities of antioxidants from pomegranate marc. **J Food Eng,** v. 99, n. 1, p. 16-23, 2010.

RIVERA GIL, P.; OBERDÖRSTER, G.; ELDER, A.; PUNTES, V.; PARAK, W. J. Correlating physico-chemical with toxicological properties of nanoparticles: The present and the future. **ACS Nano,** v. 4, n. 10, p. 5527-5531, 2010.

SCHUBERT, M. A.; MÜLLER-GOYMANN, C. C. Characterisation of surface-modified solid lipid nanoparticles (SLN): Influence of lecithin and nonionic emulsifier. **Eur J Pharm Biopharm,** v. 61, n. 1–2, p. 77-86, 2005.

SEERAM, N. P.; ADAMS, L. S.; HENNING, S. M.; NIU, Y.; ZHANG, Y.; NAIR, M. G.; HEBER, D. In vitro antiproliferative, apoptotic and antioxidant activities of punicalagin, ellagic acid and a total pomegranate tannin extract are enhanced in combination with other polyphenols as found in pomegranate juice. **J Nutr Biochem,** v. 16, n. 6, p. 360-367, 2005.

SHEETZ, M. P.; SINGER, S. Biological membranes as bilayer couples. A molecular mechanism of drug-erythrocyte interactions. **Proc Natl Acad Sci U. S. A.,** v. 71, n. 11, p. 4457-4461, 1974.

SNYDER, L. M.; FORTIER, N. L.; TRAINOR, J.; JACOBS, J.; LEB, L.; LUBIN, B.; CHIU, D.; SHOHET, S.; MOHANDAS, N. Effect of hydrogen peroxide exposure on normal human erythrocyte deformability, morphology, surface characteristics, and spectrin-hemoglobin cross-linking. **J Clin Invest,** v. 76, n. 5, p. 1971-1977, 1985.

SÖDERLIND, E.; KARLSSON, L. Haemolytic activity of maltopyranoside surfactants. **Eur J Pharm Biopharm,** v. 62, n. 3, p. 254-259, 2006.

SVETINA, S.; KUZMAN, D.; WAUGH, R. E.; ZIHERL, P.; ŽEKŠ, B. The cooperative role of membrane skeleton and bilayer in the mechanical behaviour of red blood cells. **Bioelectrochemistry,** v. 62, n. 2, p. 107-113, 2004.

SZEBENI, J. Hemocompatibility testing for nanomedicines and biologicals: predictive assays for complement mediated infusion reactions. **Eur J Nanomed.,** v. 4, p. 33-53, 2012.

TOLEDO, D. B.; CÁRDENAS, M. B.; DÍAZ, A. V.; MONTALBÁN, C. M. M.; RODRIGUEZ, N. I. Evaluación fotohemolítica in vitro de Parthenium hysterophorus L. **Revista Científica Villa Clara,** v. 16, n. 1, p. 43-48, 2012.

UGARTONDO, V.; MITJANS, M.; VINARDELL, M. P. Applicability of lignins from different sources as antioxidants based on the protective effects on lipid peroxidation induced by oxygen radicals. **Ind Crops Prod,** v. 30, n. 2, p. 184-187, 2009.

VAN ELSWIJK, D. A.; SCHOBEL, U. P.; LANSKY, E. P.; IRTH, H.; VAN DER GREEF, J. Rapid dereplication of estrogenic compounds in pomegranate (Punica granatum) using on-line biochemical detection coupled to mass spectrometry. **Phytochemistry,** v. 65, n. 2, p. 233-241, 2004.

VITTORI, D.; GARBOSSA, G.; LAFOURCADE, C.; PÉREZ, G.; NESSE, A. Human erythroid cells are affected by aluminium. Alteration of membrane band 3 protein. **Biochim Biophys Acta Biomembr,** v. 1558, n. 2, p. 142-150, 2002.

YANG, H.-L.; CHEN, S.-C.; CHANG, N.-W.; CHANG, J.-M.; LEE, M.-L.; TSAI, P.-C.; FU, H.-H.; KAO, W.-W.; CHIANG, H.-C.; WANG, H.-H.; HSEU, Y.-C. Protection from oxidative damage using Bidens pilosa extracts in normal human erythrocytes. **Food Chem.Toxicol.,** v. 44, n. 9, p. 1513-1521, 2006.

CAPÍTULO 3: DETERMINAÇÃO DA FOTOPROTEÇÃO DAS NANOEMULSÕES CONTENDO CONSTITUINTES DE *Punica grantaum* CONTRA RADIAÇÃO UVB

A utilização de compostos antioxidantes na fotoproteção constitui uma estratégia promissona na indústria farmacêutica e cosmética. Em especial, os compostos polifenólicos são de grande interesse, pois podem atuar como agentes fotoprotetores na absorção da radiação ultravioleta e na prevenção contra possíveis danos causados na pele pela radiação solar através da ação antioxidante, anti-inflamatória e anticarcinogênica (NICHOLS and KATIYAR, 2010; AFAQ and KATIYAR, 2011; CHEN et al., 2012).

Diversos trabalhos científicos relatam o potencial fotoprotetor de extratos derivados da romã (SYED et al., 2007; ZAID et al., 2007; PACHECO-PALENCIA et al., 2008; AFAQ, 2011; MANASATHIEN et al., 2011). O presente trabalho descreve a avaliação do potencial fotoprotetor das nanoemulsões contendo constituintes de *P. granatum* quanto à proteção ao dano no DNA causado pela radiação UVB em modelo *in vitro* utilizando células de queratinócitos humanos (HaCaT). Através das técnicas de espalhamento de luz dinâmico (DLS) e Crio-TEM, o comportamento das nanoemulsões uma vez em contato com o meio de cultivo celular foi verificado. A citotoxicidade *in vitro* foi determinada em células de queratinócito humano (HaCaT) e fibroblasto murino 3T3, empregando os métodos do MTT e NRU. Estudos de internalização celular foram conduzidos através da nanoemulsificação de um agente fluoróforo (vermelho de nilo) juntamente com a fração acetato de etila ou na presença da calceína, um agente fluoróforo impermeável à membrana celular. A fototoxicidade *in vitro* das nanoemulsões também foi relatada neste capítulo. Os resultados descritos neste capítulo foram publicados no *Journal of Photochemistry and Photobiology B, v. 153, p. 127-136, 2015*.

Publicação: "Photoprotection by *Punica granatum* seed oil nanoemulsion entrapping polyphenol-rich ethyl acetate fraction against UVB-induced DNA damage in human keratinocytes (HaCaT) cell line"

Journal of Photochemistry and Photobiology B 153 (2015) 127-136

Photoprotection by *Punica granatum* seed oil nanoemulsion entrapping polyphenol-rich ethyl acetate fraction against UVB-induced DNA damage in human keratinocyte (HaCaT) cell line

Thaisa Baccarin[a,c], Montserrat Mitjans[a], David Ramos[b], Elenara Lemos-Senna[c], Maria Pilar Vinardell[a*]

[a]Departament de Fisiologia, Facultat de Farmàcia, Universitat de Barcelona, Barcelona, Spain, [b] Unidad de Toxicología y Ecotoxicología del Parc Cientific de Barcelona, Barcelona, Spain

[c]Programa de Pós-Graduação em Farmácia, Universidade Federal de Santa Catarina, 88040-900, Florianópolis, Brazil.

*Corresponding author: mpvinardellmh@ub.edu. Departament de Fisiologia, Facultat de Farmàcia, Universitat de Barcelona, Av. Joan XXIII s/n, E-08028 Barcelona, Spain. Tel.: +34 934024505; fax: +34 934035901.

ABSTRACT

There has been an increase in the use of botanicals as skin photoprotective agents. Pomegranate (*Punica granatum* L.) is well known for its high concentration of polyphenolic compounds and for its antioxidant and anti-inflammatory properties. The aim of this study was to analyse the photoprotection provided by *Punica granatum* seed oil nanoemulsion entrapping the polyphenol-rich ethyl acetate fraction against UVB-induced DNA damage in the keratinocyte HaCaT cell line. For this purpose, HaCaT cells were pretreated for 1 h with nanoemulsions in a serum-free medium and then irradiated with UVB (90–200 mJ/cm^2) rays. Fluorescence microscopy analysis provided information about the cellular internalization of the nanodroplets. We also determined the *in vitro* SPF of the nanoemulsions and evaluated their phototoxicity using the 3T3 Neutral Red Uptake Phototoxicity Test. The nanoemulsions were able to protect the cells' DNA against UVB-induced damage in a concentration dependent manner.

Nanodroplets were internalized by the cells but a higher proportion was detected along the cell membrane. The SPF obtained (~25) depended on the concentration of the ethyl acetate fraction and pomegranate seed oil in the nanoemulsion. The photoprotective formulations were classified as non-phototoxic. In conclusion, nanoemulsions entrapping the polyphenol-rich ethyl acetate fraction show potential for use as a sunscreen product.

Keywords: *Punica granatum*, pomegranate seed oil, nanoemulsion, cytotoxicity, phototoxicity, cellular internalization, photoprotection.

1. INTRODUCTION

Ultraviolet radiation (UVR) is an important exogenous factor in skin pathogenesis and can lead to the development of a number of skin disorders including sunburn, immunosuppression, carcinogenesis, and photoaging. UVR can be divided in-to three types: ultraviolet C (UVC – from 200 to 290 nm); ultraviolet B (UVB - from 290 to 320 nm) and ultraviolet A (UVA - from 320 to 400 nm) (NICHOLS and KATIYAR, 2010). UVC radiation is filtered by the ozone layer before reaching the Earth. UVA is the radiation most responsible for photoaging; it penetrates deep into the epidermis and dermis of the skin and as it is barely able to excite the DNA molecule directly, it is assumed that much of its mutagenic and carcinogenic action is mediated through oxidative stress (NICHOLS and KATIYAR, 2010). UVB radiation (290-320 nm) is responsible for damage due to sunburn (erythema and edema) and, induction of oxidative stress, and is highly genotoxic agent. Direct absorption of UVB photons leads to disruption of DNA, with cyclobutane-pyrimidine dimers (CPD) and pyrimidine-pyrimidone (6-4) photoproducts as a result, which, if remaining unrepaired, can initiate photocarcinogenesis. It is less penetrating than UVA, mostly only reaches the epidermal basal cell layer of the skin and thus affects mainly epidermal cells, possibly altering the proliferation, differentiation and metabolism of these cells (SVOBODOVÁ et al., 2009; VOSTÁLOVÁ et al., 2010; PERDE-SCHREPLER et al., 2013).

Thus, protection of skin against excessive sunlight exposure is essential to forestall damage. Exogenous application of protective dermatological preparations containing sunscreens (organic and/or inorganic filters) is commonly recommended. In this regard, naturally occurring plant products have also been investigated and play a role in a

broad range of physiological processes including protection against harmful UVR. Due to their sunscreen effect and, potent antioxidant, anti-inflammatory and immunomodulatory properties, polyphenols are among the most promising group of compounds that can be exploited as chemopreventive agents for a variety of skin disorders (NICHOLS and KATIYAR, 2010; VOSTÁLOVÁ et al., 2010).

Punica granatum (pomegranate) is an ancient fruit, considered as "a pharmacy unto itself" with enormous health benefits (JURENKA, 2008; VIUDA-MARTOS et al., 2010; MELO et al., 2014). The main compounds responsible for most of its functional properties are phenolic compounds. They can be found in substantial quantities and in different parts of the fruit (bark, flower, leaves, and arils) but are much more concentrated in the peel and juice. The peel is rich in hydrolysable tannins, mainly punicalin, peduncalagin and punicalagin; hydroxybenzoic acids such as gallic acid and ellagic acid; anthocyanidins and flavonoids. They account for 92% of the antioxidant activity associated with the fruit (ISMAIL et al., 2012). The pomegranate seed oil contains phytosterols, tocopherols and a unique fatty acid mixture, mainly consisting of punicic acid (50-70 %), which is considered to be one of the strongest natural antioxidants (SCHUBERT et al., 1999).

We recently developed pomegranate seed oil nanoemulsions (PSO-NE) and medium chain triglyceride nanoemulsions (MCT-NE), both of them entrapping a pomegranate peel polyphenol-rich ethyl acetate fraction (EAF), for topical administration, and evaluated their antioxidant activity using *in vitro* methods (BACCARIN and LEMOS-SENNA, 2014). Nanoemulsions (NE) present a large surface area and with low surface tension of the oil droplets, which could help increase the permeation of the incorporated polyphenol compounds through the skin, enhancing their topical effect (MASON et al., 2006; SILVA et al., 2009; CHIME et al., 2014). In another study erythrocyte-based assays were employed to determine whether if EAF-loaded NE could protect the membrane lipid bilayer against the oxidative stress induced by oxidant agents (erythrocytes are well known as a biomembrane model that mimics a cellular environment), and to determine whether nanoemulsion component (mainly surfactants) could damage the cell membrane and lead to hemolysis (BACCARIN, MITJANS, LEMOS-SENNA, et al., 2015).

The main purpose of this study was to investigate whether the free EAF and EAF-loaded nanoemulsions have photoprotective effect

against DNA damage induced by UVB irradiation, of monolayer cultures of human keratinocyte HaCaT, and to determine the cytotoxicity and phototoxicity of the formulations. Finally, cell internalization studies were conducted to predict the possible localization of the nanoemulsion when in contact with cells.

2. MATERIALS AND METHODS

2.1 Materials

Polysorbate (Tween 80®), triethanolamine, dimethyl sulfoxide (DMSO), 2,5 diphenyl-3,-(4,5-dimethyl-2-thiazolyl) tetrazolium bromide (MTT), neutral red dye, Nile red (NR), calcein and 4,6 diamino-2-phelylindole dihydrochloride hydrate (DAPI) were purchased from Sigma-Aldrich (St. Louis, MO, USA). NaCl, Na_2HPO_4 and KH_2PO_4 were purchased from Merck (Darmstadt, Germany). Sodium acetate, ethyl acetate, dichloromethane, chloride acid, and ethanol were obtained from Vetec® (Rio de Janeiro, Brazil). Pomegranate seed oil and pomegranate fruit peel dry extract were purchased from Via Farma (São Paulo, Brazil). Soy lecithin (Lipoid® S100) was from Lipoid AG (Steinhausen, Switzerland). Medium chain triglyceride was from Brasquim (Porto Alegre, Brazil) and water was purified in a Milli-Q system (Millipore, Bedford, MA). Dulbecco's modified Eagle's medium (DMEM), fetal bovine serum (FBS), phosphate buffered saline (PBS), L-glutamine solution (200 mM), trypsin–EDTA solution (170,000 U/L trypsin and 0.2 g/L EDTA) and penicillin–streptomycin solution (10,000 U/mL penicillin and 10 mg/ml streptomycin) were obtained from Lonza (Verviers, Belgium). The 75 cm^2 flasks, 96-well and 24-well plates were obtained from TPP (Trasadingen, Switzerland).

2.2 Methods

2.2.1 Ethyl acetate fraction (EAF)

The polyphenol-rich ethyl acetate fraction (EAF) from *Punica granatum* peel extract was obtained following the method described by (PANICHAYUPAKARANANT et al., 2010) with some modifications. Briefly, the *P. granatum* fruit peel dry extract was commercially bought and then extracted for 24 hour by dynamic maceration with methanol containing 10% (v/v) water. The obtained extract was dried *in vacuo*

and then suspended in 2% aqueous acetic acid. The suspended extract was partitioned with dichloromethane and ethyl acetate. After that, the pooled ethyl acetate fractions were evaporated to dryness *in vacuo*.

2.2.2 Preparation of nanoemulsions

EAF-loaded pomegranate seed oil nanoemulsions (EAF-PSO-NE) were prepared using an ultrasonic emulsification method followed by solvent evaporation (TAN and NAKAJIMA, 2005). Briefly, the ethyl acetate fraction (EAF) (0.5%; w/v), soy lecithin (0.4%; w/v) and PSO (2%; w/v) were dissolved in 10 mL of ethyl acetate. This ethyl acetate solution was slowly poured into 40 mL of a polysorbate 80 (2.1%; w/v) aqueous solution, which was then adjusted to pH 5.0-6.5 with triethanolamine. The oil in water dispersion was sonicated for 3 minutes using an Ultrasonic Processor UP200S (Hielscher, Germany), and kept under magnetic stirring for 24 hours. The resulting nanoemulsion was evaporated under reduced pressure to a volume of 15 mL.

EAF-loaded medium chain triglyceride nanoemulsions (EAF-MCT-NE) were prepared using the spontaneous emulsification method (BOUCHEMAL et al., 2004). For this, 10 mL of an ethanolic solution containing EAF (0.5%; w/v), soy lecithin (0.4%; w/V), and MCT (1.8%, w/v) was poured into a 2.1% (w/v) polysorbate 80 aqueous solution and adjusted to pH 5.0-6.5 with triethanolamine, under magnetic stirring. The NE was then evaporated under reduced pressure to eliminate the organic solvent and concentrated to a volume of 15 mL. All formulations were filtered through 8 µm quantitative filter paper. Unloaded PSO-NE and MCT-NE were prepared in the same manner.

2.2.3 Droplet size and zeta potential

Droplet size and zeta potential were analysed by dynamic light scattering (DLS) using a Malvern Zetasizer Nano ZS (Malvern Instruments Ltd, UK) at 25ºC and a detection angle of 173º. Before measurement unloaded and EAF-loaded NE were appropriately diluted in ultrapurified water, or cell culture medium with 5% (v/v) FBS. Readings were taken immediately after preparation (t = 0 h) and after a 24 h incubation at 37 ºC (t = 24 h). Each measurement was performed using at least three sets of a minimum of 10 runs.

2.2.4 Culture of HaCaT and 3T3 cell line

The spontaneously immortalized human keratinocyte cell line HaCaT and the murine Swiss albino 3T3 fibroblast cell line were grown in DMEM medium (4.5 g L^{-1} glucose) supplemented with 10% fetal bovine serum, 2 mM L-glutamine, penicillin (100 U mL^{-1}) and streptomycin (100 µg mL^{-1}) at 37 ºC, 5% CO_2. Both cell lines were routinely cultured in 75 cm^2 culture flasks and trypsinized using trypsin/EDTA when the cells reached approximately 80% confluence. All cell lines were obtained from Eucellbank (Universitat de Barcelona, Spain).

2.2.5 Cytotoxicity assays

The cytotoxic effect of the free EAF, unloaded and EAF-loaded NE was measured by tetrazolium salt MTT assay (MOSMANN, 1983) and neutral red uptake (NRU) assay (BORENFREUND and PUERNER, 1985). 3T3 and HaCaT cells were seeded into the central 60 wells of a 96-well plate at a density of 8.5 x 10^4 cells ml^{-1} and 1 x 10^5 cells ml^{-1}, respectively. After incubation for 24 h under 5% CO2 at 37 ºC, the spent medium was replaced with 100 µL of fresh medium supplemented with 5% FBS containing free EAF, unloaded or EAF-loaded NE at the required concentration (7.8-500 µg mL^{-1}). After 24 h, the surfactant-containing medium was removed, and 100 µL of MTT in PBS (5 mg mL^{-1}) diluted 1:10 in medium without FBS and phenol red was then added to the cells. Similarly, 100 µL of 50 µg mL^{-1} NR solution in DMEM without FBS and phenol red was added to each well for the NRU assay. The plates were further incubated for 3 h, after which the medium was removed, and the cells were washed once in PBS. Thereafter, 100 µL of DMSO was added to each well to dissolve the purple formazan product (MTT assay) and for the NRU assay, 100 µL of a solution containing 50% absolute ethanol and 1% acetic acid in distilled water was added to extract the dye. After 10 min on a microtiter plate shaker at room temperature, the absorbance of the resulting solutions was measured at 550 nm using a Bio-Rad 550 microplate reader. The effect of each treatment was calculated as the percentage inhibition of cell viability compared to the respective controls.

2.2.6 Cryo-TEM

The morphology and size of the unloaded and EAF-loaded NE were analysed by cryo transmission electron microscopy (Cryo-TEM). Briefly, 5 µL of unloaded or EAF-loaded NE were appropriately diluted in ultrapure water or cell culture medium with 5% (v/v) FBS and placed on a Lacey carbon film on 200 mesh copper grids and automatically blotted against filter paper, leaving thin sample films spanning the grid holes. These films were vitrified by plunging the grids into ethane, which was kept at its melting point by liquid nitrogen, using a Vitrobot (FEI Company, Eindhoven, Netherlands) keeping the sample at 100% humidity before freezing. The temperature at which the thin films and vitrification were initiated was room temperature. The vitreous sample films were transferred to a Tecnai F20 microscope (FEI Company, Eindhoven, Netherlands) using a Gatan cryo-transfer. The images were taken at 200 Kv with a 4096x4096 pixel CCD Eagle camera (FEI Company, Eindhoven, Netherlands) at a temperature between -170 ºC and -175 ºC using low-dose imaging conditions.

2.2.7 Cell uptake studies

2.2.7.1 Intracellular localization of Nile red-labelled nanoemulsions

Nanoemulsions (NE) loaded with Nile red (NR) (NR-NE) were prepared using PSO or MCT as the oil phase. HaCaT cells were plated in 24-well plates at a density of 1×10^5 cells/mL on round cover glasses (Marlenfeld GmbH & Co.KG, Lauda-Könlgshofen, Germany) and incubated overnight at 37 ºC under 5% CO_2. When cells reached confluence, the culture medium was replaced with fresh medium containing NR-NE at a final concentration of 25 µg mL^{-1} and incubated for 2 and 24 h. After incubation, the samples were aspirated and the cells were washed four times with PBS and fixed with 4 % (v/v) formaldehyde in PBS (pH 7.4) for 15 min at room temperature and away from light. The individual cover glasses were then mounted on clean glass slides with a drop of Prolong® Gold antifade reagent (Invitrogen, OR, USA) for subsequent fluorescence microscopy analysis (Olympus BX41 microscope equipped with a UV-mercury lamp, 100 W Ushio Olympus, and a filter set type MNIGA3 540-550 nm excitation, 575-625 nm emission and 570 nm dichromatic mirror). Images were digitized on a computer through a video camera (Olympus digital camera XC50)

using an image processor (Olympus cell^B Image Acquisition Software). To calculate the mean fluorescence value of the cells, approximately 40 individual cells from different fields and images were analyzed with Image J software (version 1.46, National Institutes of Health, MD, USA) and their total fluorescence intensity was quantified, corresponding to the cell internalization of nanoemulsion (NOGUEIRA et al., 2014).

2.2.7.2 Intracellular release of calcein

HaCaT cells were plated (1×10^5 cells/mL) in 24-well plates on round cover glasses (Marlenfeld GmbH & Co.KG, Lauda-Könlgshofen, Germany) and incubated at 37 ºC under 5% CO_2 until confluence was reached. Then calcein, a membrane-impermeable fluorophore, was added to the cells at 1 mg mL^{-1} as a tracer molecule to monitor the effect of the EAF-loaded NE on endosomes after cell internalization (control). EAF-loaded NE containing of 50 µg mL^{-1} of calcein, were diluted in DMEM medium without FBS and phenol red. After 2 h incubation at 37 ºC, the cells were washed four times with PBS and incubated in DMEM medium with 10% FBS for 3 h to allow intracellular trafficking. Then cells were washed four times with PBS and fixed with 4% (v/v) formaldehyde in PBS (pH 7.4) for 15 min at room temperature. Individual cover glasses were mounted on a clean glass slide with Prolong® Gold antifade reagent (Invitrogen, OR, USA) and analyzed on an Olympus BX41 fluorescence microscope equipped with a UV-mercury lamp (100 W Ushio Olympus) and a filter set type MNIBA3 (470-495 nm excitation, 510-550 nm emission and 505 nm dichromatic mirror). Images were digitized on a computer through a video camera (Olympus digital camera XC50) using an image processor (Olympus cell^B Image Acquisition software).

Image J software was used to calculate the average pixel intensity of calcein fluorescence within regions of interest (ROI) drawn onto collected images. This was done by drawing three ROI inside the cell (excluding any calcein-containing vesicles and, thus, representing the cytoplasm only) and the results were obtained in arbitrary fluorescence units. Images of ~40 individual cells were analyzed for each formulation (NOGUEIRA et al., 2014).

2.2.8 UVB photoprotection in vitro studies

Treatment of keratinocytes with EAF and nanoemulsions

(A) To evaluate the photoprotective effect of free EAF and EAF-loaded NE, HaCaT cells were pre-treated (1 hour; cell incubator) with 20 µg mL^{-1} or 50 µg mL^{-1} of each sample in serum-free medium without phenol red, then irradiated and incubated at 37 ºC for another 2 hours.

(B) To verify the photorepair activity, HaCaT cells were first irradiated (90 mJ/cm^2) in serum-free medium without phenol red, then treated with free EAF, unloaded or EAF-loaded NE (50 µg mL^{-1}) in serum-free medium and incubated at 37 ºC for 24 hours.

UVB irradiation

The keratinocytes were UVB irradiated (90 or 200 mJ/cm^2) in culture plates placed under a Philips LP471 UVB source, with a spectral range of 280-315 nm. In parallel, non-irradiated cells were treated similarly and kept in the dark in a cell incubator. The UVB output measured by an UVB-meter (Delta OHM HD 2302.0) before each experiment in direct contact with the cell culture plate was 0.4 mW/cm^2.

2.2.9 Comet assay (single cell gel electrophoresis assay – SCGE)

Two (photoprotection) or 24 hours (photorepair) after irradiation, the cells from two wells of each treatment were trypsinized, transferred to eppendorfs and centrifuged at 1500 rpm for 5 minutes. Microscope slides containing the samples (cell pellet) mixed with a 0.9% solution of low-melting point agarose were prepared. The cells were lysed and then incubated in alkaline electrophoresis buffer for DNA unwinding and conversion of alkali-labile sites to single-strand breaks. Electrophoresis was performed in the same buffer for 30 min at 25 V and 300 mA. Next, 30 µL of 5 µg mL^{-1} DAPI solution were added to each slide for the fluorescence microscopy analysis. The migration of nuclear DNA from the cells was measured using the COMET ASSAY IV® Program (Perspective Instruments) for 50 randomly selected cell images and the mean percentage of DNA in the tail (% Tail DNA) was calculated in each trial.

2.2.10 Interleukin-8 determination

The effect of UVB and treatments on IL-8 was determined using a specific immunoassay kit (BD OptEIA™ BD, Biosciences, USA) Set for human interleukin-8 according to the manufacturer's protocol. Briefly, after centrifugation (see *Comet assay item 2.9.3*), the supernatant was collected and samples were stored at -20ºC. One hundred microliters of sample were transferred to a 96-well plate, covered with a specific capture antibody and incubated for 2 h at room temperature. The mixture was removed, wells were rinsed five times with wash buffer and the detection antibody solution was added (1 h at room temperature). Then the solution was removed, the wells were rinsed seven times with wash buffer and the substrate solution was added. After incubation (30 min at room temperature, in the dark), the stop solution was applied and a yellow-colored product was measured at 450 nm using a Bio-Rad 550 microplate reader.

2.2.11 Sun protector factor determination in vitro

The *in vitro* sun protection factor (SPF) of the free EAF, EAF-loaded NE and PSO was determined according to a previously described method (MANSUR et al., 1986). Dilute solutions of free EAF and EAF-loaded NE were tested at concentrations of 5, 20, 50 and 100 µg mL^{-1}; PSO was tested at 20, 80, 200 and 400 µg, which correspond to the amount of oil found at each concentration of NE. The absorption spectra of samples were obtained in the range of 290 to 320 nm every 5 nm, using a 1 cm quartz cell. The observed absorbance values were calculated using the equation:

$$SPF_{spectrophotometric} = CF \times \sum_{290}^{320} EE(\lambda) \times I(\lambda) \times Abs(\lambda)$$

where: CF – correction factor (10), EE (λ) – erythemal effect spectrum, I (λ) – solar intensity spectrum, Abs (λ) – absorbance values at wavelength λ. The values of EE × I are constants and were determined by (SAYRE et al., 1979).

2.2.12 Phototoxicity test

The phototoxicity test was carried out as described in the Organization for Economic Co-operation and Development (OECD)

432 guidelines with some modification. Cell lines 3T3 and HaCaT were used as *in vitro* models to predict cutaneous phototoxicity. Briefly, the 3T3 mouse fibroblast cell line and HaCaT cell line were maintained in culture for 24 h to allow the formation of monolayers. Two 96-well plates per cell line were then pre-incubated in six duplicates with EAF, EAF-PSO-NE and EAF-MCT-NE at 50 µg mL^{-1} in serum-free medium without phenol red for 1h. One plate of each cell line was then exposed to a dose of 5 J/cm^2 UVA, whereas the other plate was kept in the dark. UVA irradiation was performed using a TL-D 15 W/10 UVA lamp (Royal Philips Electronics, The Netherlands), with a spectral range of 315-400 nm. The treatment medium was then replaced with culture medium and, after 24 h, cell viability was determined by neutral red uptake assay. The neutral red uptake was measured after 3 h incubation at the absorbance of 550 nm using a Bio-Rad 550 microplate reader. Cell viability obtained with each sample at 50 µg mL^{-1} in both cell lines was compared with that of untreated controls and the percent inhibition was calculated. To predict the phototoxic potential, the cell viabilities obtained in the presence and absence of UVA radiation were compared.

2.2.13 Statistical analysis

Each experiment was run at least in triplicate. Statistical analyses were performed using one-way analysis of variance (ANOVA) followed by Dunnett's or Tukey's post-hoc test for multiple comparisons using Instat software. Differences were considered significant at $p < 0.05$.

3. RESULTS AND DISCUSSION

3.1 Characterization of nanoemulsions

The EAF and EAF-loaded NE were developed and characterized according to their physicochemical properties. The EAF contained a substantial amount of total phenolic compounds (around 638 mg g^{-1} GAE – gallic acid equivalents), the major ones being ellagic acid, gallic acid and punicalagin. The entrapment efficiency of the phenolic compounds in the nanoemulsions was near or above 50% depending on the lipophilicity of the chemical compound. The antioxidant activity determined through DPPH and FRAP assay is reported elsewhere (BACCARIN and LEMOS-SENNA, 2014).

Characterization of the nanodispersion when in contact with cell culture medium, is extremely important since the nanosystem and its components do not always behave as inert objects. The cell growth media contain serum proteins, essential amino acids, vitamins, electrolytes, and other chemicals. These components could interact with nanoparticles/nanodroplets and change their physicochemical properties and stability (ALKILANY and MURPHY, 2010). Furthermore, nanoparticles/nanodroplets can undergo aggregation or agglomeration, and proteins present in the biological medium can adsorb and change the features of the nanosystem's interaction with cells (MAIORANO et al., 2010; RIVERA GIL et al., 2010; SABBIONI et al., 2014). The unloaded and EAF-loaded NE were characterized in terms of size, zeta potential and PI when dispersed in cell culture medium (DMEM 5% FBS). Table 1 shows the DLS measurements of unloaded and EAF-loaded NE immediately after being diluted in ultrapure water or in culture medium DMEM containing 5% FBS at time 0 and 24h of incubation. The size of unloaded PSO-NE and MCT-NE did not alter when incubated in cell culture medium; EAF-PSO-NE and EAF-MCT-NE showed an increase of about 20% in particle size mainly after 24 h incubation in cell culture medium, increasing from 203 nm to 244 nm and from 185 nm to 218 nm, respectively. The zeta potential values of unloaded and EAF-loaded NE when diluted in ultrapure water were highly negative, similar to the previously reported values (BACCARIN and LEMOS-SENNA, 2014), but were close to zero when measured in cell culture medium. The first hypothesis regarding size augmentation and reduction in surface charge is that in the presence of non-ionic surfactants (i.e. polysorbate) the protein adsorption layer could be formed by hydrophobic interaction with the surfactant. The second hypothesis is that for a water/oil interface the adsorbing protein molecules could penetrate into the hydrophobic oil phase with the hydrophobic parts of the molecule (MILLER et al., 2000). As observed from the PI values of the unloaded and EAF-loaded NE, after incubation in cell culture medium the nanometric-sized dispersion remained monodisperse (PI<0.3). Cryo-TEM images (Figure 1) corroborated the mean hydrodynamic size obtained by DLS. Limited particle deformation can be seen in the cryo-TEM image due to the confining effect inside the thin film of vitreous ice (DORA et al., 2012).

Table 1. Characterization of unloaded and EAF-loaded *P. granatum* nanoemulsions in water and culture medium DMEM containing 5% FBS at incubation time 0 and 24 h.

Nanoemulsions	Ultrapure Water			5% FBS - t0			5% FBS - t24 h		
	Size (nm)	*Zeta Potential (mV)*	*PI*	*Size (nm)*	*Zeta Potential (mV)*	*PI*	*Size (nm)*	*Zeta Potential (mV)*	*PI*
EAF-PSO-NE	203.2 ± 1.8	-28.9	0.222	211.4 ± 4.0	-4.8	0.217	244.4 ± 0.9	-5.6	0.251
PSO-NE	146.1 ± 0.6	-18.6	0.124	150.2 ± 1.2	-3.6	0.121	151.2 ± 1.1	-3.0	0.123
EAF-MCT-NE	185.6 ± 0.8	-28.3	0.154	193.2 ± 1.4	-4.4	0.191	218.3 ± 1.3	-4.4	0.221
MCT-NE	168.7 ± 0.1	-15.3	0.174	170.3 ± 0.8	-1.5	0.167	170.5 ± 0.8	-3.3	0.197

PI = Polydispersity Index; Values are expressed as mean ± SD (n=3).
EAF-PSO-NE = pomegranate seed oil nanoemulsion with the pomegranate ethyl acetate fraction encapsulated.
PSO-NE = pomegranate seed oil nanoemulsion (blank).
EAF-MCT-NE = medium chain triglyceride nanoemulsion with the ethyl acetate fraction encapsulated.
MCT-NE = medium chain triglyceride nanoemulsions (blank).

Figure 1. Cryo TEM image of unloaded and EAF-loaded *P. granatum* nanoemulsions. Formulations dispersed in ultrapurified water: (A) MCT-NE; (B) EAF-MCT-NE; (C) PSO-NE; (D) EAF-PSO-NE; Formulations in DMEM 5% FBS after 24 h incubation: (E) EAF-MCT-NE and (F) EAF-PSO-NE. Scale bars correspond to 500 nm.

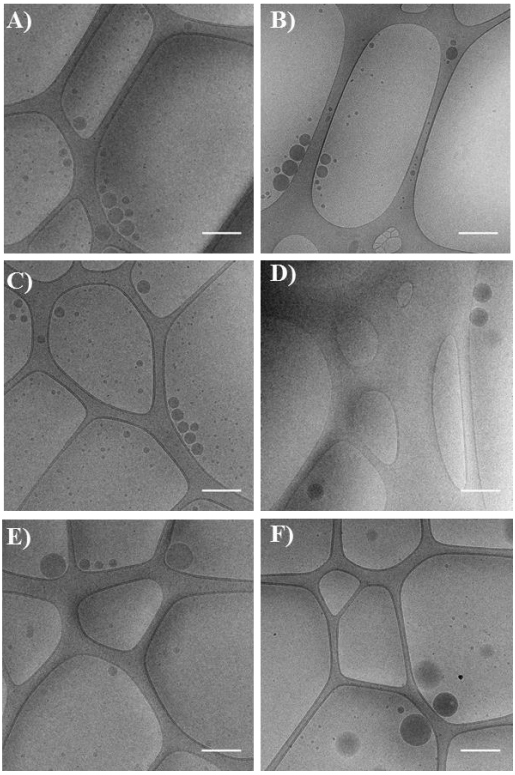

3.2 Cell viability studies

In vitro cell-culture based cytotoxicity is a highly used alternative to animal testing. To determine the IC_{50} of free EAF, unloaded and EAF-loaded NE, two endpoint assays were used - one concerning the integrity of the mitochondrial compartment (MTT) and the other the lysosomal damage (NRU). The cytotoxicity of free EAF, unloaded and

EAF-loaded NE was assessed in human keratinocyte HaCaT and fibroblast 3T3 cell lines (Table 2). For the 3T3 cell line in both endpoint assays, the unloaded PSO-NE and MCT-NE were most cytotoxic to the cells, presenting a lowest IC_{50} values. Regarding the MTT assay the EAF-PSO-NE was the least cytotoxic with the highest IC_{50} followed by free EAF and EAF-MCT-NE. On the other hand, with concern to the NRU assay the free EAF was the least cytotoxic of all samples; this differentiated behavior of samples might be due to the peculiarities of the endpoint assays employed. For the HaCaT cell line the opposite was observed, the free EAF and unloaded NE were less cytotoxic than the EAF-loaded NE with a higher IC_{50} value in both endpoint assays, probably some interaction among the EAF and nanoemulsions components might happen when they are put together which might lead to a cytotoxic event in the cells. Indeed, the cytotoxic effects of free EAF, unloaded and EAF-loaded NE showed some disparities that, in fact, might depend on the NE components, cell line and endpoint assayed.

Moreover it is noteworthy that the concentrations used in the experiments were much lower than the cytotoxic concentrations. Finally, in UV-visible measurements of MTT and neutral red dye interactions with NE alone (without the cells), there was no interference between the formulations and the assay dyes (data not shown).

Table 2. Values of IC_{50} for free EAF, unloaded and EAF-loaded nanoemulsions in 3T3 fibroblasts and HaCaT keratinocytes.

Treatment	***MTT***		***NRU***	
Assay/cell line	***IC_{50} (µg mL^{-1})***		***IC_{50} (µg mL^{-1})***	
	3T3	*HaCaT*	*3T3*	*HaCaT*
EAF	116.5 ± 0.2	166.5 ± 5.7	105.7 ± 10.4	175.2 ± 11.1
EAF-PSO-NE	168.9 ± 8.3	79.0 ± 15.2	89.0 ± 6.4	94.1 ± 1.2
EAF-MCT-NE	115.5 ± 13.6	93.2 ± 1.2	71.3 ± 9.8	93.4 ± 0.8
PSO-NE	89.5 ± 0.3	107.1 ± 6.9	91.5 ± 11.7	190.3 ± 3.7
MCT-NE	74.7 ± 11.7	132.9 ± 12.7	79.9 ± 4.2	164.0 ± 1.8

Values are expressed as mean ± SD of at least three independent experiments.
EAF = ethyl acetate fraction from pomegranate peel dry extract. EAF-PSO-NE = pomegranate seed oil nanoemulsion with the pomegranate ethyl acetate fraction encapsulated. EAF-MCT-NE = medium chain triglyceride nanoemulsion with the ethyl acetate fraction encapsulated. PSO-NE = pomegranate seed oil nanoemulsion (blank). MCT-NE = medium chain triglyceride nanoemulsions (blank).

3.3 Cellular internalization studies

The cellular uptake of fluorescent-labeled NR-NE nanodroplets by the HaCaT cell line was visualized using a fluorescence microscope after 2 and 24 h incubation (Figure 2A). It was apparent that the nanodroplets were taken up by the cells since some fluorescent punctate spots were seen in the cell cytosol. However, a larger number of fluorescent spots were detected along the cell membrane. After 24 h incubation a more intensive dotted pattern of fluorescent NR-NE nanodroplets was observed inside the cell, but again, predominantly along the cell membrane together with some diffuse fluorescence. Figure 2B shows the quantitative analysis of the images and corroborates the fact that after 24 h incubation there was an increase in the number of NR-NE nanodroplets inside the cell but much greater and more intense localization along the cell membrane.

It has previously been reported that neutral and negatively charged particles adsorb much less onto negatively charged cell-membrane surfaces and consequently show lower levels of internalization compared to positively charged particles (CHO et al., 2009; VERMA and STELLACCI, 2010; KHACHANE et al., 2015). This finding is consistent with our results on cellular internalization of EAF-loaded NE. In general, a number of nanodroplets were internalized by the cells, probably through nonspecific binding of the nanodroplets on relatively scarcer cationic sites on the plasma membrane and their subsequent endocytosis (VERMA and STELLACCI, 2010), reflecting the fact that the nanoemulsions contain non-ionic surfactant and present a large number of hydroxyl groups from the polyphenolic compounds in the EAF.

Figure 2C shows the ability of EAF-loaded NE to destabilize the endosomal membrane and release the endocytosed material into the HaCaT cell cytoplasm. The uptake of calcein, a membrane-impermeable fluorophore, and EAF-loaded NE into keratinocyte HaCaT cells was observed through fluorescence microscopy. The control cells, treated with calcein alone, showed a punctate distribution of fluorescence, which is consistent with constitutive endocytosis of the external medium and indicates that the endosome membranes were not damaged (HU et al., 2007; NOGUEIRA et al., 2014). When the calcein was co-incubated with EAF-loaded NE diffuse fluorescence was observed in the cell cytoplasm in some cells, which suggests the low release of calcein from endosomal compartments. However, quantitative analyses of the

cytosolic calcein distribution (Figure 2D) showed that the level of this fluorescence did not differ significantly from that of control cells. When cells were treated with the unloaded NE or free EAF the images and fluorescence quantification were like the untreated control cells (data not shown).

Since the main phenolic compounds identified and quantified in the EAF (ellagic acid, gallic acid and punicalagin) are partially in the ionized form (hydroxyl anion) at the pH range found within the endosomal compartments (pka=5.5; 5.0 and 5.12, respectively), an interaction between the EAF-loaded NE and the endosomal membrane and consequently release of endocytosed material into the cytoplasm might be difficult. However, EAF-loaded NE may act in the extracellular medium and throughout the cell membrane lipid bilayer (inner and outer layer) without compromising its integrity, as demonstrated in our previous study (BACCARIN, MITJANS, LEMOS-SENNA, et al., 2015). Obviously, the possibility that the EAF-loaded NE reaches the cytosol compartment through another internalization pathway cannot be ruled out.

Figure 2. (A) Localization of NR-NE by HaCaT cells after 2 and 24 h of incubation at 37 ºC. Cell uptake was visualized using fluorescence microscopy. (B) Quantitative fluorescence analysis of images like those in 'A'. (C) Fluorescence microscopy images of HaCaT cells showing the distribution of calcein fluorescence. The cells were treated with 1 mg mL^{-1} of calcein (control) and both 1 mg mL^{-1} of calcein and 50 µg mL^{-1} of each EAF-loaded NE formulation. Images were acquired at 3 h after 2 h of uptake. (D) Quantitative fluorescence analysis of images like those in 'C'. Scale bar: 50 µm. The results represent the mean value of ~ 40 cells ± SEM. Statistical analyses were performed using ANOVA ($^{***}p < 0.001$).

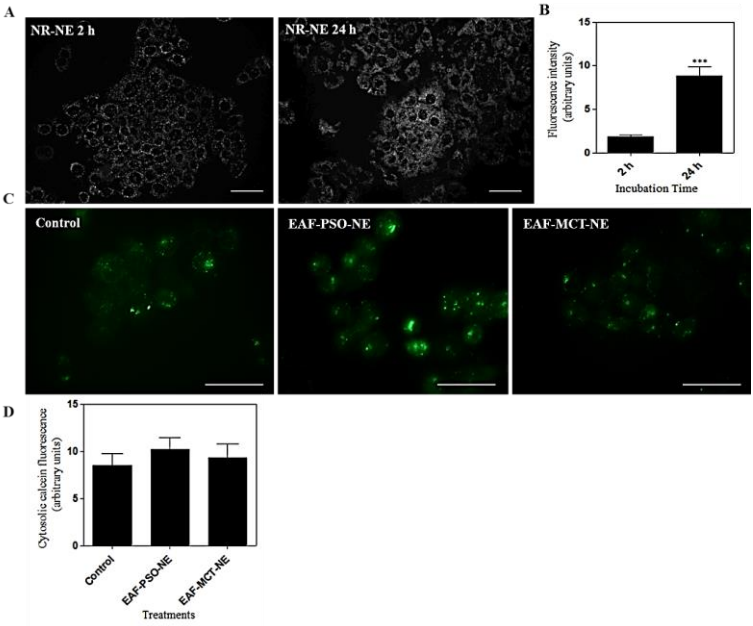

3.4 Photoprotection against UVB-induced DNA damage

DNA bases are considered to be the main targets (chromophores) of UVB irradiation, which results in base modification or dimer formation (SVOBODOVÁ et al., 2009). The DNA lesions observed in the comet assay after UVB irradiation are thought to be transient DNA breaks during the nucleotide excision repair of the photoproducts (ARORA et al., 2012; MAGDOLENOVA et al., 2014). Other mechanisms including oxidative damage to DNA due to the excess

generation of reactive oxygen species (ROS) may also contribute to the UVB-induced comet formation (NICHOLS and KATIYAR, 2010; VOSTÁLOVÁ et al., 2010; AFAQ, 2011).

The use of UV protoprotective dermatological formulations is one of the most recommended and the most common way of preventing solar UV light-caused damage to the skin. Botanical compounds as photoprotective agents in dermatological preparations has received considerable attention since these chemical compounds exhibit a wide range of biological activities (VOSTÁLOVÁ et al., 2010; AFAQ, 2011) and act either as filters, absorbing the UVB photons, or prevent photooxidative damage via the antioxidant activity mainly of their polyphenolic constituents. Previously, high concentrations of total phenolics and substantial amounts of ellagic acid, gallic acid and punicalagin were measured in the free EAF and EAF-loaded *P. granatum* NE using a HPLC-DAD method and presented great antioxidant activity, protecting the lipid bilayer of biomembranes from ROS (BACCARIN and LEMOS-SENNA, 2014; BACCARIN, MITJANS, LEMOS-SENNA, et al., 2015). Here, we evaluated the pretreatment and post-treatment (photorepair) effect of free EAF, unloaded and EAF-loaded NE on UVB-induced DNA damage in human keratinocytes HaCaT cell line.

EAF-loaded NE and free EAF were able to protect the human keratinocyte HaCaT cells from UVB-induced DNA damage, as shown in Figure 3. When cells were irradiated at a dose of 90 mJ/cm^2, the concentrations tested (20 µg mL^{-1} and 50 µg mL^1) for treatments were able to protect and reduce cell DNA damage in a dose dependent manner, by 2.0-fold and 4.7-fold, respectively. At the dose of 200 mJ/cm^2, only the concentration of 50 µg mL^{-1} was effective and reduced the DNA damage by 3.3-fold when compared to the control cells. There was no significant difference between free EAF and EAF-loaded NE in terms of photoprotection against UVB-induced DNA damage, which means that even when entrapped in the oil phase the EAF is able to deliver the same protection. The unloaded NE did not protect the cells against UVB-induced DNA damage (data not shown).

Zaid and collaborators evaluated the inhibition of UVB-mediated oxidative stress in immortalized HaCaT keratinocytes cell line by pomegranate fruit extract. The authors verified that the pretreatment of cells with the extract before an UVB irradiation dose of 15-30 mJ/cm^2, increased the cell viability and intracellular antioxidant mechanism (ZAID et al., 2007). Afaq and collaborators verified that the

pretreatment of human reconstituted skin with pomegranate-derived products before an UVB irradiation dose of 60 mJ/cm^2 protected the cells from DNA damage (AFAQ et al., 2009). At the same manner our findings demonstrates the effectiveness of EAF and EAF-loaded NE on protecting the HaCaT cells from UVB-mediated DNA damage even when higher irradiation doses are employed.

The photoprotective effect of EAF and EAF-loaded *P. granatum* NE seems to be linked to the high amount of polyphenols in the EAF, not less than 600 mg g^{-1} GAE (BACCARIN and LEMOS-SENNA, 2014), and direct elimination of ROS that prevent oxidative damage of cellular constituents, which reflect their antioxidant activity. Also, the protective activity may be related with the ability to absorb UV photons, since these chemical compounds are able to absorb in the UVB region and reduce the number of photons attacking the cell constituents. Our results corroborate those of other authors on the photoprotective activity of pomegranate derived products (ZAID et al., 2007; PACHECO-PALENCIA et al., 2008; AFAQ et al., 2009).

Figure 3. Photoprotection of free EAF and EAF-loaded *P. granatum* nanoemulsions (EAF-PSO-NE and EAF-MCT-NE) against UVB-induced DNA damage at irradiation doses of 90 mJ/cm^2 and 200 mJ/cm^2. Black bars = concentration of 20 µg mL^{-1} and white bars = 50 µg mL^{-1}. ** $p < 0.01$ when compared to non-treated irradiated control. Data are presented as mean ± SEM. Same letters mean no significant difference – ANOVA followed by Tukey's post-hoc test for multiple comparisons.

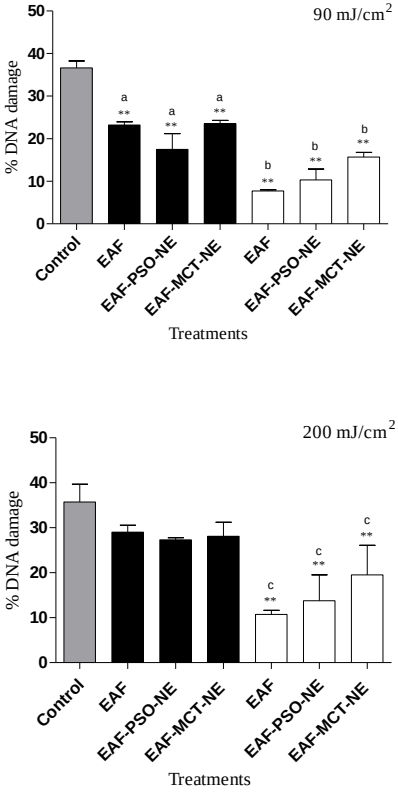

Figure 4. Keratinocyte HaCaT cell viability measured by MTT assay after UVB irradiation and 24 h incubation under photorepair conditions (*see Methods section for more details*). Cells were treated with free EAF and EAF-loaded *P. granatum* nanoemulsions. *** $p < 0.001$ when compared to non-treated irradiated control. Data is presented as mean ± SEM. Same letters mean no significant difference – ANOVA followed by Tukey's post-hoc test for multiple comparisons.

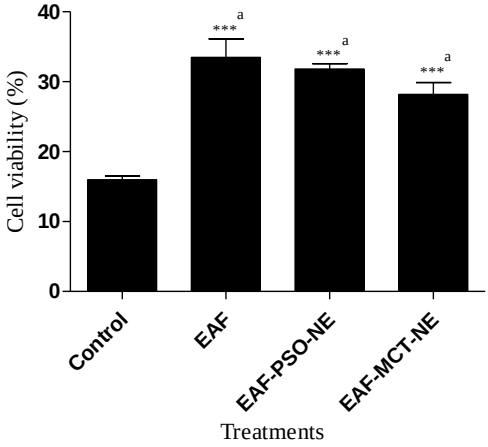

Regarding the photorepair evaluation, the EAF-loaded NE and free EAF could not repair the DNA damage after UVB radiation (data not shown), only protect against it. However, according to the MTT assay employed to characterize keratinocytes cells viability after UVB radiation at a dose of 90 mJ/cm^2 (Figure 4), the cells that were irradiated and then treated with free EAF or EAF-loaded NE, were significantly more viable (approximately 50%) after 24 h than the untreated control or the unloaded NE treated cells; the latter presented the same cell viability as the untreated control cells (data not shown).

3.5 Interleukin-8 release

Figure 5 shows the IL-8 release by keratinocyte cells after UVB irradiation doses of 90 mJ/cm^2 and 200 mJ/cm^2 or under photorepair conditions. Similarly to the photoprotection results, the free EAF and

EAF-loaded NE at 50 μg mL^{-1} reduced IL-8 release in irradiated cells when they were applied before and after (photorepair) UVB exposure. The maximal protection achieved was around 80% for the free EAF and EAF-loaded NE and these treatments were statistically the same. The cells treated with the unloaded NE released a large amount of IL-8 like the untreated control cells (data not shown).

Figure 5. UVB induced IL-8 release in keratinocyte HaCaT cell line after irradiation doses of 90 mJ/cm^2 (grey bars) and 200 mJ/cm^2 (white bars) or under photorepair conditions (black bars) (*see Methods section for more details*). Cells were treated with free EAF and EAF-loaded *P. granatum* nanoemulsions before (photoprotection) and after (photorepair) UVB exposure at the concentration of 50 μg mL^{-1}. Data are presented as mean ± SEM.

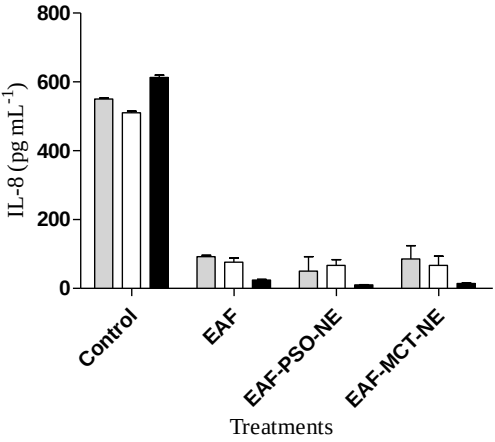

The reduction of UVB-induced IL-8 secretion by keratinocytes demonstrates an important mechanism for protection against UVB-induced skin inflammation by free EAF and EAF-loaded NE, since this cytokine is upregulated in human keratinocytes following UVB-irradiation *in vitro* and *in vivo* (KONDO et al., 1993; STRICKLAND et al., 1997). Significant IL-8 concentrations were secreted and released by the cells in the medium after UVB radiation, and the EAF and EAF-loaded NE were able to suppress the secretion to basal IL-8 levels. IL-8, a pro-inflammatory and chemotactic cytokine, is a key mediator of UVB-induced inflammation, acting as a potent chemoattractant for neutrophils, which then cause local tissue damage (WELSS et al., 2004).

Furthermore, IL-8 induces keratinocyte proliferation, angiogenesis and the growth of a variety of tumors and enhances the expression of matrix metalloproteinases (MMPs) (DI GIROLAMO et al., 2002; STOREY et al., 2004).

3.6 Sun protector factor determination

The SPF *in vitro* was determined for free EAF, EAF-loaded NE and PSO by the spectrophotometric method using the UVB region. Figure 6 shows that the EAF-PSO-NE had the highest SPF at almost all concentrations tested (20, 50 and 100 µg mL^{-1}) with the exception of 5 µg mL^{-1}, at which EAF-PSO-NE, free EAF and PSO had statistically the same SPF (~2). The highest SPF value (~25) was achieved by EAF-PSO-NE at 100 µg mL^{-1}. The SPF values obtained for all samples were concentration-dependent. The sun protection factor (SPF) is the universal indicator for describing the efficiency of sunscreen products. The *in vitro* method correlates well with the *in vivo* tests because it relates the absorbance of the substance to the erythematogenic effect of radiation and intensity of light at specific wavelengths between 290 and 320 nm (DUTRA et al., 2004; EL-BOURY et al., 2007; KAUR and SARAF, 2011; JARZYCKA et al., 2013; MOTA et al., 2013; WU et al., 2014). A synergistic effect was seen between the PSO and the EAF. Besides the phenolic compounds contained in the EAF, PSO presents a typical fatty acid profile that includes a high concentration of punicic acid (~65%), a polyunsaturated acid with three conjugated double bonds in the molecule that also absorb light.

Figure 6. Spectrophotometrically calculated sun protector factor (SPF) values of ethyl acetate fraction fraction (EAF) (grey bars), EAF-loaded *P. granatum* nanoemulsions - EAF-PSO-NE (black bars) and EAF-MCT-NE (white bars) - and pomegranate seed oil (PSO) (dotted bars) at different concentrations. Data are presented as mean ± SD. Same letters mean no significant difference – ANOVA followed by Tukey's post-hoc test for multiple comparisons.

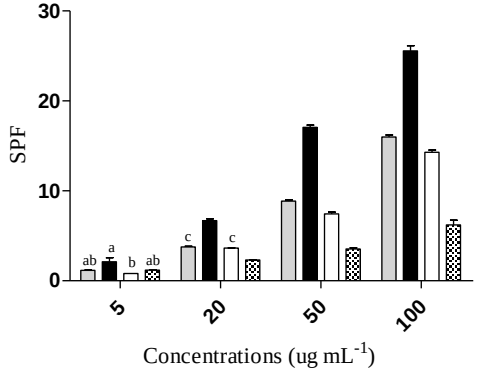

3.7 Phototoxicity

The *in vitro* 3T3 NRU phototoxicity test is a highly sensitive alternative methodology for evaluating phototoxic risk for both pharmaceutical and cosmetic formulations, especially photoirritant risk. Photoirritation is an inflammatory event in the skin that is sometimes induced by oxidative stress in the cellular membrane, triggered by both excessive accumulation of photosensitizers in the skin and exposure of the skin to a particular wavelength of light (SETO et al., 2012); photo-oxidation of lipids and proteins and binding of photosensitizers to amino acid moieties in the cellular membrane are two common causative reactions in photoirritation (SCHOTHORST et al., 1972; GIROTTI, 2001). The phototoxicity of free EAF and EAF-loaded NE was tested on 3T3 mouse fibroblasts and HaCaT human keratinocytes using the NRU assay. Cell viability (%) was mostly above 80% for non-irradiated and irradiated cell lines. which classifies the treatments at the concentration tested as non-phototoxic (OECD, 2004). These results corroborated the preliminary photosafety evaluation of EAF-loaded NE and free EAF in

a human red blood cell model demonstrated in our previous study (BACCARIN, MITJANS, LEMOS-SENNA, et al., 2015).

Figure 7. Phototoxicity of free EAF and EAF-loaded *P. granatum* nanoemulsions (EAF-PSO-NE and EAF-MCT-NE), at concentration of 50 µg mL^{-1} on 3T3 mouse fibroblasts and HaCaT human keratinocytes cell lines measured by neutral red uptake assay. White bars = non-irradiated cells and black bars = UVA 5 J/cm^2 irradiated cells. Data are presented as mean ± SEM.

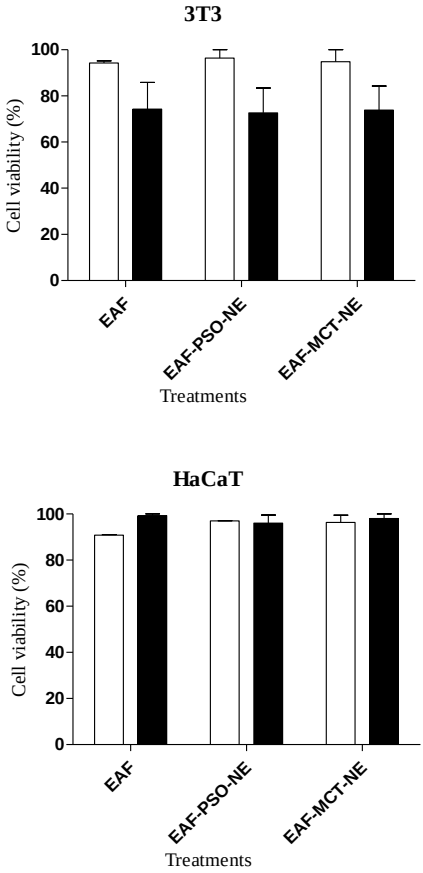

4. CONCLUSIONS

Our results suggest that pomegranate seed oil nanoemulsion entrapping pomegranate peel polyphenol-rich extract has great potential to be used as a sunscreen. EAF-loaded NE were internalized by the keratinocyte cells and also accumulated along the cell membrane. Formulations protected the cells' DNA against UVB-induced damage, protection was concentration dependent. The SPF determined for EAF-loaded NE was relatively high given that no synthetic filters were involved. No phototoxic effect was observed after incubation of EAF or EAF-loaded NE with 3T3 mouse fibroblasts or human keratinocyte HaCaT at the concentration tested. The data presented here can be considered a starting point for the initiation of the use of pomegranate seed oil nanoemulsion entrapping pomegranate peel polyphenol-rich extract for photoprotection against UVB radiation and its damaging effects on human skin. However, further studies are needed to better understand this photoprotective effect.

Conflict of Interest

The authors report no conflicts of interest. The authors alone are responsible for the content and writing of the paper.

Acknowledgment

The authors acknowledge financial support from CAPES (CAPES/PDSE Project No. BEX 5613/13-2), the Ministerio de Economía y Competitividad - Spain (Project MAT2012-38047-C02-01). The authors would like to thank Carmem Iglesias for her expert technical assistance in Cryo-TEM.

References

AFAQ, F. Natural agents: Cellular and molecular mechanisms of photoprotection. **Arch Biochem Biophys,** v. 508, n. 2, p. 144-151, 2011.

AFAQ, F.; ZAID, M. A.; KHAN, N.; DREHER, M.; MUKHTAR, H. Protective effect of pomegranate-derived products on UVB-mediated damage in human reconstituted skin. **Exp Dermatol,** v. 18, n. 6, p. 553-561, 2009.

ALKILANY, A. M.; MURPHY, C. J. Toxicity and cellular uptake of gold nanoparticles: what we have learned so far? **J Nanopart Res,** v. 12, n. 7, p. 2313-2333, 2010.

ARORA, S.; RAJWADE, J. M.; PAKNIKAR, K. M. Nanotoxicology and in vitro studies: The need of the hour. **Toxicol Appl Pharmacol,** v. 258, n. 2, p. 151-165, 2012.

BACCARIN, T.; LEMOS-SENNA, E. Pomegranate seed oil nanoemulsions encapsulating pomegranate peel polyphenol-rich ethyl acetate fraction: Development and antioxidant assessment. **J Nanopharmaceutics and Drug Delivery,** v. 2, n. 4, p. 333-343, 2014.

BACCARIN, T.; MITJANS, M.; LEMOS-SENNA, E.; VINARDELL, M. P. Protection against oxidative damage in human erythrocytes and preliminary photosafety assessment of Punica granatum seed oil nanoemulsions entrapping polyphenol-rich ethyl acetate fraction. **Toxicology in vitro,** v. Article accepted, 2015.

BORENFREUND, E.; PUERNER, J. Toxicity determined in vitro by morphological alterations and neutral red absorptio. **Toxicol Lett,** v. 24, p. 119-124, 1985.

BOUCHEMAL, K.; BRIANÇON, S.; PERRIER, E.; FESSI, H. Nano-emulsion formulation using spontaneous emulsification:solvent, oil and surfactant optimisation. **Int J Pharm,** v. 280, p. 241-251, 2004.

CHIME, S. A.; KENECHUKWU, F. C.; ATTAMA, A. A. **Nanoemulsions — Advances in Formulation, Characterization and Applications in Drug Delivery**. Croatia: Intech Books, 2014.

CHO, E. C.; XIE, J.; WURM, P. A.; XIA, Y. Understanding the role of surface charges in cellular adsorption versus internalization by selectively removing gold nanoparticles on the cell surface with a I2/KI Etchant. **Nano Lett.,** v. 9, n. 3, p. 1080-1084, 2009.

DI GIROLAMO, N.; KUMAR, R. K.; CORONEO, M. T.; WAKEFIELD, D. UVB-mediated induction of interleukim-6 and -8 in pterygia and culture human pterygium epithelial cells. **Invest Ophthalmol Visual Sci,** v. 43, n. 11, p. 3430-3437, 2002.

DORA, C. L.; SILVA, L. F. C.; PUTAUX, J. L.; NISHIYANNA, Y.; PIGNOT-PAINTRAND, I.; BORSALI, R.; LEMOS-SENNA, E. Poly(ethylene glycol) hydroxystearate-based nanosized emulsions: effect of surfactant concentration on their formation and ability to solubilize quercetin. **J Biomed Nanotechnol,** v. 8, p. 1-9, 2012.

DUTRA, E. A.; OLIVEIRA, D. A. G. C.; KEDOR-HACKMANN, E. R. M.; SANTORO, M. I. R. M. Determination of sun protection factor (SPF) of sunscreens by ultraviolet spectrophotometry. **Braz J Pharm Sci,** v. 40, n. 3, p. 381-385, 2004.

EL-BOURY, S.; COUTEAU, C.; BOULANDE, L.; PAPARIS, E.; COIFFARD, L. J. M. Effect of the combination of organic and inorganic filters on the Sun Protection Factor (SPF) determined by in vitro method. **Int J Pharm,** v. 340, p. 1-5, 2007.

GIROTTI, A. W. Photosensitized oxidation of membrane lipids: reaction pathways, cytotoxic effects, and cytoprotective mechanisms. **J. Photochem. Photobiol., B,** v. 63, p. 103-113, 2001.

HU, Y.; LITWIN, T.; NAGARAJA, A. R.; KWONG, B.; KATZ, J.; WATSON, N.; IRVINE, D. J. Cytosolic delivery of membrane-impermeable molecules in dendritic cells using pH-responsive core-shell nanoparticles. **Nano Lett,** v. 7, n. 10, p. 3056-3064, 2007.

ISMAIL, T.; SESTILI, P.; AKHTAR, S. Pomegranate peel and fruit extracts: A review of potential anti-inflammatory and anti-infective effects. **J Ethnopharmacol,** v. 143, n. 2, p. 397-405, 2012.

JARZYCKA, A.; LEWINSKA, A.; GANCARZ, R.; WILK, K. A. Assessment of extracts of Helichrysum arenarium, Crataegus monogyna, Sambucus nigra in photoprotective UVA and UVB; photostability in cosmetic emulsions. **J Photochem Photobiol B,** v. 128, p. 50-57, 2013.

JURENKA, J. Therapeutic applications of pomegranate (Punica granatum L.): a review. **Altern Med Rev,** v. 13, n. 2, p. 128-144, 2008.

KAUR, C. D.; SARAF, S. Photochemoprotective activity of alcoholic extract of *Camellia sinensis*. **Int J Pharmacol,** v. 7, n. 3, p. 400-404, 2011.

KHACHANE, P. V.; JAIN, A. S.; DHAWAN, V. V.; JOSHI, G. V.; DATE, A. A.; MULHERKAR, R.; NAGARSENKER, M. S. Cationic nanoemulsions as potential carriers for intracellular delivery. **Saudi Pharm J,** v. 23, p. 188-194, 2015.

KONDO, S.; KONO, T.; SAUDER, D. N.; MCKENZIE, R. C. IL-8 gene expression and production in human keratinocytes and their modulation by UVB. **J Invest Dermatol,** v. 101, n. 5, p. 690-694, 1993.

MAGDOLENOVA, Z.; COLLINS, A.; KUMAR, A.; DHAWAN, A.; STONE, V.; DUSINSKA, M. Mechanisms of genotoxicity. A review of in vitro and in vivo studies with engineered nanoparticles. **Nanotoxicology,** v. 8, n. 3, p. 233-278, 2014.

MAIORANO, G.; SABELLA, S.; SORCE, B.; BRUNETTI, V.; MALVINDI, M. A.; CINGOLANI, R.; POMPA, P. P. Effects of cell culture media on the dynamic formation of protein−nanoparticle complexes and influence on the cellular response. **ACS Nano,** v. 4, n. 12, p. 7481-7491, 2010.

MANSUR, J. D. S.; BREDER, M. N. R.; MANSUR, M. C. D. A.; AZULAY, R. D. Correlação entre a determinação do fator de proteção solar em seres humanos e por espectrofotometria. **An Bras Dermatol,** v. 61, n. 4, p. 167-72, 1986.

MASON, T. G.; WILKING, J. N.; MELESON, K.; CHANG, C. B.; GRAVES, S. M. Nanoemulsions: formation, structure, and physical properties. **J Phys Condens Matter,** v. 18, n. 41, p. R635, 2006.

MELO, I. L. P.; CARVALHO, E. B. T.; MANCINI-FILHO, J. Pomegranate seed oil (Punica granatum L.): A source of punicic acid (conjugated alpha-linolenic-acid). **Plant Foods Hum Nutr,** v. 2, n. 1, p. 1024, 2014.

MILLER, R.; FAINERMAN, V. B.; MAKIEVSKI, A. V.; KRÄGEL, J.; GRIGORIEV, D. O.; KAZAKOV, V. N.; SINYACHENKO, O. V. Dynamics of protein and mixed protein/surfactant adsorption layers at the water/fluid interface. **Adv Colloid Interface Sci,** v. 86, n. 1–2, p. 39-82, 2000.

MOSMANN, T. Rapid colorimetric assay to cellular growth and survival:application to proliferation and cytotoxicity assays. **J Immunol Methods,** v. 65, p. 55-63, 1983.

MOTA, A. C. V.; FREITAS, Z. M. F.; RICCI JÚNIOR, E.; DELLAMORA-ORTIZ, G. M.; SANTOS-OLIVEIRA, R.; OZZETTI, R. A.; VERGNANINI, A. L.; RIBEIRO, V. L.; SILVA, R. S.; SANTOS, E. P. In vivo and in vitro evaluation of octyl methoxycinnamate liposomes. **Int. J. Nanomed.,** v. 8, p. 4689-4701, 2013.

NICHOLS, J.; KATIYAR, S. Skin photoprotection by natural polyphenols: anti-inflammatory, antioxidant and DNA repair mechanisms. **Arch. Dermatol. Res.,** v. 302, n. 2, p. 71-83, 2010.

NOGUEIRA, D. R.; CARMEN MORÁN, M. D.; MITJANS, M.; PÉREZ, L.; RAMOS, D.; LAPUENTE, J. D.; PILAR VINARDELL, M. Lysine-based surfactants in nanovesicle formulations: the role of cationic charge position and hydrophobicity in in vitro cytotoxicity and intracellular delivery. **Nanotoxicology,** v. 8, n. 4, p. 404-421, 2014.

OECD. OECD Guidelines for the Testing of Chemicals Test No. 432: In Vitro 3T3 NRU Phototoxicity Test. 2004.

PACHECO-PALENCIA, L. A.; NORATTO, G.; HINGORANI, L.; TALCOTT, S. T.; MERTENS-TALCOTT, S. U. Protective effects of standardized pomegranate (Punica granatum L.) polyphenolic extract in ultraviolet-irradiated human skin fibroblasts. **J Agric Food Chem,** v. 56, n. 18, p. 8434-8441, 2008.

PANICHAYUPAKARANANT, P.; ITSURIYA, A.; SIRIKATITHAM, A. Preparation method and stability of ellagic acid-rich pomegranate fruit peel extract. **Pharm Biol,** v. 48, n. 2, p. 201-205, 2010.

PERDE-SCHREPLER, M.; CHERECHES, G.; BRIE, I.; TATOMIR, C.; POSTESCU, I. D.; SORAN, L.; FILIP, A. Grape seed extract as

photochemopreventive agent against UVB-induced skin cancer. **J Photochem Photobiol B,** v. 118, n. 0, p. 16-21, 2013.

RIVERA GIL, P.; OBERDÖRSTER, G.; ELDER, A.; PUNTES, V.; PARAK, W. J. Correlating physico-chemical with toxicological properties of nanoparticles: The present and the future. **ACS Nano,** v. 4, n. 10, p. 5527-5531, 2010.

SABBIONI, E.; FORTANER, S.; FARINA, M.; DEL TORCHIO, R.; PETRARCA, C.; BERNARDINI, G.; MARIANI-COSTANTINI, R.; PERCONTI, S.; DI GIAMPAOLO, L.; GORNATI, R.; DI GIOACCHINO, M. Interaction with culture medium components, cellular uptake and intracellular distribution of cobalt nanoparticles, microparticles and ions in Balb/3T3 mouse fibroblasts. **Nanotoxicology,** v. 8, n. 1, p. 88-99, 2014.

SAYRE, R. M.; AGIN, P. P.; LEVEE, G. J.; MARLOWE, E. A comparison of in vivo and in vitro testing of sunscreening formulas. **Photochem Photobiol,** v. 29, n. 3, p. 559-566, 1979.

SCHOTHORST, A. A.; VAN STEVENINCK, J.; WENT, L. N.; SUURMOND, D. Photodynamic damage of the erythrocyte membrane caused by protoporphyrin in protoporphyria and in normal red blood cells. **Clin. Chim. Acta,** v. 39, p. 161-170, 1972.

SCHUBERT, S. Y.; LANSKY, E. P.; NEEMAN, I. Antioxidant and eicosanoid enzyme inhibition properties of pomegranate seed oil and fermented juice flavonoids. **J Ethnopharmacol,** v. 66, n. 1, p. 11-17, 1999.

SETO, Y.; HOSOI, K.; TAKAGI, H.; NAKAMURA, K.; KOJIMA, H.; YAMADA, S.; ONOUE, S. Exploratory and regulatory assessments on photosafety of new drug entities. **Curr. Drug Saf.,** v. 7, n. 2, p. 140-148, 2012.

SILVA, A. P. C.; NUNES, B. R.; DE OLIVEIRA, M. C.; KOESTER, L. S.; MAYORGA, P.; BASSANI, V. L.; TEIXEIRA, H. F. Development of topical nanoemulsions containing the isoflavone genistein. **Pharmazie,** v. 64, n. 1, p. 32-35, 2009.

STOREY, A.; MCARDLE, F.; FRIEDMANN, P. S.; JACKSON, M. J.; RHODES, L. E. Eicosapentaenoic acid and docosahexaenoic acid reduce UVB- and TNF-[alpha]-induced IL-8 secretion in keratinocytes and UVB-induced IL-8 in fibroblasts. **J Investig Dermatol,** v. 124, n. 1, p. 248-255, 2004.

STRICKLAND, I.; RHODES, L. E.; FLANAGAN, B. F.; FRIEDMANN, P. S. TNF-alpha and IL-8 are upregulated in the epidermis of normal human skin after UVB exposure: Correlation with neutrophil accumulation and E-Selectin expression. **J Invest Dermatol,** v. 108, n. 5, p. 763-768, 1997.

SVOBODOVÁ, A.; ZDAŘILOVÁ, A.; VOSTÁLOVÁ, J. Lonicera caerulea and Vaccinium myrtillus fruit polyphenols protect HaCaT keratinocytes against UVB-induced phototoxic stress and DNA damage. **J Dermatol Sci,** v. 56, n. 3, p. 196-204, 2009.

TAN, C. P.; NAKAJIMA, M. β-Carotene nanodispersions: preparation, characterization and stability evaluation. **Food Chem.,** v. 92, n. 4, p. 661-671, 2005.

VERMA, A.; STELLACCI, F. Effect of Surface Properties on nanoparticle–cell interactions. **Small,** v. 6, n. 1, p. 12-21, 2010.

VIUDA-MARTOS, M.; FERNÁNDEZ-LÓPEZ, J.; PÉREZ-ÁLVAREZ, J. A. Pomegranate and its many functional components as

related to human health: A review. **Compr Rev Food Sci Food Saf,** v. 9, n. 6, p. 635-654, 2010.

VOSTÁLOVÁ, J.; ZDAŘILOVÁ, A.; SVOBODOVÁ, A. Prunella vulgaris extract and rosmarinic acid prevent UVB-induced DNA damage and oxidative stress in HaCaT keratinocytes. **Arch Dermatol Res,** v. 302, n. 3, p. 171-181, 2010.

WELSS, T.; BASKETTER, D. A.; SCHRÖDER, K. R. In vitro skin irritation: facts and future. State of the art review of mechanisms and models. **Toxicol in Vitro,** v. 18, n. 3, p. 231-243, 2004.

WU, P. S.; HUANG, L. N.; GUO, Y. C.; LIN, C. C. Effects of the novel poly(methyl methacrylate) (PMMA)-encapsulated organic ultraviolet (UV) filters on the UV absorbance and in vitro sun protection factor (SPF). **J. Photochem. Photobiol., B,** v. 131, p. 24-30, 2014.

ZAID, M. A.; AFAQ, F.; SYED, D. N.; DREHER, M.; MUKHTAR, H. Inhibition of UVB-mediated oxidative stress and markers of photoaging in immortalized HaCaT keratinocytes bu pomegranate polyphenol extract POMx. **Photochem Photobiol,** v. 83, p. 882-888, 2007.

CAPÍTULO 4: DESENVOLVIMENTO DE HIDROGÉIS CONTENDO NANOEMULSÕES DE *Punica granatum* PARA LIBERAÇÃO TÓPICA DE COMPOSTOS POLIFENÓLICOS

Hidrogéis são redes macromoleculares de polímeros hidrofílicos (iônicos ou não iônicos), que entumescem em contato com soluções aquosas formando redes reticuladas por ligações iônicas, pontes de hidrogênio ou interações hidrofóbicas (PEPPAS et al., 2000; HAMIDI et al., 2008). Os hidrogéis possuem aspecto sensorial agradável e podem atuar como sistemas de liberação de fármacos para uma ampla gama de produtos farmacêuticos e cosméticos (VAN TOMME et al., 2008). Esses sistemas ainda podem se comportar como sistemas reservatórios, modificando e controlando a taxa de difusão de susbtâncias (PEPPAS et al., 2000).

Dentre os polímeros empregados na obtenção de um hidrogel, há os polímeros que conferem ao hidrogel alterações reversíveis na presença de mudanças relacionadas ao meio externo, tais como temperatura, pH e campo elétrico. Em particular, hidrogéis termosensíveis são amplamente investigados, devido às suas características distintas de serem líquidos em baixas temperaturas e tornarem-se um gel à temperatura corporal (PEPPAS et al., 2000; VAN TOMME et al., 2008).

O poloxamer é um copolímero não iônico em tri-bloco de poli (óxido de etileno) / poli (óxido de propileno) / poli (óxido de etileno) de característica anfifílica (Figura 10), capaz de formar gel *in situ* (KLOUDA e MIKOS, 2008; VAN TOMME et al., 2008).

Figura 10. Estrutura química do poloxamer 407, onde (*x*) corresponde a 95-105 unidades de óxido de etileno e (*y*) a 54-60 unidades de óxido de propileno.

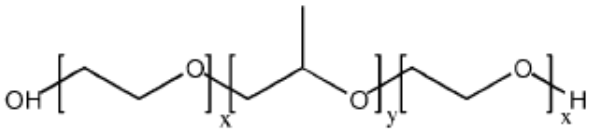

Fonte: Ruel-Gariépy e Leroux (2004).

O fenômeno de transição entre uma solução para um gel é referenciado pela temperatura de transição ($T_{sol\text{-}gel}$). Abaixo da temperatura de transição, o poloxamer encontra-se na forma de uma solução em meio aquoso e acima da temperatura de transição, o polímero se agrega em micelas devido à desidratação das cadeias poliméricas hidrofóbicas (óxido de propileno). Essas micelas são

esféricas com as cadeias hidrofóbicas voltadas para o centro (óxido de propileno) e as cadeias hidrofílicas voltadas para o meio aquoso (óxido de etileno). O hidrogel é formado devido ao arranjo destas micelas e em concentrações adequadas de poloxamer (Figura 11) (DUMORTIER et al., 2006; KLOUDA e MIKOS, 2008; VAN TOMME et al., 2008).

Figura 11. Representação esquemática do mecanismo de associação do poloxamer em água.

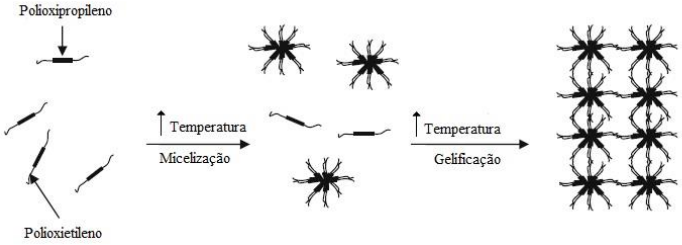

Fonte: adaptado de Dumortier et al. (2006).

Para exercer a ação fotoprotetora os compostos polifenólicos presentes nas nanoemulsões necessitam se difundir pelo veículo reter no *stratum corneum* e/ou permear até as camadas viáveis da epiderme e derme. Modelos *in vitro* têm sido amplamente utilizados para predizer a permeação e distribuição de sustâncias na pele, sendo a utilização de células de difusão a mais empregada. Neste trabalho, estudos de permeação foram realizados usando células de difusão de Franz e pele de orelha suína como modelo de membrana. Um modelo de membrana apropriado deve apresentar características estruturais, de transporte e propriedades de barreira que mimetizem a pele humana. A pele de orelha suína representa uma boa alternativa do ponto de vista histológico por apresentar semelhanças estruturais com a pele humana (BOLZINGER et al., 2012).

A microscopia confocal de varredura a laser (CLSM) é uma técnica muito empregada juntamente com os estudos de permeação para visualizar a distribuição de sistemas de liberação e/ou de substâncias isoladas após a aplicação na pele. Essa técnica é baseada na emissão de fluorescência pela amostra, podendo ser sobreposta à imagem obtida em campo claro (sem fluorescência). Além disso, permite uma melhor resolução de imagem do que um microscópio de fluorescência comum

(ALVAREZ-ROMÁN, NAIK, KALIA, FESSI, et al., 2004; VERMA e FAHR, 2006). Quando a (s) própria (s) substância (s) de interesse não emite fluorescência, um agente fluoróforo é adicionado no sistema, onde o mesmo poderá ligar-se à molécula de interesse ou a algum componente da formulação por meio de ligação covalente ou ainda estar distribuído homogeneamente no sistema (GREENSPAN et al., 1985; ALVAREZ-ROMÁN, NAIK, KALIA, GUY, et al., 2004; TSIENV et al., 2006; POPLE e SINGH, 2010). Neste trabalho, o vermelho de nilo foi usado como agente fluoróforo devido a suas características físico-químicas, como a lipofilicidade, onde o mesmo foi nanoemulsionado juntamente com a fração acetato de etila.

Este capítulo descreve o desenvolvimento e caracterização de hidrogéis termoreversíveis contendo as nanoemulsões para a liberação tópica. Os resultados obtidos encontram-se redigidos sob a forma de artigo, o qual será submetido para publicação no periódico *European Journal of Pharmaceutical Science*. Para a obtenção dos hidrogéis, diferentes concentrações de poloxamer 407 foram incorporadas nas nanoemulsões. O poloxamer 407 tem sido utilizado no desenvolvimento de hidrogéis termosensíveis para aplicação tópica na pele (BRUGUÉS et al., 2015; DJEKIC, KRAJISNIK, et al., 2015; DJEKIC, MARTINOVIC, et al., 2015) pelo fato de promover, melhorar ou retardar a permeação de substâncias através da pele, além de apresentar consistência e características sensoriais agradáveis e possibilitar a aplicação em spray.

Posteriormente os hidrogéis foram caracterizados quanto ao tamanho de gota, potencial zeta, quantificação dos compostos polifenólicos, viscosidade, textura, temperatura de gelificação e morfologia (FEG-SEM). A avaliação da permeação e retenção cutânea *in vitro* e análise por MCVL após a aplicação na pele das formulações contendo tanto a fração quanto o vermelho de nilo nanoemulsionados, também é relatada.

Publicação: "Nanoemulsion drug delivery systems for potential application in skin delivery of polyphenol constituents from pomegranate"

A ser submetida

Nanoemulsion drug delivery systems for potential application in skin delivery of polyphenol constituents from pomegranate

Thaisa Baccarin, Elenara Lemos-Senna*

Departamento de Ciências Farmacêuticas, Centro de Ciências da Saúde, Universidade Federal de Santa Catarina, Campus Universitário Trindade, 88040-900 Florianópolis, SC, Brazil.

*Corresponding author: Elenara Lemos Senna. Programa de Pós-Graduação em Farmácia, Universidade Federal de Santa Catarina, 88040-970, Florianópolis, SC, Brazil. E-mail address: lemos.senna@ufsc.br - Telephone: (+55) 48 37325067

ABSTRACT

Antioxidants such polyphenols are reported to be capable of protecting the skin against ultraviolet (UV) radiation by either absorbing photons before radiation reaches the viable epidermis and dermis or neutralizing reactive species in these skin layers. To obtain suitable viscous formulations to spray on the skin surface, topical hydrogel formulations containing pomegranate seed oil (PSO) or medium chain triglyceride (MCT) nanoemulsions (NEs) entrapping a polyphenol-rich ethyl acetate fraction (EAF) from *Punica granatum* peel extract (EAF-PSO-NE or EAF-MCT-NE) were prepared using poloxamer 407 and properly characterized. The skin permeation and distribution of three major polyphenols - gallic acid (GA), ellagic acid (EA) and punicalagin (PC) - from free EAF, EAF-loaded NEs or EAF-loaded NE gels were obtained by an *in vitro* methodology using porcine ear skin and by confocal laser scanning microscopy. The quantification of polyphenolics compounds in the skin layers and receptor fluid was performed by UFLC. Results indicated a substantial enhancement of skin permeation when the EAF was nanoemulsified. The analysed compounds were mostly retained in the *stratum corneum* and did not reach the receptor compartment. However GA and EA were also delivered in the viable epidermis and dermis. Confocal microscopy corroborated the finding that nanoemulsions drug delivery systems can improve the skin permeation. In conclusion, the skin permeation of compounds depended on the

physicochemical properties of the molecules, vehicle and possible interactions with the skin membrane. Furthermore, nanoemulsions delivery systems containing polyphenol constituents from pomegranate are promising formulations for further studies towards a new photoprotector.

Keywords: *Punica granatum*; pomegranate peel polyphenol-rich ethyl acetate fraction; pomegranate seed oil; nanoemulsions; antioxidant activity; skin permeation; confocal microscopy.

1. INTRODUCTION

Skin is the largest organ in the body whose major function is to protect the body from dehydration and unwanted effects from the external environment. The skin consists of two distinct layers. The dermis (DE), which is made up of connective tissue elements (i.e. collagen, elastin, fibroblasts), is a highly vascular tissue, and includes the sebaceous and sweat glands, hair follicles, nerves, dermal adipose cells, mast cells, and infiltrating leucocytes. The viable epidermis (EP) is basically composed by keratinocytes (95%), melanocytes, Langerhans cells and Merkel cells. The outermost nonviable layer of epidermis is the *stratum corneum* (SC), which is comprised by flattened, stacked, hexagonal, and cornified cells (corneocytes or horny cells), enveloped by a highly organized lipid-rich matrix, which has been described as a brick and mortar model. This particular structure of the SC has been considered as the rate controlling barrier for the percutaneous absorption of substances (BARRY, 2001; MENON, 2002; KONG et al., 2011).

Ultraviolet (UV) radiation is one of the major causes of formation of reactive oxygen species (ROS), which are associated with UV-induced skin damages such as erythema and sunburn, DNA damage, oxidative stress, premature skin aging and carcinoma (BITO e NISHIGORI, 2012). Topical application of natural antioxidants compounds, as polyphenols, has emerged as a successful approach for the prevention of ultraviolet-induced oxidative stress and skin alteration, due to their ability to absorb the UV photons or neutralize pro-oxidant reactive species, mainly when the levels of endogenous antioxidants are significantly depleted (AFAQ, 2011; GODIC et al., 2014). However, attention to the cutaneous permeation must be given, since antioxidant compounds should be able to reach the viable skin layers to afford satisfactory photoprotection (SAIJA et al., 2000; FREITAS et al., 2015).

Many strategies have been investigated to improve the skin permeation and efficacy of topically applied drugs. Among them is the use of nanoemulsions (NEs), which has proved to be able to enhance release and skin permeation due to its very small droplet size and low surface tension, which provides a good contact with the skin surface. Besides, the surfactant and co-surfactant components of nanoemulsions may reduce the diffusional obstruction of the *stratum corneum* by inherent penetration enhancer's activity, and its high solubilizing capacity of hydrophobic drugs may increase the thermodynamic activity towards the skin (SONNEVILLE-AUBRUN et al., 2004; TADROS et al., 2004; KOGAN and GARTI, 2006; KONG et al., 2011; MONTENEGRO et al., 2011).

In a previous study, we developed and characterized an oil-in-water nanoemulsions entrapping an ethyl acetate fraction from pomegranate peel dried extract (EAF) using the pomegranate seed oil (PSO) or medium chain triglyceride (MCT) as oil phases. Pomegranate (*Punica grantum L.*) is a seeded or granular apple consumed worldwide, which is known for its high antioxidant properties, due to the presence of polyphenolic compounds that are concentrated in the fruit peels, such as ellagic acid (EA), gallic acid (GA) and punicalagin (PC) (AVIRAM et al., 2000; LI et al., 2006; ÇAM et al., 2009; FISCHER et al., 2011; LANDETE, 2011; ISMAIL et al., 2012; MANASATHIEN et al., 2012; QU et al., 2012). Pomegranate seed oil (PSO) is found in the seeds and contains conjugated fatty acids, in which the main constituent is punicic acid (EL-NEMR et al., 2006; FADAVI et al., 2006), that it has been reported to have antioxidant properties (QU et al., 2010). The antioxidant activity of EAF-loaded NEs (EAF-PSO-NE and EAF-MCT-NE) was demonstrated through the ferric reducing antioxidant power (FRAP) and 2,2-diphenyl-1-picrylhydrazyl (DPPH) assays (BACCARIN and LEMOS-SENNA, 2014). The ability of free EAF and EAF-loaded NE to interact with the lipid bilayer of biomembrane and protect it against a radical initiator was also verified (BACCARIN, MITJANS, LEMOS-SENNA, et al., 2015). Finally, a recent study evidenced the photoprotection activity of EAF-loaded NE against UVB-induced DNA damage on the human keratinocyte HaCaT cell line (BACCARIN, MITJANS, RAMOS, et al., 2015).

Although NEs exhibit several advantages for topical delivery, the low viscosity of these drug delivery systems restrains its clinical application due to inconvenient use. To overcome this limitation, the nanoemulsions were thickened by adding poloxamer 407 into the

external phase of the colloidal dispersions. Poloxamer 407 is an amphiphilic synthetic copolymer consisting of a hydrophobic poly(oxypropylene) block between two hydrophilic poly(oxyethylene) blocks, and it is frequently used as a gelling agent to form thermosensitive hydrogels. Depending on its concentration, poloxamer dispersions exhibit a free-flowing property at room temperature, but easily form *in situ* gels when in contact with the skin temperature (BUWALDA et al., 2014). This characteristic allows spraying the formulation onto the skin, facilitating the product application.

Considering the above mentioned, in this study we described the preparation and characterization of poloxamer 407 hydrogel containing EAF-loaded nanoemulsions. We also evaluated the skin permeation and distribution of the polyphenolic compounds from pomegranate, using Franz diffusion cells and porcine ear skin as membrane model. The results obtained in this study may be useful to predict the ability of the nanoemulsions loaded with pomegranate constituents in to protect the skin against UV radiation damage.

2. MATERIALS AND METHODS

2.1 Materials

Pomegranate seed oil and pomegranate peel dried extract were purchased from Via Farma (Sao Paulo, Brazil); according to the manufacturer, pomegranate seed oil contains 65% to 85% of punicic acid, and minor amounts of others polyunsaturated fatty acids, including linoleic acid, and α- and γ-linolenic acids. Pomegranate peel dried extract is a spray-dried powder standardized to contain at least 40% of ellagic acid. Soy lecithin (Lipoid® S100) and polysorbate 80 (Tween 80®) were purchased from PharmaNostra (Rio de Janeiro, Brazil) and Sigma-Aldrich (St. Louis, MO, USA), respectively. Medium chain triglyceride (Rittamolient®) was purchased from Brasquim (Porto Alegre, Brazil). Ellagic acid, gallic acid and punicalagin standards, Folin-Ciocalteu's reagent, poloxamer 407 (polyoxyethylene-polyoxypropilene-polyoxyethylene tri-block copolymer) (Pluronic F-127®), nile red and triethanolamine were purchased from Sigma-Aldrich (St. Louis, MO, USA). Except for the methanol (Vetec®), acetonitrile (Panreac®) and acetic acid (Vetec®) (Sao Paulo, Brazil) of HPLC grade used in the analysis, all the other solvents and reagents were analytical grade.

2.2 Pomegranate polyphenol-rich ethyl acetate fraction

The pomegranate polyphenol-rich ethyl acetate fraction (EAF) was obtained and characterized as previously described (BACCARIN and LEMOS-SENNA, 2014). Briefly, the dried powder was extracted by 24 hour dynamic maceration with a 90:10 (v/v) methanol:water mixture. The extractive solution was evaporated under reduced pressure for solvent removal, and the precipitate was suspended with a 2% aqueous acetic acid solution. The resulting mixture was then partitioned with dichloromethane and ethyl acetate. Thereafter, the pooled ethyl acetate fraction was evaporated under reduced pressure to dryness.

2.3 Preparation of the nanoemulsions

EAF-loaded pomegranate seed oil-based nanoemulsions (EAF-PSO-NE) and EAF-loaded medium chain triglyceride-based nanoemulsions (EAF-MCT-NE) were prepared using the ultrasonic emulsification method followed by solvent evaporation and by the spontaneous emulsification method, respectively (BACCARIN and LEMOS-SENNA, 2014). For the first method, the EAF (0.5%; w/v), soy lecithin (0.4%; w/v) and PSO (2%; w/v) were dissolved in 10 mL of ethyl acetate. This ethyl acetate solution was slowly poured into 40 mL of a 2.1% (w/v) polysorbate 80 aqueous solution and adjusted to pH 5.0-6.5 with triethanolamine. The oil in water dispersion was sonicated for 3 minutes using an Ultrasonic Processor UP200S (Hielscher, Germany), and then it was and kept under magnetic stirring for 24 hours. The resulting nanoemulsion was evaporated under reduced pressure up to volume of 15 mL.

For the preparation of medium chain triglyceride-based nanoemulsions (EAF-MCT-NE), 10 mL of an ethanolic solution containing EAF (0.5%; w/v), soy lecithin (0.4%; w/v), and MCT (1.8%, w/v) that was poured into 40 mL of a 2.1% (w/v) polysorbate 80 aqueous solution under magnetic stirring and adjusted to pH 5.0-6.5 with triethanolamine. The nanoemulsion was then evaporated under reduce pressure to eliminate the organic solvent and concentrated up to volume of 15 mL. All formulations were filtered through 8 µm quantitative filter paper. Unloaded PSO-NE and MCT-NE were prepared as the same manner.

2.4 Preparation of the hydrogel containing nanoemulsions

To prepare the hydrogels, poloxamer 407 was added to the unloaded and EAF-loaded nanoemulsions at concentrations of 18% and 28% (w/v). Following, the mixtures were kept at 4º C during 12 hours to ensure complete wetting. Then, the hydrogels containing the nanoemulsions were stirred for mixing and were stored at 4º C for further analysis.

2.5 Characterization of the nanoemulsions and hydrogels containing nanoemulsions

2.5.1 Droplet size and zeta potential

The mean droplet size and zeta potential of NEs and hydrogels containing the nanoemulsions were determined by dynamic light scattering (DLS) and laser-Doppler anemometry, respectively, using a Zetasizer Nano Series (Malvern Instruments, Worcestershire, UK). The size analyses were performed at a scattering angle of 173º, after appropriated dilution of the samples in ultrapure water (Milli-Q®, Millipore, USA). For zeta potential analysis, the samples were diluted in Milli-Q® water and placed in electrophoretic cells where a potential of ±150 mV was applied. The zeta potential values were calculated as mean electrophoretic mobility values by using Smoluchowski's equation.

2.5.2 HPLC analysis of polyphenolic compounds

The determination of the major phenolic compounds of the EAF, which are ellagic acid (AE), gallic acid (GA) and punicalagin (PC), was performed using a HPLC method previously developed and validated (BACCARIN e LEMOS-SENNA, 2014). The experiments were conducted using a Shimadzu-HPLC system equipped with a LC-20AT binary pump, CTO-20A oven, SPD-M20A photo diode array detector and software LC Solution 1.2 (Shimadzu, Tokyo, Japan). The analyses were carried out with a Luna C18 5 µm Fusion RP 100 Å column (250 mm x 4.6 mm) (Phenomenex®, USA) coupled with a C18 guard column (Phenomenex®, USA), equilibrated at 30º C. Mobile phase consisted of acetonitrile (A) and 1% (v/v) acetic acid aqueous solution (B), which were filtered prior to use through 0.45 µm regenerated cellulose

membrane filter. The mobile phase was eluted at flow rate of 1 mL.min^{-1} using the following linear gradient program: 97% B at 0.01-3 min, 97%-94% B at 3-5 min; 94%- 90% B at 5-8 min; 90%-87% B at 8-12 min; 87%-84% B at 12-15 min, 84%-80% B at 15-18 min; 80%-77% B at 18-21 min; 77%-74% B at 21-24 min, 74%-97% B at 24-28 min; 97% B at 28-30 min. The injection volume of the samples was 20 mL and the detection was achieved at wavelengths of 270 nm, 367 nm and 378 nm for gallic acid, ellagic acid, and punicalagin, respectively.

To determine the polyphenolic compounds in the EAF-loaded nanoemulsions and in the hydrogels, 1 mL of each formulation was transferred to a 10 mL volumetric flask. Following, the samples were dissolved with 1 mL of acetonitrile (EAF-MCT-NE or EAF-MCT-NE hydrogel) or ethyl acetate (EAF-PSO-NE or EAF-PSO-NE hydrogel), the mixtures were shaken vigorously in a vortex for 2 min, and acetonitrile was added to complete the volume. The resulting solutions were filtered through a 0.2 µm PTFE syringe filter and injected in the chromatograph. All samples were analyzed in triplicate.

2.5.3 Morphology

The morphology of the hydrogels containing the nanoemulsions was evaluated using a Jeol JSM-6701F high-resolution scanning electron microscope (FEG-SEM, Japan). For that, samples were placed directly onto aluminium stubs and dried in a freeze-drying Terroni LD 1500 (Terroni®, Sao Paulo, Brazil). Thereafter, the samples were coated with colloidal gold and examined at an accelerating voltage of 5 kV.

2.6 Evaluation of the rheological properties of the hydrogels

2.6.1 Determination of gelation temperature

Gelation temperatures of the hydrogels containing the unloaded and EAF-loaded NEs were measured by the method described by Bruschi et al. (2007). A transparent beaker containing a magnetic bar and 15 g of each formulation was placed in a magnetic stirred-hot plate, and slowly heated under stirring. The sol/gel transition temperature ($T_{sol/gel}$), corresponding to the temperature in which the magnetic bar stopped from moving, was measured using a thermometer. Samples were analyzed on triplicate.

2.6.2 Textural profile analysis (TPA)

The textural properties of the hydrogels containing the nanoemulsions were measured using a TA-XTPlus Texture Analyser (Stable Micro Systems, Surrey, UK) in textural profile analysis (TPA) mode (JONES et al., 1997; HURLER et al., 2012). Approximately 15 g of the hydrogels were transferred into 10 mL transparent beakers, taking care to avoid the introduction of air into the samples. An analytical probe (10 mm diameter) was twice forced down into each sample at a defined rate (1 mms^{-1}) and to a defined depth (20 mm), allowing a delay period (10 s) between the end of the first and the beginning of the second pass. At least three replicate analyses of each sample were performed at 37 ºC. From the resulting force–time plots, the hardness, adhesiveness, springiness and cohesiveness were derived. Samples were analyzed on triplicate.

2.6.3 Viscosity determination

The viscosities of hydrogels containing the nanoemulsions were assessed at 10, 25 and 37 ºC using a rotational viscometer HAAKE VT 550-PK10 (Thermo Scientific, USA) with a PK1/1º or SVDIN rotor and coupled with a temperature controlled water bath. Shear rates ranged from 0.01 to 80 s^{-1} and the shearing rate was increased over a period of 100 s, held at the upper limit for 100 s, and then decreased over a period of 100 s. A temperature ramp from 10 to 40 ºC was made for each NE gel to evaluate the viscosity of samples as a function of temperature. The measurements were carried out in triplicate and the data was analyzed using RheoWin Job Manager and RheoWin Data Manager Software.

2.7 *In vitro* skin permeation and retention studies

In vitro skin permeation and retention studies were performed on a Franz diffusion cell with an effective diffusional area of 1.52 cm^2 and 12 mL of receiver chamber capacity using porcine ear skin as membrane model. Porcine ears were obtained from a local slaughterhouse (Antonio Carlos, Brazil). The ears were withdrawn from the animals before the scalding procedure, cleaned, wrapped in aluminium foil and stored at -20°C for a maximum time period of 1 month. On the day of the experiment, the ears were thawed, the full-thickness skin was excised

from the outer region of the ear with a scalpel, and the subcutaneous fat was removed. Then, the excised circular pig ear skin with a thickness about 0.5 to 0.8 mm was set between the donor and the receptor compartments, with the inner part facing the upper inside portion of the cell. The receptor medium consisted of a 25:75 (v/v) ethanol:water solution, which was maintained under magnetic stirring at temperature of 37 ºC throughout the experiments. For the permeation studies of pomegranate polyphenols, 1 mL of the EAF solution (0.5 %; w/v), EAF-loaded NEs or hydrogels containing the EAF-loaded NEs was placed in the donor compartment, and after 30 min, 1, 2, 4, 6 and 8 h, an aliquot of 1 mL of the receptor medium was withdrawn and immediately replaced with an equal volume of fresh diffusion medium. The samples were filtered through a 0.45 µm regenerated cellulose syringe filter and analysed by UFLC-DAD method described below. All experiments were carried out in six replicates.

Skin retention of pomegranate polyphenols was determined in the *stratum corneum* (SC), epidermis (EP), and dermis (DE). At the end of the 8-hour permeation study, the skin was removed from the cell and the excess of the formulation was removed using a cotton swab. Then, the SC was separated from whole skin using the tape stripping method (3M, Scotch, St Paul, USA). The first stripped tape was discarded, while the following 15 tapes were cut, placed into test tubes, and extracted with 5 mL of methanol for determination of the polyphenolic compounds. Next, the EP was separated from the DE using a scalpel, cut into tiny pieces, placed into separated test tubes, and extracted with 2 mL of methanol. The tubes with different skin layers were maintained in an ultrasound bath during 1 hour and left at 4 ºC overnight. Thereafter, the samples were sonicated for 5 minutes using a Ultrasonic Processor UP200S (Hielscher, Germany), transferred to microtubes, centrifuged at 6200 rpm for 20 minutes. The supernatants were then filtered through a 0.45 µm PVDF syringe filter and analysed through a UFLC-DAD method, as described below. All experiments were carried out in six replicates.

2.8 UFLC analysis

The quantification of EA, GA and PC in receptor fluid and skin layers was assessed by ultra-fast liquid chromatography (UFLC). In brief, UFLC apparatus consisted of a Shimadzu LC-20AD system (Tokyo, Japan) equipped with a model LC-20AD pump, a SPD-M20A

photo diode array detector, a DGU-20A3 degasser, a CBM-20A system controller, and a SIL-20AC auto sampler. The analyses were carried out with a Luna C18 5 µm Fusion RP 100 Å column (250 mm x 4.6 mm) (Phenomenex®, USA) coupled with a C18 guard column (Phenomenex®, USA). Mobile phase consisted of acetonitrile (A) and 1% (v/v) acetic acid aqueous solution (B), filtered prior to use through 0.45 µm regenerated cellulose membrane filter. The mobile phase was eluted at flow rate of 1 $mL.min^{-1}$ using the following linear gradient program: 97% B at 0.01-3 min, 97%-94% B at 3-5 min; 94%- 90% B at 5-8 min; 90%-87% B at 8-12 min; 87%-84% B at 12-15 min, 84%-80% B at 15-18 min; 80%-77% B at 18-21 min; 77%-74% B at 21-24 min, 74%-97% B at 24-28 min; 97% B at 28-30 min. The injection volume of the samples was 20 mL and the detection was achieved at wavelengths of 254 nm.

The UFLC-DAD method was validated according to the ICH and ANVISA guidelines (BRASIL, 2003c; ICH, 2005) according the parameters of linearity, specificity, accuracy, precision, limit of detection (LOD) and quantification (LOQ). The specificity of the method was assessed by detection of possible interferences of adhesive tape, skin (SC, EP and DE), receptor medium and hydrogel containing the unloaded nanoemulsions. The linearity of the method was assessed by construction of calibration curves in receptor medium at concentration ranging from 1 to 20 $\mu g.mL^{-1}$ for all polyphenols, and in methanol at concentrations ranging from 0.5 to 20 $\mu g.mL^{-1}$, 0.3 to 20 $\mu g.mL^{-1}$ and 5 to 40 $\mu g.mL^{-1}$ for GA, EA and PC, respectively. LOD and LOQ were calculated at signal-to-noise ratios (S/N) of 3 and 10, respectively, based on the standard deviation of the *y* intercepts of regression curves. To assess the accuracy of the method, accurate amounts at tree levels concentrations of GA, EA and PC (5, 10 and 20 $\mu g.mL^{-1}$) were added to the samples of receptor medium, adhesive tapes containing SC, EP or DE after the 8-hour permeation/retention study. The percent recovery of phenolic compounds in the samples was determined by comparing the obtained experimental concentrations with the corresponding theoretical concentrations. Finally, for precision determination, GA, EA and PC were analyzed in the receptor medium and methanol in triplicate at three concentrations levels (5, 10 and 20 $\mu g.mL^{-1}$) in one day (intra-day precision) and for another two consecutive days (inter-day precision). The results were expressed as relative standard deviation (%RSD).

2.9 Confocal fluorescence microscopy study

For confocal fluorescence experiments, nile red (NR), a fluorescent dye, was added in the organic phase during the preparation of EAF-loaded NEs to obtain formulations displaying a NR final concentration of 0.007% (w/v) (EAF_{NR}-MCT-NE or EAF_{NR}-PSO-NE). Briefly, 1 mL of a 0.007% (w/v) NR solution, EAF_{NR}-loaded NEs or hydrogel containing the EAF_{NR}-loaded NEs was placed in the donor compartment of the diffusion cells and a skin permeation study was performed under the same experimental conditions described in the *section 2.7*. After 30 minutes or 8 hours of experiment, the skin was removed from the Franz cells, cleaned with a cotton swab, submerged in a freezing medium (Tissue-Tek®, Leica Microsystems, Germany) and frozen at -20°C for 24hs. Thereafter, the samples were mounted onto a metal sample holder and transversal sections of skin cuts of 20 µm thickness were obtained using a microtome-cryostat CM 1850 UV (Leica Microsystems, Germany) equipped with high profile carbon blades (EMSCD500, Leica Microsystems, USA). The slides were evaluated using a confocal microscope Leica DMI6000 B (Leica Microsystems, Germany), with a helium–neon laser at exciting wavelength of 543 nm and emission wavelength from 585 nm to 635 nm. The images were taken at a tenfold magnification. Slides were also obtained from porcine ear skin alone and from a skin obtained after 8-hours permeation studies using a EAF-loaded NE in order to verify a possible fluorescence emission of these samples.

2.10 Data analysis

Experimental data were statistically analyzed through analysis of variance (ANOVA) ($p < 0.05$) followed by Tukey's test using the Graph-Pad Prism software (San Diego, USA).

3. RESULTS

3.1 Characterization of the poloxamer hydrogels containing EAF-loaded NEs

The results obtained in the characterization of the hydrogels containing the nanoemulsions are summarized in the Table 1. As can be observed, all hydrogels formulations exhibited droplet mean sizes in the

nanometric range, varying from 168 to 257 nm, which was similar to those values obtained for the nanoemulsions alone. The zeta potential values varied from -12.5 to -18.8 mV for the hydrogels, evidencing a decrease in the surface charge of the droplets after incorporation of the poloxamer 407 in the external phase of the nanoemulsions. The concentrations of GA, EA, and PC in the hydrogels containing the EAF-loaded NEs were similar to those reported for EAF-loaded NEs. The pH of the hydrogels varied from 5.5 to 6.3. The presence of nanodroplets with sizes of about 150 to 200 nm in the hydrogel matrix was confirmed by FEG-SEM (Figure 1), corroborating with the results obtaining by DLS.

Figure 1. FEG-SEM images of poloxamer 407 (18% w/v) hydrogel containing P. granatum EAF-loaded nanoemulsion (EAF-PSO-NE) obtained at (A) 10.000 and (B) 25.000 times of magnification.

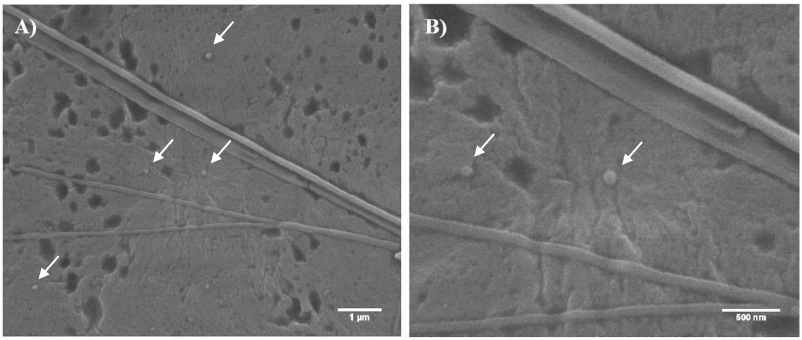

The viscosity of the poloxamer hydrogels measured at different temperatures (10 ºC, 25 ºC and 37 ºC), as well as their gelation temperature values are depicted in the Table 2. As can be seen, the viscosity of the hydrogels was dependent on both temperature and poloxamer concentration. It is noteworthy that the sol-gel transition temperature decreased with the increase of the poloxamer concentration from 18% to 28% by 5 to 8 degrees. Figure 2 also illustrates the effect of temperature on the hydrogel viscosity. At 10 ºC, the poloxamer hydrogel containing the NEs can be characterized as Newtonian fluid (Figure 2-A) and as the temperature increases, the rheological properties of the hydrogel changes, becoming a Non-Newtonian pseudo-plastic fluid (flow index <1) with thixotropic behaviour (data not shown)

(Figure 2-B, C). Figure 2-D displays the temperature ramp from 10 ºC to 40 ºC and corroborates with our findings, in which hydrogel viscosity increases with the temperature augmentation and this increasing was dependent on poloxamer concentration.

The mechanical properties of hydrogels containing the NEs are summarized in the Table 3. The increase in the copolymer concentration from 18% (w/v) to 28% (w/v) provoked a change in their mechanical properties, resulting in an increasing in the hardness, adhesiveness, springiness, and cohesiveness.

Figure 2. Effect of the temperature on the viscosity of the poloxamer hydrogels containing the NEs. Viscosity profiles were obtained at (A)10 ºC, (B) 25 ºC, and (C) 37 ºC for poloxamer 407 hydrogels containing unloaded (MCT-NE or PSO-NE) and EAF-loaded NEs (EAF-MCT-NE or EAF-PSO-NE). (D) Temperature ramp obtained from 10 ºC to 40 ºC.

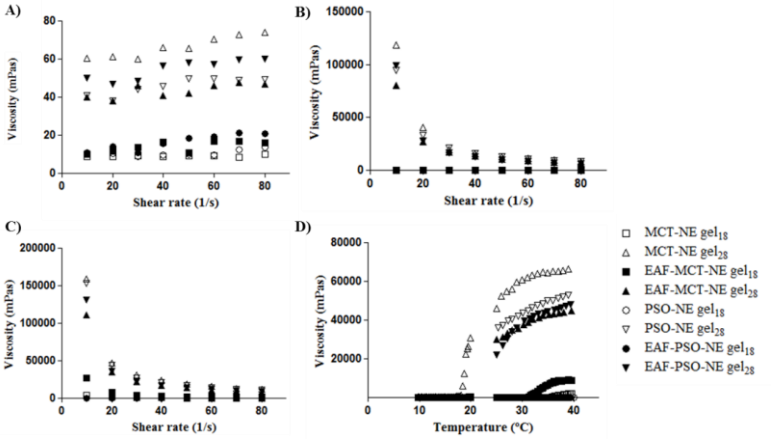

Table 1.Values of zeta potential, mean droplet size, and content of the major pomegranate polyphenols obtained for the nanoemulsions and poloxamer hydrogels containing the nanoemulsions.

Samples[a]	Zeta Potential (mV ± SD)	Size (nm ± SD)	AG (μg.mL^{-1} ± SD)	EA (μg.mL^{-1} ± SD)	PC (μg.mL^{-1} ± SD)
EAF-MCT-NE	-33.3 ± 1.4	222.0 ± 8.20	1263.6 ± 6.81	88.9 ± 11.03	460.6 ± 5.80
EAF-MCT-NE gel$_{18}$	-16.5 ± 0.2	257.0 ± 2.54	1175.5 ± 2.41	80.1 ± 4.14	576.9 ± 4.17
EAF-MCT-NE gel$_{28}$	-14.7 ± 0.2	255.9 ± 5.16	1094.1 ± 1.67	88.0 ± 5.94	480.4 ± 4.67
EAF-PSO-NE	-27.5 ± 0.9	169.0 ± 3.89	1216.4 ± 15.55	41.4 ± 7.28	471.2 ± 2.08
EAF-PSO-NE gel$_{18}$	-18.8 ± 1.3	168.5 ± 5.65	1021.5 ± 3.54	34.6 ± 1.14	454.4 ± 0.26
EAF-PSO-NE gel$_{28}$	-12.9 ± 0.3	178.0 ± 4.95	1058.1 ± 12.85	38.3 ± 4.57	457.3 ± 8.55

AG=Gallic Acid; EA=Ellagic Acid; PC=Punicalagin.
[a]The subscript number indicates the concentration of poloxamer 407 in the hydrogel.
Data are presented by mean ± standard deviation (SD) (n=3).

Table 2. Viscosity determination at 10 ºC, 25 ºC and 37 ºC, flow and gelation temperature ($T_{sol\text{-}gel}$) obtained by mechanical method of poloxamer 407 gels (18% or 28% w/v) containing blank nanoemulsions or *P. granatum* EAF-loaded nanoemulsions.

Samples[a]	**Viscosity (mPas ± SD)**			**$T_{sol\text{-}gel}$ (ºC ± SD)**
	10 ºC	**25 ºC**	**37 ºC**	
MCT-NE gel_{18}	6.72 ± 1.15	63.74 ± 1.61	486.90 ± 2.44	33,3 ± 2.08
MCT-NE gel_{28}	68.01 ± 2.53	13137.54 ± 3.10	16005.00 ± 2.89	26,2 ± 1.04
EAF-MCT-NE gel_{18}	11.83 ± 2.02	124.20 ± 2.13	2170.97 ± 1.88	32,3 ± 1.53
EAF-MCT-NE gel_{28}	43.26 ± 2.33	9224.41 ± 2.22	11435.67 ± 2.15	27,0 ± 2.00
PSO-NE gel_{18}	6.72 ± 1.49	159.64 ± 3.10	245.31 ± 2.68	33,7 ± 1.15
PSO-NE gel_{28}	47.85 ± 3.07	10773.38 ± 2.65	14207.77 ± 3.22	27,3 ± 1.15
EAF-PSO-NE gel_{18}	17.67 ± 2.68	97.21 ± 1.57	117.35 ± 3.00	34,0 ± 1.73
EAF-PSO-NE gel_{28}	57.66 ± 1.77	8455.98 ± 3.30	12039.54 ± 3.55	26,7 ±1.53

Data are presented by mean ± standard deviation (SD) (n=3).

[a]The subscript number indicates the concentration of poloxamer 407 in the hydrogel.

Table 3. The mechanical properties of poloxamer 407 gels (18% or 28% w/v) containing blank nanoemulsions or *P. granatum* EAF-loaded nanoemulsions determined by texture profile analysis.

Samples	**Hardness (*N*)**	**Adhesiveness (*N* sec)**	**Springiness (*N* sec)**	**Cohesiveness (*N* sec)**
MCT-NE gel_{18}	1.49 ± 0.13	23.340 ± 3.09	0.590 ± 0.24	0.880 ± 0.13
MCT-NE gel_{28}	60.80 ± 0.33	54.761 ± 1.41	0.693 ± 0.11	0.934 ± 0.05
EAF-MCT-NE gel_{18}	2.24 ± 0.73	17.539 ± 2.47	0.612 ± 0.16	0.914 ± 0.12
EAF-MCT-NE gel_{28}	55.27 ± 2.07	57.563 ± 0.78	0.762 ± 0.13	0.970 ± 0.21
PSO-NE gel_{18}	1.85 ± 0.64	10.062 ± 1.02	0.411 ± 0.15	0.956 ± 0.03
PSO-NE gel_{28}	75.70 ± 0.22	64.185 ± 0.95	0.793 ± 0.16	0.902 ± 0.05
EAF-PSO-NE gel_{18}	1.26 ± 0.47	0.759 ± 0.07	0.399 ± 0.10	0.876 ± 0.13
EAF-PSO-NE gel_{28}	53.92 ± 3.14	51.264 ± 6.66	0.808 ± 0.13	1.053 ± 0.18

Data are presented by mean ± standard deviation (SD) (n=3).

3.2 UFLC method validation

The UFLC method for quantification of GA, EA, and PC in the receptor medium and skin layers was validated according to the parameters of linearity, limits of detection and quantification, specificity, accuracy, and precision (Table 4). The specificity of the method was confirmed, since no interference of the excipients of the formulations, receptor fluid, adhesive tape or skin layers were observed on the peaks of the polyphenol compounds, during the chromatographic runs. The method was linear over the concentration ranges employed for the three compounds in both receptor medium and methanol ($r^2 > 0.99$). For the receptor medium, the LOD and LOQ values of GA, EA, and PC were 0.19, 0.40 and 0.48 $\mu g.mL^{-1}$, and 0.64, 1.35 and 1.60 $\mu g.mL^{-1}$, respectively. When the calibration curves were constructed using methanol to determine the polyphenols in the different skin layers, the LOD and LOQ values for GA, EA, and PC were 0.13, 0.05 and 1.50 $\mu g.mL^{-1}$, and 0.42, 0.19 and 5.01 $\mu g.mL^{-1}$, respectively. The relative standard deviation (%RSD) obtained in the intra and inter-day precision analyses were lower than 6% for all samples, while the recovery values of GA, EA and PC from SC, EP, and DE ranged between 80.55 and 99.71%. The precision and recovery results are in agreement with the values required for a complex matrix (BRASIL, 2003c). These results indicated that the UFLC method is suitable for separation and quantification of the pomegranate polyphenols in the receptor medium and skin layers in the skin permeation and retention studies.

3.3 *In vitro* skin permeation and retention studies

The results obtained in the skin permeation studies of GA, EA, and PC indicated that the most part of these polyphenols remains retained in the skin layers, since they could not be detected by the UPLC method in the receptor medium, even considering that *sink* conditions were guaranteed throughout the whole experiment. On the other hand, the polyphenol compounds could be determined in the porcine ear skin after 8 h permeation experiment, but their skin distribution was depended on the formulation tested (Figure 3). The results demonstrated that GA, EA, and PC were delivery to the SC after applying both EAF-loaded NEs or the poloxamer hydrogels containing the EAF-loaded NEs, but only gallic acid was found in this skin layer after applying the EAF-solution. The results also demonstrated the superiority of the EAF-

loaded NEs in to deliver the polyphenols to the SC when compared with the hydrogels (Figure 3-A).

When the EP and DE were analysed, GA and EA could be determined after application of the EAF-loaded NEs in the skin surface. On the other hand, after the hydrogels containing the EAF-loaded NEs were applied in the skin, none of the three polyphenols were found in these skin layers. The mean permeated amount of GA and EA found in the epidermis and in the dermis were 1.78 and 1.36 μg/cm^2, and 1.10 and 0.97 μg/cm^2, respectively. No statistical difference was verified when the results obtained after the application of EAF-PSO-NE and the EAF-MCT-NE was compared (Figure 3-B).

According with the results, the permeation of GA, EA, and PC was restricted to the SC and, among the three polyphenols, the PC displayed the lowest permeation capacity across the skin. Finally, EAF-loaded NEs were considered more convenient vehicles to deliver GA and EA in to skin deeper layers, while the EAF-loaded NE hydrogels retained the phenolic compounds in the upper layer of the skin.

3.4 Confocal fluorescence microscopy

The skin permeation of NR in solution or incorporated in the oil phase of EAF-loaded NEs was visualized by confocal fluorescence microscopy. The EAF_{NR}-MCT-NE and EAF_{NR}-PSO-NE displayed monodisperse size distributions (PDI<0.3), with mean droplet size of 225 and 140 nm, respectively and zeta potential between -20 and -30 mV. No autofluorescence was observed on untreated skin or on skin treated with formulations prepared without the NR (data not shown). When the NR solution was applied on the porcine ear skin, the fluorescence was only detected in the SC (Figure 4). After 30 min of *in vitro* permeation study, the NR´s fluorescence was visualized in the SC and in the EP for all EAF_{NR}-loaded NEs and EAF_{NR}-loaded NE hydrogels. On the other hand, after 8 h of permeation experiment, the application of the EAF_{NR}-loaded NEs conducted to the appearance of a strong fluorescence in the SC, EP and DE, indicating an enhancement of the permeation of this compound towards the deeper skin layers by the nanoemulsions. This result was not verified after application of the hydrogels containing the NEs, since only a slight fluorescence was observed in the skin deep layers after 8 hours of permeation experiment. These results corroborates with those obtained after UFLC determination of polyphenol compounds in the different skin layers, i.e.,

the incorporation of poloxamer in the external phase of nanoemulsions restrain the permeation of compounds across the skin. It is worth mentioning that several attempts were made to improve the extraction of the phenolic compounds from the skin layers being the reported here the best one. Consistent with the results reported at *section 3.3*, the NR fluorescent staining was more diffused in deeper skin layers after treatment with EAF_{NR}-loaded NEs.

Table 4. Results of the regression analysis, precision (intra-and inter-day) and accuracy of the UFLC method in the receptor medium and extraction solvent for the phenolic compounds gallic acid, ellagic acid and punicalagin.

Solvent	Compounds	r^2	Regression line	LOD ($\mu g.mL^{-1}$)	LOQ ($\mu g.mL^{-1}$)	Precision (%RSD)			Recovery (% ± RSD)	
						Level	Intra-day	Inter-day		
Receptor medium	Gallic acid	0.9943	y=37240x-24939	0.19	0.64	1	3.62	4.62		
						2	1.68	2.68	94.12 ± 3.12	
						3	1.50	1.89		
	Ellagic acid	0.9973	y=158315x-100403	0.40	1.35	1	1.98	3.64		
						2	3.45	2.54	97.15 ± 2.66	
						3	1.47	2.86		
	Punicalagin	0.9994	y=7044x-2144	0.48	1.60	1	4.68	5.68		
						2	2.95	4.22	99.09 ± 2.63	
						3	2.92	3.24		
Extraction Solvent (Methanol)	Gallic acid	0.9995	y=28092x-10998	0.13	0.42	1	1.63	5.85	SC	99.69 ± 2.77
						2	2.44	5.24	EP	92.92 ± 3.27
						3	4.98	5.66	DE	86.02 ± 3.89
	Ellagic acid	0.9903	y=140943x-95567	0.05	0.19	1	2.71	2.75	SC	96.47 ± 1.64
						2	3.09	2.20	EP	95.88 ± 2.83
						3	2.29	1.45	DE	85.45 ± 2.88
	Punicalagin	0.9991	y=10410x-10587	1.50	5.01	1	4.04	5.23	SC	99.71 ± 2.30
						2	1.94	2.31	EP	96.36 ± 3.04
						3	2.27	3.84	DE	80.55 ± 2.55

SC= *stratum corneum*; EP=epidermis; DE= dermis. n=3.

Figure 3. Pomegranate polyphenols retained in the skin layers after 8 h permeation experiments. (A) Retained amount of gallic acid (GA), ellagic acid (EA), and punicalagin (PC) in the *stratum corneum* (SC). (B) Retained amount of gallic acid (GA) and ellagic acid (EA) in the epidermis (EP) and dermis (DE). For the experiments were applied a EAF solution, EAF-loaded NEs or hydrogels containing EAF-loaded NEs prepared by the addition of 18% or 28% (w/v) of poloxamer 407 into the external phase of the colloidal dispersions. Data are presented as mean ± SD (n=6). Same letters mean no significant difference between the values. Statistical analysis was performed by ANOVA followed by Tukey's post-hoc test for multiple comparisons.

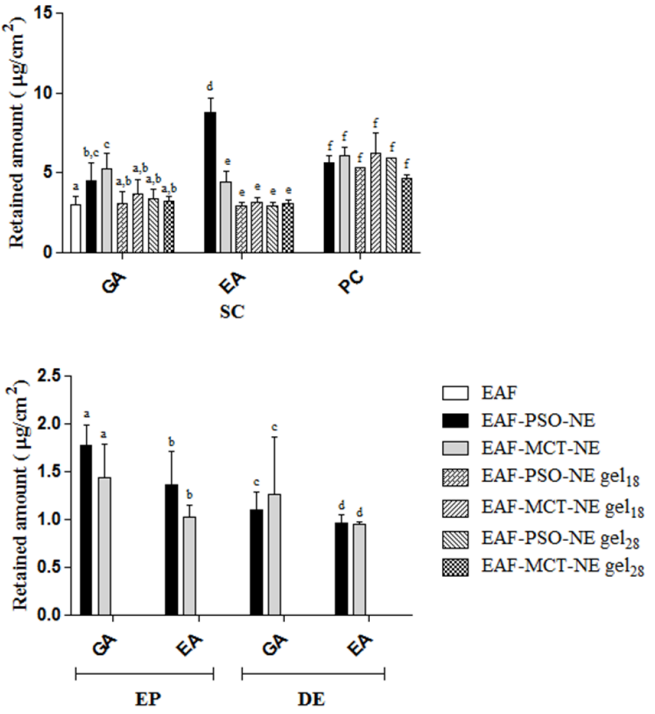

Figure 4. Confocal images of porcine ear skin obtained in 30 min or 8 h after application of a nile red (NR) solution (control), EAF_{NR}-loaded NEs or poloxamer hydrogels containing EAF_{NR}-loaded NEs. Scale bar=100 µm.

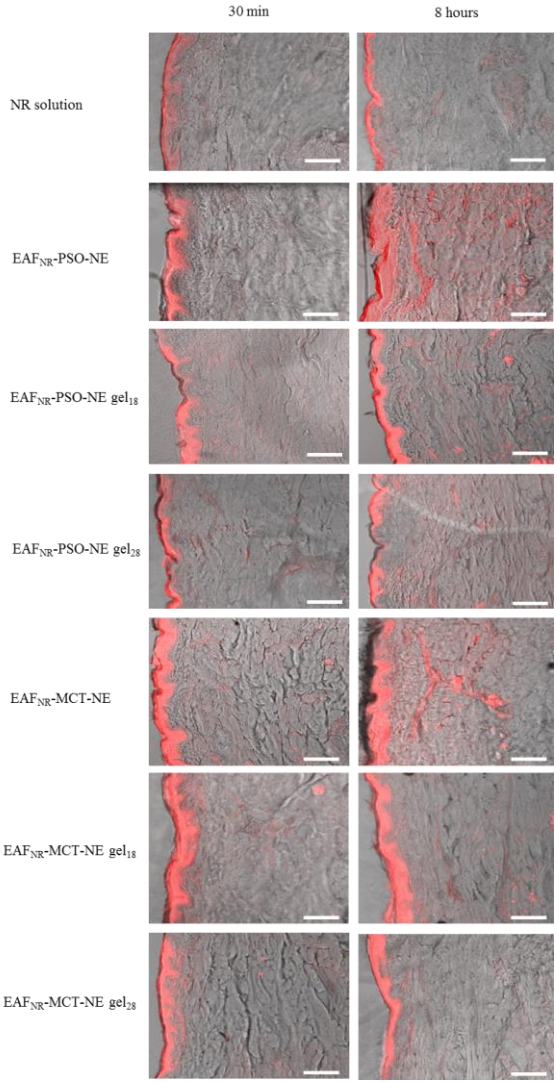

4. DISCUSSION

The most critical risk factor in the initiation and development of several skin diseases is exposure to UV solar radiation. The use of natural products, which absorb UV photons and exhibit a wide range of biological activities, such as antioxidant, anti-inflammatory and antitumor, is of great interest in UV skin protection (SVOBODOVÁ et al., 2009). Polyphenols appear particularly promising as cosmetic sunscreens because they can absorb a broad spectrum of UV radiation. Due to their great antioxidant properties, these chemical compounds can react with free radicals produced by UV radiation and inhibit or delay their harmful effects (NICHOLS e KATIYAR, 2010; JARZYCKA et al., 2013; RATZ-ŁYKO et al., 2015). However, to obtain a desired photoprotection, the polyphenols should reach the viable epidermis and dermis and, therefore, skin permeation studies should be carried out during the formulation optimization.

Nanoemulsions have been widely used in dermatological and cosmetic products due to several advantageous properties, including low skin irritation and high drug-loading capacity for topical delivery (SONNEVILLE-AUBRUN et al., 2004; TADROS et al., 2004; SOLANS et al., 2005; SHAKEEL et al., 2012). In a previous study, we prepared and characterized PSO and MCT-based NEs entrapping the EAF from *P. granatum* peel dried extract. These nanoemulsions exhibited substantial amount of pomegranate polyphenolic compounds, the major ones being GA, EA, and PC. The entrapment efficiency of these compounds varied according to their lipophilicity, i.e, PC > EA > GA (BACCARIN and LEMOS-SENNA, 2014). Both the antioxidant properties and photoprotection activity were demonstrated for these formulations ((BACCARIN and LEMOS-SENNA, 2014; BACCARIN, MITJANS, LEMOS-SENNA, et al., 2015; BACCARIN, MITJANS, RAMOS, et al., 2015).

Even though nanoemulsions show several advantages for topical delivery, their low viscosity restrain an appropriate application and retention onto the skin surface. For this purpose, the poloxamer 407, a thermosensitive triblock copolymer, was incorporated to the external phase of the nanoemulsions. The poloxamer hydrogels containing the nanoemulsions exhibited rheological behaviors depending on the temperature. Below the gelation temperature, the hydrogels exhibited a Newtonian behavior and above the gelation temperature, they become a Non-Newtonian pseudo-plastic thixotropic fluid, which is a more

desirable property for topical formulations like sunscreens (GASPAR and MAIA CAMPOS, 2003) (Figure 3). To characterize the textural properties of NE gels, TPA analysis, which has direct relevance to the sensory properties of topical formulations, was employed. In this technique, an analytical probe is twice depressed into the sample under examination, allowing a defined recovery period between successive compressions. From the resultant force-time plot, the parameters hardness (maximum force required to attain a given deformation), adhesiveness (the work necessary to overcome the attractive forces between the surface of the product and the surface of the probe), springiness (how well a product physically springs back after it has been deformed during the first compression) and cohesiveness (the work required to deform the hydrogel in the down movement of the probe) were derived (JONES et al., 1996; JONES et al., 1997; PUND et al., 2015). Our results demonstrated that increasing the poloxamer concentration from 18 % to 28 % (w/v), all the parameters evaluated were increased (Table 3), as it was also demonstrated by other authors (JONES et al., 1997; JONES et al., 2002; BRUSCHI et al., 2007). Considering the viscosity, gelation temperature and textural properties, the hydrogel prepared at poloxamer 407 at concentration of 18% (w/V) seemed to exhibit better characteristics for spraying the formulations onto the skin and pleasant feeling after the formulation application.

Regarding the skin permeation/retention studies, the permeation profile of the three major phenolic compounds of *P. granatum* EAF was evaluated during 8 h after application of the EAF alone, the EAF-loaded NEs, and the poloxamer hydrogels containing the EAF-loaded NEs onto the porcine ear skin surface. The use of a hydroalcoholic solution guaranteed the *sink* conditions throughout the whole experiment. However, none of the three polyphenols GA, EA, or PC were detected in the receptor medium. The results of these studies evidenced that the phenolic compounds were mostly retained by the skin and did not reach the receptor compartment of Franz diffusion cells (Figure 3). On the other hand, the superiority of the NEs into deliver the drugs into the deeper sink layers was demonstrated. A 2.2 fold enhancement of the GA amount in the SC was verified after EAF-loaded NEs application, when compared with the free EAF alone. Furthermore, EA and PC were not detected in the SC, when the free EAF was applied. Yet, both GA and EA were able to reach the viable EP and DE when the nanoemulsions where assayed. Although GA exhibits a hydrophilic character (log P= -0.53), it was diffused across the SC barrier and

reached these deeper skin layers in similar amounts of those reported for EA, which is a more lipophilic molecule (log P=2.44). The entrapment of GA into the oil phase of the nanoemulsions, probably promoted its access towards the EP and DE. The oil droplets of NEs containing phospholipids and fatty acids can fuse with SC lipids and modify the lipid domains of SC, and yet provoke phase separation of SC lipids, facilitating permeation of hydrophilic compounds across this barrier (WILLIAMS and BARRY, 2012). Moreover, as reported by Friedrich et al. (2015), the co-encapsulation of polyphenols could result in improved skin permeation, probably due to the different lipophilicities of these compounds. Taking this into account, the lipophilicity of other polyphenols present in the EAF-loaded NEs (i.e. ellagic acid) could potentially alter the structure of the phospholipid bilayer of the *stratum corneum*, making easier and faster the transport of GA, which subsequently accumulates in the deeper skin layers.

A skin permeation enhancement effect provided by nanoemulsions was also verified for EA. Ellagic acid is a potent antioxidant phenolic compound which displays low water solubility. In this study, the amount of EA found in the total epidermis (SC and EP) was 10 μg/cm^2. This value was around 4.5-fold and 14.2-fold higher than those found after application of a water-soluble ointment containing 5% of standardized pomegranate peel ethyl acetate fraction (MO et al., 2015) and EA-loaded niossomes (JUNYAPRASERT et al., 2013), respectively. On the other hand, it has been assumed that the skin permeation rate and SC retention are lower for molecules displaying high molecular weight (>500 g/mol) (BOS e MEINARDI, 2000; CHATELAIN et al., 2003). Our findings are in agreement with that, since most of the PC was retained in the SC and did not reach the deeper skin layers. Punicalagin is the most abundant ellagitannin in pomegranates with similar lipophilicity than EA (log P= 2.36), but displaying a high molecular weight (MW 1084 g/mol). Likewise, Alonso et al. (2014) reported that, for five polyphenols separately applied on the skin surface, the skin permeation/retention profile depended not only on the hydrophilicity and lipophilicity, but also on the molecular weight of each polyphenol studied.

The ability of a drug in a topical formulation to permeate the skin and to exert its effects depends on two consecutive events. First, the drug must diffuse out from the vehicle to the skin surface and second, it must permeate *stratum corneum* (“skin barrier”) to reach the living layers of epidermis and dermis. Both steps are dependent not only on the

physicochemical properties of the drug, but also on the physicochemical properties of the vehicle (ALVES et al., 2007). In this study, it was observed that the EAF-loaded NE hydrogels delivered the polyphenolic compounds only in the SC. Probably, when EAF-loaded NEs are thickened by the addition of poloxamer, the higher viscosity of the aqueous phase may hamper the diffusion of the compounds out from the vehicle to the skin surface, slowing down the permeation process. On the other hand, for the EAF-loaded NEs, the oily droplets might embed into the SC and directly delivered the compounds from oily droplets into the SC without a transfer via hydrophilic phase of nanoemulsions (MOU et al., 2008).

Aiming to confirm the effect of the formulation properties on the skin permeation of the pomegranate polyphenols, confocal fluorescence microscopy studies were carried out using nile red as a lipophilic fluorophore (log P= 3.65), co-encapsulated with the EAF into the nanoemulsions. The confocal images presented in the Figure 4 corroborated the skin permeation/retention findings, since it was verified that the permeation of a lipophilic compound as nile red is increased when it was incorporated into an oil phase of a nanoemulsion, but it is restrained by the addition of poloxamer as a gelling agent.

The transport of active substances through the skin membrane has been described as a complex process that depends on several factors related to biological membrane conditions, and the physicochemical properties of the molecule and vehicle (RATZ-ŁYKO et al., 2015). In the case of a polyphenol-rich extract fraction, this process is even more complex considering a mixture of compounds that present different physicochemical properties as lipophilicity or hydrophilicity, variable size and spatial structure. Antioxidants such polyphenolics compounds, should be able to permeate across the SC and to reach the deeper skin layers, EP and DE, to effectively protect skin against ROS, without significant leakage into the systemic circulation (MARTI-MESTRES et al., 2007; ALONSO et al., 2014). The approach of nanoemulsifying the EAF from pomegranate greatly enhanced the skin delivery of the biomarkers GA, EA and PC, comparing with the EAF solution, without leading to the attainment of them in the receptor compartment, and thereby suggesting an increase in the effectiveness of antioxidant activity against ROS caused by UV radiation. Furthermore, the amount of the compounds that remained on the skin surface may absorb the UV radiation before it reaches the viable skin layers.

5. CONCLUSIONS

It is reported that application of skin care products containing antioxidants may contribute for an efficiently skin protection against ROS occurring during UV radiation exposure, once the skin viable layers are reached. Furthermore, these topically applied compounds may act absorbing the incident UV radiation, thereby reducing the amount that reaches beyond the most superficial layers of the epidermis.

To obtain a formulation with an ideal viscous to spray topically, a thermosensitive copolymer was used. The 18% (w/v) poloxamer hydrogels containing the EAF-loaded NEs presented rheological and texture properties suitable for these purpose. After application of EAF-loaded NEs and hydrogels containing the EAF-loaded NEs on porcine ear skin, our investigations demonstrated that the tested formulations improved substantially, when compared with the free EAF solution, the GA, EA and PC residence in the skin, mainly located in the SC, without reaching the receptor compartment. However, the only EAF-loaded NEs were able to deliver the polyphenolic compounds in the skin deeper layers. Confocal images of a nanoemulsified lipophilic fluorophore corroborated these findings.

Thus, this study demonstrates the advantages of nanoemulsifying the EAF when topical delivery is considered to protect skin from harmful effects of UV radiation. However, the permeation profile of each phenolic compound depends on the physicochemical properties of the molecule, vehicle and interactions that may happen with the skin membrane. Finally, nanoemulsions delivery systems containing polyphenol constituents from pomegranate are promising formulations to continue the investigation towards a new photoprotector.

Conflict of interest

The authors declare the absence of conflict of interest.

Acknowledgments

The authors acknowledge the financial support from Coordination for the Improvement of Higher Education Personnel (CAPES-DS). The authors would like to thank Msc. André O'Reilly Beringhs for his technical assistance in microtome-cryostat and Professor Dr. Ruth Meri Lucinda Silva from Universidade do Vale do

Itajaí (Itajaí, Brazil) for the TPA Texture Analyser and HAAKE Rotational Viscometer use. The authors also would like to thank the Laboratório Central de Microscopia Eletrônica-LCME (Universidade Federal de Santa Catarina, Florianópolis, Brazil) for the FEG-SEM analyses and confocal images.

References

AFAQ, F. Natural agents: Cellular and molecular mechanisms of photoprotection. **Arch Biochem Biophys,** v. 508, n. 2, p. 144-151, 2011.

ALONSO, C.; RUBIO, L.; TOURIÑO, S.; MARTÍ, M.; BARBA, C.; FERNÁNDEZ-CAMPOS, F.; CODERCH, L.; LUÍS PARRA, J. Antioxidative effects and percutaneous absorption of five polyphenols. **Free Radical Biol Med,** v. 75, p. 149-155, 2014.

ALVES, M. P.; SCARRONE, A. L.; SANTOS, M.; GUTERRES, S. S. Human skin penetration and distribuition of nimesulide from hydrophilic gels containing nanocarriers. **Int J Pharm,** v. 314, p. 215-220, 2007.

AVIRAM, M.; DORNFELD, L.; ROSENBLAT, M.; VOLKOVA, N.; KAPLAN, M.; COLEMAN, R.; HAYEK, T.; PRESSER, D.; FUHRMAN, B. Pomegranate juice consumption reduces oxidative stress, atherogenic modifications to LDL, and platelet aggregation: studies in humans and in atherosclerotic apolipoprotein E–deficient mice. **Am J Clin Nutr** v. 71, n. 5, p. 1062-1076, 2000.

BACCARIN, T.; LEMOS-SENNA, E. Pomegranate seed oil nanoemulsions encapsulating pomegranate peel polyphenol-rich ethyl acetate fraction: Development and antioxidant assessment. **J Nanopharmaceutics and Drug Delivery,** v. 2, n. 4, p. 333-343, 2014.

BACCARIN, T.; MITJANS, M.; LEMOS-SENNA, E.; VINARDELL, M. P. Protection against oxidative damage in human erythrocytes and preliminary photosafety assessment of Punica granatum seed oil nanoemulsions entrapping polyphenol-rich ethyl acetate fraction. **Toxicol In Vitro,** v. Article *in press*, 2015.

BACCARIN, T.; MITJANS, M.; RAMOS, D.; LEMOS-SENNA, E.; VINARDELL, M. P. Photoprotection by Punica granatum seed oil nanoemulsion entrapping polyphenol-rich ethyl acetate fraction against UVB-induced DNA damage in human keratinocyte (HaCaT) cell line. **J Photochem Photobiol B,** v. 153, p. 127-136, 2015.

BARRY, B. W. Novel mechanisms and devices to enable successful transdermal drug delivery. **Eur J Pharm Sci,** v. 14, p. 101-114, 2001.

BITO, T.; NISHIGORI, C. Impact of reactive oxygen species on keratinocyte signaling pathways. **J Dermatol Sci,** v. 68, n. 1, p. 3-8, 2012.

BOS, J. D.; MEINARDI, M. M. H. M. The 500 Dalton rule for the skin penetration of chemical compounds and drugs. **Exp Dermatol,** v. 9, n. 3, p. 165-169, 2000.

BRASIL. Resolution RE 899 "Guide for analytical and bio-analitycal method validation". **Anvisa - Agência Nacional de Vigilância Satinária** 2003.

BRUSCHI, M. L.; JONES, D. S.; PANZERI, H.; GREMIÃO, M. P. D.; DE FREITAS, O.; LARA, E. H. G. Semisolid systems containing propolis for the treatment of periodontal disease: In Vitro release kinetics, syringeability, rheological, textural, and mucoadhesive properties. **J Pharm Sci,** v. 96, n. 8, p. 2074-2089, 2007.

BUWALDA, S. J.; BOERE, K. W. M.; DIJKSTRA, P. J.; FEIJEN, J.; VERMONDEN, T.; HENNINK, W. E. Hydrogels in a historical perspective: From simple networks to smart materials. **J Controlled Release,** v. 190, p. 254-273, 2014.

ÇAM, M.; HISIL, Y.; DURMAZ, G. Classification of eight pomegranate juices based on antioxidant capacity measured by four methods. **Food Chem,** v. 112, p. 721-726, 2009.

CHATELAIN, E.; GABARD, B.; SURBER, C. Skin penetration and sun protection factor of five UV filters: Effect of the vehicle. **Skin Pharmacol Physiol,** v. 16, n. 1, p. 28-35, 2003.

EL-NEMR, S. E.; ISMAIL, I. A.; RAGAB, M. Chemical composition of juice and seeds of pomegranate fruit. **Die Nahrung,** v. 34, n. 7, p. 601-606, 2006.

FADAVI, A.; BARZEGAR, M.; AZIZI, H. M. Determination of fatty acids and total lipid content in oilseed of 25 pomegranates varieties grown in Iran. **J Food Compost Anal,** v. 19, p. 676-680, 2006.

FISCHER, U. A.; CARLE, R.; KAMMERER, D. R. Identification and quantification of phenolic compounds from pomegranate (Punica granatum L.) peel, mesocarp, aril and differently produced juices by HPLC-DAD–ESI/MSn. **Food Chem,** v. 127, n. 2, p. 807-821, 2011.

FREITAS, J. V.; PRAÇA, F. S. G.; BENTLEY, M. V. L. B.; GASPAR, L. R. Trans-resveratrol and beta-carotene from sunscreens penetrate viable skin layers and reduce cutaneous penetration of UV-filters. **Int J Pharm,** v. 484, n. 1–2, p. 131-137, 2015.

FRIEDRICH, R. B.; KANN, B.; CORADINI, K.; OFFERHAUS, H. L.; BECK, R. C. R.; WINDBERGS, M. Skin penetration behavior of lipid-core nanocapsules for simultaneous delivery of resveratrol and curcumin. **Eur J Pharm Sci,** v. 78, p. 204-213, 2015.

GASPAR, L. R.; MAIA CAMPOS, P. M. B. G. Rheological behavior and the SPF of sunscreens. **Int J Pharm,** v. 250, n. 1, p. 35-44, 2003.

GODIC, A.; POLJAK, B.; ADAMIC, M.; DAHMANE, R. The role of antioxidants in skin cancer prevention and treatment. **Oxid Med Cell Longevity,** v. 2014, p. 1-6, 2014.

HURLER, J.; ENGESLAND, A.; POORAHMARY KERMANY, B.; ŠKALKO-BASNET, N. Improved texture analysis for hydrogel characterization: Gel cohesiveness, adhesiveness, and hardness. **J Appl Polym Sci,** v. 125, n. 1, p. 180-188, 2012.

ICH. International Conference on Harmonization of Technical Requeriments for Registration of Pharmaceuticals for Human Use, Validation of Analytical Procedures: Text and Methodology. Geneva, Switzerland 2005.

ISMAIL, T.; SESTILI, P.; AKHTAR, S. Pomegranate peel and fruit extracts: A review of potential anti-inflammatory and anti-infective effects. **J Ethnopharmacol,** v. 143, n. 2, p. 397-405, 2012.

JARZYCKA, A.; LEWINSKA, A.; GANCARZ, R.; WILK, K. A. Assessment of extracts of Helichrysum arenarium, Crataegus monogyna, Sambucus nigra in photoprotective UVA and UVB; photostability in cosmetic emulsions. **J Photochem Photobiol B,** v. 128, p. 50-57, 2013.

JONES, D. S.; LAWLOR, M. S.; WOOLFSON, A. D. Examination of the flow rheological and textural properties of polymer gels composed of poly(methylvinylether-co-maleic anhydride) and poly(vinylpyrrolidone): Rheological and mathematical interpretation of textural parameters. **J Pharm Sci,** v. 91, n. 9, p. 2090-2101, 2002.

JONES, D. S.; WOOLFSON, A. D.; BROWN, A. F. Textural, viscoelastic and mucoadhesive properties of pharmaceutical gels composed of cellulose polymers. **Int J Pharm,** v. 151, n. 2, p. 223-233, 1997.

JONES, D. S.; WOOLFSON, A. D.; DJOKIC, J. Texture profile analysis of bioadhesive polymeric semisolids: Mechanical characterization and investigation of interactions between formulation components. **J Appl Polym Sci,** v. 61, n. 12, p. 2229-2234, 1996.

JUNYAPRASERT, V. B.; SINGHSA, P.; JINTAPATTANAKIT, A. Influence of chemical penetration enhancers on skin permeability of ellagic acid-loaded niosomes. **Asian J Pharm Sci,** v. 8, n. 2, p. 110-117, 2013.

KOGAN, A.; GARTI, N. Microemulsions as transdermal drug delivery vehicles. **Adv Colloid Interface Sci,** v. 123–126, p. 369-385, 2006.

KONG, M.; CHEN, X. G.; KWEON, D. K.; PARK, H. J. Investigations on skin permeation of hyaluronic acid based nanoemulsion as transdermal carrier. **Carbohydr Polym,** v. 86, n. 2, p. 837-843, 2011.

LANDETE, J. M. Ellagitannins, ellagic acid and their derived metabolites: A review about source, metabolism, functions and health. **Food Res Int,** v. 44, n. 5, p. 1150-1160, 2011.

LI, Y.; GUO, C.; YANG, J.; WEI, J.; XU, J.; CHENG, S. Evaluation of antioxidant properties of pomegranate peel extract in comparison with pomegranate pulp extract. **Food Chem,** v. 96, n. 2, p. 254-260, 2006.

MANASATHIEN, J.; INDRAPICHATE, K.; INTARAPICHET, K.-O. Antioxidant activity and bioefficacy of pomegranate Punica granatum Linn. peel and seed extracts. **Global J Pharmacol,** v. 6, n. 2, p. 131-141, 2012.

MARTI-MESTRES, G.; MESTRES, J. P.; BRES, J.; MARTIN, S.; RAMOS, J.; VIAN, L. The "in vitro" percutaneous penetration of three antioxidant compounds. **Int J Pharm,** v. 331, n. 1, p. 139-144, 2007.

MENON, G. K. N ew insights into skin structure: scratching the surface. **Adv Drug Delivery Rev,** v. 54, p. 3-17, 2002.

MO, J.; KAEWNOPPARAT, N.; SONGKRO, S.; PANICHAYUPAKARANANT, P.; REANMONGKOL, W. Physicochemical properties, in vitro release and skin permeation studies of a topical formulation of standardized pomegranate rind extract. **Pak J Pharm Sci,** v. 28, n. 1, p. 29-36, 2015.

MONTENEGRO, L.; CARBONE, C.; PUGLISI, G. Vehicle effects on in vitro release and skin permeation of octylmethoxycinnamate from microemulsions. **Int J Pharm,** v. 405, n. 1–2, p. 162-168, 2011.

MOU, D.; CHEN, H.; DU, D.; MAO, C.; WAN, J.; XU, H.; YANG, X. Hydrogel-thickened nanoemulsion system for topical delivery of lipophilic drugs. **Int J Pharm,** v. 353, n. 1–2, p. 270-276, 2008.

NICHOLS, J.; KATIYAR, S. Skin photoprotection by natural polyphenols: anti-inflammatory, antioxidant and DNA repair mechanisms. **Arch Dermatol Res,** v. 302, n. 2, p. 71-83, 2010.

PUND, S.; PAWAR, S.; GANGURDE, S.; DIVATE, D. Transcutaneous delivery of leflunomide nanoemulgel: Mechanistic

investigation into physicomechanical characteristics, in vitro anti-psoriatic and anti-melanoma activity. **Int J Pharm,** v. 487, n. 1–2, p. 148-156, 2015.

QU, W.; BREKSA, A. P.; PAN, Z.; MA, H. Quantitative determination of major polyphenol constituents in pomegranate products. **Food Chem,** v. 132, n. 3, p. 1585-1591, 2012.

QU, W.; PAN, Z.; MA, H. Extraction modeling and activities of antioxidants from pomegranate marc. **J Food Eng,** v. 99, n. 1, p. 16-23, 2010.

RATZ-ŁYKO, A.; ARCT, J.; MAJEWSKI, S.; PYTKOWSKA, K. Influence of polyphenols on the physiological processes in the skin. **Phytother Res,** v. 29, n. 4, p. 509-517, 2015.

SAIJA, A.; TOMAINO, A.; TROMBETTA, D.; DE PASQUALE, A.; UCCELLA, N.; BARBUZZI, T.; PAOLINO, D.; BONINA, F. In vitro and in vivo evaluation of caffeic and ferulic acids as topical photoprotective agents. **Int J Pharm,** v. 199, n. 1, p. 39-47, 2000.

SHAKEEL, F.; SHAFIQ, S.; HAQ, N.; ALANAZI, F. K.; ALSARRA, I. A. Nanoemulsions as potential vehicles for transdermal and dermal delivery of hydrophobic compounds: an overview. **Expert Opin Drug Delivery,** v. 9, n. 8, p. 953-974, 2012.

SOLANS, C.; IZQUIERDO, P.; NOLLA, J.; AZEMAR, N.; GARCIA-CELMA, M. J. Nano-emulsions. **Curr Opin Colloid Interface Sci,** v. 10, n. 3–4, p. 102-110, 2005.

SONNEVILLE-AUBRUN, O.; SIMONNET, J. T.; L'ALLORET, F. Nanoemulsions: a new vehicle for skincare products. **Adv Colloid Interface Sci,** v. 108–109, p. 145-149, 2004.

SVOBODOVÁ, A.; ZDAŘILOVÁ, A.; VOSTÁLOVÁ, J. Lonicera caerulea and Vaccinium myrtillus fruit polyphenols protect HaCaT keratinocytes against UVB-induced phototoxic stress and DNA damage. **J Dermatol Sci,** v. 56, n. 3, p. 196-204, 2009.

TADROS, T.; IZQUIERDO, P.; ESQUENA, J.; SOLANS, C. Formation and stability of nano-emulsions. **Adv Colloid Interface Sci,** v. 108–109, n. 0, p. 303-318, 2004.

WILLIAMS, A. C.; BARRY, B. W. Penetration enhancers. **Adv Drug Delivery Rev,** v. 64, Supplement, n. 0, p. 128-137, 2012.

DISCUSSÃO GERAL

A romã ou pomegranate (*Punica granatum L* Punicaceae) é um fruto consumido mundialmente na forma de sucos, geleias e *in natura*. Diversas aplicações e atividades biológicas estão relacionadas aos extratos da romã como ação antioxidante, anti-inflamatória, antitumoral, cicatrizante, além da potencial ação fotoprotetora. Estas atividades biológicas são geralmente atribuídas à presença substancial de compostos polifenólicos, principalmente na casca do fruto, destacando-se as punicalaginas, o ácido elágico e ácido gálico (KASAI et al., 2006; SYED et al., 2007; ZAID et al., 2007; PACHECO-PALENCIA et al., 2008; AFAQ et al., 2009; ISMAIL et al., 2012; MANASATHIEN et al., 2012). O óleo da semente de romã (PSO), rico em ácidos graxos como o ácido oleico, esteárico, linoleico e principalmente o ácido punícico, também apresenta atividades biológicas, como antioxidante, quimiopreventiva e neuroprotetora (QU et al., 2010; RAHIMI et al., 2012; MELO et al., 2014). Contudo apesar das potenciais utilizações dos extratos da romã, principalmente do extrato das cascas, em produtos farmacêuticos e cosméticos, seu uso é limitado devido à baixa solubilidade aquosa, baixa permeabilidade e instabilidade de alguns compostos polifenólicos. Diante destes aspectos, a proposta deste trabalho foi desenvolver nanoemulsões (o/a) contendo uma fração rica em compostos polifenólicos a partir do extrato seco das cascas da romã, tendo o óleo da semente da romã como fase oleosa, para aplicação cutânea visando sua utilização na fotoproteção.

Para melhor compreensão o presente trabalho foi dividido em quatro capítulos: (1) revisão de literatura, (2) desenvolvimento e caracterização de nanoemulsões contendo constituintes de *P. granatum* e avaliação da atividade antioxidante *in vitro*, (3) determinação da fotoproteção das nanoemulsões contendo constituintes de *P. grantaum* contra radiação UVB, e (4) desenvolvimento de hidrogéis contendo nanoemulsões de *P. granatum* para liberação tópica de compostos polifenólicos.

A fração acetato de etila (EAF), rica em compostos polifenólicos, foi obtida pelo método de partição líquido-líquido a partir do extrato seco das cascas da romã adquirido comercialmente. A partição líquido-líquido foi realizada de maneira sequencial empregando os seguintes solventes de polaridade crescente: diclorometano, acetato de etila e n-butanol. A fração acetato de etila foi selecionada devido à presença de altas concentrações de compostos polifenólicos, quando comparada as frações diclorometano e n-butanol. Um método analítico por cromatografia líquida de alta eficiência (CLAE) foi desenvolvido e

validado para a identificação e quantificação dos compostos polifenólicos tanto na fração quanto nas nanoemulsões. Este método mostrou ser linear, específico, exato, preciso e robusto para os três marcadores utilizados, a punicalagina (PC), o ácido elágico (EA) e o ácido gálico (GA).

A aplicação de sistemas nanoestruturados em produtos farmacêuticos e cosméticos tem sido extensivamente pesquisada. As nanoemulsões permitem a associação de concentrações consideráveis dos polifenóis presentes na fração acetato de etila e dos lipídeos presentes no óleo em um único sistema nanoestruturado. São sistemas cineticamente estáveis e devido ao tamanho nanométrico das gotículas, apresentam grande área superficial e baixa tensão superficial, o que permite um aumento na permeação cutânea de substâncias e consequentemente uma melhora na ação tópica (BOUCHEMAL et al., 2004; SCHÄFER-KORTING et al., 2007; SARAF, 2010). Além das nanoemulsões contendo o PSO como fase oleosa (EAF-PSO-NE), nanoemulsões contendo triglicerídeo de cadeia média (MCT) como fase oleosa (EAF-MCT-NE) também foram desenvolvidas para fins de comparação, através dos métodos de emulsificação-evaporação do solvente e emulsificação espontânea, respectivamente. Todas as nanoemulsões apresentaram distribuição monodispersa e eficiência de encapsulação de acordo com a lipofilicidade do composto polifenólico. Vale ressaltar que durante os estudos de desenvolvimento das formulações, diversos tensoativos foram testados, assim como concentrações diferentes de PSO ou MCT. Pelas análises de CLAE e determinação de fenóis totais (TPC) pela técnica de Folin-Ciocalteu, quantidades substanciais de compostos polifenólicos foram evidenciadas na EAF e também nas nanoemulsões, os quais foram responsáveis pela ação antioxidante frente aos métodos de DPPH e FRAP.

A estabilidade e fotoestabilidade das nanoemulsões foram determinadas. As nanoemulsões brancas (sem a EAF) foram estáveis fisicamente por 60 dias a 4 ºC. As nanoemulsões contendo a EAF foram fisicamente estáveis por 60 dias em temperatura ambiente (25 ºC) e em refrigerador; as concentrações de TPC e GA permaneceram constantes por 60 dias, porém um aumento no EA e uma diminuição na PC foram observados a partir do décimo quinto dia indicando uma possível hidrólise da PC, a qual libera uma molécula de EA. Tanto as formulações brancas quanto as contendo a EAF nanoemulsionada foram fotoestáveis após a exposição mínima preconizada para radiação UVA e UV visível.

Com o intuito de verificar se a EAF e as nanoemulsões eram capazes de proteger a membrana celular contra dano oxidativo, eritrócitos humanos foram empregados como modelo de biomembrana. Tanto a EAF quanto as nanoemulsões foram capazes de interagir com a bicamada lipídica em toda sua extensão e proteger a membrana eritrocitária contra os danos causados pelo iniciador de radical livre AAPH. A EAF-PSO-NE apresentou menor redução nas proteínas citoesqueléticas quando comparada aos outros tratamentos, possivelmente pelo fato do PSO também apresentar atividade antioxidante e consequentemente proporcionar uma proteção mais efetiva. Ainda empregando o modelo de eritrócitos humanos, o potencial irritante e fotoirritante foram avaliados pelos ensaios de hemólise e fotohemólise, respectivamente. As nanoemulsões e EAF livre foram classificadas como seguras em relação a estes testes preliminares. Este resultado foi corroborado pela avaliação da fototoxicidade *in vitro* segundo o guia OECD 432 usando células de fibroblasto murinho 3T3 e queratinócitos humanos HaCaT, que classificou as nanoemulsões como não fototóxicas na concentração testada. Entretanto, ressalta-se a necessidade de fututros ensaios para que as formulações sejam consideradas seguras para utilização na condição de um fotoprotetor.

A citotoxicidade *in vitro* das nanoemulsões e EAF livre, foi determinada em células de fibroblasto murinho 3T3 e queratinócitos humanos HaCaT usando os métodos de avalição de viabilidade celular MTT e NRU, que avaliam a integridade da mitocôndria e dano no lisossomo, respectivamente. Os valores de IC_{50} obtidos variaram conforme a linhagem celular empregada, método de avaliação e formulação. Nos estudos de internalização celular, as nanoemulsões (nanogotículas) foram capazes de internalizar em células de queratinócitos humanos HaCaT como também de se acumularem ao redor das mesmas.

Ambas as nanoemulsões e EAF livre protegeram as células de queratinócitos humanos HaCaT contra danos no DNA nas duas doses de irradiação UVB testadas e essa proteção ocorreu de maneira dependente da concentração dos tratamentos aplicada nas células. O fator de proteção solar obtido para as nanoemulsões e EAF livre, através de um método espectrofotométrico, foi elevado considerando que nenhum outro filtro solar foi adicionado nas formulações. A EAF-PSO-NE apresentou o maior FPS, o que pode estar relacionado com a ação sinérgica entre os compostos polifenólicos presentes na EAF e os ácidos

graxos insaturados presentes no PSO, principalmente do ácido punícico, também capaz de absorver luz devido às ligações duplas conjugadas.

Com o objetivo de aumentar a viscosidade das nanoemulsões e facilitar a aplicação na pele, um polímero foi incorporado nas mesmas visando à obtenção de um hidrogel. O poloxamer 407 foi escolhido para esta finalidade devido à sua característica termosensível, o que possibilitaria a aplicação tópica das formulações na forma de spray. Com a incorporação de uma concentração adequada de poloxamer nas nanoemulsões, os hidrogéis resultantes exibiram textura agradável ao toque e as formulações apresentaram-se líquidas em temperatura ambiente e gelificadas em temperatura corporal.

Para a determinação dos compostos, AE, AG e PC nos estudos de permeação e retenção cutânea na pele de orelha suína, um método analítico foi validado em equipamento de UFLC para quantificação dos mesmos no meio receptor e extrator. O método mostrou ser específico, linear, exato e preciso tanto para o meio receptor quanto para o extrator. Após a aplicação das nanoemulsões ou hidrogéis na pele, uma maior permeação e retenção cutânea dos compostos polifenólicos foram observadas em relação à EAF livre. As concentrações dos compostos retidas no estrato córneo e permeadas até as camadas viáveis da pele sugerem a possibilidade de obtenção de um efeito fotoprotetor, tanto pela absorção de luz quanto pela ação antioxidante exercida pelos polifenóis.

CONSIDERAÇÕES FINAIS

- Nanoemulsões contendo o óleo da semente de romã ou triglicerídeo de cadeia média como fase oleosa encapsulando a fração acetato de etila do extrato seco das cascas de *Punica granatum* foram obtidas através dos métodos de emulsificação espontânea e emulsificação-evaporação do solvente, respectivamente.
- Um método analítico por cromatografia líquida de alta eficiência foi desenvolvido e validado para quantificar os principais compostos fenólicos presentes na fração acetato de etila livre ou encapsulada – ácido gálico, ácido elágico e punicalagina. Este método foi considerado linear, específico, exato, preciso e robusto.
- A eficiência de encapsulação foi dependente da lipofilicidade de cada composto fenólico.
- As nanoemulsões e fração livre apresentaram considerável potencial antioxidante *in vitro* perante os ensaios de DPPH e FRAP.
- Em ensaio preliminar *in vitro*, as nanoemulsões não demostraram ser irritantes ou fotoirritantes.
- As nanoemulsões apresentaram efeito antioxidante protetor frente ao formador de radical livre AAPH em modelo de biomembrana lipídica.
- A segurança do uso das nanoemulsões foi evidenciada no ensaio de citotoxicidade e fototoxicidade em linhagem de fibroblasto murino 3T3 e queratinócitos humanos HaCaT.
- As nanoemulsões foram capazes de internalizar e se acumular ao redor dos queratinócitos humanos HaCaT.
- O potencial efeito fotoprotetor promovido pelas nanoemulsões contra radiação UVB em queratinócitos humanos HaCaT foi evidenciado pela proteção ao dano no DNA.
- Na determinação do SPF *in vitro* foi observada uma sinergia entre os componentes da formulação da nanoemulsão contendo o óleo de romã e fração encapsulada.
- A estabilidade física e química (exceto para a punicalagina) das nanoemulsões foi evidenciada durante 60 dias.
- Hidrogéis termoreversíveis contendo as nanoemulsões foram facilmente preparados e a presença das nanogotas foi evidenciada por DLS e microscopia FEG-SEM.

- Hidrogéis formados com concentração mais baixa de polímero apresentaram características físicas favoráveis para aplicação tópica em spray.
- Um método analítico por cromatografia líquida ultra rápida foi validado para determinação dos compostos fenólicos nos estudos de permeação e retenção cutânea usando pele de orelha suína como modelo de membrana. O método demonstrou ser específico, linear, exato e preciso no meio receptor e no meio extrator.
- A retenção e permeação dos compostos fenólicos foram dependentes de características físico-químicas dos compostos, do veículo e de possíveis interações com a pele.
- A retenção no *stratum corneum* e a permeação dos compostos até as camadas viáveis da pele sugerem uma potencial aplicação como fotoprotetor atuando na absorção de fótons e na complementação antioxidante cutânea.
- As imagens dos cortes da pele obtidas por microscopia confocal corroboraram os estudos de permeação e retenção cutânea.
- Por fim, a nanoemulsão contendo óleo de semente de romã e fração acetato de etila encapsulada desenvolvida neste trabalho, como também o hidrogel termosensível, constituem uma boa estratégia para facilitar a aplicação cutânea, aprimorar a retenção e permeação de compostos fenólicos nas camadas da pele e favorecer a ação fotoprotetora.

REFERÊNCIAS

ABISMAIL, B.; CANSELIER, J. P.; WILHELM, A. M.; DELMAS, H.; GOURDON, C. Emulsification by ultrasound: drop size distribution and stability. **Ultrason Sonochem,** v. 6, n. 1–2, p. 75-83, 1999.

ABLA, M. J.; BANGA, A. K. Formulation of tocopherol nanocarriers and in vitro delivery into human skin. **Int J Cosmet Sci,** v. 36, n. 3, p. 239-246, 2014.

AFAQ, F. Natural agents: Cellular and molecular mechanisms of photoprotection. **Arch Biochem Biophys,** v. 508, n. 2, p. 144-151, 2011.

AFAQ, F.; KATIYAR, S. K. Polyphenols: Skin Photoprotection and Inhibition of Photocarcinogenesis. **Mini-Rev Med Chem,** v. 11, n. 14, p. 1200-1215, 2011.

AFAQ, F.; SALEEM, M.; KRUEGER, C. G.; REED, J. D.; MUKHTAR, H. Anthocyanin- and hydrolyzable tannin-rich pomegranate fruit extract modulates MAPK and NF-κB pathways and inhibits skin tumorigenesis in CD-1 mice. **Int J Cancer,** v. 113, n. 3, p. 423-433, 2005.

AFAQ, F.; ZAID, M. A.; KHAN, N.; DREHER, M.; MUKHTAR, H. Protective effect of pomegranate-derived products on UVB-mediated damage in human reconstituted skin. **Exp Dermatol,** v. 18, n. 6, p. 553-561, 2009.

AJILA, C. M.; PRASADA RAO, U. J. S. Protection against hydrogen peroxide induced oxidative damage in rat erythrocytes by Mangifera indica L. peel extract. **Food Chem Toxicol,** v. 46, p. 303-309, 2008.

ALAM, M. N.; BRISTI, N. J.; RAFIQUZZAMAN, M. Review on in vivo and in vitro methods evaluation of antioxidant activity. **Saudi Pharm J,** v. 21, n. 2, p. 143-152, 2013.

ALEXANDER, A.; DWIVEDI, S.; AJAZUDDIN; GIRI, T. K.; SARAF, S.; SARAF, S.; TRIPATHI, D. K. Approaches for breaking the barriers of drug permeation through transdermal drug delivery. **J Controlled Release,** v. 164, n. 1, p. 26-40, 2012.

ALKILANY, A. M.; MURPHY, C. J. Toxicity and cellular uptake of gold nanoparticles: what we have learned so far? **J Nanopart Res,** v. 12, n. 7, p. 2313-2333, 2010.

ALMEIDA, I. F.; PINTO, A. S.; MONTEIRO, C.; MONTEIRO, H.; BELO, L.; FERNANDES, J.; BENTO, A. R.; DUARTE, T. L.; GARRIDO, J.; BAHIA, M. F.; SOUSA LOBO, J. M.; COSTA, P. C. Protective effect of C. sativa leaf extract against UV mediated-DNA damage in a human keratinocyte cell line. **J Photochem Photobiol B,** v. 144, p. 28-34, 2015.

ALMEIDA, M. E.; TEIXEIRA, H. F.; KOESTER, L. S. Preparação de emulsões submicrométricas: Aspectos teóricos sobre os métodos empregados na atualidade. **Lat Am J Pharm,** v. 27, n. 5, p. 780-788, 2008.

ALONSO, C.; RUBIO, L.; TOURIÑO, S.; MARTÍ, M.; BARBA, C.; FERNÁNDEZ-CAMPOS, F.; CODERCH, L.; LUÍS PARRA, J. Antioxidative effects and percutaneous absorption of five polyphenols. **Free Radical Biol Med,** v. 75, p. 149-155, 2014.

ALVAREZ-ROMÁN, R.; NAIK, A.; KALIA, Y. N.; FESSI, H.; GUY, R. H. Visualization of skin penetration using confocal laser scanning microscopy. **Eur J Pharm Biopharm,** v. 58, n. 2, p. 301-316, 2004.

ALVAREZ-ROMÁN, R.; NAIK, A.; KALIA, Y. N.; GUY, R. H.; FESSI, H. Skin penetration and distribution of polymeric nanoparticles. **J Controlled Release,** v. 99, n. 1, p. 53-62, 2004.

ALVAREZ-SUAREZ, J. M.; GIAMPIERI, F.; GONZÁLEZ-PARAMÁS, A. M.; DAMIANI, E.; ASTOLFI, P.; MARTINEZ-SANCHEZ, G.; BOMPADRE, S.; QUILES, J. L.; SANTOS-BUELGA, C.; BATTINO, M. Phenolics from monofloral honeys protect human erythrocyte membranes against oxidative damage. **Food Chem Toxicol,** v. 50, n. 5, p. 1508-1516, 2012.

ALVES, M. P.; SCARRONE, A. L.; SANTOS, M.; GUTERRES, S. S. Human skin penetration and distribuition of nimesulide from hydrophilic gels containing nanocarriers. **Int J Pharm,** v. 314, p. 215-220, 2007.

AMAKURA, Y.; OKADA, M.; TSUJI, S.; TONOGAI, Y. High-performance liquid chromatographic determination with photodiode array detection of ellagic acid in fresh and processed fruits. **J Chromatogr A,** v. 896, n. 1–2, p. 87-93, 2000.

AMAN, S.; MOIN, S.; OWAIS, M.; SIDDIQUI, M. U. Antioxidant activity of thymol: protective role in AAPH-induced hemolysis in diabetic erythrocytes. **Int J Pharm Sci Invent,** v. 2, n. 3, p. 55-60, 2013.

AN, B.-J.; KWAK, J.-H.; PARK, J.-M.; LEE, J.-Y.; PARK, T.-S.; LEE, J.-T.; SON, J.-H.; JO, C.; BYUN, M.-W. Inhibition of Enzyme Activities and the Antiwrinkle Effect of Polyphenol Isolated from the Persimmon Leaf (Diospyros kaki folium) on Human Skin. **Dermatol Surg,** v. 31, p. 848-855, 2005.

ANTON, N.; BENOIT, J.-P.; SAULNIER, P. Design and production of nanoparticles formulated from nano-emulsion templates—A review. **J Controlled Release,** v. 128, n. 3, p. 185-199, 2008.

ARCT, J.; PYTKOWSKA, K. Flavonoids as components of biologically active cosmeceuticals. **Clin Dermatol,** v. 26, n. 4, p. 347-357, 2008.

ARORA, R.; AGGARWAL, G.; HARIKUMAR, S. L.; KAUR, K. Nanoemulsion Based Hydrogel for Enhanced Transdermal Delivery of Ketoprofen. **Advances in Pharmaceutics,** v. 2014, p. 12, 2014.

ARORA, S.; RAJWADE, J. M.; PAKNIKAR, K. M. Nanotoxicology and in vitro studies: The need of the hour. **Toxicol Appl Pharmacol,** v. 258, n. 2, p. 151-165, 2012.

ARULMOZHI, V.; PANDIAN, K.; MIRUNALINI, S. Ellagic acid encapsulated chitosan nanoparticles for drug delivery system in human oral cancer cell line (KB). **Colloids Surf B,** v. 110, p. 313-320, 2013.

ARUOMA, O. Free radicals, oxidative stress, and antioxidants in human health and disease. **J Am Oil Chem Soc,** v. 75, n. 2, p. 199-212, 1998.

ASHARA, K. C.; PAUN, J. S.; SONIWALA, M. M.; CHAVADA, J. R.; MORI, N. M. Micro-emulsion based emulgel: a novel topical drug

delivery system. **Asian Pac J Trop Dis,** v. 4, Supplement 1, n. 0, p. S27-S32, 2014.

ASLAM, M. N.; LANSKY, E. P.; VARANI, J. Pomegranate as a cosmeceutical source: Pomegranate fractions promote proliferation and procollagen synthesis and inhibit matrix metalloproteinase-1 production in human skin cells. **J Ethnopharmacol,** v. 103, n. 3, p. 311-318, 2006.

AULTON, M. E. **Delineamento de formas farmacêuticas**. 2. Artmed, 2005. 678

AVACHAT, A. M.; PATEL, V. G. Self nanoemulsifying drug delivery system of stabilized ellagic acid–phospholipid complex with improved dissolution and permeability. **Saudi Pharm J,** v. 23, n. 3, p. 276-289, 2015.

AVIRAM, M.; DORNFELD, L.; ROSENBLAT, M.; VOLKOVA, N.; KAPLAN, M.; COLEMAN, R.; HAYEK, T.; PRESSER, D.; FUHRMAN, B. Pomegranate juice consumption reduces oxidative stress, atherogenic modifications to LDL, and platelet aggregation: studies in humans and in atherosclerotic apolipoprotein E–deficient mice. **Am J Clin Nutr** v. 71, n. 5, p. 1062-1076, 2000.

AVIRAM, M.; VOLKOVA, N.; COLEMAN, R.; DREHER, M.; REDDY, M. K.; FERREIRA, D.; ROSENBLAT, M. Pomegranate phenolics from the peels, arils, and flowers are antiatherogenic: Studies in vivo in atherosclerotic apolipoprotein E-deficient (E0) mice and in vitro in cultured macrophages and lipoproteins. **J Agric Food Chem,** v. 56, n. 3, p. 1148-1157, 2008.

BACCARIN, T.; LEMOS-SENNA, E. Pomegranate seed oil nanoemulsions encapsulating pomegranate peel polyphenol-rich ethyl acetate fraction: Development and antioxidant assessment. **J Nanopharmaceutics and Drug Delivery,** v. 2, n. 4, p. 333-343, 2014.

BACCARIN, T.; MITJANS, M.; LEMOS-SENNA, E.; VINARDELL, M. P. Protection against oxidative damage in human erythrocytes and preliminary photosafety assessment of Punica granatum seed oil nanoemulsions entrapping polyphenol-rich ethyl acetate fraction. **Toxicol In Vitro,** v. Article *in press*, 2015.

BACCARIN, T.; MITJANS, M.; RAMOS, D.; LEMOS-SENNA, E.; VINARDELL, M. P. Photoprotection by Punica granatum seed oil nanoemulsion entrapping polyphenol-rich ethyl acetate fraction against UVB-induced DNA damage in human keratinocyte (HaCaT) cell line. **J Photochem Photobiol B,** v. 153, p. 127-136, 2015.

BADEN, H. P.; GIFFORD, A. M. Isometric contraction of epidermis and stratum corneum with heating. **J Invest Dermatol,** v. 54, n. 4, p. 298-303, 1970.

BALA, I.; BHARDWAJ, V.; HARIHARAN, S.; KHARADE, S. V.; ROY, N.; RAVI KUMAR, M. N. V. Sustained release nanoparticulate formulation containing antioxidant-ellagic acid as potential prophylaxis system for oral administration. **J Drug Targeting,** v. 14, n. 1, p. 27-34, 2006.

BALA, I.; BHARDWAJ, V.; HARIHARAN, S.; RAVI KUMAR, M. N. V. Analytical methods for assay of ellagic acid and its solubility studies. **J Pharm Biomed Anal,** v. 40, n. 1, p. 206-210, 2006.

BANERJEE, A.; KUNWAR, A.; MISHRA, B.; PRIYADARSINI, K. I. Concentration dependent antioxidant/pro-oxidant activity of curcumin: Studies from AAPH induced hemolysis of RBCs. **Chem-Biol Interact,** v. 174, n. 2, p. 134-139, 2008.

BANIHANI, S.; SWEDAN, S.; ALGURAAN, Z. Pomegranate and type 2 diabetes. **Nutr Res,** v. 33, n. 5, p. 341-348, 2013.

BAROLI, B. Penetration of nanoparticles and nanomaterials in the skin: fiction or reality? **J Pharm Sci,** v. 99, n. 1, p. 21-50, 2010.

BARRY, B. W. Novel mechanisms and devices to enable successful transdermal drug delivery. **Eur J Pharm Sci,** v. 14, p. 101-114, 2001.

BARZEGAR, M.; FADAVI, A.; AZIZI, M. H. An investigation on the physico-chemical composition of various pomegranates (Punica granatum L.) grown in Yazd. **Iran J Food Sci Technol,** v. 2, p. 9-14, 2004.

BASHIR, S. J.; CHEW, A.-L.; ANIGBOGU, A.; DREHER, F.; MAIBACH, H. I. Physical and physiological effects of stratum corneum tape stripping. **Skin ResTechnol,** v. 7, n. 1, p. 40-48, 2001.

BASU, A.; PENUGONDA, K. Pomegranate juice: a heart-healthy fruit juice. **Nutr Rev,** v. 67, p. 49-56, 2009.

BEDAF, M. T.; BAHAR, M.; SHARIFNABI, B.; YAMCHI, A. Evaluation of genetic diversity among Iranian pomegranate (Punica granatum L.) cultivars, using ISSR and RAPD markers. **Taxon Biosyst,** v. 3, n. 8, p. 35-44, 2011.

BEHREND, O.; SCHUBERT, H. Influence of hydrostatic pressure and gas content on continuous ultrasound emulsification. **Ultrason Sonochem,** v. 8, n. 3, p. 271-276, 2001.

BEKIR, J.; MARS, M.; SOUCHARD, J. P.; BOUAJILA, J. Assessment of antioxidant, anti-inflammatory, anti-cholinesterase and cytotoxic activities of pomegranate (Punica granatum) leaves. **Food Chem Toxicol,** v. 55, n. 0, p. 470-475, 2013.

BEN NASR, C.; AYED, N.; METCHE, M. Quantitative determination of the polyphenolic content of pomegranate peel. **Z Lebensm Unters For,** v. 203, n. 4, p. 374-378, 1996.

BENSON, H. A. Transdermal drug delivery: penetration enhancement techniques. **Curr drug delivery,** v. 2, n. 1, p. 23-33, 2005.

BENZIE, I. F. F.; STRAIN, J. J. The Ferric Reducing Ability of Plasma (FRAP) as a Measure of "Antioxidant Power": The FRAP Assay. **Anal Biochem,** v. 239, n. 1, p. 70-76, 1996.

BIDONE, J.; ARGENTA, D. F.; KRATZ, J.; PETTENUZZO, L. F.; HORN, A. P.; KOESTER, L. S.; BASSANI, V. L.; SIMÕES, C. M. O.; TEIXEIRA, H. F. Antiherpes activity and skin/mucosa distribution of flavonoids from Achyrocline satureioides extract incorporated into topical nanoemulsions. **Biomed Res Int,** v. 2015, p. 238010, 2015.

BIDONE, J.; ZORZI, G. K.; CARVALHO, E. L. S.; SIMÕES, C. M. O.; KOESTER, L. S.; BASSANI, V. L.; TEIXEIRA, H. F.

Incorporation of Achyrocline satureioides (Lam.) DC extracts into topical nanoemulsions obtained by means of spontaneous emulsification procedure. **Ind Crops Prod,** v. 62, n. 0, p. 421-429, 2014.

BITO, T.; NISHIGORI, C. Impact of reactive oxygen species on keratinocyte signaling pathways. **J Dermatol Sci,** v. 68, n. 1, p. 3-8, 2012.

BLASA, M.; CANDIRACCI, M.; ACCORSI, A.; PIACENTINI, M. P.; PIATTI, E. Honey flavonoids as protection agents against oxidative damage to human red blood cells. **Food Chem,** v. 104, n. 4, p. 1635-1640, 2007.

BOLZINGER, M.-A.; BRIANÇON, S.; PELLETIER, J.; CHEVALIER, Y. Penetration of drugs through skin, a complex rate-controlling membrane. **Curr Opin Colloid Interface Sci,** v. 17, n. 3, p. 156-165, 2012.

BORENFREUND, E.; PUERNER, J. Toxicity determined in vitro by morphological alterations and neutral red absorptio. **Toxicol Lett,** v. 24, p. 119-124, 1985.

BOS, J. D.; MEINARDI, M. M. H. M. The 500 Dalton rule for the skin penetration of chemical compounds and drugs. **Exp Dermatol,** v. 9, n. 3, p. 165-169, 2000.

BOTTA, A.; MARTÍNEZ, V.; MITJANS, M.; BALBOA, E.; CONDE, E.; VINARDELL, M. P. Erythrocytes and cell line-based assays to evaluate the cytoprotective activity of antioxidant components obtained from natural sources. **Toxicol In Vitro,** v. 28, n. 1, p. 120-124, 2014.

BOUCHEMAL, K.; BRIANÇON, S.; PERRIER, E.; FESSI, H. Nano-emulsion formulation using spontaneous emulsification:solvent, oil and surfactant optimisation. **Int J Pharm,** v. 280, p. 241-251, 2004.

BOUWSTRA, J. A.; HONEYWELL-NGUYEN, P. L.; GOORIS, G. S.; PONEC, M. Structure of the skin barrier and its modulation by vesicular formulations. **Prog Lipid Res,** v. 42, p. 1-36, 2003.

BRADFORD, M. M. A rapid and sensitive method for the quantitation of microgram quantities of protein utilizing the principle of protein-dye binding. **Anal Biochem,** v. 72, n. 1–2, p. 248-254, 1976.

BRAGA, L. C.; SHUPP, J. W.; CUMMINGS, C.; JETT, M.; TAKAHASHI, J. A.; CARMO, L. S.; CHARTONE-SOUZA, E.; NASCIMENTO, A. M. A. Pomegranate extract inhibits Staphylococcus aureus growth and subsequent enterotoxin production. **J Ethnopharmacol,** v. 96, n. 1–2, p. 335-339, 2005.

BRASIL. Guia para avaliação de segurança de produtos cosméticos. **Agência Nacional de Vigilância Sanitária**, p. 1-47, 2003a.

BRASIL. Resolution RE 899 "Guide for analytical and bio-analitycal method validation". **Anvisa - Agência Nacional de Vigilância Satinária** 2003.

BRAVO, L. Polyphenols: Chemistry, dietary sources, metabolism, and nutritional significance. **Nutr Rev,** v. 56, n. 11, p. 317-333, 1998.

BRUGUÉS, A. P.; NAVEROS, B. C.; CALPENA CAMPMANY, A. C.; PASTOR, P. H.; SALADRIGAS, R. F.; LIZANDRA, C. R. Developing cutaneous applications of paromomycin entrapped in stimuli-sensitive block copolymer nanogel dispersions. **Nanomedicine,** v. 10, n. 2, p. 227-240, 2015.

BRUSCHI, M. L.; JONES, D. S.; PANZERI, H.; GREMIÃO, M. P. D.; DE FREITAS, O.; LARA, E. H. G. Semisolid systems containing propolis for the treatment of periodontal disease: In Vitro release kinetics, syringeability, rheological, textural, and mucoadhesive properties. **J Pharm Sci,** v. 96, n. 8, p. 2074-2089, 2007.

BURANAJAREE, S.; DONSING, P.; JEENAPONGSA, R.; VIYOCH, J. Depigmenting action of a nanoemulsion containing heartwood extract of Artocarpus incisus on UVB-induced hyperpigmentation in C57BL/6 mice. **J Cosmet Sci,** v. 62, n. 1, p. 1-14, 2011.

BUWALDA, S. J.; BOERE, K. W. M.; DIJKSTRA, P. J.; FEIJEN, J.; VERMONDEN, T.; HENNINK, W. E. Hydrogels in a historical

perspective: From simple networks to smart materials. **J Controlled Release,** v. 190, p. 254-273, 2014.

ÇAM, M.; HISIL, Y.; DURMAZ, G. Classification of eight pomegranate juices based on antioxidant capacity measured by four methods. **Food Chem,** v. 112, p. 721-726, 2009.

CECHINEL FILHO, V.; YUNES, R. A. Estrategies for obtaining pharmacologically active compounds from medicinal plants: concepts about structural modification for improve the activity. **Quim Nova,** v. 21, n. 1, p. 99-105, 1998.

CELIK, I.; TEMUR, A.; ISIK, I. Hepatoprotective role and antioxidant capacity of pomegranate (Punica granatum) flowers infusion against trichloroacetic acid-exposed rats. **Food Chem Toxicol,** v. 47, p. 145-149, 2009.

CERQUEIRA, F. M.; MEDEIROS, M. H. G. D.; AUGUSTO, O. Antioxidantes dietéticos: controvérsias e perspectivas. **Quim Nova,** v. 30, p. 441-449, 2007.

CEVC, G. Lipid vesicles and other colloids as drug carriers on the skin. **Adv Drug Delivery Rev,** v. 56, n. 5, p. 675-711, 2004.

CEVC, G.; VIERL, U. Nanotechnology and the transdermal route: A state of the art review and critical appraisal. **J Controlled Release,** v. 141, n. 3, p. 277-299, 2010.

CHAIITTIANAN, R.; SRIPANIDKULCHAI, B. Development of a nanoemulsion of Phyllanthus emblica L. branch extract. **Drug Dev Ind Pharm,** v. 40, n. 12, p. 1597-1606, 2014.

CHATELAIN, E.; GABARD, B.; SURBER, C. Skin penetration and sun protection factor of five UV filters: Effect of the vehicle. **Skin Pharmacol Physiol,** v. 16, n. 1, p. 28-35, 2003.

CHEN, H.; KHEMTONG, C.; YANG, X.; CHANG, X.; GAO, J. Nanonization strategies for poorly water-soluble drugs. **Drug Discovery Today,** v. 16, n. 7–8, p. 354-360, 2011.

CHEN, L.; HU, J. Y.; WANG, S. Q. The role of antioxidants in photoprotection: A critical review. **J Am Acad Dermatol,** v. 67, n. 5, p. 1013-1024, 2012.

CHIDAMBARA MURTHY, K. N.; REDDY, V. K.; VEIGAS, J. M.; MURTHY, U. D. Study on Wound Healing Activity of Punica granatum Peel. **J Med Food,** v. 7, n. 2, p. 256-259, 2004.

CHIME, S. A.; KENECHUKWU, F. C.; ATTAMA, A. A. **Nanoemulsions — Advances in Formulation, Characterization and Applications in Drug Delivery**. Croatia: Intech Books, 2014.

CHIRINOS, R.; CAMPOS, D.; WARNIER, M.; PEDRESCHI, R.; REES, J.-F.; LARONDELLE, Y. Antioxidant properties of mashua (Tropaeolum tuberosum) phenolic extracts against oxidative damage using biological in vitro assays. **Food Chem,** v. 111, n. 1, p. 98-105, 2008.

CHO, E. C.; XIE, J.; WURM, P. A.; XIA, Y. Understanding the role of surface charges in cellular adsorption versus internalization by selectively removing gold nanoparticles on the cell surface with a I2/KI etchant. **Nano Lett,** v. 9, n. 3, p. 1080-1084, 2009.

CHOI, C. W.; KIM, S. C.; HWANG, S. S.; CHOI, B. K.; AHN, H. J.; LEE, M. Y.; PARK, S. H.; KIM, S. K. Antioxidant activity and free radical scavenging capacity between Korean medicinal plants and flavonoids by assay-guided comparison. **Plant Sci,** v. 163, n. 6, p. 1161-1168, 2002.

CLIFFORD, M. N.; SCALBERT, A. Ellagitannins – nature, occurrence and dietary burden. **J Sci Food Agric,** v. 80, n. 7, p. 1118-1125, 2000.

CONCEA. Conselho Nacional de Controle de Experimentação Animal. Resolução Normativa nº 17 de 03 de julho de 2014.

DAHLGREN, R.; THORNE, R. F. The order myrtales: circumscription, variation, and relationships. **Ann Mo Bot Gard,** v. 71, n. 3, p. 633-699, 1984.

DAVIDSON, M. H.; MAKI, K. C.; DICKLIN, M. R.; FEINSTEIN, S. B.; WITCHGER, M. S.; BELL, M.; MCGUIRE, D. K.; PROVOS, J. C.; LIKER, H.; AVIRAM, M. Effects of consumption of pomegranate juice on carotid intima-media thickness in men and women at moderate risk for coronary heart disease. **Am J Cardiol,** v. 104, n. 7, p. 936-942, 2009.

DE BOER, J.; HOEIJMAKERS, J. H. J. Nucleotide excision repair and human syndromes. **Carcinogenesis,** v. 21, n. 3, p. 453-460, 2000.

DE GRUIJL, F. R. [33] Photocarcinogenesis: UVA vs UVB. In: LESTER PACKER, H. S. (Ed.). **Methods in Enzymology**: Academic Press, v.Volume 319, 2000. p.359-366.

DE OLIVEIRA JUNIOR, R. G.; DE SOUZA ARAÚJO, C.; SOUZA, G. R.; GUIMARÃES, A. L.; DE OLIVEIRA, A. P.; DE LIMA-SARAIVA, S. R. G.; MORAIS, A. C. S.; RIBEIRO, J. S. In vitro antioxidant and photoprotective activities of dried extracts from Neoglaziovia variegata (Bromeliaceae). **J Appl Pharm Sci,** v. 3, n. 01, p. 122-127, 2013.

DEPIERI, L. V.; PRAÇA, F. S. G.; CAMPOS, P. M.; BENTLEY, M. V. L. B. Advances in the bioanalytical study of drug delivery across the skin. **Ther Delivery,** v. 6, n. 5, p. 173-196, 2015.
DEVARAJAN, V.; RAVICHANDRAN, V. Nanoemulsions: as modified drug delivery tool. **Pharm Globale,** v. 2, p. 1-5, 2011.

DI GIROLAMO, N.; KUMAR, R. K.; CORONEO, M. T.; WAKEFIELD, D. UVB-mediated induction of interleukim-6 and -8 in pterygia and culture human pterygium epithelial cells. **Invest Ophthalmol Visual Sci,** v. 43, n. 11, p. 3430-3437, 2002.

DINKOVA-KOSTOVA, A. T. Phytochemicals as protectors against ultraviolet radiation: versatility of effects and mechanisms. **Planta Med,** v. 74, n. 13, p. 1548, 2008.

DIVSALAR, A.; SABOURY, A. A.; NABIUNI, M.; ZARE, Z.; KEFAYATI, M. E.; SEYEDARABI, A. Characterization and side effect analysis of a newly designed nanoemulsion targeting human serum albumin for drug delivery. **Colloids Surf B,** v. 98, n. 0, p. 80-84, 2012.

DJEKIC, L.; KRAJISNIK, D.; MARTINOVIC, M.; DJORDJEVIC, D.; PRIMORAC, M. Characterization of gelation process and drug release profile of thermosensitive liquid lecithin/poloxamer 407 based gels as carriers for percutaneous delivery of ibuprofen. **Int J Pharm,** v. 490, n. 1–2, p. 180-189, 2015.

DJEKIC, L.; MARTINOVIC, M.; STEPANOVIĆ-PETROVIĆ, R.; TOMIĆ, M.; MICOV, A.; PRIMORAC, M. Design of block copolymer costabilized nonionic microemulsions and their in vitro and in vivo assessment as carriers for sustained regional delivery of ibuprofen via topical administration. **J Pharm Sci,** v. 104, n. 8, p. 2501-2512, 2015.

DOKTOROVOVA, S.; SOUTO, E. B.; SILVA, A. M. Nanotoxicology applied to solid lipid nanoparticles and nanostructured lipid carriers – A systematic review of in vitro data. **Eur. J. Pharm. Biopharm.,** v. 87, n. 1, p. 1-18, 2014.

DORA, C. L.; SILVA, L. F. C.; PUTAUX, J. L.; NISHIYANNA, Y.; PIGNOT-PAINTRAND, I.; BORSALI, R.; LEMOS-SENNA, E. Poly(ethylene glycol) hydroxystearate-based nanosized emulsions: effect of surfactant concentration on their formation and ability to solubilize quercetin. **J Biomed Nanotechnol,** v. 8, p. 1-9, 2012.

DUMORTIER, G.; GROSSIORD, J.; AGNELY, F.; CHAUMEIL, J. A review of poloxamer 407 pharmaceutical and pharmacological characteristics. **Pharm Res,** v. 23, n. 12, p. 2709-2728, 2006.

DUTRA, E. A.; OLIVEIRA, D. A. G. C.; KEDOR-HACKMANN, E. R. M.; SANTORO, M. I. R. M. Determination of sun protection factor (SPF) of sunscreens by ultraviolet spectrophotometry. **Braz J Pharm Sci,** v. 40, n. 3, p. 381-385, 2004.

EL-BOURY, S.; COUTEAU, C.; BOULANDE, L.; PAPARIS, E.; COIFFARD, L. J. M. Effect of the combination of organic and inorganic filters on the Sun Protection Factor (SPF) determined by in vitro method. **Int J Pharm,** v. 340, p. 1-5, 2007.

EL-NEMR, S. E.; ISMAIL, I. A.; RAGAB, M. Chemical composition of juice and seeds of pomegranate fruit. **Die Nahrung,** v. 34, n. 7, p. 601-606, 2006.

ELANGO, S.; BALWAS, R.; PADMA, V. V. Gallic acid isolated from pomegranate peel extract induces reactive oxygen species mediated apoptosis in A549 cell line. **J Cancer Ther,** v. 2, p. 638-645, 2011.

ELFALLEH, W.; TLILI, N.; NASRI, N.; YAHIA, Y.; HANNACHI, H.; CHAIRA, N.; YING, M.; FERCHICHI, A. Antioxidant capacities of phenolic compounds and tocopherols from Tunisian pomegranate (Punica granatum) Fruits. **J Food Sci,** v. 76, n. 5, p. C707-C713, 2011.

ERCISLI, S.; AGAR, G.; ORHAN, E.; YILDIRIM, N.; HIZARCI, Y. Interspecific variability of RAPD and fatty acid composition of some pomegranate cultivars (Punica granatum L.) growing in Southern Anatolia Region in Turkey. **Biochem Syst Ecolo,** v. 35, n. 11, p. 764-769, 2007.

ESCOBAR-CHÁVEZ, J. J.; MERINO-SANJUÁN, V.; LÓPEZ-CERVANTES, M.; URBAN-MORLAN, Z.; PIÑÓN-SEGUNDO, E.; QUINTANAR-GUERRERO, D.; GANEM-QUINTANAR, A. The tape stripping technique as a method for drug quantification in skin. **J Pharm Pharm Sci,** v. 11, p. 104-130, 2008.

ESMAILLZADEH, A.; TAHBAZ, F.; GAIENI, I.; ALAVI-MAJD, H.; AZADBAKHT, L. Cholesterol-lowering effect of concentrated pomegranate juice consumption in type II diabetic patients with hyperlipidemia. **Int J Vitam Nutr Res,** v. 76, n. 3, p. 147-151, 2006.

FADAVI, A.; BARZEGAR, M.; AZIZI, H. M. Determination of fatty acids and total lipid content in oilseed of 25 pomegranates varieties grown in Iran. **J Food Compost Anal,** v. 19, p. 676-680, 2006.

FADAVI, A.; BARZEGAR, M.; AZIZI, M. H.; BAYAT, M. Physicochemical composition of ten pomegranate cultivars (Punica granatum L.) grown in Iran. **Food Sci Technol Int,** v. 11, p. 113-119, 2005.

FAIRBANKS, G.; STECK, T. L.; WALLACH, D. F. H. Electrophoretic analysis of the major polypeptides of the human erythrocyte membrane. **Biochemistry,** v. 10, n. 13, p. 2606-2617, 1971.

FANG, J.-Y.; HUNG, C.-F.; HWANG, T.-L.; WONG, W.-W. Transdermal delivery of tea catechins by electrically assisted methods. **Skin Pharmacol Physiol,** v. 19, n. 1, p. 28-37, 2006.

FERNANDEZ, C.; MARTI-MESTRES, G.; RAMOS, J.; MAILLOLS, H. LC analysis of benzophenone-3: II application to determination of 'in vitro' and 'in vivo' skin penetration from solvents, coarse and submicron emulsions. **J Pharm Biomed Anal,** v. 24, n. 1, p. 155-165, 2000.

FERREIRA, L. M.; CERVI, V. F.; GEHRCKE, M.; DA SILVEIRA, E. F.; AZAMBUJA, J. H.; BRAGANHOL, E.; SARI, M. H. M.; ZBOROWSKI, V. A.; NOGUEIRA, C. W.; CRUZ, L. Ketoprofen-loaded pomegranate seed oil nanoemulsion stabilized by pullulan: Selective antiglioma formulation for intravenous administration. **Colloids Surf B,** v. 130, n. 0, p. 272-277, 2015.

FISCHER, U. A.; CARLE, R.; KAMMERER, D. R. Identification and quantification of phenolic compounds from pomegranate (Punica granatum L.) peel, mesocarp, aril and differently produced juices by HPLC-DAD–ESI/MSn. **Food Chem,** v. 127, n. 2, p. 807-821, 2011.

FJAERAA, C.; NÅNBERG, E. Effect of ellagic acid on proliferation, cell adhesion and apoptosis in SH-SY5Y human neuroblastoma cells. **Biomed Pharmacother,** v. 63, n. 4, p. 254-261, 2009.

FLOR, J.; DAVOLOS, M. R.; CORREA, M. A. Protetores solares. **Quim Nova,** v. 30, p. 153-158, 2007.

FLOURY, J.; BELLETTRE, J.; LEGRAND, J.; DESRUMAUX, A. Analysis of a new type of high pressure homogeniser. A study of the flow pattern. **Chem Eng Sci,** v. 59, n. 4, p. 843-853, 2004.

FLOURY, J.; LEGRAND, J.; DESRUMAUX, A. Analysis of a new type of high pressure homogeniser. Part B. study of droplet break-up and recoalescence phenomena. **Chem Eng Sci,** v. 59, n. 6, p. 1285-1294, 2004.

FLOYD, R. A.; LEWIS, A. C. Hydroxyl free radical formation from hydrogen peroxide by ferrous iron-nucleotide complexes. **Biochem,** v. 22, p. 2645-2649, 1983.

FLYNN, T. P.; ALLEN, D. W.; JOHNSON, G. J.; WHITE, J. G. Oxidant damage of the lipids and proteins of the erythrocyte membranes in unstable hemoglobin disease. Evidence for the role of lipid peroxidation. **J Clin Invest,** v. 71, p. 1215-1223, 1983.

FOLDVARI, M. Non-invasive administration of drugs through the skin: challenges in delivery system design. **Pharm Sci Technol Today,** v. 3, n. 12, p. 417-425, 2000.

FORT, J. J.; MITRA, A. K. Effects of epidermal/dermal separation methods and ester chain configuration on the bioconversion of a homologous series of methotrexate dialkyl esters in dermal and epidermal homogenates of hairless mouse skin. **Int J Pharm,** v. 102, n. 1–3, p. 241-247, 1994.

FRANZ, T. J. Percutaneous absorption - on the relevance of *in vitro* data. **J Invest Dermatol,** v. 64, n. 3, p. 190-195, 1975.

FRASER, P. D.; BRAMLEY, P. M. The biosynthesis and nutritional uses of carotenoids. **Prog Lipid Res,** v. 43, n. 3, p. 228-265, 2004.

FREITAS, J. V.; PRAÇA, F. S. G.; BENTLEY, M. V. L. B.; GASPAR, L. R. Trans-resveratrol and beta-carotene from sunscreens penetrate viable skin layers and reduce cutaneous penetration of UV-filters. **Int J Pharm,** v. 484, n. 1–2, p. 131-137, 2015.

FRIDOVICH, I. Oxygen toxicity: a radical explanation. **J Exp Biol,** v. 201, n. 8, p. 1203-1209, 1998.

FRIEDMAN, D. I.; SCHWARZ, J. S.; WEISSPAPIR, M. Submicron emulsion vehicle for enhanced transdermal delivery of steroidal and nonsteroidal antiinflammatory drugs. **J Pharm Sci,** v. 84, n. 3, p. 324-329, 1995.

FRIEDRICH, R. B.; KANN, B.; CORADINI, K.; OFFERHAUS, H. L.; BECK, R. C. R.; WINDBERGS, M. Skin penetration behavior of lipid-core nanocapsules for simultaneous delivery of resveratrol and curcumin. **Eur J Pharm Sci,** v. 78, p. 204-213, 2015.

FRONZA, T.; CAMPOS, A.; TEIXEIRA, H. Nanoemulsões como sistemas de liberação para fármacos oftálmicos. **Acta Farm Bonaerense,** v. 23, n. 4, p. 558-566, 2004.

GANESAN, P.; KUMAR, C. S.; BHASKAR, N. Antioxidant properties of methanol extract and its solvent fractions obtained from selected Indian red seaweeds. **Bioresour Technol,** v. 99, n. 8, p. 2717-2723, 2008.

GAOE, H.; PANG, Z.; PAN, S.; CAO, S.; YANG, Z.; CHEN, C.; JIANG, X. Anti-glioma effect and safety of docetaxel-loaded nanoemulsion. **Arch Pharmacal Res,** v. 35, n. 2, p. 333-341, 2012/02/01 2012.

GARATINI, T.; MEDEIROS, M. H. G.; COLEPICOLO, P. Antioxidantes na manutenção do equilíbrio redox cutâneo: uso e avaliação de sua eficácia. **Quim Nova,** v. 30, n. 1, p. 206-213, 2007.

GASPAR, L. R.; MAIA CAMPOS, P. M. B. G. Rheological behavior and the SPF of sunscreens. **Int J Pharm,** v. 250, n. 1, p. 35-44, 2003.

GEORGE, J.; SINGH, M.; SRIVASTAVA, A. K.; BHUI, K.; SHUKLA, Y. Synergistic growth inhibition of mouse skin tumors by pomegranate fruit extract and diallyl sulfide: Evidence for inhibition of activated MAPKs/NF-κB and reduced cell proliferation. **Food Chem Toxicol,** v. 49, n. 7, p. 1511-1520, 2011.

GEUSENS, B.; STROBBE, T.; BRACKE, S.; DYNOODT, P.; SANDERS, N.; GELE, M. V.; LAMBERT, J. Lipid-mediated gene delivery to the skin. **Eur J Pharm Sci,** v. 43, n. 4, p. 199-211, 2011.

GIL, M. I.; TOMÁS-BARBERÁN, F. A.; HESS-PIERCE, B.; HOLCROFT, D. M.; KADER, A. A. Antioxidant Activity of Pomegranate Juice and Its Relationship with Phenolic Composition and Processing. **J Agric Food Chem,** v. 48, n. 10, p. 4581-4589, 2000.

GILABERTE, Y.; GONZÁLEZ, S. Update on Photoprotection. **Actas Dermo-Sifiliogr (English Edition),** v. 101, n. 8, p. 659-672, 2010.

GIROTTI, A. W. Photosensitized oxidation of membrane lipids: reaction pathways, cytotoxic effects, and cytoprotective mechanisms. **J Photochem Photobiol B,** v. 63, p. 103-113, 2001.

GODIC, A.; POLJAK, B.; ADAMIC, M.; DAHMANE, R. The role of antioxidants in skin cancer prevention and treatment. **Oxid Med Cell Longevity,** v. 2014, p. 1-6, 2014.

GODIN, B.; TOUITOU, E. Transdermal skin delivery: Predictions for humans from in vivo, ex vivo and animal models. **Adv Drug Delivery Rev,** v. 59, p. 1152-1161, 2007.

GOLUBOVIC-LIAKOPOULOS, N.; SIMON, S. R.; SHAH, B. Nanotechnology use with cosmeceuticals. **Semin Cutaneous Med Surg,** v. 30, n. 3, p. 176-180, 2011.

GONZÁLEZ, N.; RIBEIRO, D.; FERNANDES, E.; NOGUEIRA, D. R.; CONDE, E.; MOURE, A.; VINARDELL, M. P.; MITJANS, M.; DOMÍNGUEZ, H. Potential use of Cytisus scoparius extracts in topical applications for skin protection against oxidative damage. **J Photochem Photobiol B,** v. 125, n. 0, p. 83-89, 2013.

GONZÁLEZ, S.; FERNÁNDEZ-LORENTE, M.; GILABERTE-CALZADA, Y. The latest on skin photoprotection. **Clin Dermatol,** v. 26, n. 6, p. 614-626, 2008.

GOULA, A. M.; ADAMOPOULOS, K. G. A method for pomegranate seed application in food industries: Seed oil encapsulation. **Food Bioprod Process,** v. 90, n. 4, p. 639-652, 2012.

GREENSPAN, P.; MAYER, E. P.; FOWLER, S. D. Nile red: a selective fluorescent stain for intracellular lipid droplets. **J Cell Biol,** v. 100, n. 3, p. 965-973, 1985.

GROOT, H. D.; RAUEN, U. Tissue injury by reactive oxygen species and the protective effects of flavonoids. **Fundam Clin Pharmacol,** v. 12, n. 3, p. 249-255, 1998.

GUARATINI, T.; MEDEIROS, M. H. G.; COLEPICOLO, P. Antioxidantes na manutenção do equilíbrio redox cutâneo: uso e avaliação de sua eficácia. **Quim Nova,** v. 30, p. 206-213, 2007.

GUGLIELMINI, G. Nanostructured novel carrier for topical application. **Clin Dermatol,** v. 26, n. 4, p. 341-346, 2008.

GÜLÇIN, İ. Antioxidant activity of caffeic acid (3,4-dihydroxycinnamic acid). **Toxicol,** v. 217, n. 2–3, p. 213-220, 2006.

GUPTA, S. S.; GHOSH, S.; MAITI, P.; GHOSH, M. Microencapsulation of conjugated linolenic acid–rich pomegranate seed oil by an emulsion method. **Food Sci Technol Int,** v. 18, n. 6, p. 549-558, December 1, 2012 2012.

GUTTERIDGE, J. M. Lipid peroxidation and antioxidants as biomarkers of tissue damage. **Clin Chem,** v. 41, n. 12, p. 1819-28, December 1, 1995 1995.

HA, T. V. A.; KIM, S.; CHOI, Y.; KWAK, H.-S.; LEE, S. J.; WEN, J.; OEY, I.; KO, S. Antioxidant activity and bioaccessibility of size-different nanoemulsions for lycopene-enriched tomato extract. **Food Chem,** v. 178, p. 115-121, 2015.

HADGRAFT, J. Skin, the final frontier. **Int J Pharm,** v. 224, p. 1-18, 2001.

HADGRAFT, J. Skin deep. **Eur J Pharm Biopharm,** v. 58, p. 291-299, 2004.

HADGRAFT, J.; PUGH, W. J. The selection and design of topical and transdermal agents: a review. Journal of Investigative Dermatology Symposium Proceedings, 1998. p.131-135.

HAIDARI, M.; ALI, M.; CASSCELLS, S. W.; MADJID, M. Pomegranate (Punica granatum) purified polyphenol extract inhibits influenza virus and has a synergistic effect with oseltamivir. **Phytomedicine,** v. 16, n. 12, p. 1127-1136, 2009.

HALLIWELL, B.; CLEMENT, M. V.; LONG, L. H. Hydrogen peroxide in the human body. **FEBS Lett,** v. 486, p. 10-13, 2000.

HAMAD, A. W.; AL-MOMENE, W. Separation and purification of crude ellagic acid from white flesh of pomegranate fruits as a potent anti-carcinogenic. **New Biotechnol,** v. 25, n. 1, p. 286, 2009.

HAMIDI, M.; AZADI, A.; RAFIEI, P. Hydrogel nanoparticles in drug delivery. **Adv Drug Delivery Rev,** v. 60, n. 15, p. 1638-1649, 2008.

HARBORNE, J. B. General procedures and measurements of total phenolics. In: HARBORNE, J. B. (Ed.). **Methods in plant biochemistry. Plant phenolics**. London: Academic Press, v.1, 1989.

HASLAM, E. Vegetable tannins – Lessons of a phytochemical lifetime. **Phytochemistry,** v. 68, n. 22–24, p. 2713-2721, 2007.

HAYOUNI, E. A.; MILED, K.; BOUBAKER, S.; BELLASFAR, Z.; ABEDRABBA, M.; IWASKI, H.; OKU, H.; MATSUI, T.; LIMAM, F.; HAMDI, M. Hydroalcoholic extract based-ointment from Punica granatum L. peels with enhanced in vivo healing potential on dermal wounds. **Phytomedicine,** v. 18, n. 11, p. 976-984, 2011.

HENRY, S.; MCALLISTER, D. V.; ALLEN, M. G.; PRAUSNITZ, M. R. Microfabricated microneedles: A novel approach to transdermal drug delivery. **J Pharm Sci,** v. 87, n. 8, p. 922-925, 1998.

HEURTAULT, B.; SAULNIER, P.; PECH, B.; PROUST, J.-E.; BENOIT, J.-P. Physico-chemical stability of colloidal lipid particles. **Biomaterials,** v. 24, n. 23, p. 4283-4300, 2003.

HOELLER, S.; SPERGER, A.; VALENTA, C. Lecithin based nanoemulsions: A comparative study of the influence of non-ionic surfactants and the cationic phytosphingosine on physicochemical behaviour and skin permeation. **Int J Pharm,** v. 370, n. 1–2, p. 181-186, 2009.

HORA, J. J.; MAYDEW, E. R.; LANSKY, E. P.; DWIVEDI, C. Chemopreventive Effects of Pomegranate Seed Oil on Skin Tumor Development in CD1 Mice. **J Med Food,** v. 6, n. 3, p. 157-161, 2003.

HOU, S.-Z.; SU, Z.-R.; CHEN, S.-X.; YE, M.-R.; HUANG, S.; LIU, L.; ZHOU, H.; LAI, X.-P. Role of the interaction between puerarin and the erythrocyte membrane in puerarin-induced hemolysis. **Chem-Biol Interact,** v. 192, n. 3, p. 184-192, 2011.

HSEU, Y.-C.; CHANG, W.-C.; HSEU, Y.-T.; LEE, C.-Y.; YECH, Y.-J.; CHEN, P.-C.; CHEN, J.-Y.; YANG, H.-L. Protection of oxidative damage by aqueous extract from Antrodia camphorata mycelia in normal human erythrocytes. **Life Sci,** v. 71, n. 4, p. 469-482, 2002.

HSIEH, C.-L.; YEN, G.-C.; CHEN, H.-Y. Antioxidant Activities of Phenolic Acids on Ultraviolet Radiation-Induced Erythrocyte and Low Density Lipoprotein Oxidation. **J Agric Food Chem,** v. 53, n. 15, p. 6151-6155, 2005.

HU, Y.; LITWIN, T.; NAGARAJA, A. R.; KWONG, B.; KATZ, J.; WATSON, N.; IRVINE, D. J. Cytosolic delivery of membrane-impermeable molecules in dendritic cells using pH-responsive core-shell nanoparticles. **Nano Lett,** v. 7, n. 10, p. 3056-3064, 2007.

HURLER, J.; ENGESLAND, A.; POORAHMARY KERMANY, B.; ŠKALKO-BASNET, N. Improved texture analysis for hydrogel characterization: Gel cohesiveness, adhesiveness, and hardness. **J Appl Polym Sci,** v. 125, n. 1, p. 180-188, 2012.

ICH. Guideline Stability Testing: Photostability Testing of New Drug Substances and Products. **Q1B, Current Step,** v. 4, 1996.

ICH. International Conference on Harmonization of Technical Requeriments for Registration of Pharmaceuticals for Human Use, Validation of Analytical Procedures: Text and Methodology. Geneva, Switzerland 2005.

ISMAIL, T.; SESTILI, P.; AKHTAR, S. Pomegranate peel and fruit extracts: A review of potential anti-inflammatory and anti-infective effects. **J Ethnopharmacol,** v. 143, n. 2, p. 397-405, 2012.

JAHFAR, M.; VIJAYAN, K. K.; AZADI, P. Studies on a polysaccharide from the fruit rind of Punica granatum. **Res J Chem Environ,** v. 7, p. 43-50, 2003.

JARZYCKA, A.; LEWINSKA, A.; GANCARZ, R.; WILK, K. A. Assessment of extracts of Helichrysum arenarium, Crataegus monogyna, Sambucus nigra in photoprotective UVA and UVB; photostability in cosmetic emulsions. **J Photochem Photobiol B,** v. 128, p. 50-57, 2013.

JONES, D. S.; LAWLOR, M. S.; WOOLFSON, A. D. Examination of the flow rheological and textural properties of polymer gels composed of poly(methylvinylether-co-maleic anhydride) and poly(vinylpyrrolidone): Rheological and mathematical interpretation of textural parameters. **J Pharm Sci,** v. 91, n. 9, p. 2090-2101, 2002.

JONES, D. S.; WOOLFSON, A. D.; BROWN, A. F. Textural, viscoelastic and mucoadhesive properties of pharmaceutical gels composed of cellulose polymers. **Int J Pharm,** v. 151, n. 2, p. 223-233, 1997.

JONES, D. S.; WOOLFSON, A. D.; DJOKIC, J. Texture profile analysis of bioadhesive polymeric semisolids: Mechanical characterization and investigation of interactions between formulation components. **J Appl Polym Sci,** v. 61, n. 12, p. 2229-2234, 1996.

JUNYAPRASERT, V. B.; SINGHSA, P.; JINTAPATTANAKIT, A. Influence of chemical penetration enhancers on skin permeability of ellagic acid-loaded niosomes. **Asian J Pharm Sci,** v. 8, n. 2, p. 110-117, 2013.

JURENKA, J. Therapeutic applications of pomegranate (Punica granatum L.): a review. **Altern Med Rev,** v. 13, n. 2, p. 128-144, 2008.

JURKIEWICZ, B. A.; BUETTNERF, G. R. EPR Detection of free radicals in UV-irradiated skin: mouse versus human. **Photochem Photobiol,** v. 64, n. 6, p. 918-922, 1996.

KAGAN, V. E.; SERBINOVA, E. A.; BAKALOVA, R. A.; STOYTCHEV, T. S.; ERIN, A. N.; PRILIPKO, L. L.; EVSTIGNEEVA, R. P. Mechanisms of stabilization of biomembranes by alpha-tocopherol. The role of the hydrocarbon chain in the inhibition of lipid peroxidation. **Biochem Pharmacol,** v. 40, n. 11, p. 2403-2413, 1990.

KASAI, K.; YOSHIMURA, M.; KOGA, T.; ARII, M.; KAWASAKI, S. Effects of oral administration of ellagic acid-rich pomegranate extract on ultraviolet-induced pigmentation in the human skin. **J Nutr Sci Vitaminol,** v. 52, n. 5, p. 383-388, 2006.

KATZ, S. R.; NEWMAN, R. A.; LANSKY, E. P. Punica granatum: heuristic treatment for diabetes mellitus. **J Med Food,** v. 10, n. 2, p. 213-217, 2007.

KAUR, C. D.; SARAF, S. Photochemoprotective activity of alcoholic extract of *Camellia sinensis*. **Int J Pharmacol,** v. 7, n. 3, p. 400-404, 2011.

KAUR, C. D.; SARAF, S. Development of photoprotective creams with antioxidant polyphenolic herbal extracts. **Res J Med Plant,** v. 6, p. 83-91, 2012a.

KAUR, C. D.; SARAF, S. Photoprotective herbal extract loaded nanovesicular creams inhibiting ultraviolet radiations induced photoaging. **Int J Drug Delivery,** v. 3, n. 4, p. 699-711, 2012b.

KAY, M. M.; BOSMAN, G. J.; SHAPIRO, S. S.; BENDICH, A.; BASSEL, P. S. Oxidation as a possible mechanism of cellular aging: vitamin E deficiency causes premature aging and IgG binding to erythrocytes. **Proc Natl Acad Sci,** v. 83, n. 8, p. 2463-2467, 1986.

KENTISH, S.; WOOSTER, T. J.; ASHOKKUMAR, M.; BALACHANDRAN, S.; MAWSON, R.; SIMONS, L. The use of ultrasonics for nanoemulsion preparation. **Innov Food Sci Emerg Technol,** v. 9, n. 2, p. 170-175, 2008.

KHACHANE, P. V.; JAIN, A. S.; DHAWAN, V. V.; JOSHI, G. V.; DATE, A. A.; MULHERKAR, R.; NAGARSENKER, M. S. Cationic nanoemulsions as potential carriers for intracellular delivery. **Saudi Pharm J,** v. 23, p. 188-194, 2015.

KLOUDA, L.; MIKOS, A. G. Thermoresponsive hydrogels in biomedical applications. **Eur J Pharm Biopharm,** v. 68, n. 1, p. 34-45, 2008.

KOGAN, A.; GARTI, N. Microemulsions as transdermal drug delivery vehicles. **Adv Colloid Interface Sci,** v. 123–126, n. 0, p. 369-385, 2006.

KOMAIKO, J.; MCCLEMENTS, D. J. Low-energy formation of edible nanoemulsions by spontaneous emulsification: Factors influencing particle size. **J Food Eng,** v. 146, n. 0, p. 122-128, 2015.

KONDO, S.; KONO, T.; SAUDER, D. N.; MCKENZIE, R. C. IL-8 gene expression and production in human keratinocytes and their modulation by UVB. **J Invest Dermatol,** v. 101, n. 5, p. 690-694, 1993.

KONG, M.; CHEN, X. G.; KWEON, D. K.; PARK, H. J. Investigations on skin permeation of hyaluronic acid based nanoemulsion as transdermal carrier. **Carbohydr Polym,** v. 86, n. 2, p. 837-843, 2011.

KREILGAARD, M. Influence of microemulsions on cutaneous drug delivery. **Adv Drug Delivery Rev,** v. 54, Supplement, n. 0, p. S77-S98, 2002.

LADEMANN, J.; JACOBI, U.; SURBER, C.; WEIGMANN, H. J.; FLUHR, J. W. The tape stripping procedure – evaluation of some critical parameters. **Eur J Pharm Biopharm,** v. 72, n. 2, p. 317-323, 2009.

LAMBERS, H.; PIESSENS, S.; BLOEM, A.; PRONK, H.; FINKEL, P. Natural skin surface pH is on average below 5, which is beneficial for its resident flora. **Int J Cosmet Sci,** v. 28, n. 5, p. 359-370, 2006.

LAN, J.; LEI, F.; HUA, L.; WANG, Y.; XING, D.; DU, L. Transport behavior of ellagic acid of pomegranate leaf tannins and its correlation with total cholesterol alteration in HepG2 cells. **Biomed Chromatogr,** v. 23, n. 5, p. 531-536, 2009.

LANDETE, J. M. Ellagitannins, ellagic acid and their derived metabolites: A review about source, metabolism, functions and health. **Food Res Int,** v. 44, n. 5, p. 1150-1160, 2011.

LANE, M. E. Skin penetration enhancers. **Int J Pharm,** v. 447, n. 1–2, p. 12-21, 2013.

LANSKY, E.; SHUBERT, S.; NEEMAN, I. Pharmacological and therapeutic properties of pomegranate. **Serie A. Séminaires Méditerranées,** v. 42, p. 231-235, 2000.

LANSKY, E. P.; NEWMAN, R. A. Punica granatum (pomegranate) and its potential for prevention and treatment of inflammation and cancer. **J Ethnopharmacol,** v. 109, n. 2, p. 177-206, 2007.

LARROSA, M.; GARCÍA-CONESA, M. T.; ESPÍN, J. C.; TOMÁS-BARBERÁN, F. A. Ellagitannins, ellagic acid and vascular health. **Mol Aspects Med,** v. 31, n. 6, p. 513-539, 2010.

LAWRENCE, G. H. Taxonomy of vascular plants. **New york,** v. 9, p. 628-629, 1951.

LEE, C. J.; CHEN, L. G.; LIANG, W. L.; WANGA, C. C. Anti-inflammatory effects of Punica granatum Linne in vitro and in vivo. **Food Chem,** v. 118, p. 315-322, 2010.

LEELAPORNPISID, P.; KIATTISIN, K.; JANTRAWUT, P.; PHRUTIVORAPONGKUL, A. Nanoemulsion loaded with marigold flower extract (Tagetes erecta Linn) in gel preparations as anti-wrinkles cosmeceutical. **Int J Pharm Pharm Sci,** v. 6, n. 2, p. 231-236, 2014.

LI, Y.; GUO, C.; YANG, J.; WEI, J.; XU, J.; CHENG, S. Evaluation of antioxidant properties of pomegranate peel extract in comparison with pomegranate pulp extract. **Food Chem,** v. 96, n. 2, p. 254-260, 2006.

LI, Z.; GU, L. Effects of mass ratio, pH, temperature, and reaction time on fabrication of partially purified pomegranate ellagitannin−gelatin nanoparticles. **J Agric Food Chem,** v. 59, n. 8, p. 4225-4231, 2011.

LIAO, K.-L.; YIN, M.-C. Individual and combined antioxidant effects of seven phenolic agents in human erythrocyte membrane ghosts and phosphatidylcholine liposome systems: Importance of the partition coefficient. **J Agric Food Chem,** v. 48, n. 6, p. 2266-2270, 2000.

LIEBERMAN, H. A.; RIEGER, M. M.; BANKER, G. S. **Pharmaceutical Dosage Forms: Disperse Systems**. New York, NY, USA: Marcel Dekker, 1989. 427-455

LIM H. W., G.; WORTIS, M.; MUKHOPADHYAY, R. Stomatocyte–discocyte–echinocyte sequence of the human red blood cell: Evidence for the bilayer– couple hypothesis from membrane mechanics. **Proc Natl Acad Sci U. S. A.,** v. 99, n. 26, p. 16766-16769, 2002.

LIU, X.; KRUGER, P.; MAIBACH, H.; COLDITZ, P. B.; ROBERTS, M. S. Using skin for drug delivery and diagnosis in the critically ill. **Adv Drug Delivery Rev,** v. 77, n. 20, p. 40-49, 2014.

LU, J.; DING, K.; YUAN, Q. Determination of punicalagin isomers in pomegranate husk. **Chromatographia,** v. 68, n. 3-4, p. 303-306, 2008.
LUO, X. D.; BASILE, M. J.; KENNELLY, E. J. Polyphenolic antioxidants from the fruits of Chrysophyllum cainito L. (Star Apple). **J Agric Food Chem,** v. 50, n. 6, p. 1379-1382, 2002.

MAA, Y.-F.; HSU, C. C. Performance of Sonication and microfluidization for liquid–liquid emulsification. **Pharm Dev Technol,** v. 4, n. 2, p. 233-240, 1999.

MADARIAGA, Y. G.; CÁRDENAS, M. B.; TOLEDO, D. B.; ALFONSO, O. C.; MONTALBÁN, C. M. M.; BERNAL, Y. M. In vitro photohemolitic assessment of Cissus sicyoides L. and Achyranthes aspera. **Rev Cubana Plant Med,** v. 15, n. 3, p. 126-132, 2010.

MAGALHÃES, A. S.; SILVA, B. M.; PEREIRA, J. A.; ANDRADE, P. B.; VALENTÃO, P.; CARVALHO, M. Protective effect of quince (Cydonia oblonga Miller) fruit against oxidative hemolysis of human erythrocytes. **Food Chem Toxicol,** v. 47, n. 6, p. 1372-1377, 2009.

MAGDOLENOVA, Z.; COLLINS, A.; KUMAR, A.; DHAWAN, A.; STONE, V.; DUSINSKA, M. Mechanisms of genotoxicity. A review of in vitro and in vivo studies with engineered nanoparticles. **Nanotoxicology,** v. 8, n. 3, p. 233-278, 2014.

MAGHRABY, G. M.; BARRY, B. W.; WILLIAMS, A. C. Liposomes and skin:From drug delivery to model membranes. **Eur J Pharm Sci,** v. 34, p. 203-222, 2008.

MAHARLOOEI, M. K.; MOHAMMADI, A. A.; FARSI, A.; AHRARI, I.; ATTAR, A.; MONABATI, A. A comparison between different

existing methods used to separate epidermal cells from skin biopsies for autologous transplantation. **Indian J Dermatol,** v. 56, n. 6, p. 666-669, 2011.

MAHDI, E. S.; NOOR, A. M.; SAKEENA, M. H.; ABDULLAH, G. Z.; ABDULKARIM, M. F.; SATTAR, M. A. Formulation and in vitro release evaluation of newly synthesized palm kernel oil esters-based nanoemulsion delivery system for 30% ethanolic dried extract derived from local Phyllanthus urinaria for skin antiaging. **Int J Nanomed,** v. 6, p. 2499-2512, 2011.

MAIORANO, G.; SABELLA, S.; SORCE, B.; BRUNETTI, V.; MALVINDI, M. A.; CINGOLANI, R.; POMPA, P. P. Effects of cell culture media on the dynamic formation of protein−nanoparticle complexes and influence on the cellular response. **ACS Nano,** v. 4, n. 12, p. 7481-7491, 2010.

MALIK, A.; AFAQ, F.; SARFARAZ, S.; ADHAMI, V. M.; SYED, D. N.; MUKHTAR, H. Pomegranate fruit juice for chemoprevention and chemotherapy of prostate cancer. **Proc Natl Acad Sci U. S. A,** v. 102, n. 41, p. 14813-14818, 2005.

MANASATHIEN, J.; INDRAPICHATE, K.; INTARAPICHET, K.-O. Antioxidant activity and bioefficacy of pomegranate Punica granatum Linn. peel and seed extracts. **Global J Pharmacol,** v. 6, n. 2, p. 131-141, 2012.

MANASATHIEN, J.; KUPITTAYANANT, S.; INDRAPICHATE, K. Protective efficacy of pomegranate (Punica granatum Linn., Punicaceae) peel ethanolic extracts on UVB-irradiated rat skin. **American-Eurasian Journal of Toxicology Sciences 3,** v. 4, p. 250-258, 2011.

MANOSROI, A.; JANTRAWUT, P.; AKAZAWA, H.; AKIHISA, T.; MANOSROI, W.; MANOSROI, J. Transdermal absorption enhancement of gel containing elastic niosomes loaded with gallic acid from Terminalia chebula galls. **Pharm Biol,** v. 49, n. 6, p. 553-562, 2011.

MANSUR, J. D. S.; BREDER, M. N. R.; MANSUR, M. C. D. A.; AZULAY, R. D. Correlação entre a determinação do fator de proteção

solar em seres humanos e por espectrofotometria. **An Bras Dermatol,** v. 61, n. 4, p. 167-72, 1986.

MARCZAK, A. Fluorescence anisotropy of membrane fluidity probes in human erythrocytes incubated with anthracyclines and glutaraldehyde. **Bioelectrochemistry,** v. 74, n. 2, p. 236-239, 2009.
MARTI-MESTRES, G.; MESTRES, J. P.; BRES, J.; MARTIN, S.; RAMOS, J.; VIAN, L. The "in vitro" percutaneous penetration of three antioxidant compounds. **Int J Pharm,** v. 331, n. 1, p. 139-144, 2007.

MARTÍNEZ, V.; UGARTONDO, V.; VINARDELL, M. P.; TORRES, J. L.; MITJANS, M. Grape epicatechin conjugates prevent erythrocyte membrane protein oxidation. **J Agric Food Chem,** v. 60, p. 4090-4095, 2012.

MASON, T. G.; WILKING, J. N.; MELESON, K.; CHANG, C. B.; GRAVES, S. M. Nanoemulsions: formation, structure, and physical properties. **J Phys Condens Matter,** v. 18, n. 41, p. R635, 2006.

MEERTS, I. A. T. M.; VERSPEEK-RIP, C. M.; BUSKENS, C. A. F.; KEIZER, H. G.; BASSAGANYA-RIERA, J.; JOUNI, Z. E.; VAN HUYGEVOORT, A. H. B. M.; VAN OTTERDIJK, F. M.; VAN DE WAART, E. J. Toxicological evaluation of pomegranate seed oil. **Food Chem Toxicol,** v. 47, n. 6, p. 1085-1092, 2009.

MEGWA, S. A.; CROSS, S. E.; BENSON, H. A. E.; ROBERTS, M. S. Ion-pair formation as a strategy to enhance topical delivery of salicylic acid. **J Pharm Pharmacol,** v. 52, n. 8, p. 919-928, 2000.

MEHNERT, W.; MADER, K. Solid lipid nanoparticles: Production, characterization and applications. **Adv Drug Delivery Rev,** v. 47, n. 2-3, p. 165-196, 2001.

MELO, I. L. P.; CARVALHO, E. B. T.; MANCINI-FILHO, J. Pomegranate seed oil (Punica granatum L.): A source of punicic acid (conjugated alpha-linolenic-acid). **Plant Foods Hum Nutr,** v. 2, n. 1, p. 1024, 2014.

MENON, G. K. New insights into skin structure: scratching the surface. **Adv Drug Delivery Rev,** v. 54, p. 3-17, 2002.

MIKI, M.; TAMAI, H.; MINO, M.; YAMAMOTO, Y.; NIKI, E. Free-radical chain oxidation of rat red blood cells by molecular oxygen and its inhibition by α-tocopherol. **Arch Biochem Biophys,** v. 258, n. 2, p. 373-380, 1987.

MILLER, R.; FAINERMAN, V. B.; MAKIEVSKI, A. V.; KRÄGEL, J.; GRIGORIEV, D. O.; KAZAKOV, V. N.; SINYACHENKO, O. V. Dynamics of protein and mixed protein/surfactant adsorption layers at the water/fluid interface. **Adv Colloid Interface Sci,** v. 86, n. 1–2, p. 39-82, 2000.

MIRDEHGHAN, S. H.; RAHEMI, M. Seasonal changes of mineral nutrients and phenolics in pomegranate (Punica granatum L.) fruit. **Sci Hortic,** v. 111, n. 2, p. 120-127, 2007.

MISHRA, A.; RAM, S.; GHOSH, G. Dynamic light scattering and optical absorption in biological nanofluids of gold nanoparticles in poly(vinyl pyrrolidone) molecules. **J Phys Chem C,** v. 113, n. 17, p. 6976-6982, 2009.

MITRI, K.; SHEGOKAR, R.; GOHLA, S.; ANSELMI, C.; MÜLLER, R. H. Lipid nanocarriers for dermal delivery of lutein: preparation, characterization, stability and performance. **Int J Pharm,** v. 414, n. 1, p. 267-275, 2011.

MIZRAHI, M.; FRIEDMAN-LEVI, Y.; LARUSH, L.; FRID, K.; BINYAMIN, O.; DORI, D.; FAINSTEIN, N.; OVADIA, H.; BEN-HUR, T.; MAGDASSI, S.; GABIZON, R. Pomegranate seed oil nanoemulsions for the prevention and treatment of neurodegenerative diseases: the case of genetic CJD. **Nanomed-Nanotechnol,** v. 10, n. 6, p. 1353-1363, 2014.

MO, J.; KAEWNOPPARAT, N.; SONGKRO, S.; PANICHAYUPAKARANANT, P.; REANMONGKOL, W. Physicochemical properties, in vitro release and skin permeation studies of a topical formulation of standardized pomegranate rind extract. **Pak J Pharm Sci,** v. 28, n. 1, p. 29-36, 2015.

MOHAGHEGHI, M.; REZAEI, K.; LABBAFI, M.; EBRAHIMZADEH MOUSAVI, S. M. Pomegranate seed oil as a functional ingredient in beverages. **Eur J Lipid Sci Technol,** v. 113, n. 6, p. 730-736, 2011.

MONTENEGRO, L.; CARBONE, C.; PUGLISI, G. Vehicle effects on in vitro release and skin permeation of octylmethoxycinnamate from microemulsions. **Int J Pharm,** v. 405, n. 1–2, p. 162-168, 2011.

MORTON, J. F. Pomegranate, Punica granatum L. In: MORTON, J. F. (Ed.). **Fruits of Warm Climates**. Miami: Purdue New Crops Profile, 1987. p.352-355.

MOSER, K.; KRIWET, K.; NAIK, A.; KALIA, Y. N.; GUY, R. H. Passive skin penetration enhancement and its quantification in vitro. **Eur J Pharm Biopharm,** v. 52, n. 2, p. 103-112, 2001.
MOSMANN, T. Rapid colorimetric assay to cellular growth and survival:application to proliferation and cytotoxicity assays. **J Immunol Methods,** v. 65, p. 55-63, 1983.

MOTA, A. C. V.; FREITAS, Z. M. F.; RICCI JÚNIOR, E.; DELLAMORA-ORTIZ, G. M.; SANTOS-OLIVEIRA, R.; OZZETTI, R. A.; VERGNANINI, A. L.; RIBEIRO, V. L.; SILVA, R. S.; SANTOS, E. P. In vivo and in vitro evaluation of octyl methoxycinnamate liposomes. **Int J Nanomed,** v. 8, p. 4689-4701, 2013.

MOU, D.; CHEN, H.; DU, D.; MAO, C.; WAN, J.; XU, H.; YANG, X. Hydrogel-thickened nanoemulsion system for topical delivery of lipophilic drugs. **Int J Pharm,** v. 353, n. 1–2, p. 270-276, 2008.

MOUSAVINEJAD, G.; EMAM-DJOMEH, Z.; REZAEI, K.; KHODAPARAST, M. H. H. Identification and quantification of phenolic compounds and their effects on antioxidant activity in pomegranate juices of eight Iranian cultivars. **Food Chem,** v. 115, p. 1274-1278, 2009.

NAQVI, S. A.; KHAN, M. S.; VOHORA, S. B. Antibacterial, antifungal, and antihelminthic investigations on Indian medicinal plants. **Fitoterapia,** v. 62, p. 221-228, 1991.

NAZ, S.; SIDDIQI, R.; AHMAD, S.; RASOOL, S. A.; SAYEED, S. A. Antibacterial activity directed isolation of compounds from Punica granatum. **J Food Sci,** v. 72, n. 9, p. M341-M345, 2007.

NEGI, P. S.; JAYAPRAKASHA, G. K. Antioxidant and antibacterial activities of Punica granatum peel extracts. **J Food Sci,** v. 68, n. 4, p. 1473-1477, 2003.

NEGI, P. S.; JAYAPRAKASHA, G. K.; JENA, B. S. Antioxidant and antimutagenic activities of pomegranate peel extracts. **Food Chem,** v. 80, n. 3, p. 393-397, 2003.

NEMEN, D.; LEMOS-SENNA, E. Preparação e caracterização de suspensões coloidais de nanocarreadores lipídicos contendo resveratrol destinados à administração cutânea. **Quim Nova,** v. 34, n. 3, p. 408-413, 2011.

NEUHOFER, H.; WITTE, L.; GORUNOVIC, M.; CZYGAN, F. C. Alkaloids in the bark of Punica granatum L. (pomegranate) from Yugoslavia. **Pharmazie,** v. 48, p. 398-391, 1993.

NEYRINCK, A. M.; VAN HÉE, V. F.; BINDELS, L. B.; DE BACKER, F.; CANI, P. D.; DELZENNE, N. M. Polyphenol-rich extract of pomegranate peel alleviates tissue inflammation and hypercholesterolaemia in high-fat diet-induced obese mice: potential implication of the gut microbiota. **Br J Nutr,** v. 109, n. 05, p. 802-809, 2013.

NGUYEN, M.-H.; HWANG, I.-C.; PARK, H.-J. Enhanced photoprotection for photo-labile compounds using double-layer coated corn oil-nanoemulsions with chitosan and lignosulfonate. **J Photochem Photobiol B,** v. 125, n. 0, p. 194-201, 2013.

NICHOLS, J.; KATIYAR, S. Skin photoprotection by natural polyphenols: anti-inflammatory, antioxidant and DNA repair mechanisms. **Arch Dermatol Res,** v. 302, n. 2, p. 71-83, 2010.

NOGUEIRA, D.; MITJANS, M.; MORÁN, M. C.; PÉREZ, L.; VINARDELL, M. P. Membrane-destabilizing activity of pH-responsive cationic lysine-based surfactants: role of charge position and alkyl chain length. **Amino Acids,** v. 43, n. 3, p. 1203-1215, 2012.

NOGUEIRA, D. R.; CARMEN MORÁN, M. D.; MITJANS, M.; PÉREZ, L.; RAMOS, D.; LAPUENTE, J. D.; PILAR VINARDELL, M. Lysine-based surfactants in nanovesicle formulations: the role of

cationic charge position and hydrophobicity in in vitro cytotoxicity and intracellular delivery. **Nanotoxicology,** v. 8, n. 4, p. 404-421, 2014.

NOGUEIRA, D. R.; MITJANS, M.; BUSQUETS, M. A.; PÉREZ, L.; VINARDELL, M. P. Phospholipid bilayer-perturbing properties underlying lysis induced by pH-sensitive cationic lysine-based surfactants in biomembranes. **Langmuir,** v. 28, n. 32, 2012.
OECD. OECD Guidelines for the Testing of Chemicals Test No. 432: In Vitro 3T3 NRU Phototoxicity Test. 2004.

OLIVEIRA, E. M. M.; LIMA, I. S.; CARNEIRO, B. T.; NOGUEIRA, R. I.; FREITAS-SILVA, O. **Aplicabilidade da técnica PCR-RAPD para a determinação do perfil genotípico de variedades de romã (*Punica granatum*)**. II Congresso Brasileiro de Recursos Genéticos. Belém**:** 1-5 p. 2012.

ONOUE, S.; SETO, Y.; GANDY, G.; YAMADA, S. Drug-induced phototoxicity; an early in vitro identification of phototoxic potential of new drug entities in drug discovery and development. **Curr Drug Saf,** v. 4, n. 2, p. 123-136, 2009.

PACHECO-PALENCIA, L. A.; NORATTO, G.; HINGORANI, L.; TALCOTT, S. T.; MERTENS-TALCOTT, S. U. Protective effects of standardized pomegranate (Punica granatum L.) polyphenolic extract in ultraviolet-irradiated human skin fibroblasts. **J Agric Food Chem,** v. 56, n. 18, p. 8434-8441, 2008.

PAILLER-MATTEI, C.; GUERRET-PIÉCOURT, C.; ZAHOUANI, H.; NICOLI, S. Interpretation of the human skin biotribological behaviour after tape stripping. **J R Soc Interface,** v. 8, n. 60, p. 934-941, 2011.
PANICHAYUPAKARANANT, P.; ITSURIYA, A.; SIRIKATITHAM, A. Preparation method and stability of ellagic acid-rich pomegranate fruit peel extract. **Pharm Biol,** v. 48, n. 2, p. 201-205, 2010.

PAPE, W. J. W.; HOPPE, U. In vitro methods for the assessment of primary local effects of topically applied preparations. **Skin Pharmacol,** v. 4, n. 3, p. 205-212, 1991.

PAPE, W. J. W.; MAURER, T.; PFANNENBECKER, U.; STEILING, W. The red blood cell phototoxicity test (photohaemolysis and

haemoglobin oxidation): EU/COLIPA validation programme on phototoxicity (phase II). **ATLA, Altern. Lab. Anim.,** v. 29, n. 2, p. 145-162, 2001.

PAPE, W. J. W.; PFANNENBECKER, U.; HOPPE, U. Validation of the red blood cell system as in vitro assay for rapid screening of irritation potential of surfactants. **Mol Toxicol,** v. 1, n. 4, p. 525-536, 1987.

PARDEIKE, J.; HOMMOSS, A.; MÜLLER, R. H. Lipid nanoparticles (SLN, NLC) in cosmetic and pharmaceutical dermal products. **Int J Pharm,** v. 366, n. 1–2, p. 170-184, 2009.

PASTORE, S.; LULLI, D.; FIDANZA, P.; POTAPOVICH, A. I.; KOSTYUK, V. A.; DE LUCA, C.; MIKHAL'CHIK, E.; KORKINA, L. G. Plant polyphenols regulate chemokine expression and tissue repair in human keratinocytes through interaction with cytoplasmic and nuclear components of epidermal growth factor receptor system. **Antioxid Redox Signaling,** v. 16, n. 4, p. 314-328, 2012.

PATTISON, D.; DAVIES, M. Actions of ultraviolet light on cellular structures. In: (Ed.). **Cancer: Cell Structures, Carcinogens and Genomic Instability**: Birkhäuser Basel, v.96, 2006. cap. 6, p.131-157. (Experientia Supplementum). ISBN 978-3-7643-7156-2.

PELLE, E.; HUANG, X.; MAMMONE, T.; MARENUS, K.; MAES, D.; FRENKEL, K. Ultraviolet-B-induced oxidative DNA base damage in primary normal human epidermal keratinocytes and inhibition by a hydroxyl radical scavenger. **J Investig Dermatol,** v. 121, n. 1, p. 177-183, 2003.

PEPPAS, N. A.; BURES, P.; LEOBANDUNG, W.; ICHIKAWA, H. Hydrogels in pharmaceutical formulations. **Eur J Pharm Biopharm,** v. 50, n. 1, p. 27-46, 2000.

PERDE-SCHREPLER, M.; CHERECHES, G.; BRIE, I.; TATOMIR, C.; POSTESCU, I. D.; SORAN, L.; FILIP, A. Grape seed extract as photochemopreventive agent against UVB-induced skin cancer. **J Photochem Photobiol B,** v. 118, n. 0, p. 16-21, 2013.

POPLE, P. V.; SINGH, K. K. Targeting tacrolimus to deeper layers of skin with improved safety for treatment of atopic dermatitis. **Int J Pharm,** v. 398, n. 1–2, p. 165-178, 2010.

POTTS, R.; GUY, R. Predicting skin permeability. **Pharm Res,** v. 9, n. 5, p. 663-669, 1992.

PRETE, A. C. L.; MARIA, D. A.; RODRIGUES, D. B. G.; VALDUGA, C. J.; IBAÑEZ, O. C. M.; MARANHÃO, R. C. Evaluation in melanoma-bearing mice of an etoposide derivative associated to a cholesterol-rich nanoemulsion. **J Pharm Pharmacol,** v. 58, n. 6, p. 801-808, 2006.

PROW, T. W.; GRICE, J. E.; LIN, L. L.; FAYE, R.; BUTLER, M.; BECKER, W.; WURM, E. M. T.; YOONG, C.; ROBERTSON, T. A.; SOYER, H. P.; ROBERTS, M. S. Nanoparticles and microparticles for skin drug delivery. **Adv Drug Delivery Rev,** v. 63, n. 6, p. 470-491, 2011.

PUGLIA, C.; DAMIANI, E.; OFFERTA, A.; RIZZA, L.; TIRENDI, G. G.; TARICO, M. S.; CURRERI, S.; BONINA, F.; PERROTTA, R. E. Evaluation of nanostructured lipid carriers (NLC) and nanoemulsions as carriers for UV-filters: Characterization, in vitro penetration and photostability studies. **Eur J Pharm Sci,** v. 51, n. 0, p. 211-217, 2014.

PUND, S.; PAWAR, S.; GANGURDE, S.; DIVATE, D. Transcutaneous delivery of leflunomide nanoemulgel: Mechanistic investigation into physicomechanical characteristics, in vitro anti-psoriatic and anti-melanoma activity. **Int J Pharm,** v. 487, n. 1–2, p. 148-156, 2015.

QU, W.; BREKSA, A. P.; PAN, Z.; MA, H. Quantitative determination of major polyphenol constituents in pomegranate products. **Food Chem,** v. 132, n. 3, p. 1585-1591, 2012.

QU, W.; PAN, Z.; MA, H. Extraction modeling and activities of antioxidants from pomegranate marc. **J Food Eng,** v. 99, n. 1, p. 16-23, 2010.

QUIDEAU, S.; FELDMAN, K. S. Ellagitannin chemistry. **Chemical Reviews,** v. 96, n. 1, p. 475-504, 1996.

RAHIMI, H. R.; ARASTOO, M.; OSTAD, S. N. A Comprehensive review of Punica granatum (Pomegranate) properties in toxicological, pharmacological, cellular and molecular biology researches. **Iran J Pharm Res,** v. 11, n. 2, p. 385-400, Spring 2012.

RATZ-ŁYKO, A.; ARCT, J.; MAJEWSKI, S.; PYTKOWSKA, K. Influence of polyphenols on the physiological processes in the skin. **Phytother Res,** v. 29, n. 4, p. 509-517, 2015.

RAVANAT, J.-L.; DOUKI, T.; CADET, J. Direct and indirect effects of UV radiation on DNA and its components. **J Photochem Photobiol B,** v. 63, n. 1–3, p. 88-102, 2001.

REITER, R. J.; MAESTRONI, G. J. Melatonin in relation to the antioxidative defense and immune systems: possible implications for cell and organ transplantation. **J Mol Med,** v. 77, n. 1, p. 36-39, 1999.

RIVERA GIL, P.; OBERDÖRSTER, G.; ELDER, A.; PUNTES, V.; PARAK, W. J. Correlating physico-chemical with toxicological properties of nanoparticles: The present and the future. **ACS Nano,** v. 4, n. 10, p. 5527-5531, 2010.

ROLAND, I.; PIEL, G.; DELATTRE, L.; EVRARD, B. Systematic characterization of oil-in-water emulsions for formulation design. **Int J Pharm,** v. 263, n. 1–2, p. 85-94, 2003.

ROVER JÚNIOR, L.; HÖEHR, N. F.; VELLASCO, A. P.; KUBOTA, L. T. Sistema antioxidante envolvendo o ciclo metabólico da glutationa associado a métodos eletroanalíticos na avaliação do estresse oxidativo. **Quim Nova,** v. 24, p. 112-119, 2001.

RUDRA, P.; SHRESTHA, S.; GULAM, M.; JAVED, A.; SANJULA, B. Vitamin E loaded resveratrol nanoemulsion for brain targeting for the treatment of Parkinson's disease by reducing oxidative stress. **Nanotechnology,** v. 25, n. 48, p. 485102, 2014.

RUEL-GARIÉPY, E.; LEROUX, J.-C. In situ-forming hydrogels—review of temperature-sensitive systems. **Eur J Pharm Biopharm,** v. 58, n. 2, p. 409-426, 2004.

RÜNGER, T. M. Role of UVA in the pathogenesis of melanoma and non-melanoma skin cancer: A short review. **Photodermatol Photoimmunol Photomed,** v. 15, n. 6, p. 212-216, 1999.

SABBIONI, E.; FORTANER, S.; FARINA, M.; DEL TORCHIO, R.; PETRARCA, C.; BERNARDINI, G.; MARIANI-COSTANTINI, R.; PERCONTI, S.; DI GIAMPAOLO, L.; GORNATI, R.; DI GIOACCHINO, M. Interaction with culture medium components, cellular uptake and intracellular distribution of cobalt nanoparticles, microparticles and ions in Balb/3T3 mouse fibroblasts. **Nanotoxicology,** v. 8, n. 1, p. 88-99, 2014.

SAIJA, A.; TOMAINO, A.; TROMBETTA, D.; DE PASQUALE, A.; UCCELLA, N.; BARBUZZI, T.; PAOLINO, D.; BONINA, F. In vitro and in vivo evaluation of caffeic and ferulic acids as topical photoprotective agents. **Int J Pharm,** v. 199, n. 1, p. 39-47, 2000.

SANDER, C. S.; CHANG, H.; SALZMANN, S.; MULLER, C. S. L.; EKANAYAKE-MUDIYANSELAGE, S.; ELSNER, P.; THIELE, J. J. Photoaging is associated with protein oxidation in human skin in vivo. **J Invest Dermatol,** v. 118, n. 4, p. 618-625, 2002.

SARAF, A. S. Applications of novel drug delivery system for herbal formulations. **Fitoterapia,** v. 81, p. 680-689, 2010.

SARAF, S.; GUPTA, D.; KAUR, C. D.; SARAF, S. Microneedles: from micromachining to transdermal drug delivery. **Int J Cur Biomed Phar Res,** v. 1, n. 2, p. 80-87, 2011.

SARKHOSH, A.; ZAMANI, Z.; FATAHI, R.; EBADI, A. RAPD markers reveal polymorphism among some Iranian pomegranate (Punica granatum L.) genotypes. **Sci Hortic,** v. 111, n. 1, p. 24-29, 2006.

SARTORELLI, P.; ANDERSEN, H. R.; ANGERER, J.; CORISH, J.; DREXLER, H.; GÖEN, T.; GRIFFIN, P.; HOTCHKISS, S. A. M.; LARESE, F.; MONTOMOLI, L.; PERKINS, J.; SCHMELZ, M.; VAN DE SANDT, J.; WILLIAMS, F. Percutaneous penetration studies for

risk assessment. **Environ Toxicol Pharmacol,** v. 8, n. 2, p. 133-152, 2000.

SAYRE, R. M.; AGIN, P. P.; LEVEE, G. J.; MARLOWE, E. A comparison of in vivo and in vitro testing of sunscreening formulas. **Photochem Photobiol,** v. 29, n. 3, p. 559-566, 1979.

SCHÄFER-KORTING, M.; MEHNERT, W.; KORTING, H. C. Lipid nanoparticles for improved topical application of drugs for skin diseases. **Adv Drug Delivery Rev,** v. 59, p. 427-443, 2007.

SCHMID, M. H.; KORTING, H. C. Liposomes for atopic dry skin: the rationale for a promising approach. **Clin Invest,** v. 71, n. 8, p. 649-653, 1993.

SCHOTHORST, A. A.; VAN STEVENINCK, J.; WENT, L. N.; SUURMOND, D. Photodynamic damage of the erythrocyte membrane caused by protoporphyrin in protoporphyria and in normal red blood cells. **Clin Chim Acta,** v. 39, p. 161-170, 1972.

SCHRAMM, L. L. In: (Ed.). **Emulsions, foams and suspensions: fundamentals and applications**. Germany: Wiley-VCH, 2005. p.4-5.

SCHUBERT, M. A.; MÜLLER-GOYMANN, C. C. Characterisation of surface-modified solid lipid nanoparticles (SLN): Influence of lecithin and nonionic emulsifier. **Eur J Pharm Biopharm,** v. 61, n. 1–2, p. 77-86, 2005.

SCHUBERT, S. Y.; LANSKY, E. P.; NEEMAN, I. Antioxidant and eicosanoid enzyme inhibition properties of pomegranate seed oil and fermented juice flavonoids. **J Ethnopharmacol,** v. 66, n. 1, p. 11-17, 1999.

SCHULMAN, J. H.; MCROBERTS, T. S. On the structure of transparent water and oil dispersions (solubilized oils). **Trans Faraday Soc,** v. 42, n. 165-170, 1946.

SEERAM, N. P.; ADAMS, L. S.; HENNING, S. M.; NIU, Y.; ZHANG, Y.; NAIR, M. G.; HEBER, D. In vitro antiproliferative, apoptotic and antioxidant activities of punicalagin, ellagic acid and a total

pomegranate tannin extract are enhanced in combination with other polyphenols as found in pomegranate juice. **J Nutr Biochem,** v. 16, n. 6, p. 360-367, 2005.

SERGEEV, P. V.; UKHINA, T. V.; SHIMANOVSKII, N. L. Effects of sex steroid hormones on lipid peroxidation and glutathione antioxidant system in rat skin. **Bull Exp Biol Med,** v. 128, n. 6, p. 1235-1238, 1999.

SESSA, M.; CASAZZA, A.; PEREGO, P.; TSAO, R.; FERRARI, G.; DONSÌ, F. Exploitation of polyphenolic extracts from grape marc as natural antioxidants by encapsulation in lipid-based nanodelivery systems. **Food Bioprocess Technol,** v. 6, n. 10, p. 2609-2620, 2013.

SETO, Y.; HOSOI, K.; TAKAGI, H.; NAKAMURA, K.; KOJIMA, H.; YAMADA, S.; ONOUE, S. Exploratory and regulatory assessments on photosafety of new drug entities. **Curr Drug Saf,** v. 7, n. 2, p. 140-148, 2012.

SHAH, P.; BHALODIA, D.; SHELAT, P. Nanoemulsion: A pharmaceutical review. **Syst Rev Pharm,** v. 1, n. 1, p. 24-32, 2012.
SHAH, V. P.; FLYNN, G. L.; YACOBI, A.; MAIBACH, H. I.; BON, C.; FLEISCHER, N. M.; FRANZ, T. J.; KAPLAN, S. A.; KAWAMOTO, J.; LESKO, L. J. Bioequivalence of topical dermatological dosage forms–methods of evaluation of bioequivalence. **Skin Pharmacol Physiol,** v. 11, n. 2, p. 117-124, 1998.

SHAKEEL, F.; BABOOTA, S.; AHUJA, A.; ALI, J.; AQIL, M.; SHAFIQ, S. Nanoemulsions as vehicles for transdermal delivery of aceclofenac. **AAPS PharmSciTech,** v. 8, n. 4, p. 191-199, 2007.

SHAKEEL, F.; BABOOTA, S.; AHUJA, A.; ALI, J.; SHAFIQ, S. Skin permeation mechanism and bioavailability enhancement of celecoxib from transdermally applied nanoemulsion. **J Nanobiotechnol,** v. 6, p. 8-8, 2008.

SHAKEEL, F.; SHAFIQ, S.; HAQ, N.; ALANAZI, F. K.; ALSARRA, I. A. Nanoemulsions as potential vehicles for transdermal and dermal delivery of hydrophobic compounds: an overview. **Expert Opin Drug Delivery,** v. 9, n. 8, p. 953-974, 2012.

SHEETZ, M. P.; SINGER, S. Biological membranes as bilayer couples. A molecular mechanism of drug-erythrocyte interactions. **Proc Natl Acad Sci U. S. A.,** v. 71, n. 11, p. 4457-4461, 1974.

SHIRODE, A. B.; BHARALI, D. J.; NALLANTHIGHAL, S.; COON, J. K.; MOUSA, S. A.; RELIENE, R. Nanoencapsulation of pomegranate bioactive compounds for breast cancer chemoprevention. **Int J Nanomed,** v. 10, p. 475-484, 2015.

SILVA, A. P. C.; NUNES, B. R.; DE OLIVEIRA, M. C.; KOESTER, L. S.; MAYORGA, P.; BASSANI, V. L.; TEIXEIRA, H. F. Development of topical nanoemulsions containing the isoflavone genistein. **Pharmazie,** v. 64, n. 1, p. 32-35, 2009.

SINGH, R. P.; CHIDAMBARA MURTHY, K. N.; JAYAPRAKASHA, G. K. Studies on the antioxidant activity of pomegranate (Punica granatum) peel and seed extracts using in vitro models. **J Agric Food Chem,** v. 50, n. 1, p. 81-86, 2002.

SLOAN, K. B.; WASDO, S. Designing for topical delivery: Prodrugs can make the difference. **Med Res Rev,** v. 23, n. 6, p. 763-793, 2003.

SNYDER, L. M.; FORTIER, N. L.; TRAINOR, J.; JACOBS, J.; LEB, L.; LUBIN, B.; CHIU, D.; SHOHET, S.; MOHANDAS, N. Effect of hydrogen peroxide exposure on normal human erythrocyte deformability, morphology, surface characteristics, and spectrin-hemoglobin cross-linking. **J Clin Invest,** v. 76, n. 5, p. 1971-1977, 1985.

SÖDERLIND, E.; KARLSSON, L. Haemolytic activity of maltopyranoside surfactants. **Eur J Pharm Biopharm,** v. 62, n. 3, p. 254-259, 2006.

SOLANS, C.; IZQUIERDO, P.; NOLLA, J.; AZEMAR, N.; GARCIA-CELMA, M. J. Nano-emulsions. **Curr Opin Colloid Interface Sci,** v. 10, n. 3–4, p. 102-110, 2005.

SONNEVILLE-AUBRUN, O.; SIMONNET, J. T.; L'ALLORET, F. Nanoemulsions: a new vehicle for skincare products. **Adv Colloid Interface Sci,** v. 108–109, n. 0, p. 145-149, 2004.

SOUSA, C. M. M.; ROCHA-SILVA, H.; VIEIRA-JR, G. M.; AYRES, M. C. C.; COSTA, C. L. S.; ARAÚJO, D. S.; CAVALCANTE, L. C. D.; BARROS, E. D. S.; ARAÚJO, P. B. M.; BRANDÃO, M. S.; CHAVES, M. H. Fenóis totais e atividade antioxidante de cinco plantas medicinais. **Quim Nova,** v. 30, n. 2, p. 351-355, 2007.

STOREY, A.; MCARDLE, F.; FRIEDMANN, P. S.; JACKSON, M. J.; RHODES, L. E. Eicosapentaenoic acid and docosahexaenoic acid reduce UVB- and TNF-[alpha]-induced IL-8 secretion in keratinocytes and UVB-induced IL-8 in fibroblasts. **J Investig Dermatol,** v. 124, n. 1, p. 248-255, 2004.

STRICKLAND, I.; RHODES, L. E.; FLANAGAN, B. F.; FRIEDMANN, P. S. TNF-alpha and IL-8 are upregulated in the epidermis of normal human skin after UVB exposure: Correlation with neutrophil accumulation and E-Selectin expression. **J Invest Dermatol,** v. 108, n. 5, p. 763-768, 1997.

SUTRADHAR KUMAR, B.; AMIN MD, L. Nanoemulsions: increasing possibilities in drug delivery. **Eur J Nanomed,** v. 5, n. 2, p. 97-110, 2013.

SVETINA, S.; KUZMAN, D.; WAUGH, R. E.; ZIHERL, P.; ŽEKŠ, B. The cooperative role of membrane skeleton and bilayer in the mechanical behaviour of red blood cells. **Bioelectrochemistry,** v. 62, n. 2, p. 107-113, 2004.

SVOBODOVÁ, A.; ZDAŘILOVÁ, A.; VOSTÁLOVÁ, J. Lonicera caerulea and Vaccinium myrtillus fruit polyphenols protect HaCaT keratinocytes against UVB-induced phototoxic stress and DNA damage. **J Dermatol Sci,** v. 56, n. 3, p. 196-204, 2009.

SYED, D. N.; AFAQ, F.; MUKHTAR, H. Pomegranate derived products for cancer chemoprevention. **Semin Cancer Biol,** v. 17, p. 377-385, 2007.

SYED, D. N.; MALIK, A.; HADI, N.; SARFARAZ, S.; AFAQ, F.; MUKHTAR, H. Photochemopreventive effect of pomegranate fruit extract on UVA-mediated activation of cellular pathways in normal

human epidermal keratinocytes. **Photochem Photobiol,** v. 82, n. 2, p. 398-405, 2006.

SZEBENI, J. Hemocompatibility testing for nanomedicines and biologicals: predictive assays for complement mediated infusion reactions. **Eur J Nanomed,** v. 4, p. 33-53, 2012.

TADROS, T.; IZQUIERDO, P.; ESQUENA, J.; SOLANS, C. Formation and stability of nano-emulsions. **Adv Colloid Interface Sci,** v. 108–109, n. 0, p. 303-318, 2004.

TAN, C. P.; NAKAJIMA, M. β-Carotene nanodispersions: preparation, characterization and stability evaluation. **Food Chem,** v. 92, n. 4, p. 661-671, 2005.

TANG, W.; BHUSHAN, B. Adhesion, friction and wear characterization of skin and skin cream using atomic force microscope. **Colloids Surf B,** v. 76, n. 1, p. 1-15, 2010.

TAYLOR, P. Ostwald ripening in emulsions. **Adv Colloid Interface Sci,** v. 75, n. 2, p. 107-163, 1998.

TAYLOR, P. Ostwald ripening in emulsions: estimation of solution thermodynamics of the disperse phase. **Adv Colloid Interface Sci,** v. 106, n. 1–3, p. 261-285, 2003.

TEIXEIRA DA SILVA, J. A.; RANA, T. S.; NARZARY, D.; VERMA, N.; MESHRAM, D. T.; RANADE, S. A. Pomegranate biology and biotechnology: A review. **Sci Hortic,** v. 160, p. 85-107, 2013.

THIELE, J. J.; TRABER, M. G.; PACKER, L. Depletion of human stratum corneum vitamin E: an early and sensitive in vivo marker of UV induced photo-oxidation. **J Invest Dermatol,** v. 110, n. 5, p. 756-761, 1998.

THRING, T. S. A.; HILI, P.; NAUGHTON, D. P. Anti-collagenase, anti-elastase and anti-oxidant activities of extracts from 21 plants. **BMC Complementary and Alternative Medicine,** v. 9, p. 27-27, 2009.

TOLEDO, D. B.; CÁRDENAS, M. B.; DÍAZ, A. V.; MONTALBÁN, C. M. M.; RODRIGUEZ, N. I. Evaluación fotohemolítica in vitro de Parthenium hysterophorus L. **Revista Científica Villa Clara,** v. 16, n. 1, p. 43-48, 2012.

TRONCOSO, E.; AGUILERA, J.; MCCLEMENTS, D. Development of nanoemulsions by an emulsification-evaporation technique. Food process engineering in a changing world. Proceedings of the 11th International Congress on Engineering and Food, 2011. p.929-930.

TSIENV, R. Y.; ERNST, L.; WAGGONER, A. Fluorophores for Confocal Microscopy: Photophysics and Photochemistry. In: PAWLEY, J. B. (Ed.). **Handbook of Biological Confocal Microscopy**. Berlin: Springer Science Business Media, 2006. p.338-352.

UE - União Européria. Regulamento nº 1223/2009 do Parlamento Europeu e do Conselho de 30 de novembro de 2009 relativo aos produtos cosméticos. CapítuloV - Ensaios em Animais.

UGARTONDO, V.; MITJANS, M.; VINARDELL, M. P. Applicability of lignins from different sources as antioxidants based on the protective effects on lipid peroxidation induced by oxygen radicals. **Ind Crops Prod,** v. 30, n. 2, p. 184-187, 2009.

USÓN, N.; GARCIA, M. J.; SOLANS, C. Formation of water-in-oil (W/O) nano-emulsions in a water/mixed non-ionic surfactant/oil systems prepared by a low-energy emulsification method. **Colloids Surf A,** v. 250, n. 1–3, p. 415-421, 2004.

VALENTA, C.; SIMAN, U.; KRATZEL, M.; HADGRAFT, J. The dermal delivery of lignocaine: influence of ion pairing. **Int J Pharm,** v. 197, n. 1–2, p. 77-85, 2000.

VAN ELSWIJK, D. A.; SCHOBEL, U. P.; LANSKY, E. P.; IRTH, H.; VAN DER GREEF, J. Rapid dereplication of estrogenic compounds in pomegranate (Punica granatum) using on-line biochemical detection coupled to mass spectrometry. **Phytochemistry,** v. 65, n. 2, p. 233-241, 2004.

VAN HAL, D. A.; JEREMIASSE, E.; JUNGINGER, H. E.; SPIES, F.; BOUWSTRA, J. A. Structure of Fully Hydrated Human Stratum Corneum: A Freeze-Fracture Electron Microscopy Study. **J Investig Dermatol,** v. 106, n. 1, p. 89-95, 1996.

VAN TOMME, S. R.; STORM, G.; HENNINK, W. E. In situ gelling hydrogels for pharmaceutical and biomedical applications. **Int J Pharm,** v. 355, n. 1–2, p. 1-18, 2008.

VERMA, A.; STELLACCI, F. Effect of Surface Properties on Nanoparticle–Cell Interactions. **Small,** v. 6, n. 1, p. 12-21, 2010.

VERMA, D. D.; FAHR, A. Confocal Laser Scanning Microscopy: An Excellent Tool for Tracking Compounds in the Skin. In: SMITH, W. E. e MAIBACH, H. I. (Ed.). **Percutaneous Penetration Enhancers**. Abingdon: Taylor & Francis Group 2006. p.335-357.

VITALE, S. A.; KATZ, J. L. Liquid Droplet Dispersions Formed by Homogeneous Liquid−Liquid Nucleation: "The Ouzo Effect". **Langmuir,** v. 19, n. 10, p. 4105-4110, 2003.

VITTORI, D.; GARBOSSA, G.; LAFOURCADE, C.; PÉREZ, G.; NESSE, A. Human erythroid cells are affected by aluminium. Alteration of membrane band 3 protein. **Biochim Biophys Acta Biomembr,** v. 1558, n. 2, p. 142-150, 2002.

VIUDA-MARTOS, M.; FERNÁNDEZ-LÓPEZ, J.; PÉREZ-ÁLVAREZ, J. A. Pomegranate and its Many Functional Components as Related to Human Health: A Review. **Compr Rev Food Sci Food Saf,** v. 9, n. 6, p. 635-654, 2010.

VOSTÁLOVÁ, J.; ZDAŘILOVÁ, A.; SVOBODOVÁ, A. Prunella vulgaris extract and rosmarinic acid prevent UVB-induced DNA damage and oxidative stress in HaCaT keratinocytes. **Arch Dermatol Res,** v. 302, n. 3, p. 171-181, 2010/04/01 2010.

WELSS, T.; BASKETTER, D. A.; SCHRÖDER, K. R. In vitro skin irritation: facts and future. State of the art review of mechanisms and models. **Toxicol in Vitro,** v. 18, n. 3, p. 231-243, 2004.

WERTZ, P. W. The nature of the epidermal barrier: biochemical aspects. **Adv Drug Delivery Rev,** v. 18, p. 283-294, 1996.

WILLIAMS, A. C.; BARRY, B. W. Penetration enhancers. **Adv Drug Delivery Rev,** v. 64, Supplement, n. 0, p. 128-137, 2012.

WU, H.; RAMACHANDRAN, C.; WEINER, N. D.; ROESSLER, B. J. Topical transport of hydrophilic compounds using water-in-oil nanoemulsions. **Int J Pharm,** v. 220, n. 1–2, p. 63-75, 2001.

WU, P. S.; HUANG, L. N.; GUO, Y. C.; LIN, C. C. Effects of the novel poly(methyl methacrylate) (PMMA)-encapsulated organic ultraviolet (UV) filters on the UV absorbance and in vitro sun protection factor (SPF). **J Photochem Photobiol B,** v. 131, p. 24-30, 2014.

XU, K. Z. Y.; ZHU, C.; KIM, M. S.; YAMAHARA, J.; LI, Y. Pomegranate flower ameliorates fatty liver in an animal model of type 2 diabetes and obesity. **J Ethnopharmacol,** v. 123, n. 2, p. 280-287, 2009.

XU, Q.; NAKAJIMA, M.; LIU, Z.; SHIINA, T. Soybean-based Surfactants and Their Applications. In: NG, T.-B. (Ed.). **Soybean - Applications and Technology**. Croatia: In Tech, 2011. p.341-364.

XU, X.; LUO, J. Marangoni flow in an evaporating water droplet. **Appl Phys Lett,** v. 91, n. 12, p. 124102, 2007.

YANG, H.-L.; CHEN, S.-C.; CHANG, N.-W.; CHANG, J.-M.; LEE, M.-L.; TSAI, P.-C.; FU, H.-H.; KAO, W.-W.; CHIANG, H.-C.; WANG, H.-H.; HSEU, Y.-C. Protection from oxidative damage using Bidens pilosa extracts in normal human erythrocytes. **Food ChemToxicol,** v. 44, n. 9, p. 1513-1521, 2006.

YEH, M.-I.; HUANG, H.-C.; LIAW, J.-H.; HUANG, M.-C.; HUANG, K.-F.; HSU, F.-L. Dermal delivery by niosomes of black tea extract as a sunscreen agent. **Int J Dermatol,** v. 52, n. 2, p. 239-245, 2013.

YOU, Y.-H.; LEE, D.-H.; YOON, J.-H.; NAKAJIMA, S.; YASUI, A.; PFEIFER, G. P. Cyclobutane pyrimidine dimers are responsible for the

vast majority of mutations induced by UVB irradiation in mammalian cells. **J Biol Chem,** v. 276, n. 48, p. 44688-44694, 2001.

YU, M.; MA, H.; LEI, M.; LI, N.; TAN, F. In vitro/in vivo characterization of nanoemulsion formulation of metronidazole with improved skin targeting and anti-rosacea properties. **Eur J Pharm Biopharm,** v. 88, n. 1, p. 92-103, 2014.

ZAID, M. A.; AFAQ, F.; SYED, D. N.; DREHER, M.; MUKHTAR, H. Inhibition of UVB-mediated oxidative stress and markers of photoaging in immortalized HaCaT keratinocytes bu pomegranate polyphenol extract POMx. **Photochem Photobiol,** v. 83, p. 882-888, 2007.

ZHAI, Y.; ZHAI, G. Advances in lipid-based colloid systems as drug carrier for topic delivery. **J Controlled Release,** v. 193, p. 90-99, 2014.

ZHOU, H.; YUE, Y.; LIU, G.; LI, Y.; ZHANG, J.; GONG, Q.; YAN, Z.; DUAN, M. Preparation and characterization of a lecithin nanoemulsion as a topical delivery system. **Nanoscale Res Lett,** v. 5, n. 1, p. 224-230, 2010.

APÊNDICE A

Estudos de estabilidade e fotoestabilidade das nanoemulsões contendo constituintes polifenólicos presentes na fração acetato de etila do extrato das cascas da romã

1 METODOLOGIA

2.2 Quantificação de compostos polifenólicos por CLAE

A quantificação dos principais compostos polifenólicos presentes nas nanoemulsões foram realizadas por cromatografia líquida de alta eficiência (CLAE) empregando um cromatógrafo Shimadzu LC-10A equipado com bomba LC-20AD, forno CTO-20A, detector de diodo SPD-M20A e software LC Solution 1.2 (Shimadzu, Kyoto, Japão). As análises foram executadas em coluna de fase reversa Luna C18 Fusion RP 100 Å (250 mm×4.6 mm) (Phenomenex®, USA), acoplada a uma pré-coluna C18 (Phenomenex®, USA), empregando método previamente desenvolvido e validado quanto aos parâmetros de especificidade, linearidade, limites de detecção e quantificação, precisão, exatidão e robustez (BACCARIN e LEMOS-SENNA, 2014). O sistema foi operado à 30ºC utilizando como fase móvel (A) acetonitrila e (B) água acidificada com ácido acético (1% v/v), filtrada previamente em membrana de celulose regenerada 0,45 µm. O fluxo da fase móvel foi de 1,0 mL/min usando o seguinte gradiente: 0,01–3 min 97% B, 3–5 min 97%–94% B; 5–8 min 94%–90% B; 8–12 min 90%–87% B; 12–15 min 87%–84% B; 15–18 min 84%–80% B; 18–21 min 80%–77% B; 21–24 min 77%–74% B; 24–28 min 74%–97% B; 28–30 min 97% B. O volume de injeção de amostra foi de 20 µL e a detecção foi realizada em 270 nm, 367 nm e 378 nm para o ácido gálico, ácido elágico e punicalagina, respectivamente.

2.3 Determinação da concentração de fenóis totais

A determinação espectrofotométrica dos compostos fenólicos totais presentes nas nanoemulsões foi realizada de acordo com metodologia previamente descrita, utilizando-se o método de Folin-Ciocalteu (BACCARIN e LEMOS-SENNA, 2014). Resumidamente, 1 mL de cada formulação foi transferido para uma balão volumétrico de 10 mL. Em seguida, as amostras foram dissolvidas em 1 mL de acetonitrila (EAF-MCT-NE) ou em 1 mL de acetato de etila (EAFPSO-NE), agitadas vigorosamente em vórtex durante 2 min, e completadas

até o volume total do balão com acetonitrila. Após, 2 mL desta solução foram transferidos para um balão volumétrico de 25 mL, 500 µL de reagent de Folin-Ciocalteu e 10 mL de água destilada foram adicionado e a solução foi agitada por 1 min. Logo após, 2 mL de NaCO3 (15% p/v) foram adicionados, a solução foi agitada por 30 segundos, e o volume do balão foi completado com água destilada até 25 mL. As amostras foram incubadas protegidas da luz por 2 horas; seguidamente, a absorbância das amostras foi medida em espectrofotômetro Shimadzu® UV-1800, Software UV Probe 2.33, no comprimento de onda de 750 nm. Os resultados foram expressos como miligrama de equivalentes de ácido gálico (EAG) por mililitro de nanoemulsão e as análises foram realizadas em triplicata.

2.4 Análise do tamanho de gota, distribuição de tamanho e potencial zeta

O diâmetro médio da gota, a distribuição de tamanho e potencial zeta das nanoemulsões, foram determinados por espectroscopia de correlação fotônica e Anemometria laser Doppler, respectivamente, utilizando um Zetasizer Nano Series (Malvern Instruments, Worcestershire, UK). As medidas foram realizadas a 25℃ após diluição apropriada das amostras em água ultrapura. Cada análise foi obtida com um ângulo de detecção de 173 °. Para determinar o potencial zeta, as amostras foram colocadas em célula eletroforética, onde um potencial de ± 150 mV foi estabelecido. Os valores potenciais foram calculados com a média dos valores da mobilidade eletroforética utilizando a equação de Smoluchowski.

2.5 Estudo de estabilidade

Um estudo de estabilidade de curto prazo foi realizado, armazenando as nanoemulsões contendo a com o óleo de semente da romã ou triglicerídeo de cadeia média encapsulando a fração acetato de etila, EAF-PSO-NE e EAF-MCT-NE respectivamente, em temperatura ambiente 25 ºC (TA) e na refrigeração a 4 ºC (GE) durante um período total de 60 dias, em frasco de vidro transparente. Nos tempos de 1, 7, 15, 30 e 60 dias, foi realizada uma coleta de cada amostra e os seguintes parâmetros físico-químicos foram avaliados: tamanho médio das gotículas e a distribuição de tamanho das mesmas, potencial zeta,

determinação da concentração de fenóis totais e quantificação dos principais compostos polifenólicos por CLAE.

2.6 Estudo de fotoestabilidade

O estudo de fotoestabilidade foi conduzido de acordo com o Guia para estudos de fotoestabilidade da *International Conference Harmonization* (ICH) (ICH, 1996), nas dependências da Central de Laboratórios de Ensaios Analíticos, na Universidade do Vale do Itajaí. As nanoemulsões contendo a fração acetato de etila (EAF-PSO-NE e EAF-MCT-NE), armazenadas em frasco de vidro transparente, foram colocadas em uma câmara de fotoestabilidade (Mecalor® CE / 0,2 / AR-F, São Paulo, Brasil) e irradiadas com lâmpada fluorescente ultravioleta (UV) nos comprimentos de onda ultravioleta A (UVA -320-400 nm) e visível (400-700 nm). As amostras foram irradiadas nas doses de 1,2 milhões de lux.hora e 200 wats hora/metro^2, para a luz visível e UVA, respectivamente. Os parâmetros avaliados no início ao final do estudo foram aspectos visuais, tamanho de gota e distribuição de tamanho, potencial zeta, TFC e quantificação dos principais compostos fenólicos através de análise por CLAE. Como controles, amostras embrulhadas em folha de alumínio, porém irradiadas, foram usadas para avaliar a influência da temperatura sobre as características físico-químicas das amostras. O ensaio foi realizado em triplicata para cada nanoemulsão.

2 RESULTADOS E DISCUSSÃO

2.1 Estabilidade

No início do teste de estabilidade as concentrações de fenóis totais, ácido gálico, ácido elágico e punicalagina foram semelhantes aos relatados anteriormente (BACCARIN e LEMOS-SENNA, 2014). No entanto, a partir do 15º dia em diante, as amostras apresentaram contaminação fúngica visível e na análise correspondente ao 60º dia as amostras armazenadas à temperatura ambiente apresentaram contaminação fúngica severa, o que tornou inviável a análise por CLAE para estas amostras. Tanto nas formulações mantidas à temperatura ambiente quanto na geladeira (Figura 10-A, B), as concentrações de fenóis totais e de ácido gálico permaneceram semelhantes durante todo o experimento de estabilidade. Observou-se que a partir do 15º dia, houve um aumento na concentração de ácido elágico e diminuição na

concentração de punicalagina (Figura 10-C, D). Uma hipótese para este evento seria que ao sofrer degradação, a punicalagina estaria liberando uma molécula de ácido elágico, resultando em um aumento da concentração do mesmo nas nanoemulsões. As nanoemulsões permaneceram monodispersas durante o experimento, com valores de potencial zeta próximo a -30 mV e tamanho médio da gota de aproximadamente 180 nm e 225 nm para EAF-PSO-NE e EAF-MCT-NE, respectivamente (Figura 10-E). As nanoemulsões contendo a fração acetato de etila que foram armazenadas na geladeira, permaneceram fisicamente estáveis por 60 dias sem apresentar floculação, cremação ou coalescência. Finalmente, de uma maneira geral, as formulações mantidas em temperatura ambiente apresentaram alterações físico-químicas mais pronunciadas que as formulações mantidas na geladeira.

Figura 10. Caracterização físico-química das nanoemulsões contendo a fração acetato de etila do extrato das cascas de *P. granatum* (EAF-PSO-NE e EAF-MCT-NE) durante os 60 dias de estudo de estabilidade em temperatura ambiente (TA) e geladeira (GE-4 ºC). A- Concentração de fenóis totais; B- Concentração de ácido gálico; C- Concentração de ácido elágico; D- Concentração de punicalagina; E- Tamanho de gota (símbolos fechados) e potencial zeta (símbolos abertos) das nanoemulsões – EAF-MCT-NE GE (■□); EAF-MCT-NE RT (▲△); EAF-PSO-NE GE (▼▽); EAF-PSO-NE TA (●○). Os resultados estão apresentados pela média ± desvio padrão (n=3).

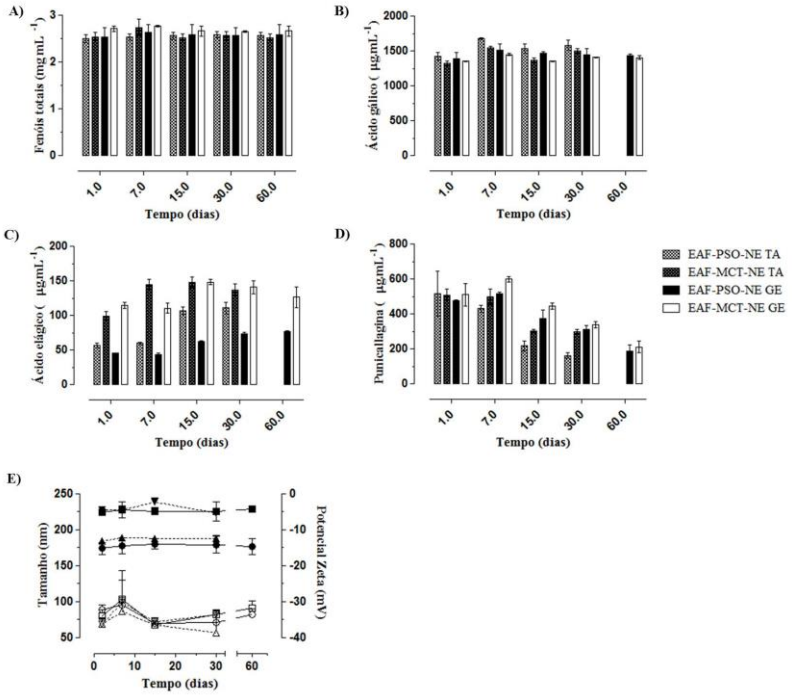

2.2 Fotoestabilidade

De acordo com os resultados obtidos no estudo de fotoestabilidade (Tabela 2), foi constatado que as nanoemulsões contendo a fração acetato de etila do extrato seco das cascas da romã (EAF-PSO-NE e EAF-MCT-NE), apresentaram distribuição de tamanho de gota monodispersa (IPD<0,3), e valores de potencial zeta e tamanho

médio de gota semelhante entre as amostras antes e após a irradiação UVA e UV-visível; os valores de potencial zeta obtidos foram entre -20 e -30 mV e o tamanho médio de gota de aproximadamente 150 nm e 212 nm, para EAF-PSO-NE e EAF-MCT-NE, respectivamente. As concentrações de TPC, AE, AG e de PC obtidas após a irradiação também foram semelhantes àquelas obtidas antes da irradiação, em torno de 2,3 $mg.mL^{-1}$, 58 $\mu g.mL^{-1}$, 1200 $\mu g.mL^{-1}$ e 450 $\mu g.mL^{-1}$, respectivamente. Nenhuma alteração física foi observada nas amostras após a irradiação. Além disso, não houve nenhuma alteração nas características físico-químicas das amostras controle, evidenciando que o aumento da temperatura provocada pela incidência de luz dentro da câmara de fotoestabilidade não teve influência sobre as amostras. Em suma, as nanoemulsões foram consideradas fotoestáveis após a irradiação mínima preconizada para a luz UVA e UV-visível.

Tabela 2. Caracterização físico-química das nanoemulsões contendo a fração acetato de etila do extrato das cascas de *P. granatum* no estudo de fotoestabilidade antes e após a irradiação UVA e luz visível.

		Amostras	Potencial Zeta (mV ± DP)	Tamanho (nm ± DP)	IPD	EAG ($mg.mL^{-1}$ ± DP)	AG ($\mu g.mL^{-1}$ ± DP)	EA ($\mu g.mL^{-1}$ ± DP)	PC ($\mu g.mL^{-1}$ ± DP)
		EAF-MCT-NE							
		I	-22,4 ± 0,8	232,2 ± 0,8	0,170	2,1 ± 0,03	1125,5 ± 14,33	87,3 ± 4,53	463,2 ± 6,21
		II	-23,0 ± 2,4	199,3 ± 2,4	0,148	2,1 ± 0,04	1147,3 ± 35,21	82,5 ± 2,93	469,9 ± 3,28
		III	-24,1 ± 1,3	216,3 ± 2,7	0,152	2,1 ± 0,08	1204,1 ± 29,20	89,2 ± 7,62	474,5 ± 3,18
Antes da irradiação		**IV**	-21,3 ± 0,7	200,0 ± 2,0	0,141	2,1 ± 0,05	1164,8 ± 43,20	88,2 ± 5,24	454,3 ± 7,66
		EAF-PSO-NE							
		I	-24,6 ± 3,7	154,8 ± 4,3	0,116	2,5 ± 0,13	1073,1 ± 27,60	39,9 ± 0,50	402,9 ± 6,68
		II	-23,4 ± 1,1	144,3 ± 2,8	0,075	2,3 ± 0,06	1095,4 ± 5,54	38,8 ± 1,40	471,7 ± 30,50
		III	-24,6 ± 0,6	156,0 ± 4,0	0,109	2,3 ± 0,06	1139,3 ± 18,00	36,5 ± 1,93	405,7 ± 17,67
		IV	-23,1 ± 1,0	147,3 ± 2,8	0,103	2,4 ± 0,11	1106,2 ± 3,29	38,2 ± 2,25	454,3 ± 5,74
		EAF-MCT-NE							
	UVA	**I**	-23,8 ± 1,3	217,2 ± 4,5	0,161	2,1 ± 0,14	1316,13 ± 2,76	81,3 ± 2,09	438,8 ± 3,52
	UVA*	**II**	-24,1 ± 2,8	197,0 ± 0,3	0,144	2,3 ± 0,21	1310,54 ± 35,4	83,8 ± 3,98	461,7 ± 3,38
	VIS	**III**	-25,1 ± 1,4	227,6 ± 0,8	0,143	2,4 ± 0,12	1254,98 ± 28,2	85,0 ± 4,26	407,9 ± 15,10
Após a irradiação	VIS*	**IV**	-21,0 ± 0,7	205,8 ± 0,2	0,150	2,3 ± 0,21	1285,55 ± 32,9	83,2 ± 3,83	419,3 ± 4,84
		EAF-PSO-NE							
	UVA	**I**	-25,0 ± 0,9	146,2 ± 0,7	0,087	2,4 ± 0,07	1239,14 ± 10,82	40,4 ± 2,09	391,9 ± 5,65
	UVA*	**II**	-25,4 ± 1,9	147,5 ± 2,1	0,101	2,3 ± 0,20	1268,78 ± 2,76	39,2 ± 3,98	465,4 ± 24,90
	VIS	**III**	-24,5 ± 0,5	149,2 ± 3,4	0,099	2,1 ± 0,10	1204,13 ± 9,47	38,5 ± 4,26	395,4 ± 23,30
	VIS*	**IV**	-24,2 ± 0,3	150,8 ± 0,7	0,100	2,2 ± 0,18	1221,36 ± 5,71	39,5 ± 3,83	421,7 ± 4,60

IPD=Índice de Polidispersão; EAG= Concentração de fenóis totais expressos em equivalentes de ácido gálico; AG=Ácido Gálico; EA=Ácido Elágico; PC=Punicalagina. *Amostras controle envolvidas em folha de alumínio, porém irradiadas, para avaliar somente a influencia da temperatura nas características físico-químicas das amostras. Os resultados estão apresentados como média ± desvio padrão (DP) (n=3).